1

Emerging approaches to investigate musculoskeletal health from HR-pQCT imagery

Andrew Burghardt[1]

1. University of California San Francisco, San Francisco, CA, United States

Abstract Coming Soon

2

VFA's: You "aorta" look beyond vertebral fractures.

Joshua Lewis[1]

1. Edith Cowan University, Perth, WA, Australia

Modern bone density machines can easily and seamlessly capture lateral spine images to detect prevalent vertebral fractures and monitor for incident vertebral fractures. These vertebral fracture assessment images or VFAs are increasingly being recommended and captured at the time of bone density testing in people with low bone mineral density. The abdominal aorta is the largest artery in the abdomen and supplies oxygenated blood from the heart to the abdominal organs, pelvis and lower limbs. Healthy aortas should not be visible on VFAs. Calcium deposition within the aortic wall or abdominal aortic calcification (AAC) is a marker of advanced blood vessel disease and is commonly seen on these VFA images. However AAC is rarely reported to patients or their healthcare providers. This is in part due to difficulties in assessing AAC and uncertainties over its prognostic importance.

In this presentation I will discuss what AAC is and why it is important for cardiovascular health. I will also discuss how AAC is currently assessed on VFAs, the limitations of this approach and state-of-the-art developments for VFA-derived AAC as well as describe the links between AAC with musculoskeletal health outcomes.

Acknowledgments: The salary of J.R.L. is supported by a National Heart Foundation of Australia, Future Leader Fellowship.

AI-driven image classification of radiographic data for prospective fracture prediction – global state and current work at the I²Lab.

Timo Damm[1]

Lars Schmarje [2], Niklas Koser [1], Stefan Reinhold [2], Eren Yilmaz [1], Nicolai Krekiehn [1], Li-Yung Lui [3], Steven R. Cummings [3], John T. Schousboe [4,5], Reinhard Koch [2], Claus-C. Glueer [1]

1) Section Biomedical Imaging, Intelligent Imaging Lab (I²Lab), Department of Radiology and Neuroradiology, University Hospital Schleswig-Holstein (UKSH), Kiel University, Germany

2) Department of Computer Science, Multimedia Information Processing Group (MIP), Kiel University, Germany

3) California Pacific Medical Center, San Francisco, CA, USA

4) Park Nicollet Clinic and HealthPartners Institute

5) University of Minnesota

Corresponding author: timo.damm@rad.uni-kiel.de

Background/Aim: Automated analysis of plain radiographs for prospective fracture (HF) risk prediction using artificial intelligence (AI) methods could expand availability of diagnostic tests, automate, and potentially improve the overall identification of patients at risk.

AI-driven computer vision, first applied in 1958, is by far not a new technique. Enduring several “AI winters”, key contributions to the field eventually let to breakthroughs, in particular of the deep convolutional neural networks (CNNs). Most notably the jump in image classification accuracy of AlexNet in the 2012 ImageNet challenge triggered the so-called “AI spring”.

At the Intelligent Imaging Lab (I2Lab) in Kiel, different AI-related approaches are investigated, both for diagnostic and prospective outcomes. Besides image classification tasks (e.g. COVID-19, stroke, osteoporosis, fractures or anomalies) on radiographs, computed tomography (CT) and/or magnetic resonance imaging (MRI) data, localization and segmentation tasks for identification, labeling and placement of regions/volumes of interest (ROI/VOI) are also an important and substantial part of the desired automated processing pipeline.

AI approaches require big and good data. At I2Lab, we started one prognostic hip fracture (HF) risk prediction study: “Study of Osteoporotic Fracture” (SOF) - Investigation by Artificial Intelligence” (SOFIA) and will present our findings in relation to other similar prognostic studies. To better access the required big data for future studies, we at I2Lab are keen to cooperate in federated learning studies.

Methods: In SOFIA, we investigate, how these deep CNNs in conjunction with automatic ROI placement based on a key-point-detector CNN (CenterNet) predict hip fracture risk based on digitized pelvic radiographs. We developed and tested three different AI models pre-trained on ImageNet data, whereas two were based on Resnet50 and one on DenseNet121. The femoral neck region (aBMD_FN) from dual X-ray Absorptiometry (DXA) data served as reference standard and Cox proportional hazard models incorporating aBMD_FN or AI based risk estimates without and with age & BMI adjustment were compared for difference in Harrell’s C.

Results: Of a total of 7964 women (age 71.6±5.1 at baseline) preprocessing resulted in a dataset of 6338 women for training and validation of the DCNNs (with 924 incident HF during 14.0±6.3 years of follow-up) and of 1252 women for the test dataset (with 184 incident HF during 15.0±5.7 years of follow-up). aBMD_FN and all of the AI predictors were significantly associated with HF incidence in univariate and in age & BMI adjusted models (all p<0.001, table). Age & BMI adjusted DenseNet based predictors showed significantly better predictive power than age-adjusted aBMD_FN on same subjects (p<0.05).

Conclusion: Automated AI-driven analysis of pelvic radiographs based on a DenseNet121 model predicts HF better than DXA-based aBMD of the femoral neck and shows potential for predictive power better than DXA and thus may enable sites without DXA access to achieve high-quality HF risk predictions.

Table: Prediction of hip fracture in SOFIA

	univariate			age- & BMI-adjusted		
Predictor	sHR	Harrell’s C	AICc	adj. sHR	Harrell’s C	AICc
aBMD FN	2.1(1.8-2.5)	0.682±.020	2373.9	1.9(1.5-2.3)	**0.711±.020**	2342.9
AI ResNet1	1.9(1.6-2.3)	0.667±.021	2386.1	1.7(1.4-2.1)	0.707±.020	2348.3
AI ResNet2	2.0(1.7-2.3)	0.688±.019	2370.5	1.8(1.5-2.1)	0.720±.018	2339.1
AI DenseNet	2.2(1.8-2.5)	0.705±.019	2347.2	2.1(1.7-2.4)	**0.741±.018***	2314.6

*: significantly better than age- & BMI-adjusted aBMD model on same subjects

sHR: standardized Hazard Ratio, AICc: corrected Akaike Information Criterion

Treating osteoporosis and dementia with anti-dementia medication acetylcholinesterase inhibitors may have therapeutic benefits on osteoporotic bone by attenuating osteoclastogenesis and bone resorption

Charles Inderjeeth[1], Shangfu Li[2], Dian Teguh[3], Depeng Wu[2], Lesong Liu[2], Jinbo Yuan[3], Jiake Xu[3]

1. North Metropolitan Health & University of Western Australia, Nedlands, WA, Australia

2. Spine Surgery, Third Affiliated Hospital of Sun Yat-sen University, Guangzhou, Guangdong, China

3. School of Biomedical Science, University of Western Australia, Perth, WA, Australia

Background; Osteoporosis and dementia are common and often concurrent in ageing populations. Identifying common pathogenesis and treatment targets may be useful.

Aims: This study was designed to determine whether the use of acetylcholinesterase inhibitors (AChEIs), a group of drugs that stimulate Acetylcholine receptors and used to treat Alzheimer's disease, is associated with osteoporosis protection and inhibition of osteoclast differentiation and function.

Methods: We examined the effects of AChEI on RANKL-induced osteoclast differentiation and function with osteoclastogensis and bone resorption assays. Next, we investigated impacts of AChEIs on RANKL-induced NF-κB and NFATc1 activation and expression of osteocalst marker genes of CA-2, CTSK and NFATc1, and dissected the MAPK signaling in osteoclasts in vitro by using luciferase assay and Western Blotting. Finally, we assessed the in vivo efficacy of AChEIs using an ovariectomy - induced osteoporosis model, which was analyzed using micro-computed tomography, in vivo osteoclast and osteoblast parameters were assessed using bone histomorphometry.

Results: We found that Donepezil and Rivastigmine inhibited RANKL-induced osteoclastogenesis and impaired osteoclastic activity and bone resorption. Moreover, AChEIs reduced the RANKL-induced transcription of NFATc1, and expression of osteocalst marker genes to varying degrees (mainly Donepezil and Rivastigmine but not Galanthamine). Furthermore, AChEIs variably inhibited RANKL-indued MAPK signaling. Finally, AChEIs protected against OVX-induced bone loss mainly by inhibiting osteoclast activity.

Conclusions: AChEIs (mainly Donepezil and Rivsatigmine) exerted powerfull effect on bone protection by inhibiting osteoclast function through MAPK signaling pathway. Our findings will influence drug choice in those patients with both Alzheimer's disease and osteoporosis.

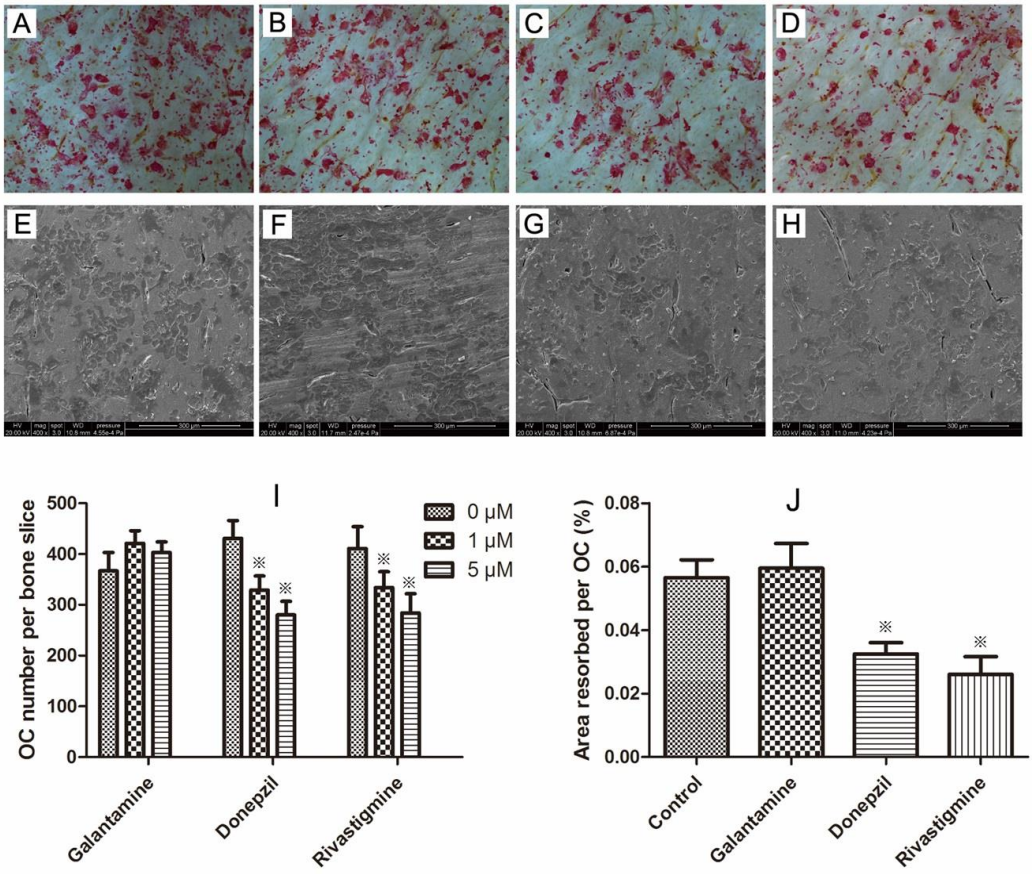

5

Bisphosphonates may boost immune responses to pulmonary infection by acting on tissue-resident macrophages in the lung

Marcia A Munoz[1], Emma K Fletcher[1], Oliver P Skinner[1], Esther Kristianto[2], Mark P Hodson[3], Michael J Rogers[1]

1. Skeletal Diseases Program, Garvan Institute of Medical Research, Sydney, NSW, Australia

2. VCCRI Innovation Centre, Victor Chang Cardiac Research Institute, Sydney, NSW, Australia

3. School of Pharmacy, University of Queensland, Woolloongabba, QLD, Australia

Bisphosphonate drugs inhibit bone resorption but also appear to have actions outside the skeleton by mechanisms that are poorly understood. Clinical and epidemiological studies suggest that nitrogen-containing bisphosphonate (N-BP) therapy is associated with reduced risk of infection and mortality from pneumonia. To better understand how N-BPs may have beneficial effects in the lung we employed various approaches including multicolour flow cytometry, mass spectrometry and single-cell RNA sequencing, and identified alveolar macrophages (aMac) as targets of N-BPs.

Flow cytometric analysis of bronchoalveolar lavage cells, isolated from mice after a single intravenous injection of a fluorescently-tagged analogue of the N-BP zoledronate (AF647-ZOL), revealed drug uptake by >97% of aMac ($CD11b^{lo/-}$ $CD11c^{hi}CD64^{+}$) and 34% of interstitial ($CX3CR1^{+}CD11b^{hi}$) macrophages. AF647-ZOL was still detectable in aMac one week after administration. Intracellular accumulation of unprenylated proteins and build-up of the metabolite isopentenyl diphosphate (IPP) are hallmarks of the pharmacological actions of N-BPs. Consistent with intracellular uptake of labelled ZOL, using mass spectrometry and a customised biochemical assay we detected a clear build-up of IPP and unprenylated Rab GTPases in aMac 48 hours after one intravenous dose of ZOL. Importantly, single-cell RNA sequencing of aMac, isolated from mice challenged intranasally with LPS endotoxin, revealed enhanced gene expression of cytokines and chemokines (including *Il1b, Cxcl2, Cxcl3, Ccl3* and *Ccl4*) in a subpopulation of aMac in ZOL-treated mice compared to controls. This was accompanied by higher levels of these cytokines and chemokines in bronchoalveolar lavage fluid from ZOL-treated mice after LPS-challenge, as measured by multiplex cytokine assays.

These studies dispel the dogma that N-BPs act only in bone and clearly demonstrate that they also affect lung-resident macrophages. In addition to preventing bone loss, we propose that N-BP treatment may boost the initial immune response of aMac to pulmonary infections, therefore conferring protection from pneumonia.

6

Endothelial cells require mitochondrial transfer from osteocytes to promote vascularization in cortical bone

Peng Liao[1], Long Chen[2], Hao Zhou[3], Jiong Mei[1], Guangyi Li[1], Changqing Zhang[1], Ming-Hao Zheng[4, 5], Delin Liu[4, 5], Junjie Gao[1]

1. Department of Orthopaedics, Shanghai Jiao Tong University Affiliated Shanghai Sixth People's Hospital, Shanghai, China

2. State Key Laboratory of Cell Biology, Shanghai Institute of Biochemistry and Cell Biology, CAS Center for Excellence in Molecular Cell Science, Chinese Academy of Sciences, University of Chinese Academy of Sciences, Shanghai, China

3. Department of Orthopedics,The Second Affiliated Hospital of Zhejiang University School of Medicine, Hangzhou, Zhejiang Province, China

4. Centre for Orthopaedic Research, Medical School, The University of Western Australia, Perth, WA, Australia

5. Perron Institute for Neurological and Translational Science, Perth, WA, Australia

Vascularization is an energy-consuming process which highly relies on mitochondria to orchestrate ROS level in endothelial cells[1,2]. Transcellular mitochondrial movement has been previously demonstrated to coordinate tissue homeostasis, survival and repair[3]. Here, we reported that osteocytes play critical roles in maintaining mature network of trans-cortical blood vessels (TCVs), and that endothelial cells of TCVs require osteocytes-derived mitochondria to facilitate vascularization. We first showed that osteocytes extend dendritic network to TCVs in cortical bone by confocal imaging analyses. Using $Dmp1^{cre}$-$DTA^{ki/wt}$ mice we showed that ablation of osteocytes in cortical bone cause regression of TCVs accompanying with the decreased expression of angiogenic genes. Using osteocyte-specific mitochondrial fluorescent mice we showed that acquisition of osteocytes-derived mitochondria by endothelial cells was integral to the structure of TCVs. Co-culture of osteocyte MLO-Y4 transfected with mitochondrial fluorescent protein Dendra2 and endothelial cells (bEnd.3) showed that osteocytes transfer mitochondria to rescue damaged endothelial cells evidenced by decreasing oxidative stress, increasing proliferation and wound healing ability of endothelial cells. Finally, conditional knockout of Miro1, the critical mitochondrial transport machinery protein, in mouse osteocytes resulted in significant compromise of TCVs morphological network. In conclusion, our studies demonstrated that the vascularization of endothelial cells in cortical bone relies on the osteocytes and their dendritic network. Osteocytes transfer mitochondria to endothelial cells for the maintenance of TCV integrity. Our results provide a new insight for bone-blood vessel interaction in mineralized tissue.

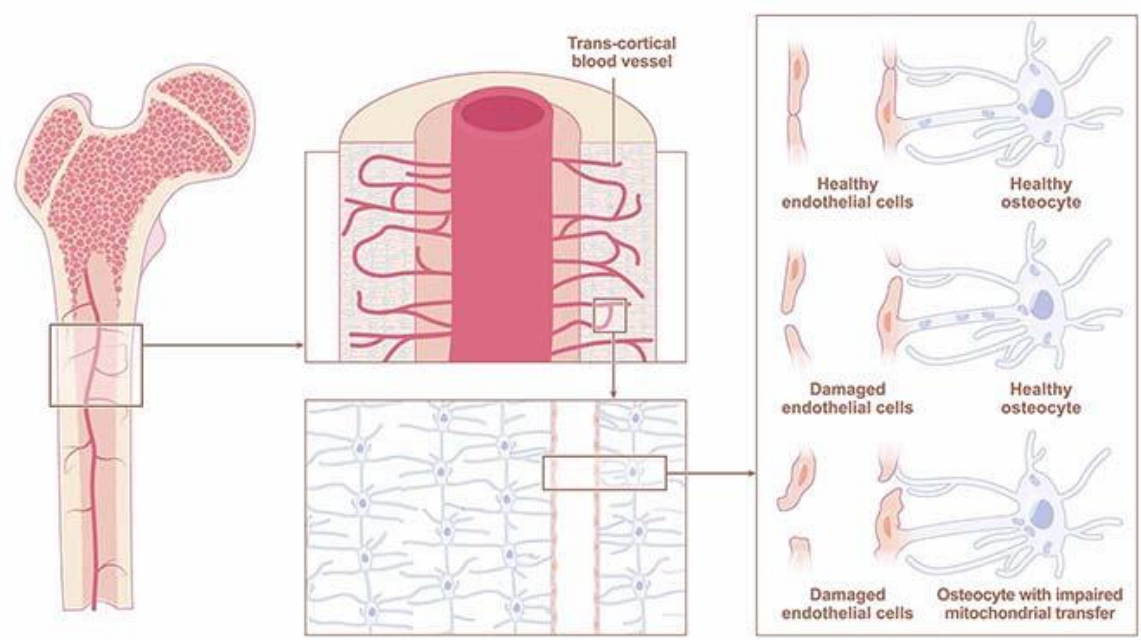

1. Jezek, P., and Hlavatá, L. (2005). Mitochondria in homeostasis of reactive oxygen species in cell, tissues, and organism. Int J Biochem Cell Biol 37, 2478-2503.
2. Reichard, A., and Asosingh, K. (2019). The role of mitochondria in angiogenesis. Mol Biol Rep 46, 1393-1400.
3. Gao, J., Qin, A., Liu, D., Ruan, R., Wang, Q., Yuan, J., Cheng, T.S., Filipovska, A., Papadimitriou, J.M., Dai, K., et al. (2019). Endoplasmic reticulum mediates mitochondrial transfer within the osteocyte dendritic network. Sci Adv 5, eaaw7215.

Epidemiology of fractures in different ethnic groups across the lifespan in New Zealand

Subhajit Konar[1], Emma Buckels[1], David Musson[1], Sarah-Jane Paine[1], Brya Matthews[1]

1. University of Auckland, Auckland, New Zealand

Fractures lead to increased morbidity and mortality in the elderly, but they are a musculoskeletal issue that occurs at all ages. Fracture rates are often estimated based on hospitalisation data, which only gives a complete picture for certain fracture types. In New Zealand, injuries are covered by a no-fault national insurance system known as ACC. Most fractures that require clinical attention are recorded as ACC claims. The aim of this study was to determine the frequency of fractures in New Zealand overall and at key sites in different genders and ethnic groups across the lifespan.

Individualised fracture claim data were obtained from ACC for 2010-2019. 945,041 fracture claims were included in the analysis. Prioritised ethnicity was reported (order of priority: Māori, Pacific peoples, Asian/Other, European) for 98% of claims. Census data was used to calculate fracture incidence. A setting where the injury occurred was reported in 91% of claims.

Males accounted for 52.7% of fractures in the entire dataset, however over the age of 50, fracture incidence is 70% higher in women (Table). Europeans had the highest incidence overall, and Māori and Pacific people have lower incidence of fractures than Europeans in all age groups in women and all but 20-39 years of age in men. Asian people had the lowest incidence of fracture in young adults, but similar rates to Europeans in the elderly. Hip fractures mainly occur in the elderly and show lower incidence in Māori and Pacific people than Europeans (Table). Almost half of all fractures occurred at home, rising to over 80% in the elderly. 30% of fractures in people aged 10-39 occurred in a place of recreation/sports. Age, gender and ethnicity all affect fracture incidence, with peaks in adolescents and the elderly. Māori and Pacific people, particularly women, generally have lower fracture rates than Europeans.

.

Table: Total fracture incidence in New Zealand 2010-2019 (per 10,000 people/year)

	Female					Male				
Age	European	Maori	Pacific Peoples	Asian/ Other	All	European	Maori	Pacific Peoples	Asian/ Other	All
0 -9	249	139	153	160	199	243	148	164	169	201
10 -19	363	185	159	182	279	555	353	378	318	462
20 -29	160	106	79	62	125	306	299	292	123	266
30 -39	138	104	75	63	114	206	217	190	105	187
40 -49	140	95	64	76	122	174	155	117	97	160
50 -59	189	115	84	127	170	146	129	91	88	137
60 -69	224	117	107	184	211	125	104	72	90	121
70 -79	259	142	126	254	255	135	109	90	114	135
80+	508	251	295	616	520	276	174	197	282	284
All	227	131	112	118	192	237	217	213	143	221
50+	259	126	110	184	241	151	120	89	101	145
Hip fractures										
50+	26.6	7.2	8.6	12.8	24.2	12.9	5.2	4.7	6.0	12.0
80+	133.6	62.2	89.2	154.1	139.6	74.6	41.0	53.3	70.3	78.2

Fracture risk in women with osteoporosis treated with gastro-resistant (ec) risedronate versus immediate release risedronate or alendronate: a claims data analysis in the United States

John Eisman[1], Friedrike Thomasius[2], Mitra Boolell[3], Francis Vekeman[4], Asif Alam[3], Jason Heroux[4], Bernard Cortet[5]

1. Garvan Institute of Medical Research, Darlinghurst, NSW, Australia

2. Rheumatology , Frankfurter Hormon Und Osteoporosezentrum, Frankfurt, Germany

3. Medical Department, Theramex, London, UK

4. Econometrics, STATLOG , Montreal, Quebec

5. Service de rhumatologie, hôpital Roger-Salengro, CHU de Lille ; université Lille-2, Lille, France

Objective(s): Risedronate immediate release (Ris-IR) and delayed release (GR/EC) formulations and alendronate (Ale; IR formulation) are used by women with osteoporosis (OP) in the US. We compared risk of fractures between women on GR(EC) Ris and those on (a) IR Ris and (b) Ale.

Material and Methods: Women aged ≥ 60 yr with ≥ 2 oral bisphosphonate (OBPs) prescription fills with OP diagnosis and/or history of fracture were selected from a claims database (2009-2019). The index date and study cohorts (GR/EC Ris, IR Ris, Ale) were based on the first observed OBPs dispensing. All eligible women on GR/EC Ris were analyzed (N = 1,080). Comparator cohorts, randomly selected from women initiated on IR Ris and Ale to match the index year of women on GR/EC Ris. Adjusted incidence rate ratios (IRRs) were used to compare fracture risk between GR/EC Ris and IR Ris/Ale; and in women with high fracture risk.

Results: Women in the GR/EC Ris, IR Ris and Ale cohorts were followed for 3.0, 3.2, and 3.2 yr, respectively (mean age: 69, 69, and 70 yr). Unadjusted rates of any fracture per 1,000 women-yr were highest among women aged ≥70 yr (GR/EC Ris: 67 vs. 58 among women aged ≥65 yr, 60 among those at high risk with comorbidity/medications, and 51 among any GR/EC Ris; IR Ris: 97 vs. 88, 77, 65; Ale: 102 vs 87, 80, 67; respectively). Adjusted IRRs for GR/EC Ris vs IR Ris /Ale generally indicated lower risk of fracture for the GR/EC Ris (IRRs <1; Figure).

IRRs were statistically lower for GR/EC for pelvis fractures and for select fractures(Figure).

Conclusions: Results suggest GR/EC Ris offers a lower risk of fracture than IR Ris or Ale among women with OP with higher baseline risk of fracture.

Disclosures: The study was funded by Theramex.

Figure.

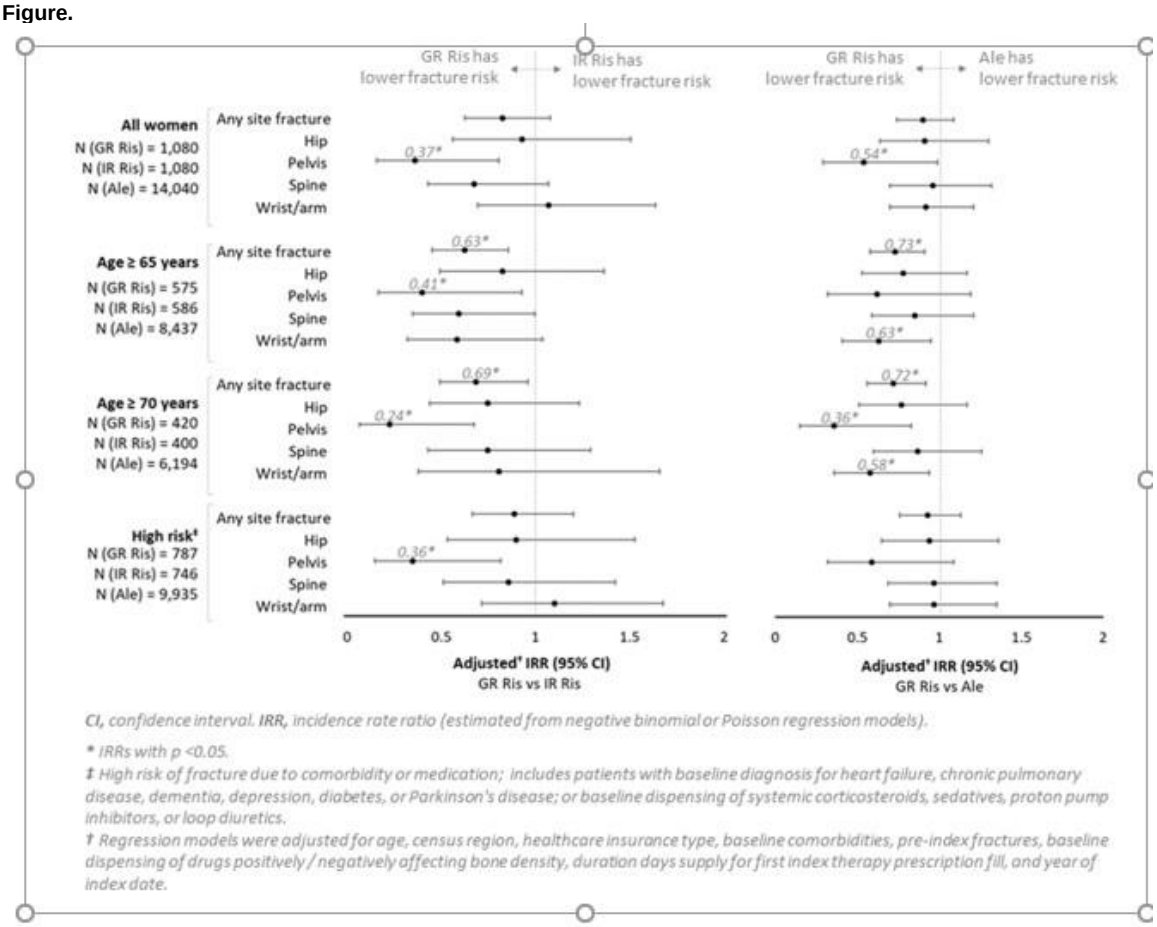

CI, confidence interval. IRR, incidence rate ratio (estimated from negative binomial or Poisson regression models).

** IRRs with p <0.05.*

‡ High risk of fracture due to comorbidity or medication; includes patients with baseline diagnosis for heart failure, chronic pulmonary disease, dementia, depression, diabetes, or Parkinson's disease; or baseline dispensing of systemic corticosteroids, sedatives, proton pump inhibitors, or loop diuretics.

† Regression models were adjusted for age, census region, healthcare insurance type, baseline comorbidities, pre-index fractures, baseline dispensing of drugs positively / negatively affecting bone density, duration days supply for first index therapy prescription fill, and year of index date.

9

Estradiol increases bone mass and strength in a pre-clinical mouse model of male-to-female transition during adulthood

Tian Nie[1], Varun Venkatesh[1], Suzanne Golub[1], Kathryn Stok[2], Reena Desai[3], David Handelsman[3], Jeffrey Zajac[1], Mathis Grossmann[1], Rachel Davey[1]

1. Department of Medicine, Austin Health, University of Melbourne, Melbourne, Vic, Australia

2. Department of Biomedical Engineering, University of Melbourne, Melbourne, VIC, Australia

3. ANZAC Research Institute, University of Sydney and Concord Repatriation General Hospital, Concord, NSW, Australia

Publish consent withheld

1. Handelsman, David J., Emma Gibson, Susan Davis, Blanka Golebiowski, Kirsty A. Walters, and Reena Desai. 2020. "Ultrasensitive Serum Estradiol Measurement by Liquid Chromatography-Mass Spectrometry in Postmenopausal Women and Mice." Journal of the Endocrine Society 4 (9): 1–12. https://doi.org/10.1210/jendso/bvaa086.

10

RANKL discovery: a model for basic science research?

David Findlay[1]

1. The Discipline of Orthopaedics and Trauma and Centre for Orthopaedic and Trauma Research, The University of Adelaide, Adelaide, SA

The research environment that led eventually to the discovery of RANK ligand was one in which basic, curiosity-driven, 'blue sky' investigation was considered valuable. A large proportion of discoveries in biomedical research, and also research in general, have historically been made by curious, observant, bright, plugged in (keeping abreast of current knowledge) people and these discoveries have often been serendipitous. When we look at the line-up of researchers, whose work enabled the identification of RANK ligand as a molecule central to the formation and activation of osteoclasts (among other actions), we see these characteristics writ large. In this talk, I will seek to honour at least some of those contributors to the RANKL story, in a short, fast and furious history of this fascinating molecule. I will list some of the ways in which the identification of RANKL has impacted bone physiology and pathology, and also try to fit in some updates on RANKL biology. Lastly, I will advocate, and attempt to recruit the audience as advocates, for the support of basic science, and in particular basic science as it relates to the human skeleton.

11

Sugar transporter Slc37a2 regulates bone metabolism via a dynamic tubular lysosomal network in osteoclasts

Amy Ribet[1], Pei Ying Ng[1], Qiang Guo[1], Benjamin H Mullin[2], Jamie W.Y Tan[1], Euphemie Landao-Bassonga[1], Sébastien Stephens[3], Kai Chen[1], Laila Abudulai[4, 1], Maike Bollen[4, 5], Edward T.T.T. Nguyen[1], Jasreen Kular[1], John M Papadimitriou[6], Kent Søe[7, 8], Rohan D. Teasdale[9], Jiake Xu[1], Robert G. Parton[10], Hiroshi Takanayagi[11], Nathan J. Pavlos[1]

1. School of Biomedical Science, UWA, CRAWLEY, WA, Australia

2. Department of Endocrinology & Diabetes, Sir Charles Gairdner Hospital, Perth, WA, Australia

3. School of Medicine and Dentistry, Griffith University, Southport, QLD, Australia

4. Centre for Microscopy Analysis and Characterisation, UWA, CRAWLEY, WA, Australia

5. School of Molecular Science, UWA, CRAWLEY, WA, Australia

6. PathWest Laboratory Medicine , CRAWLEY, WA, Australia

7. Pathology Research Unit, Department of Clinical Research, University of Southern Denmark, Odense, Denmark

8. Department of Pathology, Odense University Hospital, Odense, Denmark

9. School of Biomedical Sciences, The University of Queensland, St Lucia, QLD, Australia

10. Institute for Molecular Biosciences and Centre for Microscopy and Microanalysis, , The University of Queensland, St Lucia, QLD, Australia

11. Department of Immunology, Graduate School of Medicine and Faculty of Medicine, The University of Tokyo, Tokyo, Japan

Bone-digesting osteoclasts harbour specialized lysosome-related organelles termed secretory lysosomes (SLs). SLs store cathepsin K and give rise to the osteoclast ruffled border (RB) upon fusion with the bone-oriented plasmalemma. Despite serving as a membrane precursor for RB genesis, and therefore fertile grounds for the discovery of new homeostatic regulators of bone mass, our understanding of the molecular composition of osteoclast SLs remains incomplete. Here, by integrating the organelle proteome of enriched SLs isolated from mouse osteoclasts with human GWAS of estimated bone mineral density, we identified member a2 of the solute carrier 37 family (Slc37a2) as a new SL sugar transporter associated with the physiological regulation of bone mass. In situ, we demonstrate that among bone-lineage cells, Slc37a2 expression is restricted to osteoclasts where it localizes to the limiting membrane of SLs and the RB. Using live-cell microscopy, we unexpectedly find that Slc37a2+ve SLs adopt a dynamic tubular organization in osteoclasts that radiates throughout the cytoplasm and fuses with the bone-apposed plasmalemma. Physiologically, bones from mice lacking Slc37a2 (*Slc37a2*^{KO}) exhibit a profound increase in trabecular bone mass, which affords protection against age-associated bone loss. At the cellular level, this dramatic increase in bone mass is driven primarily by impaired bone resorption by osteoclasts coupled with imbalanced remodelling-based osteoblastic bone formation. Mechanistically, SLs in *Slc37a2*^{KO} osteoclasts are engorged and dysfunctional owing to disturbances in the luminal export of monosaccharide sugars, a prerequisite necessary for SL organelle resolution, tubulation and delivery to the RB. Accordingly, *Slc37a2*^{KO} osteoclasts exhibit disturbances in RB maturation and decreased delivery and secretion of cathepsin K. Altogether, our findings: (i) unmask Slc37a2 as a SL sugar transporter critical for physiological bone metabolism, (ii) highlight previously unappreciated plasticity of the osteoclast's specialized lysosome-related organelle(s) and; (iii) posit Slc37a2 as potential therapeutic target for metabolic bone diseases.

12

Structural and cellular characterisation of the osteochondral tissue in hip and knee osteoarthritis.

Dzenita Muratovic[1], David M Findlay[1], Ryan D Quarrington[1], Lucian B Solomon[1, 2], Gerald J Atkins[1]

1. Centre for Orthopaedic & Trauma Research, The University of Adelaide, Adelaide, South Australia, Australia

2. Orthopaedic and Trauma Service, The Royal Adelaide Hospital and the Central Adelaide Local Health Network, Adelaide, SA, Australia

INTRODUCTION: Osteoarthritis (OA) is a multifactorial disease of the whole joint and it is most commonly seen in hip and knee. It is unclear whether osteoarthritis in hip and knee has different aetiologies and if different factors influence progression and degenerative changes characterising this disease in different joints. This study investigated the type and extent of structural changes at tissue and cellular level between hip and knee osteoarthritis.

METHODS: Tibial plateaus were collected from 11 patients (5 females aged 70±8 years) undergoing total knee replacement surgery and 8 femoral heads (4 females aged 64±12 years) from patients undergoing total hip replacement surgery. Upon receiving surgical samples, two bone core biopsies were sampled per subject. From tibial plateau, biopsies were obtained from anterior and posterior aspects of medial condyle, while biopsies from femoral heads were obtained from anterior superior and anterior inferior aspects. Synchrotron micro-CT imaging was performed on each sample to obtain parameters describing bone microstructure, osteocyte-lacunar network and bone matrix vascularity. Osteocyte density, viability and connectivity were obtained histologically.

RESULTS: The sclerotic appearance of bone microstructure is more pronounced adjacent to severe cartilage loss in both hip and knee OA. However, significantly lower osteocyte cell density ($p<0.0001$), viability ($p=0.02$) and connectivity ($p<0.0001$) were found in hip OA when comparing to knee OA, irrespective of disease severity. Also, significantly lower bone matrix vascularity ($p=0.03$) was found in hip OA when compared to knee OA.

DISCUSSION: This study provides evidence that OA in hip and knee demonstrate different characteristics at the tissue and cellular levels. Importantly, the results from this study suggest that the mechanisms and phenotypes of OA disease differ across joints. In addition, findings from this study may potentially lead to identify potentially effective therapeutic targets and allow more targeted and tailored treatment in patients.

Strain Distributions Within the Proximal Tibia Calculated Using Digital Volume Correlation of Micro-CT Images

Kieran J Bennett[1, 2], Lauren Wearne[1], Sophie Rapagna[1], Saulo Martelli[3], Bogdan Solomon[4], Egon Perilli[1], Dominic Thewlis[2, 4]

1. Medical Devices Research Institute, Flinders University, Tonsley

2. Centre for Orthopaedic and Trauma Research, The University of Adelaide, Adelaide

3. Queensland University of Technology, Brisbane

4. Department of Orthopaedics and Trauma, Royal Adelaide Hospital, Adelaide

The internal mechanical response of the proximal tibia to load has been limited to those implied from finite element models. Digital volume correlation (DVC), applied on micro-CT images, has been previously used to estimate the internal strains within virtual cores of the proximal tibia due to external load. However, whole organ strains have not been investigated. In this study, we aimed to quantify the internal 3D strains within the proximal tibia due to joint loading using DVC.

Two cadaveric knees were obtained, and all soft tissues except for the articular cartilage and menisci were removed. The femur and tibia were mounted within a loading stage, positioned within a large-volume micro-CT scanner (Nikon XT H 225, Nikon Metrology, UK). Scans were performed at 46 µm isotropic pixel size in unloaded and then loaded conditions. Axial loads corresponding to three bodyweights were applied. DVC analysis was undertaken to calculate von-Mises equivalent strains across the proximal tibia (DaVis software). The final DVC subvolume size was a 34 voxel (1.564 mm) subvolume length, required 100GB of memory and 20 core-hours to compute for each scan pair. Trabecular bone subvolumes more than 68 voxels from the cortical bone.

The median internal strains within the proximal tibia (Fig. 1) were 1890µε (interquartile range 1190µε) and 1962µε (interquartile range 1328µε) for specimens 1 and 2 respectively, with the distribution showing heterogeneity across the plateau.

Whole organ internal strains within the proximal tibia under load were quantified using DVC from large-volume micro-CT images. These data will enable relationships between the internal mechanical response and trabecular bone microarchitecture to be further explored.

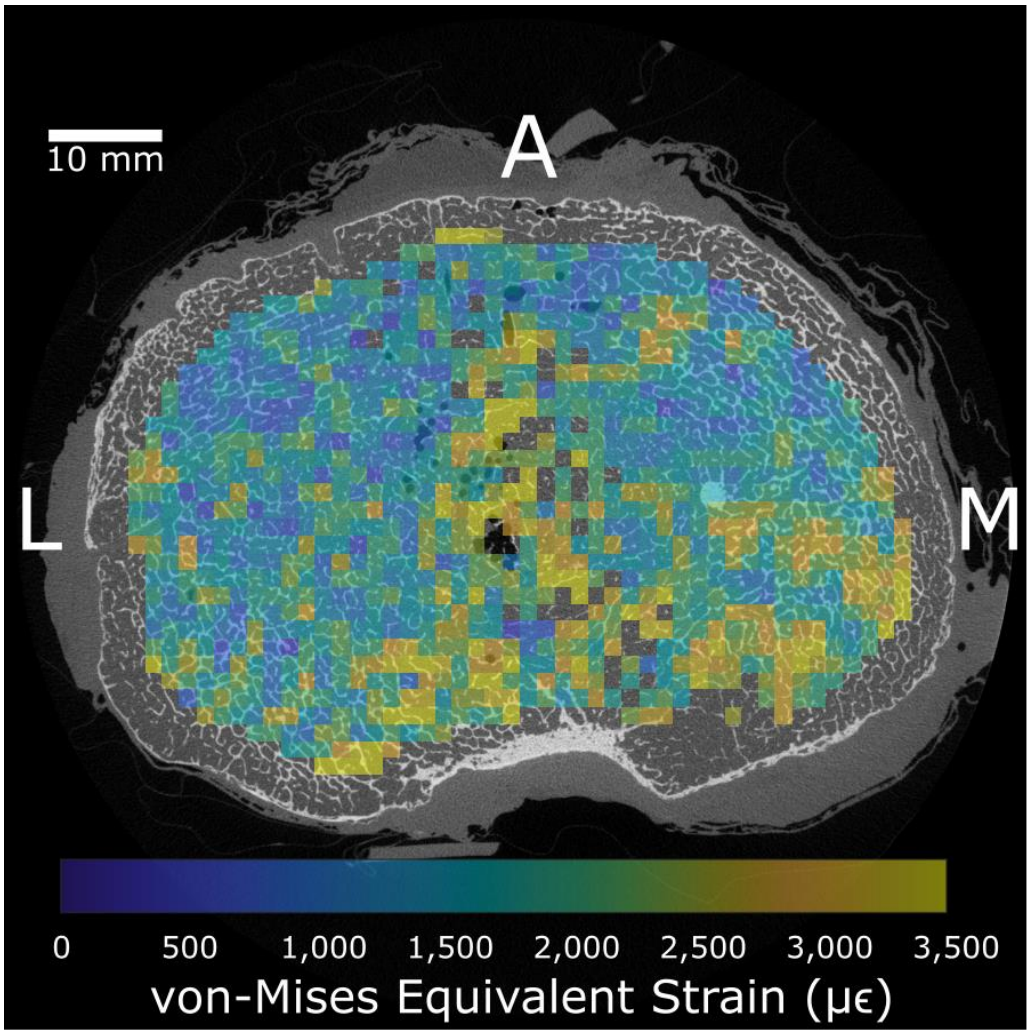

Figure 1. Micro-CT cross section of a human proximal tibia with strains due to external load calculated using DVC overlaid.

Functional group differences in the biomechanical and biochemical properties of human hand tendons

Carina Blaker[1], Dylan Ashton[1], Samantha Hefferan[1], Yolanda Liu[2], David Chang[3], Richard Lawson[3], Christopher Little[2], Elizabeth Clarke[1]

1. Murray Maxwell Biomechanics Laboratory, Institute of Bone and Joint Research, Kolling Institute, University of Sydney, Sydney, NSW, Australia

2. Raymond Purves Bone and Joint Research Laboratories, Institute of Bone and Joint Research, Kolling Institute, University of Sydney, Sydney, NSW, Australia

3. Department of Hand Surgery, Royal North Shore Hospital, Northern Sydney Local Health District, Sydney, NSW, Australia

Traumatic injury is common in hand tendons, with variable long-term outcomes in different tendons[1,2]. Understanding variations in tendon properties is critical for improving treatments designed to restore functional capacity. The aim of the study was to measure the biomechanical and biochemical properties of upper limb tendons and compare differences between functional groups.

Twenty-four different hand/wrist tendons (grouped by function, Fig1a) were sourced from 8 fresh-frozen human cadavers (3 female, 5 male; 49-65years). Tendons were tested to failure under tension (5% strain/s). Biomechanical outcomes included cross-sectional area (CSA), maximum load, ultimate tensile strength (UTS), and elastic modulus. A mid-region sample was papain digested to measure glycosaminoglycan and hydroxyproline contents. Differences between tendon groups were analysed using mixed-effects linear regression models (covariates: sex and interactions with age). Group comparisons were evaluated at the mean age (56y), and Benjamini-Hochberg used for multiple comparisons.

Wrist flexors and extensors had the greatest maximum loads (1018.2±501.4N; 1162.2±327.7N) and CSA (12.9±7.0mm^2; 13.2±4.3mm^2) while digital extensors had the lowest (load: 486.0±146.8N; CSA: 5.0±1.4mm^2). After normalising by CSA, there were fewer significant differences between tendon groups for UTS and modulus (Fig1b,c). Digital extensors were significantly stronger than wrist (P=0.0004) and digital (P≤0.0082) flexors. Thumb extensors had significantly higher moduli than both wrist flexors and extensors (P≤0.0005), and digital flexors (P≤0.0048). Glycosaminoglycan content was similar across extensors and significantly lower in most flexors (P≤0.0201) except for deep digital (Fig1d). There were many between group differences in hydroxyproline content (P≤0.0054; Fig1e) and it was lowest in digital extensor tendons (77.6±7.7ug/mg).

The results of this study highlight unique mechanical and compositional differences between tendon functional groups in the human hand. Improved understanding of unique, normal tendon properties assists the development of more precise benchmark targets for the development and selection of graft materials and bench testing of responses to new therapeutics.

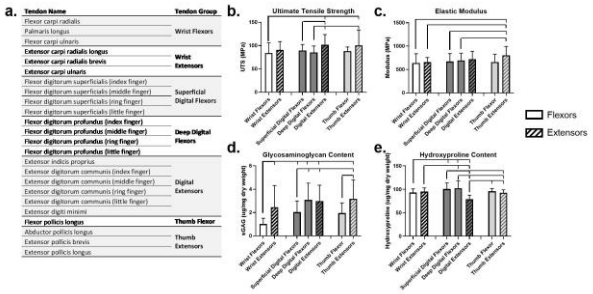

Figure 1. a. List of hand/wrist tendons and designated functional groups. **b-e.** Outcomes by tendon groups (mean ± SD). Overhead bars indicate significant differences between tendon groups. **b.** Ultimate tensile strength. **c.** Elastic modulus. **d.** Glycosaminoglycan content. **e.** Hydroxyproline content.

1. Newport ML, Tucker RL. New Perspectives on Extensor Tendon Repair and Implications for Rehabilitation. J Hand Ther. 2005;18(2):175-181
2. Dy CJ, Daluiski A, Do HT, Hernandez-Soria A, Marx R, Lyman S. The Epidemiology of Reoperation After Flexor Tendon Repair. The Journal of Hand Surgery. 2012;37(5):919-924

15

EphrinB2 and lysosomes in osteocytes are essential for collagen arrangement in the extracellular matrix

Martha Blank[1, 2], Mriga Dutt[3], Benjamin L Parker[3], Cameron J Nowell[4], T. John Martin[1, 2], Natalie A Sims[1, 2]

1. Bone Cell Biology and Disease Unit, St. Vincent's Institute of Medical Research, Melbourne, VIC, Australia

2. Department of Medicine, The University of Melbourne, St. Vincent's Hospital, Melbourne, VIC, Australia

3. Department of Anatomy and Physiology, The University of Melbourne, Melbourne, VIC, Australia

4. Drug Discovery Biology Theme, Monash Institute of Pharmaceutical Sciences, Parkville, VIC, Australia

Lysosomes are acidic intracellular vesicles. They contain enzymes that degrade collagen matrix in bone, and are essential for osteoclast-mediated bone resorption. However, their importance in osteocytes is unknown. We recently observed lysosome deficiency in cultured osteocytes with EphrinB2 (*Efnb2*) knockdown, and that *Efnb2*-deficiency in osteocytes (*Dmp1Cre.Efnb2*) caused a phenotype of fragile bones with greater mineral and collagen content than controls. Here we sought to identify the lysosomal enzymes affected by *Efnb2*-deficiency in osteocytes and determine how they regulate the collagen matrix.

To investigate how *Efnb2*-deficiency influences lysosomal collagen-degrading enzymes in osteocytes, we performed proteomics on cultured *Efnb2*-deficient and vector control Ocy454 cells. Multiple collagen-degrading proteins were lower in *Efnb2*-deficient cells compared to controls. This included matrix metallopeptidases 2 (MMP2) and 14 (MMP14), procathepsin L (CTSL), cathepsin B (CTSB) and cathepsin D (CTSD).

Next, we assessed whether the absence of these enzymes effects the ability of osteocytes to remodel collagen in a 3D culture system. Control osteocytes caused significant collagen contraction, to 25% of the original area at day 15 and only 15% at day 21. In contrast, collagen containing *Efnb2*-deficient Ocy454 cells showed no matrix contraction at day 15, and less contraction than controls (30% of original area) at day 21.

To determine how the absence of collagen-degrading enzymes in osteocytes affects the collagen matrix *in vivo*, we assessed collagen fiber architecture in tibial cortical bone from 12 week old *Dmp1Cre.Efnb2* mice by second harmonic generation imaging. *Dmp1Cre.*Efnb2 bones had thicker collagen fiber bundles with less parallel orientation than control bones.

These data indicate that the absence of collagen-degrading enzymes in osteocytes resulting from EphrinB2-deficiency limits osteocyte-dependent collagen contraction *in vitro* and collagen arrangement *in vivo*. This suggests a novel role for osteocyte-derived lysosomes to prevent aggregation of collagen in their surrounding matrix to preserve optimum bone quality and strength.

16

MicroRNA cargo of extracellular vesicles released by skeletal muscle negatively regulates the bone quality in obese mice

Ahmed AA Al Saedi[1, 2], Emily EP Parker [3], Meghan MM McGee-Lawrence[3], Gustavo GD Duque[1, 2], Mark MH Hamrick[3]

1. Department of Medicine – Western Health, The University of Melbourne, St Albans, VIC, Australia

2. Australian Institute for Musculoskeletal Science (AIMSS), The University of Melbourne and Western Health, St Albans, VIC, Australia

3. Department of Cellular Biology and Anatomy, Medical College of Georgia, Augusta university, Augusta, GEORGIA, United States

Bone and muscle closely interacted anatomically, chemically, and metabolically. Various muscle-derived humoral factors, known as myokines, affect bone. Extracellular vesicles (EVs) play a vital role in physiological and pathophysiological processes by transferring their contents to distant tissues, including bone metabolism. However, the amount and cargo of released EVs, consisting of microRNAs (miRNAs), mRNA, proteins, and DNA, are altered in obesity. Therefore, the roles of EVs in muscle-bone interactions in obesity remain unknown. The present study investigated the effects of EVs secreted from obese and lean mice muscles on bone cells, strength, and quality.

EVs were isolated from muscle samples of leptin receptor mutant *db/db* mice (obese) and myostatin null mice (lean) to determine the size, concentration, and miRNA profile. EVs were stained with CD63 and visualized under Electron Microscopy. In addition, femurs and tibias were extracted for micro-CT, 3-point bending, and bone histomorphometry. Furthermore, bones were stained for adiponectin, PPAR gamma, and perilipin RNA levels by RNA scope.

Compared to lean mice, muscle-derived EVs obtained from *db/bd* mice showed significant upregulation (3.5 fold) of mir-465 miRNA, which associates with three genes (CDC37, DAPK1, and Tirap). These genes are associated with Leucine-Rich Repeat Kinase 1 (LRRK1), a vital regulator of osteoclastogenesis. In addition, LRRK1 levels were significantly higher in femurs of *db/db* mice than in lean mice. Furthermore, we showed that *db/db* mice had a 23% increase in osteoclast numbers and a 10% decrease in osteoblast numbers compared to lean mice. Furthermore, we showed that *db/db* mice had significantly lower bone quality by micro-CT and 3-point bending compared to lean mice. Lastly, *db/db* mice also showed increased adiponectin, PPAR gamma, and perilipin RNA levels compared to lean mice.

In conclusion, these findings suggest that muscle EVs from obese mice directly impact bone cells and quality via their microRNA cargo.

Identifying genes involved in hip osteoarthritis and describing the cells in which they are differentially expressed

Kaitlyn A Flynn[1], Ryan C Chai[2, 3], Weng Hua Khoo[2, 3], Paul Baldock[2], Genetics of Osteoarthritis Consortium[4], Duncan Bassett[5], Graham R Williams[5], Peter I Croucher[2, 3], John P Kemp[1, 6]

1. Institute for Molecular Bioscience, The University of Queensland, Brisbane, QLD, Australia

2. Bone Biology, Garvan Institute of Medical Research, Sydney, NSW, Australia

3. St. Vincent's Clinical School, University of New South Wales, Sydney, NSW, Australia

4. https://www.genetics-osteoarthritis.com/home/index.html, Germany

5. Molecular Endocrinology Laboratory, Imperial College London, London, England, United Kingdom

6. MRC Integrative Epidemiology Unit (IEU) , University of Bristol, Bristol, England, United Kingdom

Background: Hip osteoarthritis (HipOA) is a complex disorder that adversely affects joint function. Genome-wide association studies (GWAS) have identified 45 HipOA-associated loci. Many genes underlying these associations remain unknown, impairing understanding of disease pathogenesis. We hypothesise that HipOA susceptibility genes can be systematically identified by integrating single cell-RNA sequencing (scRNA-seq), GWAS, and knockout mouse models.

Methods: Bone and marrow cells were isolated from mouse femora, and transcriptomes were mapped by scRNA-seq. Seurat analysis identified sets of differentially expressed genes (DEGs) that distinguished each cell type from all other cells. Gene set analysis (GSA) was used in conjunction with the largest HipOA GWAS to test whether DEGs that defined each cell type were enriched with HipOA-associated genes. HipOA-associated genes that were differentially expressed in enriched cell types were followed up in skeletal dysplasia databases.

Results: scRNA-seq analysis of 133,942 cells identified 34 cell types, each defined by a set of DEGs. GSA showed that DEGs that defined osteoblasts ($P<3.9\times10^{-4}$), chondrocytes ($P<9\times10^{-5}$) and pre-neutrophils ($P<7\times10^{-6}$) were more strongly associated with HipOA, than genes that were not differentially expressed in these cells. Seventeen HipOA-associated genes were differentially expressed in enriched cell types. Nine resulted in abnormal skeletal phenotypes when mutated. *Col11a1* (differentially expressed in osteoblasts and chondrocytes relative to all other cells), *Ltbp3* (osteoblasts), and *Mdfi* (osteoblasts and chondrocytes) caused osteoarthritis in humans and/or mice. *Tacc3* (pre-neutrophils) and *Creb3l2* (chondrocytes) resulted in abnormal cartilage morphology. Eight had no known skeletal annotations. *Tenascin-C* (*Tnc*) represented a compelling candidate that was robustly associated with HipOA ($P<2\times10^{-18}$); expression by osteoblasts was >4 fold higher than other cells, and previous studies show that *Tnc* is upregulated in response to mechanical loading, and under pathological conditions caused by inflammation.

Conclusions: We highlighted several HipOA-associated genes that are differentially expressed in cells that may be involved in osteoarthritis pathogenesis.

Skeletal glucocorticoid signalling plays a critical role in bone loss driven by circadian rhythm disruption

Eugenie Macfarlane[1], Lauryn Cavanagh[1], Colette Fong-Yee[1], Eleanor Imlay[1], Markus J Seibel[1], Hong Zhou[1]

1. ANZAC Research Institute, University of Sydney, Concord, NSW, Australia

Chronic disruption of circadian rhythms (CR) from shiftwork or sleep disorders is associated with bone loss and low bone mineral density (BMD). Glucocorticoid secretion follows a diurnal rhythm and is a potent regulator of CR by synchronising cell-autonomous clocks throughout the body. We therefore investigated whether chronic CR disruption induced-bone loss is mediated through glucocorticoid signalling in osteoblasts/osteocytes.

Mice lacking the glucocorticoid receptor in osteoblasts/osteocytes (obGRKO) and their wild-type (WT) litter-mates were exposed to an established model of chronic CR disruption for 22-weeks. Mice were maintained on either a normal 12hr:12hr light-dark cycle ('non-shifted') or exposed to weekly 12-hr phase-shifts, equivalent to spending alternate weeks in Sydney and London ('shifted'; Fig.1A).

Micro-CT analysis revealed tibiae trabecular BV/TV and BMD were reduced in shifted compared to non-shifted-WT mice. Although non-shifted-obGRKO mice had their own phenotype with lower BV/TV and BMD compared to non-shifted-WT mice, shifted-obGRKO mice had increased BV/TV, while BMD was maintained (Fig.1B-D).

Consistent with lower BMD, shifted-WT mice exhibited a greater proportion of empty osteocyte lacunae, indicative of increased osteocyte apoptosis, compared to non-shifted-WT mice. In contrast, osteocyte apoptosis was similar in shifted and non-shifted obGRKO mice (Fig.1D-F).

To analyse rhythmic changes in serum corticosterone and tibial gene expression, samples were collected at 6am and 6pm. Diurnal rhythmicity of circulating corticosterone was dampened in all shifted mice (Fig.1G) and expression of glucocorticoid target clock genes Bmal1, Per2, and Cry2 were significantly disrupted in tibiae of shifted mice. Notably, rhythmic expression of Bmal1 was flattened in shifted-WT but maintained in shifted-obGRKO mice (Fig.1H). Furthermore, clock target genes including Sost and RankL were increased in shifted-WT mice, whereas Col1a was increased in shifted-obGRKO mice. In conclusion, local osteoblast/osteocyte glucocorticoid signalling is a critical mediator of bone loss during CR disruption by regulating skeletal clock genes and their downstream rhythmic targets

Figure 1.

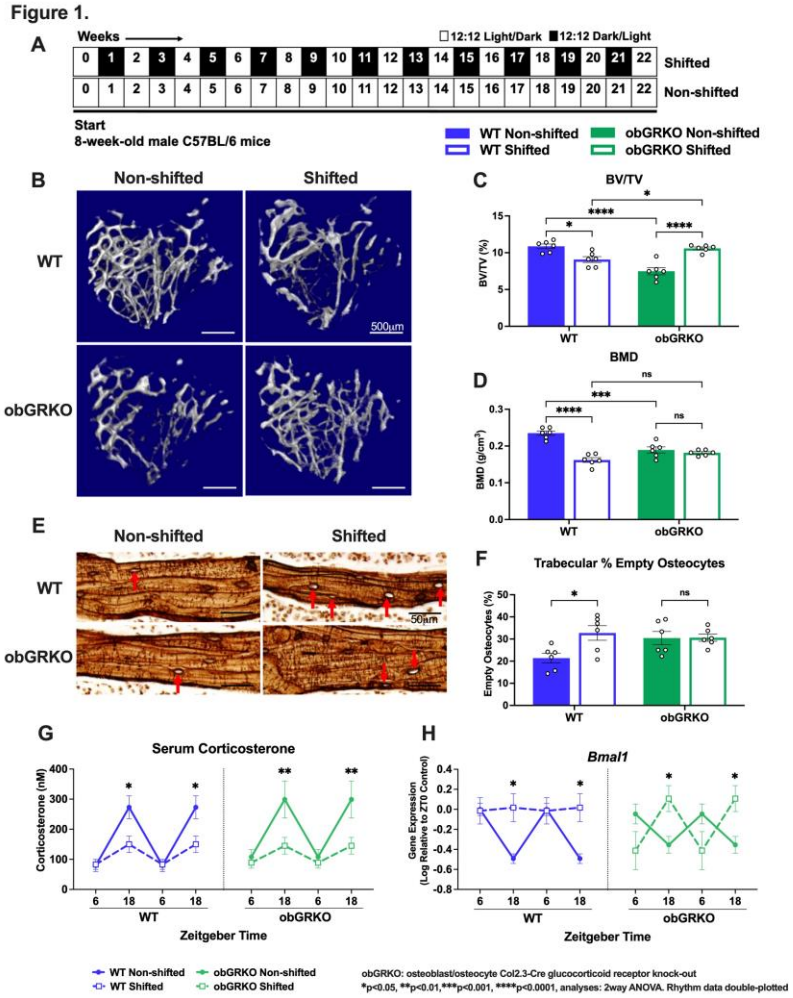

19

Asymptomatic vertebral fractures predict subsequent clinical fracture in both men and women

Ruth Frampton[1], Dana Bliuc[2], Jackie Center[2]

1. The Canberra Hospital, Garran, ACT, Australia

2. Garvan Institute of Medical Research, Darlinghurst, NSW, Australia

Asymptomatic vertebral fractures are common in the elderly, however their impact on clinical fracture risk has not been fully elucidated.

Data from 4442 women and 1755 men aged 50+ participating in the Canadian Multicentre Osteoporosis Study were analysed. Lateral thoracic and lumbar spine radiographs (T4-L4) at baseline were assessed using the Genant method (Grade 1 defined as vertebral height reduction 20 - 25%, Grade 2 26 - 40%, Grade 3 >40%).

At baseline, 13.8% of women and 14.5% of men had at least one asymptomatic vertebral fracture. For women, 6.6% had maximum Genant grade 1 fracture, 4.8% grade 2 and 2.4% grade 3. For men, 8.6% had maximum grade 1, 4.3% grade 2, and 1.5% grade 3. Incidence of clinical fracture was 24.9 per 1000 person years (95% CI 24.3-25.6) for women and 14.8 per 1000 person years (95% CI 13.9-15.8) for men.

Number of baseline asymptomatic vertebral fractures increased risk of incident clinical fracture for men and women after adjusting for age, body mass index, bone mineral density, prior clinical fracture and falls. The adjusted hazard of clinical fracture for each additional baseline vertebral fracture was 1.12 (95% CI 1.08-1.18) for women and 1.15 (95% CI 1.03-1.28) for men.

Genant grade 1 vertebral fractures did not increase risk of subsequent fracture for either sex after adjustment for other risk factors. However, compared to women with no vertebral fracture, higher Genant grade was associated with increased fracture risk [1.39 (95% CI 1.10-1.76) for grade 2, and 2.40 (95% CI 1.83-3.17) for grade 3]. For men, fracture risk was similar for Genant grade 2 [1.86 (95% CI 1.20-2.87)]. There were insufficient grade 3 fractures in men for analysis.

This study demonstrates that asymptomatic vertebral fracture number and severity (Genant grade>2) are associated with increased fracture risk, highlighting their clinical importance.

20

Identification of asymptomatic vertebral fracture using Artificial Intelligence (AI)

Huy G Nguyen[1, 2], Hoa T Nguyen[3], Linh T.T Nguyen[4], Thach S Tran[5], Sai H Ling[1], Lan T Ho-Pham[2], Tuan V Nguyen[1, 6]

1. School of Biomedical Engineering, The University of Technology Sydney, Sydney, NSW, Australia

2. Bone and Muscle Research Group, Ton Duc Thang University, Ho Chi Minh, Vietnam

3. Can Tho University of Medicine, Can Tho, Vietnam

4. The 108 Military Central Hospital, Ha Noi, Vietnam

5. Biology of Bone, The Garvan Institute of medical research, Sydney, NSW, Australia

6. School of Population Health, University of New South Wales, Sydney, NSW, Australia

Vertebral fracture (VF) is common in the elderly and is associated with increased risks of subsequent fracture and mortality. More than two-thirds of VF are asymptomatic and thus not treated. Existing methods were hard-to-interpret or black-boxes and vertebral morphometric properties were not explored. Therefore, we sought to develop an artificial intelligent (AI) method for identifying asymptomatic VF.

We analysed 1,016 lateral spinal X-rays from the Vietnamese Osteoporosis Study. VF was diagnosed by a rheumatologist using the Genant semiquantitative method. Our AI algorithm extracts the edge of a vertebral body into six identifiable vertices used to quantify the loss in height (Branched-Unet). A vertebra is considered normal, mild, moderate or severe if the height loss was <20%, 20-24%, 25-40% and >40%, respectively. We evaluated the prognostic performance of the AI algorithm on vertebra-level and person-level. We calculated sensitivity, specificity, and area under the receiver (AUC) to assess the classification performance of our AI algorithm.

We trained Branched-Unet on 98 films, and validated on 55 films, and achieved a dice-coefficient (DSC) of 90. The prevalence of vertebral fracture ascertained by clinician was 3.2% (28 / 863). At the individual level (n=863 films), the algorithm achieved a sensitivity of 89% and specificity of 62%. At the vertebral level (n=5913 vertebrae), the algorithm yielded a sensitivity of 71% and specificity of 91%. Further analysis showed a good concordance for non-fracture (91%, 5364/5875), mild (82%, 19/23) and severe (60%, 3/5) but not for moderate fracture (50%, 5/10). The AUC was 85% for both levels.

These results suggest that our AI algorithm can accurately identify asymptomatic vertebral fractures on plain radiographs without sacrificing interpretability. The rapid and automated approach can improve the efficiency of vertebral fractures in high-volume setting.

Table 1. Concordance between clinician diagnosis and AI classification over 863 films or 5913 vertebrae

Metrices	Vertebra-level	Person-level
Sensitivity	71.1 (54.1 84.6)	89.3 (71.8 97.7)
Specificity	91.3 (91.0 92.0)	61.9 (58.5 65.2)
Accuracy	91.2 (90.4 91.9)	62.8 (59.5 66.0)
AUC	84.4	85.0

Bayesian Network Meta-Analysis of All-Cause Mortality in Trials of Osteoporosis Therapies

Alexander H Seeto[1], Kevin Leow[2], Joshua Long[1], Mina Tadrous[3], Abadi Kahsu Gebre[4], Joshua R Lewis[4], Howard A Fink[5], Peter R Ebeling[6], Alexander J Rodriguez[6]

1. Griffith University, Southport, QLD, Australia

2. The Canberra Hospital, Canberra, ACT

3. Leslie Dan Faculty of Pharmacy, University of Toronto, Toronto

4. Institute for Nutrition Research, School of Medical and Health Sciences, Edith Cowan University, Joondalup

5. Geriatric Research Education and Clinical Center, VA Health Care System, Minneapolis

6. Bone and Muscle Health Research Group, Monash University, Clayton

Fractures appear to have an adverse impact on mortality with controversy over whether this is beyond pre-existing comorbidities. There are also data from observational studies and randomised controlled trials suggesting anti-osteoporosis therapies may reduce mortality. Conventional meta-analyses have examined this question in bisphosphonates, with remaining uncertainties for other anti-osteoporosis therapies. Therefore, we conducted a network meta-analysis (NMA) examining all-cause mortality data from randomised trials of anti-osteoporosis therapies in postmenopausal women.

Trials were identified from recent NMAs of osteoporosis therapies for fracture reduction, updated to December 2020. Included trials enrolled >100 women per study, randomised to placebo or an active comparator (bisphosphonate, denosumab, parathyroid [PTH] analogues, romosozumab, or menopausal hormone therapy [MHT] such as selective estrogen receptor modulators or direct estrogen and/or progesterone supplementation), and reported primary skeletal outcomes. We investigated all-cause mortality and all adverse events (for internal validity). Data were synthesized in a random-effects NMA using Bayesian modelling. Relative to placebo, point estimates for the odds ratio with 95% credible intervals were generated. Probabilistic ranking of treatment safety was performed.

We identified 71 trials, enrolling 143,388 women. Over a mean follow-up of 24 months, 1,990 deaths occurred in all studies (1.39%). There were 835 deaths in 56,460 women randomised to placebo (1.48%) and 1161 deaths in 90,722 women randomised to active therapies (1.28%). Compared with placebo, no osteoporosis therapy was significantly associated with mortality or overall adverse events. Probabilistic ranking found bisphosphonates were less likely to have increased risk of mortality than placebo, while denosumab, romosozumab, MHT, and PTH analogues ranked more likely to have increased risk of mortality than placebo.

Despite known fracture reduction benefits, we found no pooled direct/indirect evidence that anti-osteoporosis therapies significantly affected mortality risk relative to placebo. More data are now needed to understand mortality risks in the age of sequential therapies.

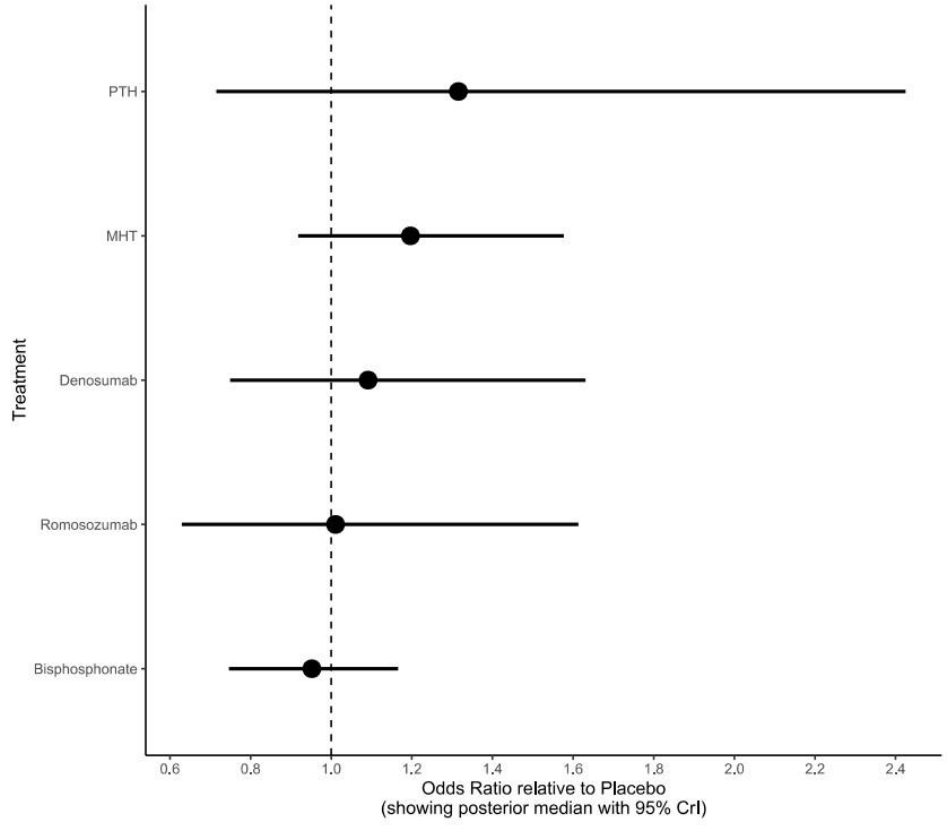

A low serum alkaline phosphatase may signal the presence of hypophosphatasia in patients with reduced bone mineral density or fragility fractures

Elisabeth Ng[2, 1], Claudia Ashkar[2], Ego Seeman[3, 4], Hans-Gerhard Schneider[2, 5], Hanh Nguyen[1, 6], Peter Ebeling[1, 6], Shoshana Sztal-Mazer[2, 7, 8]

1. Department of Endocrinology, Monash Health, Clayton, VIC, Australia

2. Department of Endocrinology & Diabetes, Alfred Health, Melbourne, VIC, Australia

3. Department of Medicine, The University of Melbourne, Melbourne, VIC, Australia

4. Department of Endocrinology, Austin Health, Melbourne, VIC, Australia

5. Clinical Biochemistry Unit, Alfred Pathology Service, Alfred Health, Melbourne, VIC, Australia

6. Department of Medicine, School of Clinical Sciences, Monash University, Clayton, VIC, Australia

7. School of Public Health, Monash University, Melbourne, VIC, Australia

8. School of Medicine, Monash University, Melbourne, VIC Australia

Introduction

Hypophosphatasia (HPP) is an inherited disorder associated with impaired primary mineralisation of osteoid (osteomalacia). HPP may be misdiagnosed as osteoporosis, a reduction in the volume of normally mineralized bone. Both illnesses may result in fragility fractures. Antiresorptive therapy, first-line treatment for osteoporosis, is contraindicated in HPP. Misdiagnosis and mistreatment can be avoided by recognising a low serum alkaline phosphatase (ALP).

Methods

The prevalence of a low ALP (<30 IU/L) was determined in a study of patients attending an Osteoporosis Clinic at a tertiary hospital during 8 years (2012-2020). Patients were categorised into those with a low ALP during one month, during at least two months but less than half of all months when ALP was measured, and in over half of all months when ALP was measured. The third group identified a persistently low ALP, minimising inclusion of patients with serial low levels within a brief time period.

Results

Of 1839 patients, 168 (9%) had at least one low ALP, 50 (2.7%) had low ALP during at least two months and seven (0.4%) had low ALP levels for at least half of all months when the ALP was measured. HPP has been diagnosed in four patients, three of whom had persistently low ALP levels. The prevalence of HPP was 0.22% of patients in the Osteoporosis Clinic and 2.38% of patients with at least one low ALP.

Conclusion

Persistently low ALP in Osteoporosis Clinic attendees signals the likelihood of a diagnosis of hypophosphatasia, a condition that may be mistaken for osteoporosis and incorrectly treated with antiresorptive therapy.

23

Patients on dialysis are at lower risk for mortality when treated with non-calcium-based phosphate binders.

Grahame J Elder[1, 2, 3], Tuan V Nguyen[4, 5], Thao P Ho-Le[5], Jacqueline R Center[3, 6]

1. Department of Renal Medicine, Westmead Hospital, Sydney, NSW, Australia

2. Medical faculty, University of Notre Dame, Sydney, NSW, Australia

3. Skeletal Diseases Program, Garvan Institute of Medical Research, Sydney, NSW, Australia

4. School of Biomedical Engineering and Centre for Health Technologies, University of Technology Sydney, Sydney, NSW, Australia

5. School of Population Health, UNSW Medicine, Sydney, NSW, Australia

6. St Vincent's Medical School, UNSW , Sydney, NSW, Australia

Background: Most patients on dialysis take oral calcium-based phosphate binders because elevated serum phosphate is associated with increased cardiovascular risk and mortality. More recently, some patients changed to newer, non calcium-based binders, sevelamer hydrochloride and lanthanum carbonate. This study tested the hypothesis that the progressive displacement of calcium-based binders is associated with reduced all-cause mortality.

Methods: The study utilised the Australian New Zealand Dialysis and Transplant Registry (ANZDATA) and included all patients ³18 years commencing dialysis in Australia from 1/2005, ending 12/2013. ANZDATA was linked to the Pharmaceutical Benefits Scheme. Data concerning demographic, anthropometric, comorbidities, biochemistry, mortality and drug treatments were collected. The outcome variable was the incidence of mortality during follow-up. The exposure variables were medication use classified into 2 major groups; sevelamer or lanthanum and calcium-based phosphate binders. A mixed-effects Cox's proportional hazards model was used to assess the association between medication use and time to mortality. Propensity score matching was applied to all analyses to deal with potential selection bias on drug treatment.

Results: The study included 7660 women and 12018 men with mean entry ages of 60.5 (15.9) and 62.0 (15.5) years respectively ($p<0.001$). Median follow-up was 32 (3-120) months, with death occurring in 34.3% of women (106.3/1000 person-years) and 35.1% of men (112.1 per 1000 person-years). Relative to calcium-based phosphate binders, use of the non calcium-based binders was associated with a 62% lower mortality risk (hazard ratio [HR] 0.38; 95% confidence interval [CI] 0.35-0.41) after adjusting for gender, age, comorbidities, and drugs that may influence survival.

Conclusions: For patients on dialysis, non calcium-based phosphate binder use was associated with markedly reduced mortality when compared to calcium-based binders. These results support the concept that positive calcium balance predisposes to increased mortality and support the use of non calcium-based phosphate binders in patient management.

24

The proportion of patients who reach the BMD surrogate threshold effect on romosozumab: a post hoc analysis of the randomised FRAME and ARCH phase 3 trials

Jeffrey Hassall[1], R. Chapurlat[2], J. van den Bergh[3], S. H. Ralston[4], S. Ferrari[5], M. McClung[6], M. Lorentzon[6, 7, 8], P. Makras[9], M. Lewiecki[10], T. Matsumoto[11], J. Timoshanko[12], Z. Wang[13], C. Libanati[14]

1. Amgen Australia, Sydney, NSW, Australia

2. INSERM UMR 1033, University Claude Bernard, Lyon, France

3. VieCuri Medisch Centrum, Venlo, Netherlands

4. Centre for Genomic and Experimental Medicine, MRC Institute for Genetics and Cancer, University of Edinburgh, Edinburgh, UK

5. Geneva University Hospital, Geneva, Switzerland

6. Mary MacKillop Institute for Health Research, Australian Catholic University, Melbourne, VIC, Australia

7. Sahlgrenska Osteoporosis Centre, Institute of Medicine, University of Gothenburg, Gothenburg, Sweden

8. 7Geriatric Medicine, Region Västra Götaland, Sahlgrenska University Hospital, , Mölndal, Sweden

9. 251 Hellenic Air Force & VA General Hospital, Athens, Greece

10. New Mexico Clinical Research & Osteoporosis Center, Albuquerque, New Mexico, USA

11. Tokushima University, Tokushima , Japan

12. UCB Pharma, Slough, UK

13. Amgen Inc, Thousand Oaks, CA, USA

14. UCB, Brusseles, Belgium

Table: Proportion of patients with total hip BMD percentage change from baseline ≥STE at 12 and 24 months.

Fracture risk reduction	STE (%)[1]	FRAME		ARCH			
		Romo Month 12 (N=3186) % (n)	Romo-DMAB Month 24 (N=2895) % (n)	Romo Month 12 (N=1773) % (n)	Romo-ALN Month 24 (N=1619) % (n)	ALN Month 12 (N=1778) % (n)	ALN-ALN Month 24 (N=1624) % (n)
All fractures							
Any	1.8	87.1 (2775)	93.6 (2711)	83.1 (1474)	85.1 (1377)	62.1 (1105)	68.6 (1114)
>30%	5.1	57.0 (1815)	77.1 (2233)	55.1 (977)	62.9 (1019)	25.0 (445)	33.7 (548)
Vertebral fractures							
Any	1.4	89.2 (2843)	94.4 (2734)	85.4 (1514)	87.5 (1417)	66.5 (1183)	72.7 (1180)
>50%	4.6	62.3 (1985)	80.9 (2342)	59.8 (1060)	66.8 (1081)	29.4 (522)	38.6 (627)
Hip fracture							
Any	3.2	75.9 (2418)	88.9 (2573)	73.0 (1294)	77.1 (1249)	45.2 (804)	54.8 (890)
>30%	5.8	49.2 (1567)	71.3 (2063)	49.7 (882)	57.9 (938)	18.8 (335)	27.4 (445)
Nonvertebral fracture							
Any	2.1	85.4 (2721)	93.0 (2692)	81.0 (1437)	83.5 (1352)	58.7 (1043)	66.5 (1080)
>20%	6.2	44.8 (1428)	67.9 (1966)	45.7 (810)	54.8 (887)	15.6 (278)	23.5 (382)

For each fracture category, STEs required for any and for maximal reductions in fracture risk (ranging from >20% to >50%) reported by Eastell et al[1] are shown. ALN: alendronate; DMAB: denosumab; PBO: placebo; Romo: romosozumab; STE: surrogate threshold effect.

Objective(s): The FNIH-ASBMR SABRE project[1] defined the bone mineral density (BMD) surrogate threshold effect (STE) required to predict a significant reduction in fracture (fx) at the study level. STEs in the FNIH-ASBMR SABRE project were calculated using difference in BMD percentage change at 24 months (M) between active and placebo (PBO).[1] In practice, a more clinically relevant measure is whether patients' (pts') BMD has improved with treatment from their own baseline (BL) values. This post hoc analysis of data from FRAME (NCT01575834) and ARCH (NCT01631214) assessed the percentage of pts achieving the established FNIH STE thresholds[1] with romosozumab (Romo) or alendronate (ALN) at 12M and 24M when compared to their own BMD values at BL.[2,3]

Materials and Methods: Postmenopausal women with osteoporosis were randomised to Romo 210mg monthly (QM) or comparator (FRAME: PBO QM; ARCH: alendronate [ALN] 70mg QW) for 12M). After 12M all pts received ALN in ARCH or denosumab (DMAB) in FRAME. Here, we report the proportion of pts that achieved total hip BMD percentage changes at 12M and 24M that meet STEs for vertebral, nonvertebral, hip and any fx risk reduction (observed case), without comparison to PBO.

Results: The table displays the percentage of patients achieving BMD changes from BL corresponding to the STEs for each fracture category.

Conclusion(s): Within 12M of treatment with Romo, most patients achieved the FNIH-SABRE STEs for any reduction in fx risk. At both 12 and 24M, higher proportions of patients met the STEs with Romo compared to ALN for all fx types.

References: 1. Eastell, R. JBMR 2021; Epub; 2. Cosman F. NEJM 2016;375:1532–431; 3. Saag K. NEJM 2017;377:1417–27.

25

Fabrication of bio-textile collagen rope for ACL regeneration

Peilin Chen[1], Ziming Chen[1], Tao Wang[1], Ming-Hao Zheng[1]

1. University of Western Australia, Nedlands, WA, Australia

Publish consent withheld

26

Comparative Effects of Surgical And Non-Surgical Therapy on Hip Contact Force For Femoroacetabular Impingement Syndrome

Azadeh Nasseri[1], Laura Diamond[1], Trevor Savage[1], Tamara Grant[1], Michelle Hall[2], Kim Bennell[2], Jilian Eyles[3], Libby Spiers[2], David Hunter[3], David Lloyd[1], David Saxby[1]

1. Griffith University, Gold Coast, QLD, Australia

2. The University of Melbourne, Melbourne, VIC, Australia

3. The University of Sydney, Sydney, NSW, Australia

Femoroacetabular impingement syndrome (FAIS) is a motion-related clinical disorder of the hip common in young active adults, whereby abnormal morphology of the femur and/or acetabulum can cause hip and groin pain, and physical dysfunction [1]. Both arthroscopy and non-operative care approaches are used to treat FAIS. However, the comparative effects of these treatments on hip joint loading have not been examined. Current study compared 12-month effects of arthroscopy versus non-operative physiotherapist-led Personalised Hip Therapy (PHT) on hip contact force (HCF) during walking.

A subset of the Australian FASHIoN trial [2], consisting of 38 individuals with FAIS, attended biomechanical testing sessions before and 12 months after they were randomised to receive either arthroscopy or PHT. Three-dimensional whole-body motion, ground reaction forces, and surface electromyography were acquired during walking. A neuromusculoskeletal modelling framework was used to estimate external biomechanics, lower limb muscle forces, and HCF. Two-way repeated measures analysis of variance applied through Statistical Parametric Mapping to compare the 12-month main effects of, and interactions between, treatment and time on HCF during the gait cycle.

There were no significant differences in HCF between the two treatment groups at follow-up. Both treatments resulted in statistically significant increase in HCF magnitude from baseline to follow-up, across most of the gait cycle. No interaction effects were found.

No differences between treatment groups at follow-up means both treatments similarly increased the HCF. Following arthroscopy and PHT, the average increase in HCF was ~0.87 and 0.91 BW, respectively. Due to lack of untreated control group, it is unclear whether the increased HCF seen in both groups was an effect of treatment or due to natural progression. However, HCF at follow-up were of comparable magnitudes to those previously reported in healthy controls [3] and we speculate the observed increase in HCF could be an effect of treatment.

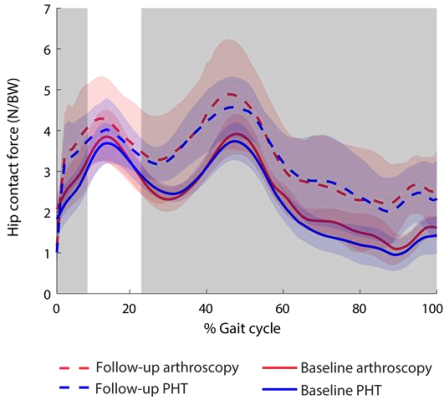

Figure 1: Ensemble average (±1 standard deviation) hip contact force over the gait cycle at baseline (solid) and 12-months follow-up (broken) for arthroscopy (red) and Personalised Hip Therapy, PHT (blue). Grey shading represents significant main effect of time (baseline versus follow-up).

1. Griffin et al, Br J Sports Med, 50(19):1169-1176, 2016.
2. Hunter et al, BMC Musculoskelet Disord, 22(1):697, 2021.
3. Savage et al, Med Sci Sport Exe, in press, 2022.

Intervertebral disc-on-a-chip: a precision-engineered platform for low back pain studies

Saie Sunil Bangar[1], David Wen[1], Louise Cole[2], Amy Bottomley[2], Joanne Tipper[1], Javad Tavakoli[1]

1. Centre for Health Technologies, School of Biomedical Engineering, Faculty of Engineering and Information Technology, , University of Technology Sydney, Sydney, NSW, Australia

2. Microbial Imaging Facility, Australian Institute for Microbiology and Infection, Faculty of Science, University of Technology Sydney, Sydney, NSW, Australia

Intervertebral disc (IVD) degeneration is associated with chronic low back pain, a leading cause of disability worldwide. Current back pain treatment options are unable to fully address symptoms and have limited long-term efficacy. In addition, IVD regeneration strategies have shown promise in preclinical studies; however, despite such potential, no such therapies have been broadly adopted clinically. Understanding the mechanisms of IVD degeneration to stop or reverse this process is a challenge at the intersection of biomaterials, biomechanics, and cell biology which would benefit from having a reproducible and adaptable 3D model able to recapitulate the relevant complexity of the IVD. The IVD models available at present are standard in vitro cultures in 2D and 3D, ex vivo systems employing human or animal IVDs and bioreactors (Fig 1). Unfortunately, none of the current models can truly represent the IVD structure and function or resemble the microenvironment of the degenerated IVD.

We have pioneered and developed a unique technique (simultaneous sonication and alkali digestion) to selectively eliminate extracellular matrix and cells to reveal the collagen and elastic fibers of the IVD (Fig 1), which has identified its novel structural features not reported previously [1-8]. These new insights have significantly enhanced knowledge about the IVD structure-function relationship over multiple scales. Building on these, we successfully employed additive manufacturing techniques to develop the first reproducible and adaptable 3D IVD-on-a-chip organ model that recapitulates the relevant IVD function and its structural complexity (Fig 1). Our organ model allows real-time monitoring in a controlled microenvironment, precise tuning of material, mechanical and biological properties, and IVD research that targets precise questions. We have so far successfully employed our organ model to evaluate cell viability and to understand the impact of IVD microstructure on cell behavior.

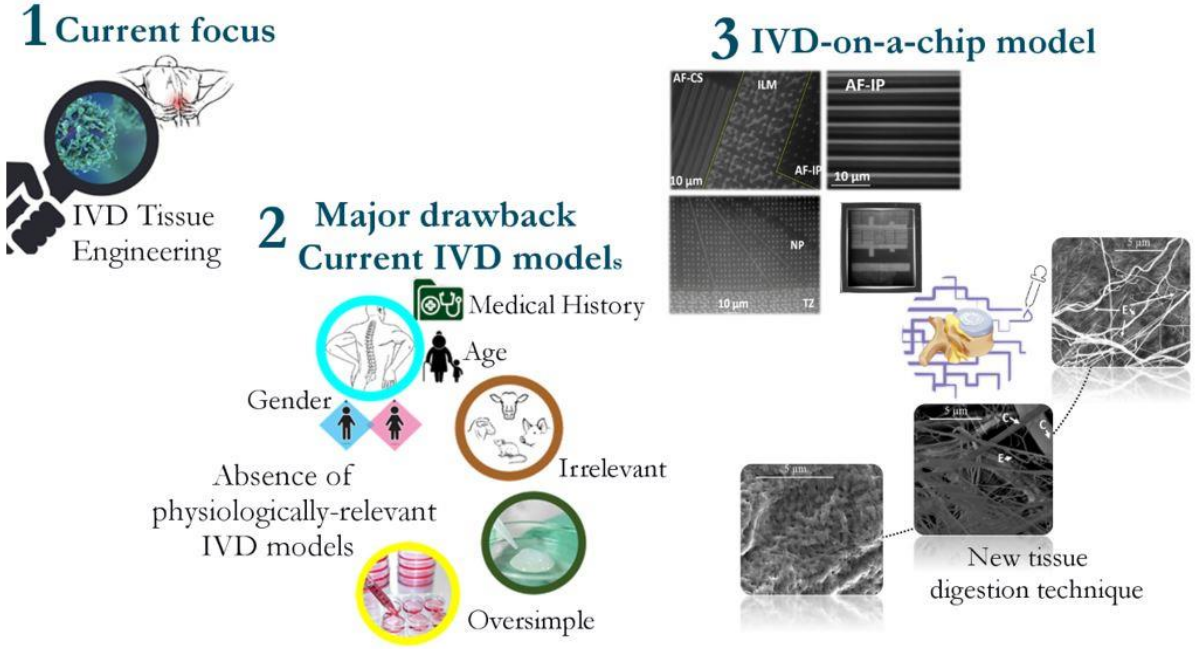

Figure 1- Reasons for development of IVD-on-a-chip model: 1. IVD tissue engineering is the current research focus. 2. The absence of physiologically and clinically relevant efficacy IVD models is one of the major reasons for the unsuccessful outcomes to date. 3 These previous reasons have provided the motivation to develop the first IVD-on-a-chip organ model for low back pain studies.

1. [1]Tavakoli, J. et al., Acta Biomater 148, 2022; [2]Tavakoli, J. et al., Acta Biomater 123, 2021; [3]Tavakoli, J. et al., Acta Biomater 114, 2020; [4]Tavakoli, J. et al., Acta Biomater 113, 2020; [5]Tavakoli, J. et al., Acta Biomater 77, 2018; [6]Tavakoli, J. et al., Acta Biomater 71, 2018; [7] Tavakoli, J. et al., Acta Biomater 68, 2018; [8] Tavakoli, J. et al., Acta Biomater 58, 2017

28

On stem cell therapy for osteoarthritis: An *in vitro* investigation to explain clinical outcomes

Jiao Jiao Li[1, 2], Christopher B. Little[2]

1. University of Technology Sydney, Ultimo, NSW, Australia

2. Kolling Institute, St Leonards, NSW, Australia

Publish consent withheld

1. Fernández-Francos S, Eiro N, Costa LA, Escudero-Cernuda S, Fernández-Sánchez ML, Vizoso FJ. Mesenchymal stem cells as a cornerstone in a galaxy of intercellular signals: Basis for a new era of medicine. Int J Mol Sci. 2021;22:3576.
2. Jiang P, Mao L, Qiao L, Lei X, Zheng Q, Li D. Efficacy and safety of mesenchymal stem cell injections for patients with osteoarthritis: a meta-analysis and review of RCTs. Arch Orthop Trauma Surg. 2021;141:1241-1251.
3. Ha C-W, Park Y-B, Kim SH, Lee H-J. Intra-articular mesenchymal stem cells in osteoarthritis of the knee: A systematic review of clinical outcomes and evidence of cartilage repair. Arthroscopy. 2019;35:277-288.e272.

29

Vertebral Body Tethering Functions as an Internal Brace for Patients with Adolescent Idiopathic Scoliosis

Megan J Roser[1, 2], Geoff N Askin[1, 2], Robert D Labrom[1, 2], Maree T Izatt[1], J Paige Little[1]

1. Biomechanics and Spine Research Group, South Brisbane, QLD, Australia

2. Orthopaedics, Queensland Children's Hospital, South Brisbane, QLD, Australia

Background

Vertebral Body Tethering (VBT) has been proposed to work via growth modulation to correct the deformity of idiopathic scoliosis by applying asymmetric forces across the growth plates of the vertebral bodies. This aim of this study is to determine the amount of growth modulation VBT has on skeletally immature patients.

Methods

A retrospective study of patients who have undergone VBT for idiopathic scoliosis. All patients were treated by one surgeon working at two centres in Brisbane, Australia. Data was prospectively collected. Pre and post-operative patient demographics, level of skeletal immaturity, Cobb angle measurements and regular post op follow up were collected.

Results

14 patients met the inclusion criteria. The mean age was 12.1 years (CI95% 10.5-13.6). The median Risser score was 0 (CI95% 0-0.6), median Sanders score was 2.5 (CI95% 1.7-3.3). The percentage of female patients was 79% and of these, all were premenarchal. The mean main thoracic Cobb angle was 52.5° (CI95% 45.1-59.9°), this corrected to 17.0° (CI95% 10.6-23.4°) on bending films. The mean rib prominence was 15.8° (CI95% 12.0-19.6°). The main thoracic curve corrected to 26.1° (CI95% 19.4-32.8°) at one week, 28.6° (CI95% 21.5-35.7°) an 2 months, 24.0° (CI95% 16.7-31.2°) at 6 months, 28.0° (CI95% 16.7-39.3°) at 12 months, 33.4° (CI95% 21.2-46.7°) at 18 months, and 34.7° (CI95% 22.0-47.3°) at 2 years follow up. At the final follow up, the mean age was 14.2 years (12.9-15.4), median Risser score was 5 (CI95% 2.8-7.2), and 85% were post-menarche.

Conclusion

Research seen in animal models and early human studies demonstrated VBT could induce significant growth modulation. The results seen in this study demonstrate that VBT functions as an internal brace to prevent curve progression and reduce deformity, to an acceptable severity that allows patients to avoid a spinal fusion when skeletally mature.

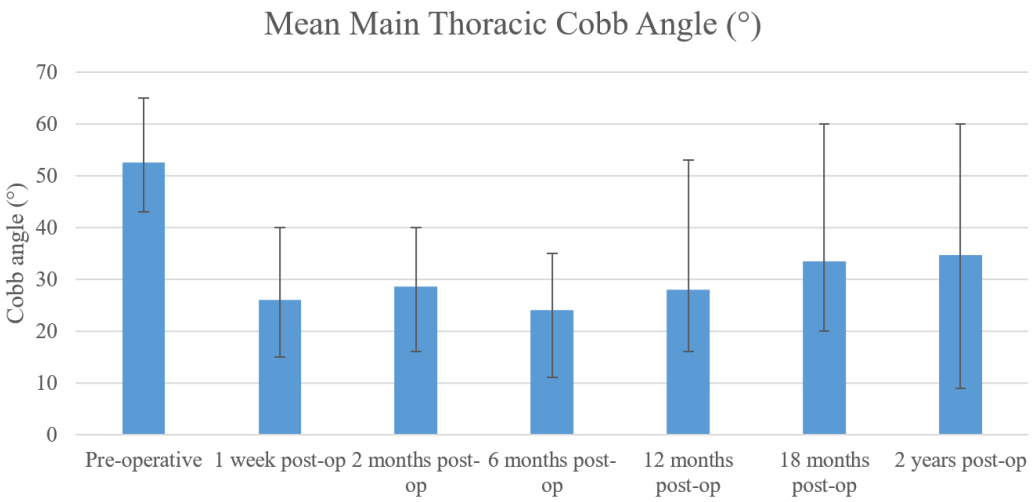

Mechanical effects of semitendinosus tendon harvesting on knee function

William S du Moulin[1], Matthew N Bourne[1], Laura E Diamond[1], Jason Konrath[2], Christopher Vertullo[3], David G Lloyd[1], David J Saxby[1]

1. Griffith University, Gold Coast, QLD, Australia

2. Principia Technology, Perth, WA, Australia

3. Knee Research Australia, Gold Coast, QLD, Australia

Objectives

Anterior cruciate ligament reconstruction (ACLR) using semitendinosus (ST) autograft results in donor muscle atrophy and uncertain tendon regeneration. The effects of harvesting these muscles on muscle moment arm and torque generating capacity have not been well described. This study aimed to determine between-limb differences (ACLR vs uninjured contralateral) in muscle moment arm and torque generating capacity across a full range of hip and knee motions.

Methods

A secondary analysis of magnetic resonance imaging was undertaken from 8 individuals with unilateral history of ST autograft ACLR with complete ST tendon regeneration. All hamstring muscles and ST tendons were manually segmented. Muscle length (cm), peak cross-sectional area (CSA) (cm^2), and volume (cm^3) were measured in ACLR and uninjured contralateral limbs. OpenSim was used to simulate and evaluate the mechanical consequences of changes in normalised moment arm (m) and torque generating capacity (N.m) between ACLR and uninjured contralateral limbs.

Results

Compared to uninjured contralateral limbs, regenerated ST tendon re-insertion varied proximal (+) (mean = 0.66cm, maximum = 3.44cm, minimum = -2.17cm, range = 5.61cm) and posterior (+) (mean = 0.38cm maximum = 0.71cm, minimum = 0.02cm, range = 0.69cm) locations relative to native anatomical position. Compared to uninjured contralateral limbs, change in ST tendon insertion point in ACLR limbs resulted in 2.5% loss in peak moment arm and a 3.4% loss in peak torque generating capacity. Accounting for changes to both max isometric force and ST moment, the ST had a 14.79% loss in peak torque generating capacity.

Conclusion

There are significant deficits in ST muscle morphology and insertion points following ST autograft ACLR. The ST atrophy and insertion point migration following ACLR may affect force transmission and distribution

Stribeck curves of cartilage-on-cartilage shearing: a comparison of healthy versus mildly degenerate tissue

Ashvin Thambyah[1]

1. University of Auckland, Auckland, AUCKLAND, New Zealand

Introduction: The Stribeck curve is a plot of the coefficient-of-friction (COF) versus the Hersey number. The latter is a function of the dynamic viscosity (Pa.s) of the fluid, multiplied by the shearing speed (Hz), and divided by the compressive stress (Pa). When the Hersey number is small, the friction mechanism is dominated by 'solid' material-to-material contact *Boundary Lubrication* and the COF is relatively large. When the Hersey number is large, fluid interface mechanics dominate and the COF is small – and this phase is known as *Hydrodynamic Lubrication*. Articular cartilage covering the bone ends in weight-bearing joints allow ultra-low friction during activities of daily living while withstanding compressive stresses in the mega Pascal range. The aim of this study was to determine the Stribeck curves for cartilage-cartilage shearing, and how pre-osteoarthritic collagen fibrillar matrix changes[1,2] affect the surface shear response.

Methods and Results: A dynamic shear test (refer to figure) was applied to eight pairs of cartilage obtained from bovine patellae of varying matrix health [1], confirmed using post-test microstructural imaging (Differential Interference Contrast Microscopy). The ratio of shear force and compressive force was used to obtain the COF. The dynamic viscosity of saline was used and the different speeds from 1Hz to 8Hz. The following Stribeck curves were obtained (below right).

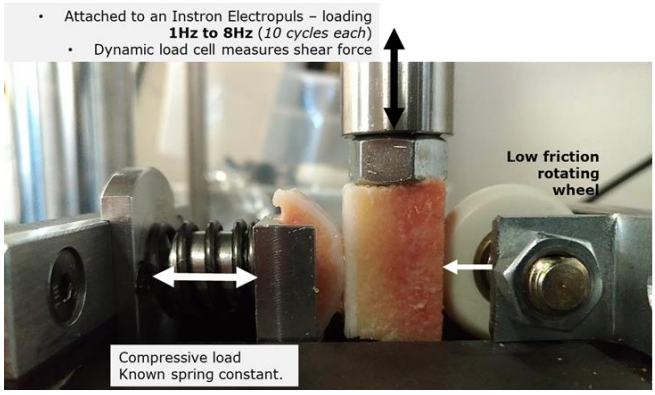

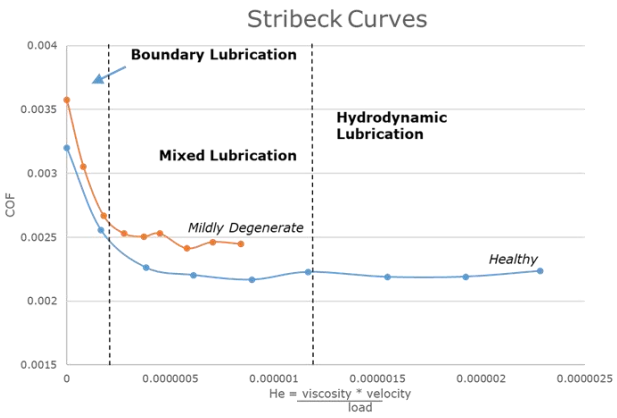

Conclusion: It appears that collagen matrix 'destructuring', occurring at the sub-micron level, results in more boundary lubrication mechanics, which may indicate a vulnerability to cartilage wear at high-velocities.

1. Hargrave-Thomas EJ, Thambyah A, McGlashan SR, Broom ND. The bovine patella as a model of early osteoarthritis. J Anat. 2013 Dec;223(6):651-642

2. Thambyah A, Zhao JY, Bevill SL, Broom ND. Macro-, micro- and ultrastructural investigation of how degeneration influences the response of cartilage to loading. J Mech Behav Biomed Mater. 2012 Jan;5(1):206-15.

A six-dimensional envelope to describe failure in an amputated femur with an osseointegrated implant under external loads

Hans A Gray[1], Dale L Robinson[1], Ryan Tiew[1], David Ackland[1], Peter Lee[1]

1. The University of Melbourne, Melbourne, VIC, Australia

Osseointegrated implants for femoral amputation are gaining popularity over conventional socket designs. However, these implants are associated with a high rate of femoral fractures [1]. To help understand these femoral fractures better, we aimed to expand the concept of a failure envelope [2] to six dimensions. The aim of this study was to use finite element analysis to quantify all external loading conditions (forces and moments) that when applied externally on the osseointegrated implant were just sufficient to fracture the femur.

A patient-specific finite element (FE) model of one right femur with an osseointegrated implant was created from CT data (details in [3]). A set of 116,444 six-dimensional (6D) unit vectors defined unique linear combinations of three moment and three force components that were applied to the distal end of the implant. The force and moment components were scaled up gradually until femoral fracture occurred. Femoral fracture was predicted when the volume of contiguous failed elements reached 350 mm^3 [4]. The points in 6D space that describe the failure loads defined the surface of the failure envelope in 6D space.

The largest direct force the implant-femur construct was able to withstand was in the superior direction (3.4 BW = 2768 N, Fig. 1C) while the largest moment was about the mediolateral direction (1.1 BWK = 138 Nm, Fig. 1A).

A six-dimensional failure envelope for the implanted femur in a transfemoral amputee was created. Published mean force and moment data measured for level walking across 10 patients [5] fell within the envelope throughout the entire activity with a minimum safety factor of 1.2. The methods described in the current study used in conjunction with experimental validation may provide useful data to understand femoral fractures and inform the design of safer osseointegrated implants.

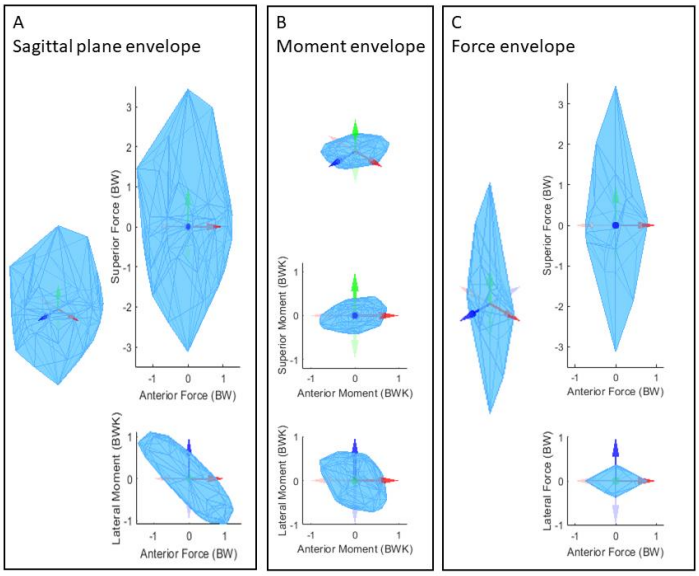

Figure 1. The six-dimensional (6D) failure envelope for the amputated femur with an osseointegrated implant. Given that it is not possible to plot a 6D object, only 3D views of the 6D envelope are shown in each box. Box A – three views of the 3D envelope for the sagittal plane (when lateral force and moments about the superior and anterior axes are zero). Box B - three views of the 3D moment envelope (when all applied forces on the implant are zero). Box A – three views of the 3D force envelope (when all applied moments at the implant are zero). The moment generated at the distal end of the implant about the medial-lateral axis by an anterior force of 1 BW (1 Body Weight, 814 N) applied at the knee was considered 1 BWK (1 Body Weight at the Knee, 125 Nm) of moment.

1. J. S. Hoellwarth et al., “Periprosthetic osseointegration fractures are infrequent and management is familiar,” Bone Jt. J., vol. 102 B, no. 2, pp. 162–169, 2020, doi: 10.1302/0301-620X.102B2.BJJ-2019-0697.R2.
2. R. Korabi, K. Shemtov-Yona, A. Dorogoy, and D. Rittel, “The Failure Envelope Concept Applied To The Bone-Dental Implant System,” Sci. Rep., vol. 7, no. 1, p. 2051, 2017, doi: 10.1038/s41598-017-02282-2.
3. D. L. Robinson et al., “Load response of an osseointegrated implant used in the treatment of unilateral transfemoral amputation: An early implant loosening case study,” Clin. Biomech., vol. 73, no. January, pp. 201–212, 2020, doi: 10.1016/j.clinbiomech.2020.01.017.
4. W. B. Edwards and K. L. Troy, “Finite element prediction of surface strain and fracture strength at the distal radius,” Med. Eng. Phys., vol. 34, no. 3, pp. 290–298, 2012, doi: 10.1016/j.medengphy.2011.07.016.
5. L. Frossard, “Loading characteristics data applied on osseointegrated implant by transfemoral bone-anchored prostheses fitted with basic components during daily activities,” Data Br., vol. 26, p. 104492, 2019, doi: https://doi.org/10.1016/j.dib.2019.104492.

33

Harnessing peptide-based therapy to control inflammatory disease

Scott N Byrne[1, 2], Anneliese S Ashhurst[1, 2, 3], Joshua WC Maxwell[3, 4], Jack Rawlings[1, 2], Skye Stockdale[1], Anica Avila[1, 2], David M McDonald[1, 3], Akane Tanaka[5], Kirstie M Bertram[1, 2], Cameron C Hanna[3], Rahael R Ireland[1, 2], Angela L Ferguson[1], Sheila Donnelly[5], Andrew N Harman[1, 2], Richard J Payne[3, 4]

1. The University of Sydney, School of Medical Sciences, Faculty of Medicine and Health, NSW, Australia.

2. The Westmead Institute for Medical Research, Centre for Immunology and Allergy Research, NSW, Australia.

3. School of Chemistry, Faculty of Science, The University of Sydney, NSW, Australia.

4. Australian Research Council Centre of Excellence for Innovations in Peptide and Protein Science, The University of Sydney, Sydney NSW 2006, Australia

5. School of Life Sciences, Faculty of Science, The University of Technology Sydney, NSW, Australia.

Inflammatory skin diseases such as psoriasis, which affects up to 4% of the Western population, can be highly debilitating. Current therapies are not consistently efficacious, can be costly and risk substantial adverse effects. New therapies that provide cost-effective and targeted suppression of inflammation are needed. We have uncovered a novel role for a human peptide in modulating and suppressing inflammation. A version of this peptide (called RP23) was produced by chemical synthesis with modifications to enhance ease of production. Culture of primary macrophages with RP23 led to reduced IL-12/23(p40) and IL-6 release after TLR-stimulation. When injected intra-dermally into human skin explants, RP23 reduced activation of dermal dendritic cells. In a mouse model of contact dermatitis, an injection of RP23 prior to sensitisation significantly suppressed elicitation of inflammation. Further, in a murine model of imiquimod-induced psoriasis, RP23 reduced erythema, skin thickness and scaling, reduced T-cells in psoriatic skin and increased the proportion of $FoxP3^+$ $CD4^+$ T-cells in local lymph nodes. Upon application in a topical formulation, RP23 penetrated the stratum corneum and colocalised with cells in the epidermis and dermis of human skin explants. Importantly, topical RP23 significantly suppressed psoriatic disease in mice when given either prophylactically or therapeutically, and synergistically enhanced therapeutic efficacy of topical steroid use. Reductions in disease were isolated to the local area in which RP23 was delivered, unlike topical glucocorticoid or injected monoclonal antibody therapy, which caused systemic immune suppression. RP23 therefore offers potential for development as a novel, locally acting peptide-based therapy for patients seeking improved management of inflammatory skin diseases.

34

Immunomodulatory human peptide RP23 alleviates atopic dermatitis-like inflammation in an oxazolone-induced murine model of disease

Jack W Rawlings[2, 1], Anneliese S Ashhurst[2, 1, 3], Joshua WC Maxwell[3, 4], Rachael A Ireland[2, 1], Richard J Payne[3, 4], Scott N Byrne[2, 1]

1. Centre for Immunology and Allergy Research, Westmead Institute of Medical Research, Westmead, NSW, Australia

2. School of Medical Sciences, Faculty of Medicine and Health, University of Sydney, Camperdown, NSW, Australia

3. School of Chemistry, The University of Sydney, Camperdown, NSW, Australia

4. Australian Research Council Centre of Excellence for Innovations in Peptide and Protein Science, The University of Sydney, Camperdown, NSW

Atopic dermatitis (AD) represents the most common chronic inflammatory skin disease in Australia, with prevalence estimated to be as high as 20% in infants and 7% of the general population. Further, one in five of those affected are considered to have moderate-to-severe disease. Topical and systemic corticosteroids are the most prescribed medications for AD but pose considerable risk of adverse effects. Additionally, while JAK inhibitors, such as baricitinib, have proven effective, their associated costs of production are considerably high. Therefore, the identification of novel and cost-effective treatment approaches would significantly aid in the long-term management of this disease. In this study, we tested the ability of a novel immunomodulatory human peptide (RP23) to treat the murine oxazolone-induced atopic dermatitis model. Mice receiving topical RP23 saw a significant reduction in back skin-fold thickness and scaling compared to untreated, vehicle and scrambled peptide controls. The reduction in scaling was comparable to that of a low-dose topical steroid, 0.01% betamethasone dipropionate (BD). However, unlike BD-treated mice, those receiving topical RP23 had no evidence of systemic immune suppression. Taken together, these results suggest that RP23 represents a potentially new treatment option for atopic dermatitis. Indeed, considering its low cost of production and low toxicity, RP23 could provide superior treatment options for long-term management of this disease.

35

Understanding $CD8^+$ T cell killing mechanisms in UV-induced tumour models

Zhen Zeng[1, 2], Margaret Veitch[1], Shoaib Anwaar[1], Ian Frazer[1], Brian Gabrielli[2], Jazmina-Libertad Gonzalez-Cruz[1], James Wells[1]

1. UQDI, Woolloongabba, QLD, Australia

2. Mater Research Institute, Woolloongabba, QLD, Australia

Publish consent withheld

37

Targeting hematoma regulation via platelet membrane coating for advanced clot-immunomodulation

Wendong Gao[1], Lan Xiao[1], Yin Xiao[1]

1. Queensland University of Technology, Brisbane, QLD, Australia

The formation of hematoma, particularly the fibrin network and fibrin network-mediated early inflammatory responses, plays a pivotal role in determining the eventual tissue repair or regeneration after an injury. Due to the critical role of the interplay between the fibrin network and immune response, it is of great significance to modulate the parameters of the fibrin network to achieve a favourable hematoma-immune response. Since platelets are involved in hematoma formation and can specifically bind to fibrinogen through its surface protein, and calcium ions play an important role in fibrin fibre growth and lateral aggregation, the platelet membrane was coated on the bioactive glass to modulate the fibrin formation process. The as-prepared platelet membrane-coated bioactive glass (PBG) is introduced as fibrinogen polymerization nuclei through specific binding and modulates the subsequent fibrin formation process through ion release. The PBG could reduce the coagulation time and increase fibre thickness and network porosity. Importantly, the PBG-modulated fibrin network shows a faster degradation rate with higher growth factor release from the fibrin network, which further supports the migration, proliferation, and differentiation of infiltrated macrophages. Besides, the PBG-modulated fibrin network the production of pro-inflammatory cytokines by macrophages through potential signaling pathways of fibrinolysis-immunomodulation and efferocytosis. In conclusion, the successful regulation of the clot-immune responses through advanced engineering of nanoparticles indicates the feasibility of developing novel clot-immune regulatory materials.

38

Understanding the burden of disease for those living with X-Linked Hypophosphatemia: a consumer perspective.

Jessica Sandy[1], Naomi Ford[2], Peter Simm[3], Christine Rodda[4], Aris Siafarikas[5], Christine Wall[1], Andrew Biggin[1], Sandy Bevc[2], Craig F Munns[6, 7]

1. Endocrinology and Diabetes, The Children's Hospital at Westmead, Westmead, NSW, Australia

2. XLH Australia , Brisbane, QLD, Australia

3. Endocrinology and Diabetes, The Royal Children's Hospital , Melbourne, VIC, Australia

4. Endocrinology and Diabetes, Sunshine Hospital, Melbourne, VIC, Australia

5. Endocrinology and Diabetes, Perth Children's Hospital, Perth, WA, Australia

6. Endocrinology and Diabetes, Queensland Children's Hospital, South Brisbane, QLD, Australia

7. The University of Queensland, South Brisbane, QLD, Australia

Aim: To describe the physical, social and psychological burden of disease in a cohort of children and adults with X-linked hypophosphatemia (XLH).

Method: In December 2021 and January 2022, XLH Australia Incorporated (in collaboration with Kyowa Kirin Australia) conducted a nationwide online survey of patients and carers of those living with X-linked hypophosphataemia (XLH).

Background: Much research has been conducted into the cause of the inherited X-linked Hypophosphatemia but little is known about the true burden of disease for consumers, particularly in Australia. This is the first Australian consumer survey targeting patients, and carers of patients, living with XLH. XLH impacts approximately 1:20,000 world-wide. The number of Australians living with XLH is uncertain.

Results: 250 consumers and carers known to XLH Australia were sent the survey, with a total of n=46 people (18%) participating (23 carers and 23 people with XLH), with 87% experiencing self-reported moderate or severe XLH. 32 of those with XLH were female and 15 were <18 years of age and 1 respondent was >75 years of age. XLH was reported to impact psychological wellbeing in 80% of those with XLH, with 54% reporting the psychological and physical impacts of XLH were equally burdensome. XLH was felt to impact daily life (Table). 70% of respondents were on medical therapy for XLH and 85% had undergone orthopaedic surgery (50% had undergone >5 surgical procedures).

Conclusion: This study showed that consumers experienced physical, social and psychological impacts from living with XLH that starts from an early age and lasts throughout adult life. These data highlight the need to ensure that there is a wholistic approach to management.

Table:

Challenge	Percent reported by those under 18 years of age	Percent reported by those 18 years of age and older
General daily activities	87	84
Bullying	80	74
Mental health	60	77
Discrimination	40	55
Social isolation	40	39
Educational / Employment	40	32
Difficulty keeping friends / relationships	33	42

39

Fall prevention – how to translate into client management of bone health

Anne-Marie Hill[1]

1. The University of Western Australia, Crawley, WA, Australia

Falls are the leading cause of hospitalised injuries (77%) each year among older Australians. Over 93% of hip fractures and 90% of wrist fractures are caused by falls, hence preventing falls is a fundamental approach to preventing fractures. Screening middle-aged and older adults for fall risk at the time of osteoporosis diagnosis, or after a first fracture, follows osteoporosis guidelines and allows a tailored fall prevention management plan to be implemented. This can be delivered alongside a progressive, resistive, strengthening exercise program for bone health. This presentation provides an overview and summary of a "how to" clinical assessment and management of fall risk in community-dwelling older adults. All health professionals should be prepared to provide evidence-based guideline advice and management of fall risk factors for their older clients. Key management and advice will include recommending exercise as an established means of preventing falls and prescribing an evidence-based multifaceted exercise program that improves balance and functional mobility. This program will include strengthening exercises that are also helpful for maintaining bone strength. Other recommendations focus on vision, medication, footwear, diet, home modifications and managing medical comorbidities, such as dizziness. Key strategies and frameworks assist in understanding how to address identified barriers and enablers to increase older adults' sustained engagement in these fall preventive strategies.

40

Understanding the burden of disease for those living with X-Linked Hypophosphatemia: a consumer perspective

Jessica Sandy[1], Naomi Ford[2], Peter Simm[3], Christine Rodda[4], Aris Siafarikas[5], Christie Wall[1], Andrew Biggin[1], Sandy Bevc[2], Craig F Munns[7, 6]

1. Endocrinology and Diabetes, The Children's Hospital at Westmead, Westmead, NSW, Australia

2. XLH Australia, Brisbane, QLD, Australia

3. Endocrinology and Diabetes, The Royal Children's Hospital, Melbourne, VIC, Australia

4. Endocrinology and Diabetes, Sunshine Hospital, Melbourne, VIC, Australia

5. Endocrinology and Diabetes, Perth Children's Hospital, Perth, WA, Australia

6. Endocrinology and Diabetes, Queensland Children's Hospital, South Brisbane, QLD, Australia

7. The University of Queensland, South Brisbane, QUEENSLAND, Australia

Aim: To describe the physical, social and psychological burden of disease in a cohort of children and adults with X-linked hypophosphatemia (XLH).

Method: In December 2021 and January 2022, XLH Australia Incorporated (in collaboration with Kyowa Kirin Australia) conducted a nationwide online survey of patients and carers of those living with X-linked hypophosphataemia (XLH).

Background: Much research has been conducted into the cause of the inherited X-linked Hypophosphatemia but little is known about the true burden of disease for consumers, particularly in Australia. This is the first Australian consumer survey targeting patients, and carers of patients, living with XLH. XLH impacts approximately 1:20,000 world-wide. The number of Australians living with XLH is uncertain.

Results: 250 consumers and carers known to XLH Australia were sent the survey, with a total of n=46 people (18%) participating (23 carers and 23 people with XLH), with 87% experiencing self-reported moderate or severe XLH. 32 of those with XLH were female and 15 were <18 years of age and 1 respondent was >75 years of age. XLH was reported to impact psychological wellbeing in 80% of those with XLH, with 54% reporting the psychological and physical impacts of XLH were equally burdensome. XLH was felt to impact daily life (Table). 70% of respondents were on medical therapy for XLH and 85% had undergone orthopaedic surgery (50% had undergone >5 surgical procedures).

Conclusion: This study showed that consumers experienced physical, social and psychological impacts from living with XLH that starts from an early age and lasts throughout adult life. These data highlight the need to ensure that there is a wholistic approach to management.

Table

Challenge	Percent reported by those under 18 years of age	Percent reported by those 18 years of age and older
General daily activities	87	84
Bullying	80	74
Mental health	60	77
Discrimination	40	55
Social isolation	40	39
Educational / Employment	40	32
Difficulty keeping friends / relationships	33	42

Mice lacking ephrinB1 in the osteogenic lineage display craniomaxillofacial abnormalities

Samuel Bereza[1], Robin Yong[1], Stan Gronthos[3, 2], Sarbin Ranjitkar[1], Peter Anderson[1, 2, 4], Agnieszka Arthur[5, 2]

1. Adelaide Dental School, The University of Adelaide, Adelaide, SA, Australia

2. South Australian Health and Medical Research Institute, Adelaide, SA, Australia

3. Mesenchymal Stem Cell Laboratory, School of Biomedicine, The University of Adelaide, Adelaide, SA, Australia

4. Australian Craniofacial Unit, Women's and Children's Hospital, Adelaide, SA

5. Musculoskeletal Cellular Communication laboratory, School of Biomedicine, The University of Adelaide, Adelaide, SA, Australia

Mutations in human ephrinB1 (*EFNB1*) manifest in craniofrontonasal dysplasia (CFND), several features include craniomaxillofacial abnormalities such as midface dysplasia, orbital hypertelorism and coronal craniosynostosis. The only current treatment for children with CFND is repeated surgical intervention. There are limited tools available to investigate ephrinB1 induced CFND. The present study aimed to determine whether loss of *EfnB1* in the murine osteogenic linage, under the regulation of the *Osterix* (*Osx*) promoter caused CFND associated craniomaxillofacial abnormalities. *Osterix* is a transcription factor essential for osteogenesis and is expressed within the cranium from embryonic day (E)12.5-13.5.

Female and male skulls from 4-week and 8-week-old mice with a *Cre* mediated deletion of *EfnB1* in osteoprogenitors, under the control of the *Osx* promoter ($EfnB1_{OB}^{-/-}$) were compared to control (*Osx:Cre*) mice (n = 6 / group). These samples underwent three-dimensional micro-computed tomography (µCT), reconstruction and morphometric analysis. Coronal and sagittal sutures were subsequently processed and stained for haematoxylin and eosin.

Morphometric analysis demonstrated that $EfnB1_{OB}^{-/-}$ skulls from female and male mice collectively were smaller at 4 weeks-of-age and bigger at 8 weeks-of-age compared to the *Osx:Cre* controls (MANOVA, $p < 0.05$). More specifically, 8-week-old $EfnB1_{OB}^{-/-}$ mice exhibited a significant increase in cranial height, interorbital (between the eyes) width and nasal width, and a reduction in maxillary (upper jaw) width when compared to the *Osx:Cre* controls ($p < 0.05$). There were no significant changes in mandibular (lower jaw) dimensions between *Osx:Cre* controls and $EfnB1_{OB}^{-/-}$ mice ($p > 0.05$). However, histological assessment of 8-week-old coronal sutures morphology identified early signs of suture fusion and changes in connective tissue in $EfnB1_{OB}^{-/-}$ mice compared to *Osx:Cre* mice.

Collectively, this data suggests that $EfnB1_{OB}^{-/-}$ mice display phenotypic craniofacial characteristics partially consistent with the human CFND phenotype. This model could be utilised to investigate the cellular and molecular mechanisms involved in cranial morphogenesis.

Lupus patients have increased fracture risk, recurrent fracture risk and 5 year mortality

Warren Raymond[1, 2], Charles Inderjeeth[1, 2], David Preen[3, 2], Helen Keen[2], Hans Nossent[1, 2]

1. North Metropolitan Health and University of Western Australia, Nedlands, WA, Australia

2. WARDER, University of Western Australia, Perth, WA, Australia

3. Population Health, University of Western Australia, Perth, WA, Australia

Background:

systemic lupus erythematosus (SLE) patients have higher fracture risk, driven by inflammation and glucocorticoids treatment. However, there is limited data on fracture recurrence and post-fracture mortality in this vulnerable population.

Objectives:

We describe the association between SLE and the risk of fracture; 5 and 10-year recurrent fracture and 5-year post-fracture mortality compared to hospital-based controls in Western Australia (WA) from 1980 - 2014.

Methods:

Population-level cohort study of patients (n=2,440, 28,002 person-years) and

population comparators (controls) (n=10,220; 161,392 person-years) identified within the

Western Australia (WA) Rheumatic Disease Epidemiological Registry (WARDER). Patients

18-80 years old (identified by ICD-9-CM: 695.4, 710.0, ICD-10-AM: L93.0, M32.0) were matched (5:1) for age, sex, Aboriginality, and temporality. Follow-up was from index SLE hospitalisation to fracture-related hospitalisation or death. Using longitudinal linked health data, we determined the relative risk of (low impact) fracture, 5 and 10-year recurrent fractures and 5-year post-fracture mortality between patients and controls with multivariate Cox proportional hazards regression models.

Results:

Patients had higher multivariate-adjusted fracture risk (aHR 2.44, 95%CI 2.08, 2.87; P<0.01) regardless of sex, Aboriginality, age group (highest in those <50 years of age) or study period. Patients had higher risk of hand, wrist and forearm fractures (aHR 1.95), vertebral fractures (aHR 5.73), hip fractures (aHR 1.83), and lower limb, ankle and foot fractures (aHR 2.14). Patients had higher risk of 5 (aHR 2.89) and 10-year (aHR 3.00) fracture recurrence. Patients had higher (aHR 1.56, 95%CI 1.16, 2.09; P<0.01) risk of 5-year post-fracture mortality. Mortality was increased in females (aHR 1.45), ≥70 years-old (aHR 1.72) and remained increased post 2000 (aHR 1.57).

Conclusion:

SLE patients have an increased risk of fractures, 5- and 10-year recurrent fractures and 5-year

mortality post-fracture compared to controls from the general population. This study highlights the need for improved primary prevention of osteoporosis in SLE patients.

Gram negative bacterial infections drive neurogenic heterotopic ossification after spinal cord or brain injury in mice and humans

Kylie A Alexander[1], Hsu-Wen Tseng[1], Marjorie Salga[2, 3], Selwin G Samuel[1], Aurélien Dinh[4], Sébastien Kerever[5], Paer-Sélim Abback[6], Catherine Paugam[6, 7], François Genêt[2, 3], Jean-Pierre Levesque[1]

1. Mater Research, The University of Queensland, Brisbane, QLD, Australia

2. Department of Physical Medicine and Rehabilitation, Raymond Poincaré Hospital, APHP, CIC 1429, Garches, France

3. University of Versailles Saint Quentin en Yvelines, END:ICAP U1179 INSERM, UFR Simone Veil-Santé, Montigny le Bretonneux, France

4. Department of Infectious Disease, Raymond Poincaré Hospital, APHP, CIC 1429, Garches, France

5. Department of Anesthesiology and Critical Care, Lariboisière University Hospital, AP-HP, Paris, France

6. Department of Intensive Care Unit, Beaujon Hospital, Clichy, France

7. University of Paris VII Denis-Diderot, Paris, France

Neurogenic heterotopic ossifications (NHO) are incapacitating complications of traumatic brain and spinal cord injuries (SCI) which manifest as abnormal heterotopic bones in periarticular muscles. NHOs are debilitating, causing pain, joint ankylosis, as well as vascular and nerve compression. The mechanisms leading to NHO are largely unknown and the only effective treatment remains surgical resection. To elucidate NHO pathophysiology we developed the first model of NHO following SCI, in genetically unmodified mice. Using this model, we have established numerous inflammatory pathways that drive NHO pathogenesis. Several retrospective studies have shown that NHO prevalence is higher in patients who suffer concomitant infections. However, it is unclear whether these infections directly contribute to NHO development or reflect the immunodepression observed in SCI patients.

Using our NHO mouse model consisting of a SCI (T11-13) and a muscle injury via an intramuscular injection of cardiotoxin (CDTX), we demonstrate that infection with gram-negative bacteria, mimicked via the intramuscular administration of lipopolysaccharide (LPS, purified from the wall of gram-negative *Escherishia coli*), resulted in an exacerbation of NHO volumes measured via micro-computed tomography. Systemic LPS administration to mimic endotoxemia also increased NHO. The effect of LPS was TLR4-dependent as LPS did not increase NHO in $TLR4^{-/-}$ mice, and TLR4 transcripts and protein were expressed by muscle fibro-adipogenic progenitors. Using mice knocked-out for MyD88 or TRIF/Ticam1 adaptors, we also established that LPS enhances NHO via the endosomal TLR4/TRIF pathway, not via the plasma membrane TLR4/MyD88 pathway. Finally, we examined the presence of infection and NHO development in patients admitted to ICU after neurological injury. Interestingly, the presence of gram-negative bacterial infections (more specifically *Pseudomonas aeruginosa*) correlated with increased NHO development. Together these data demonstrate a correlation between infection and NHO development, and further identify specific bacterial agents and pathways associated with the formation of NHO in mouse and human.

A case of hypophosphatasia treated with asfotase alfa

Liyan Wang[1], Thomas Hadwen[1]

1. Sunshine Coast University Hospital, Birtinya, QLD, Australia

Hypophosphatasia is a rare, genetic condition due to a loss of function mutation in tissue non-specific alkaline phosphatase (TNSALP). This results in low serum alkaline phosphatase (ALP) levels as well as accumulation of phosphocompounds (substrates of TNSALP), namely inorganic pyrophosphate (PPi), phosphoethanolamine (PEA), and pyridoxal-5-phosphate (PLP). PPi in particular, is a potent inhibitor of bone mineralisation. Clinical manifestations of hypophosphatasia are broad, ranging from severe perinatal death in-utero to milder forms presenting in adulthood. Asfotase alfa is a human, recombinant TNSALP enzyme replacement therapy that was approved worldwide in 2015 and is indicated for paediatric onset hypophosphatasia.

We present the case report of a 64 years old female with childhood onset hypophosphatasia with complications of skull malformation requiring craniotomy, stress fractures requiring bilateral femoral fixation and new right tibial stress fracture, commencing on asfotase alfa enzyme replacement therapy. Within three months of initiation of treatment, her pain and mobility had significantly improved. Repeated imaging showed evidence of tibial fracture healing, thus no orthopaedic intervention was required. Health related quality of life measured using the SF-36 questionnaire showed improvement in domains of physical functioning, physical role limitations, vitality, social functioning, pain, emotional wellbeing and general health perceptions. Three months post treatment pathology tests had shown a reduction in urine phosphoethanolamine from 120mmol/mol creat to 26mmol/mol creat compared to pre-treatment baseline. Corrected calcium levels mildly reduced from 2.62mmol/L to 2.51mmol/L with treatment which has been reported in the literature and thought to be related to bone remineralisation. Local injection site reaction was the only side effect and responded well to antihistamine therapy.

Improvement in symptomology, biochemical markers as well as radiological evidence of fracture healing was seen within three months of initiation of asfotase alfa treatment in our patient with childhood onset hypophosphatasia with minimal side effects.

1. Whyte MP. Hypophosphatasia: Enzyme Replacement Therapy Brings New Opportunities and New Challenges. J Bone Miner Res. 2017 Apr;32(4):667-675. doi: 10.1002/jbmr.3075. Epub 2017 Jan 31. PMID: 28084648.
2. Stürznickel J, Schmidt FN, von Vopelius E, Delsmann MM, Schmidt C, Jandl NM, Oheim R, Barvencik F. Bone healing and reactivation of remodeling under asfotase alfa therapy in adult patients with pediatric-onset hypophosphatasia. Bone. 2021 Feb;143:115794. doi: 10.1016/j.bone.2020.115794. Epub 2020 Dec 8. PMID: 33301963.
3. Whyte MP. Hypophosphatasia - aetiology, nosology, pathogenesis, diagnosis and treatment. Nat Rev Endocrinol. 2016 Apr;12(4):233-46. doi: 10.1038/nrendo.2016.14. Epub 2016 Feb 19. PMID: 26893260.
4. Whyte MP. Hypophosphatasia: An overview For 2017. Bone. 2017 Sep;102:15-25. doi: 10.1016/j.bone.2017.02.011. Epub 2017 Feb 24. PMID: 28238808.
5. Simon S, Resch H, Klaushofer K, Roschger P, Zwerina J, Kocijan R. Hypophosphatasia: From Diagnosis to Treatment. Curr Rheumatol Rep. 2018 Sep 10;20(11):69. doi: 10.1007/s11926-018-0778-5. PMID: 30203264.

45

Bioengineering humanized bone microenvironment models for cancer research applications.

Nathalie Bock[1]

1. School of Biomedical Sciences, Queensland University of Technology, Woolloongabba, QLD, Australia

Researching new therapies for bone pathologies has traditionally involved the use of 2D cell culture systems with different types of bone cells, often murine cell lines, with, at most, the addition of isolated extracellular components to recapitulate some signals present in the bone microenvironment. Mostly used for mechanistic purposes and preclinical drug screening, these 2D models are further transitioned into animal models for drug validation, prior to clinical testing. In over 90% of cases, clinical failures are however observed, partly due to inherent species differences. In cancer-related diseases, the bone tumour microenvironment is often a metastatic site, representing such a source of heterogeneity between patients, cancer subtypes and treatment histories, that the current approaches only diminish the chances of treatment efficacy. In the last three decades, advances in tissue engineering and bioengineering have been put forward to address this unmeet need and will be discussed in this talk. It is now established that three-dimensional (3D) microenvironment models better mimic structural and biochemical properties, including critical cell-to-cell and cell-to-matrix interactions. Three-dimensional cell culture using scaffolds, hydrogels, mineral addition, chemical treatments and mechanical stimulation enable human primary cells to be cultured in more chemically- and mechanically-relevant contexts than 2D models, a step closer to human bone. More recently, the use of patient-derived xenografts with 3D tissue engineered bone models have further proven to enable better physiological relevance as an *in vitro model* for drug discovery and screening. Lastly, the use of tissue-engineered human bone models as humanized xenograft models in rats and mice have been used, either ectopically or orthotopically, so far for the study of advanced breast, prostate and multiple myeloma cancers and osteosarcomas, enabling novel mechanistic insights in human disease. For primary and secondary cancers in bone alike, tissue engineering and rodent humanization represent a promising tool for studying advanced human tumour niches in bone.

46

Wearable sensors show differences in functional outcomes between robotic and conventional total knee arthroplasty

Faseeh Zaidi[1], Scott M Bolam[2], Megan Lovatt[1], Ted C Yeung[3], Michael Hanlon[2], Jacob T Munro[2], Thor F Besier[3], Andrew P Monk[2]

1. Faculty of Medical and Health Sciences, University of Auckland, Auckland, New Zealand

2. Department of Orthopaedics, Auckland City Hospital, Auckland, New Zealand

3. Auckland Bioengineering Institute, University of Auckland, Auckland, New Zealand

Introduction: Traditional patient-reported outcome measures (PROMs) have failed to highlight differences in outcome when comparing knee replacement designs and implantation techniques. Wearable sensors, such as ankle-worn inertial measurement units (IMUs), can be used to remotely measure and monitor the bi-lateral impact load of patients, augmenting traditional PROMs with objective data. The aim of this study was to compare IMU-based outcomes with PROMs in patients who had undergone robotic total knee arthroplasty (RA-TKA) and conventional TKA (TKA) in the early post-operative period.

Methods: 50 patients undergoing primary knee arthroplasty (20 RA-TKA and 30 TKA) for osteoarthritis were prospectively enrolled. Remote patient monitoring was performed pre-operatively, then weekly from post-operative weeks two to six using bilateral ankle-worn IMUs and PROMs. IMU-based outcomes included: cumulative impact load, bone stimulus, and impact load asymmetry. PROMs scores included: Oxford Knee Score (OKS), EuroQol Five-dimension with EuroQol visual analogue scale, and the Forgotten Joint Score.

Results: Differences in IMU-based outcomes and PROMs were observed in the initial six weeks after surgery between RA-TKA and TKA. The mean change scores for OKS over the early post-operative period were 7.5 and 11.4 for RA-TKA and TKA, respectively (P=0.179). However, this did not always reflect the same trend as IMU-based impact loads between RA-TKA and TKA groups. Notably, improvements in OKS were consistent with IMU outcomes in the RA-TKA group, but the conventional TKA group did not reflect the same trend in improvement as OKS, demonstrating a functional decline from post-operative week three.

Conclusion: Our wearables show that there are differences in bi-lateral impact loads between patients who undergo RA-TKA and conventional TKA, which are overlooked by using PROMs alone.

Comparing statistical shape modelling and contralateral mirroring in regenerating hemipelvis surface geometry

Praveen Krishna[1], Dale Robinson[1], Peter Lee[1], Andrew Bucknill[2]

1. University of Melbourne, Carlton, VIC, Australia

2. Department of Orthopaedic Surgery, Royal Melbourne Hospital, Parkville, VIC, Australia

Fracture plates are typically used to secure unstable pelvic ring fractures and facilitate bone healing. Due to the highly varied and often complex nature of such fractures, personalised fracture plates may offer benefits over off-the-shelf fracture plates. However, in order to design personalised fracture plates, the fracture must be virtually reduced, a time-consuming and subjective process involving manual segmentation of the fractured pelvis and repositioning of bone segments. This study compared two methods to reconstruct the hemipelvis from varying amounts of bone geometry as alternatives to manual fracture reduction: statistical shape models (SSMs) and contralateral mirroring. 33 pelvis CT scans were used to train SSMs using a leave-one-out approach. The root-mean-squared error (RMSE) of the SSM reconstruction as well as that of the mirrored hemipelvis was quantified over the entire surface of the hemipelvis and within specific regions. Deviations of pelvic landmarks from their original positions were also computed. The reconstruction of the entire hemipelvis surface based on contralateral mirroring (Figure 1a) produced an RMSE value of 1.21±0.29 mm which was not significantly different to the reconstruction from SSMs using the entire hemipelvis surface (Figure 1b, RMSE value of 1.11±0.29 mm). Landmark deviations generated from contralateral mirroring were found to be significantly lower or statistically equivalent to the deviations generated from SSMs. These results indicate that contralateral mirroring tends to be more accurate for reduction of unilateral pelvis fractures. However, in cases of bilateral pelvic fractures or for pelvic anatomies that are known to be highly asymmetric, SSMs may still be a viable method for rapidly reducing fractures.

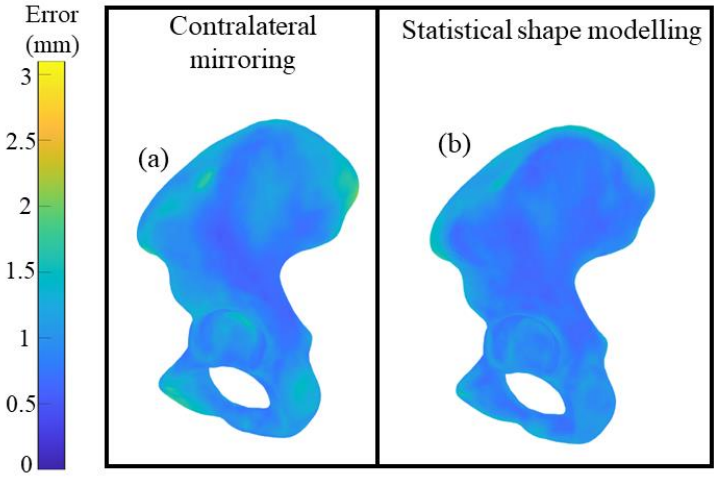

Figure 1: Contour plots showing average error (mm) at every element for the contralateral hemipelvis (a), and the SSM reconstructions based on the whole hemipelvis (b)

49

Gold Nanocluster-induced Immunomodulation for Tissue regeneration via Mitophagy Regulation: A Perspective on Materiobiology

Lan Xiao[1], Wendong Gao[1], Tianqing Liu[2], Yin Xiao[1]

1. Queensland University of Technology, Red Hill/Brisbane, QLD, Australia

2. Western Sydney University, NICM Health Research Institute, Sydney, NSW, Australia

Recent advances in biomaterials have revealed the importance of material-biology interplay, which is termed as "materiobiology" to describe the regulatory effects of biomaterial properties on biological functions at cell, tissue, organ, and the whole organism levels. A typical example of materiobiology is material-induced host immune response, the earliest biological behavior after material implantation in vivo, which plays a determinant role in material application, especially for tissue engineering/regeneration. It is therefore necessary to dissect the cellular and biochemical mechanisms under material-immune cell interaction, which will facilitate the design/development of biomaterials with the capacity to induce an ideal immune environment for tissue regeneration. In the current study, we found that dihydrolipoic acid-gold nanoclusters (AuNCs), a type of fluorescent materials for biolabelling and bioimaging, effectively regulated macrophage inflammatory response. AuNCs made up of 10 to 100 atoms have ultra-small size (< 3 nm) and therefore could efficiently accumulate in macrophages. The results showed that under inflammatory stimulation, AuNC-uptake effectively suppressed macrophage response by inducing the phenotype switch from inflammatory M1 towards tissue-regenerative M2 in a dose-dependent manner, which was achieved through activation of autophagy in inflammatory macrophage. The activated autophagy facilitated the clearance of damaged mitochondria (termed as mitophagy), an effect not only preventing intracellular accumulation of reactive oxygen species (ROS), but also shifting the energy metabolism pattern from glycolysis into oxidative phosphorylation (mitochondria-dependent). This reprogramed macrophage response was found to facilitate both osteogenic differentiation and bone regeneration in vitro and in vivo, suggesting that AuNC-application could generate a favourable immune microenvironment for tissue regeneration. Therefore, our study has discovered a novel mechanism under nanomaterial-induced immunomodulation on macrophage response, which also provides a potential approach for translational tissue regeneration in the future.

50

Translation from bench to bedside: testing a novel antimicrobial bone allograft in a standard rabbit distal femoral defect model

Katrina Browne[1, 2], Rema Oliver[2], Vedran Lovric[2], James Crowley[2], Rajesh Kuppusamy[1], Naresh Kumar[1], William R Walsh[2]

1. School of Chemistry, UNSW Sydney, Kensington, NSW, Australia

2. Prince of Wales Clinical School, Surgical and Orthopaedic Research Laboratories , Randwick, NSW, Australia

Antibiotics are critical to the success of surgical procedures, especially those using implantable biomaterials. However, antibiotic resistance is increasing rapidly, with some bacterial strains resistant to every commercial antibiotic (1). Orthopaedic infections are some of the most challenging to treat, with severe consequences for patients. There remains an unmet clinical need for the development and application of novel antibiotics. Peptidomimetics are a new class of antibiotic in preclinical development that address the drawbacks of current antibiotic therapy. They are inspired by natural antimicrobial peptides, that disrupt bacterial cell membrane integrity, resulting in rapid cell lysis (2). Due to their unique mechanism of action, these compounds have activity against antibiotic-resistant bacterial isolates, biofilm activity and a lower propensity of resistance development (3). In this study we assessed the biocompatibility of a two novel peptidomimetics, Melimine and RK758, when loaded into bone allograft. A critical-size defect was made in a rabbit distal femur defect model and filled with peptidomimetic loaded bone allograft. Bone healing was assessed across 3, 6 and 12 week timepoints. Histology of the defect site was used to assess the host tissue response and the formation of new bone in the presence of test implant materials. Bloodwork analysis and histology of the major organs were assessed for any signs of systemic toxicity. No adverse reactions were noted for any of the peptidomimetic treatment groups. Comparative micro-computed tomography analysis revealed a similar increase in bone surface area and volume between peptidomimetic groups and controls. By 12-weeks, the defects were completely closed with mature bone and bone marrow. In conclusion, peptidomimetics offer a novel solution for the prevention and treatment of antibiotic-resistant infections. This study supports the advance of these compounds in the antibiotic research and development pipeline.

1. Chen, L. (2017). Notes from the field: pan-resistant New Delhi metallo-beta-lactamase-producing Klebsiella pneumoniae—Washoe County, Nevada, 2016. MMWR. Morbidity and mortality weekly report, 66.
2. Browne, K., Chakraborty, S., Chen, R., Willcox, M. D., Black, D. S., Walsh, W. R., & Kumar, N. (2020). A new era of antibiotics: The clinical potential of antimicrobial peptides. International Journal of Molecular Sciences, 21(19), 7047.
3. Willcox, M. D. P., Hume, E. B. H., Aliwarga, Y., Kumar, N., & Cole, N. (2008). A novel cationic-peptide coating for the prevention of microbial colonization on contact lenses. Journal of applied microbiology, 105(6), 1817-1825.

Skin and bones: systemic mastocytosis and osteoporosis

Mawson Wang[1], Markus Seibel[1]

1. Department of Endocrinology & Metabolism, Concord Hospital, Concord

Clinical Case:

A 69-year-old female was referred to the dermatology clinic with asymptomatic pigmented macules and papules which began on her abdomen and gradually spread to affect her face, neck, back and proximal limbs [**Images 1a-c**]. Stroking of the lesions evoked urticaria (positive Darier sign) consistent with cutaneous mastocytosis, which was confirmed by punch biopsy. She reported increasing lethargy, diarrhoea and intermittent flushing episodes, without weight loss, night sweats, or anaphylactic episodes. Serum tryptase was elevated at 220 mcg/L (NR <11). Bone marrow biopsy demonstrated 60% infiltration of bone marrow by abnormal mast cells expressing CD117, CD2, CD25 and tryptase. CT lumbar spine demonstrated multiple sclerotic foci within L2, L4, L5 vertebral bodies, sacrum and ileum without lytic bony lesions or pathological fractures [**Image 2a-c**]. Management included the protein kinase inhibitor midostaurin, antihistamines and topical corticosteroids.

Her other medical background included hypertension, hypercholesterolemia, and a distant history of a left humerus fracture following a traumatic fall.

The patient was well-known to the osteoporosis clinic for management of significantly reduced bone mineral density. She had received a single dose of intravenous zoledronic acid 4 mg several years prior, which was followed by a pronounced acute phase reaction. A DEXA scan performed shortly after the patient had been diagnosed with systemic mastocytosis demonstrated significant interval decline with LS T-score -2.5 SD (-5.3% over 2 years), left total hip T-score -1.0 SD (-5.3%), although her true bone density may be even lower due to osteosclerosis [**Image 3**]. Subcutaneous denosumab 60mg was commenced and careful post-dosing supervision documented no hypersensitivity reaction. At current review in May 2022, the patient continues on six-monthly denosumab with calcium and Vitamin D supplementation, without minimal trauma fractures. A recent DEXA scan showed significant improvement at the LS (+18.7% since denosumab commencement) and left total hip (+10.3%). Her serum tryptase levels remain elevated between 160-200 mcg/L on midostaurin 100 mg twice daily [**Image 4**].

Laboratory and Medical Imaging Findings:

[Image 1] Cutaneous pigmented macules and papules

1a- Lower abdomen- time of diagnosis

1b- Neck region- current

1c- Upper chest- current

[Image 2a-c] CT lumbar spine with multiple sclerotic foci within lumbar vertebral bodies and pelvis, without lytic lesions or loss of vertebral height.

[Image 3] Lumbar spine and left total hip BMD in relation to antiresorptive therapy and diagnosis of SM

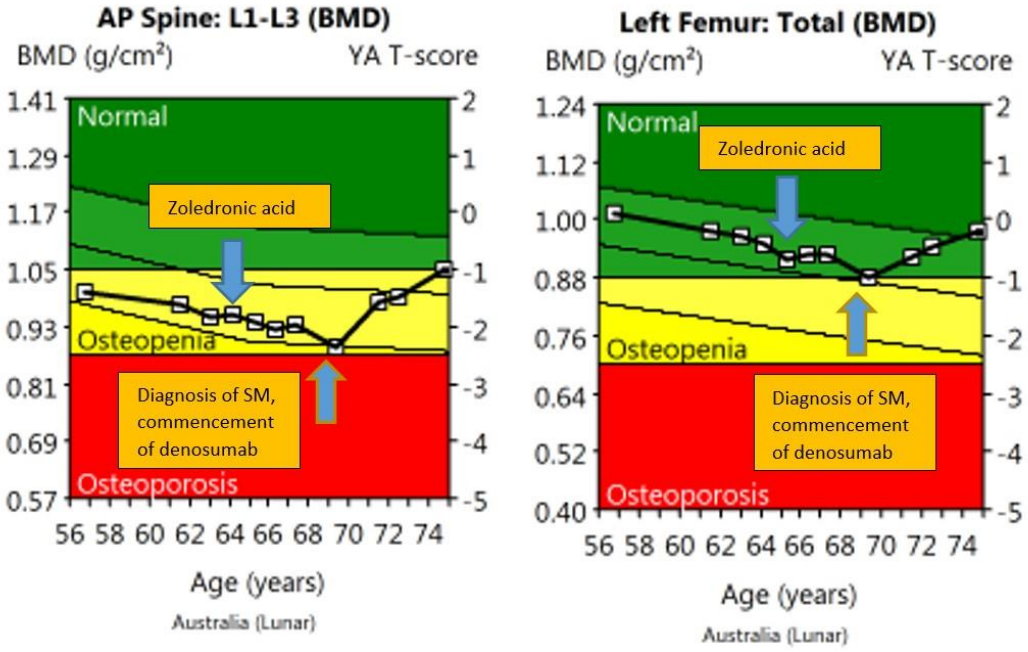

[Image 4] Serum tryptase levels

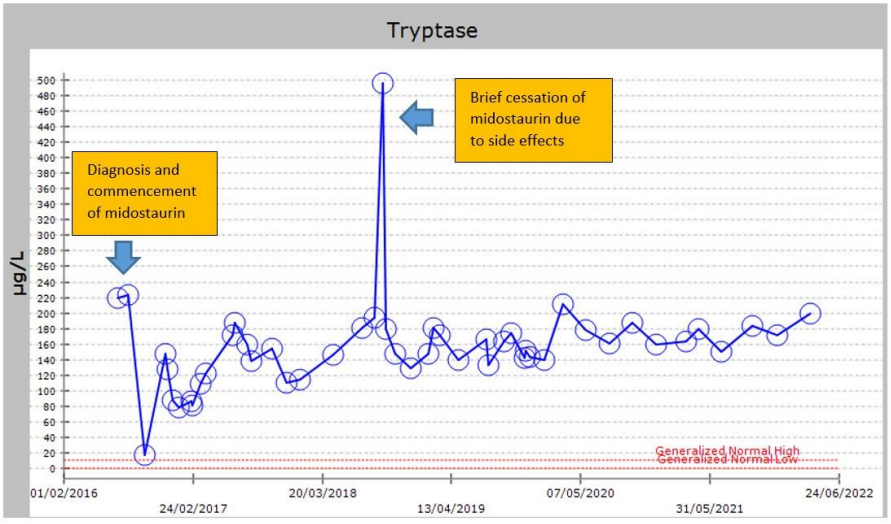

Literature Review:

Systematic mastocytosis (SM) arises from clonal proliferation of abnormal mast cells that accumulate in various tissues including the skin, bone, gastrointestinal tract, spleen and lymph nodes [1]. Activating mutations of the receptor tyrosine kinase KIT on the surface of mast cells have been implicated in the pathogenesis. Mastocytosis can present as a spectrum, ranging from cutaneous mastocytosis and indolent SM, to more aggressive forms including hematological neoplasms and mast cell leukaemia [1]. The multikinase inhibitor midostaurin inhibits KIT D816V, the driver mutation present in SM, with response rates of 60% in an open-label study [2].

Infrequently, mastocytosis may initially present as osteoporosis with fractures or sclerotic/lytic bone lesions on imaging, and bony pain due to marrow infiltration. Skeletal involvement occurs in up to 70% of SM, and prevalence of osteoporosis ranges between 18-37% [3]. Vertebral fractures were are common, affecting up to 14-20% of patients [4]. Older age, male sex and higher urinary histamine metabolites are independent predictors of osteoporotic fractures [3, 5].

The lumbar spine is the most common site of involvement [5]. Osteoporosis may result from bone marrow infiltration of mast cells, or due to the release of tryptase, histamine and heparin directly activating osteoclasts and the RANK-L pathway to promote excess bone resorption [5]. Studies examining associations between bone mineral density and urinary histamine metabolite excretion have theorised that mediators favouring osteoclast activity predominate in patients with moderate increase in mast cells, whereas mediators favouring osteoblast activity prevail in those with much higher increases in mast cell numbers [6]. This is supported by findings in advanced SM, where the majority of patients had increased bone mineral density or osteosclerosis, with higher marrow mast cell burden and tryptase levels [7]. Osteosclerosis in this setting, as in other haematological neoplasms, is associated with more aggressive phenotype and poorer prognosis [7].

Predominance of osteoclastic activity and bone resorption is the driver of SM-related osteoporosis, and thus antiresorptive agents have been utilized in its treatment. Zoledronic acid and denosumab have been studied in small case series with significant improvements in bone mineral density and suppression of bone turnover markers [8, 9]. In particular, upregulation of RANK-L signaling in SM and the effects of denosumab in inhibiting this pathway makes this a potentially promising therapeutic agent. Furthermore, the denosumab study showed decrease in serum tryptase levels in all four patients, raising the hypothesis of a negative feedback signal to mast cells from suppressed osteoclast activity, or possibly a direct effect on mast cell function [8]. The role of newer osteoanabolic agents affecting the WNT/β-catenin pathway may also be revealing, as increased levels of sclerostin have been reported in SM patients [10].

In summary, SM is an uncommon cause of secondary osteoporosis and should be suspected particularly when there are symptoms suggestive of mast cell activation. SM can be confirmed with serum tryptase and bone marrow biopsy. Our case highlighted the efficacy of denosumab in reversing the associated decline in bone mineral density.

Take Home Messages:

1. SM results from abnormal mast cell proliferation and accumulation in various organs, commonly affecting the skin and skeleton.
2. SM is a rare cause of secondary osteoporosis and should be suspected in a patient with unexplained osteoporosis, symptoms of mast cell activation and elevated serum tryptase.
3. Osteoporosis associated with SM may be related to tryptase, histamine and heparin release from mast cells activating osteoclasts and RANK-L pathway.
4. Antiresorptive therapy with RANK- L inhibitors remains the mainstay of osteoporosis treatment by counteracting mast cell-induced bone resorption.

1. Pardanani A. Systemic mastocytosis in adults: 2021 Update on diagnosis, risk stratification and management. Am J Hematol. 2021 Apr 1;96(4):508-525.
2. Gotlib J, Kluin-Nelemans HC, George TI, Akin C, Sotlar K, Hermine O, Awan FT, Hexner E, Mauro MJ, Sternberg DW, Villeneuve M, Huntsman Labed A, Stanek EJ, Hartmann K, Horny HP, Valent P, Reiter A. Efficacy and Safety of Midostaurin in Advanced Systemic Mastocytosis. N Engl J Med. 2016 Jun 30;374(26):2530-41.
3. van der Veer E, van der Goot W, de Monchy JG, Kluin-Nelemans HC, van Doormaal JJ. High prevalence of fractures and osteoporosis in patients with indolent systemic mastocytosis. Allergy. 2012 Mar;67(3):431-8.
4. Rossini M, Zanotti R, Viapiana O, Tripi G, Orsolini G, Idolazzi L, Bonadonna P, Schena D, Escribano L, Adami S, Gatti D. Bone involvement and osteoporosis in mastocytosis. Immunol Allergy Clin North Am. 2014 May;34(2):383-96.
5. Rossini M, Zanotti R, Orsolini G, Tripi G, Viapiana O, Idolazzi L, Zamò A, Bonadonna P, Kunnathully V, Adami S, Gatti D. Prevalence, pathogenesis, and treatment options for mastocytosis-related osteoporosis. Osteoporos Int. 2016 Aug;27(8):2411-21.
6. Johansson C, Roupe G, Lindstedt G, Mellström D. Bone density, bone markers and bone radiological features in mastocytosis. Age Ageing. 1996 Jan;25(1):1-7
7. Riffel P, Schwaab J, Lutz C, Naumann N, Metzgeroth G, Fabarius A, Schoenberg SO, Hofmann WK, Valent P, Reiter A, Jawhar M. An increased bone mineral density is an adverse prognostic factor in patients with systemic mastocytosis. J Cancer Res Clin Oncol. 2020 Apr;146(4):945-951.
8. Orsolini G, Gavioli I, Tripi G, Viapiana O, Gatti D, Idolazzi L, et al. Denosumab for the Treatment of Mastocytosis-Related Osteoporosis: a Case Series. Calcif Tissue Int. 2017;100(6):595–598
9. Laroche M, Livideanu C, Paul C, Cantagrel A. Interferon alpha and pamidronate in osteoporosis with fracture secondary to mastocytosis. Am J Med. 2011;124(8):776–8.
10. Hermine O, Lortholary O, Leventhal PS, Catteau A, Soppelsa F, Baude C, Cohen-Akenine A, Palmérini F, Hanssens K, Yang Y, Sobol H, Fraytag S, Ghez D, Suarez F, Barete S, Casassus P, Sans B, Arock M, Kinet JP, Dubreuil P, Moussy A. Case-control cohort study of patients' perceptions of disability in mastocytosis. PLoS One. 2008 May 28;3(5):e2266.

The RANK-L's with Polyostotic Fibrous Dysplasia Treatment in Adulthood

Emma Croker[1], Judy Luu[1]

1. Department of Endocrinology, John Hunter Hospital, New Lambton, NSW, Australia

CASE:

This case reviews the role and current evidence for treatment for polyostotic fibrous dysplasia (FD)/McCune-Albright Syndrome (MAS), with focus on denosumab in the adult patient with high skeletal burden. Our case is that of a 49-year-old mother-of-one with severe, disabling FD/MAS (**figure 1a**). In infancy she was noted to have Coast-of -Maine-shaped Café au Lait spots on her nape and trunk. At age 3 she suffered a fractured femur and went on to suffer fractures at a rate of "one-per-year" during childhood. She was treated for precocious puberty, her only MAS-associated endocrinopathy. She had hypophosphataemia, managed with calcitriol and phosphate replacement.

By her late teens she was wheelchair-bound with pan-skeletal fibrous dysplasia. Following a fractured femur at age 20, she was commenced on pamidronate and risedronate, continuing for 5 years. Alkaline phosphatase (ALP) reduced to 400-500 IU/L (reference interval 30 – 110) (**figure 2**), her pain improved, her bone mineral density increased, and she was able to mobilise without a wheelchair. Interestingly around this time she developed compressive optic neuropathy, which, despite multiple decompressive surgeries, would ultimately leave her blind. She went on to have Zoledronic acid (ZA) therapy **(figure 2)** but despite this suffered frequent fractures and required admissions to manage pain. Her ALP never reduced below 300IU/L. She developed a non-healing left pre-tibial ulcer related to underlying bone disease (**figure 1b**) and she later proceeded to a below knee amputation. She has required multiple operations including bilateral hip replacements. At age 39, after a successful pregnancy, she was treated with further ZA, but her ALP and pain did not improve.

Despite years of cumulative bisphosphonate use, she had ongoing pain, recurrent fractures and ALP remained persistently greater than 300 IU/L (**figure 2**). Therefore, 7 years ago, denosumab was commenced (60mg subcutaneously 6-monthly). There was reduction in ALP and pain improved. Prior to the second dose it was noted that she developed rebound increase in ALP, in keeping with the expected wear-off of action of denosumab (**figure 2**). Denosumab therapy has continued with dramatic suppression of bone turnover markers after each dose (**table 1**) followed by rebound rise prior to the next dose. She continues to have reasonable control of background chronic pain, has suffered only one fracture, and has not required admission for pain relief. Based on recent case reports and series, we hypothesise that increasing dose and frequency of denosumab could lead to further biochemical and clinical improvement.

LABORATORY AND IMAGING:

FIGURE 1a and Figure 1b.

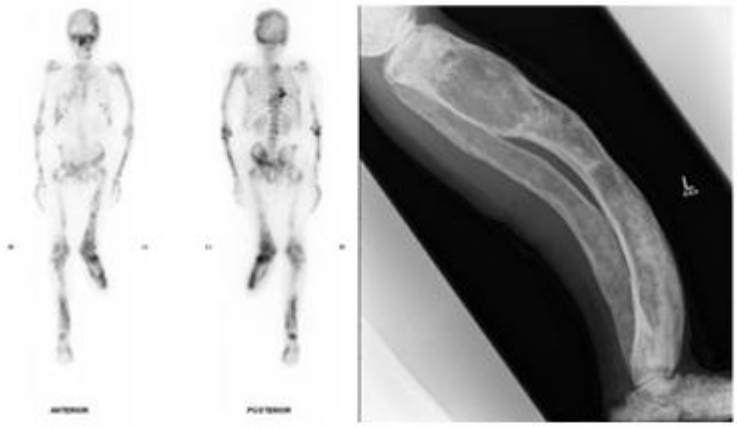

FIGURE 1a. Recent whole body nuclear medicine scan (Tc 99m hydroxydiphosphonate)

FIGURE 1b. Left lower limb prior to amputation

TABLE 1.

Analyte	Result – just prior to denosumab dose	Result – post-denosumab dose	Reference interval
Corrected calcium	2.42 mmol/L	2.28 mmol/L	2.1 -2.6
Phosphate	0.96 mmol/L	0.52 mmol/L*	0.75 – 1.50
FGF-23	151 ng/L *	86.3 ng/L	23.2 – 95.4
P1NP	868 ug/L**	181ug/L*	15 – 170
CTX	3105 ng/L**	291 ng/L	150 – 800
Vitamin D	134 nmol/L	X	50 – 140

FIGURE 2. Alkaline Phosphatase levels and therapy timeline

LITERATURE REVIEW

FD is a rare, heterogenous, debilitating disorder with no known cure. An activating post-zygotic mosaic mutation of the gene coding for the alpha subunit of the G-coupled protein receptor (*GNAS* Ch20q.13.3) results in stimulation of immature bone marrow stromal cells, producing fibro-osseus bone tissue.[1] Distorted bone architecture causes skeletal deformities, recurrent fractures, pain, nerve impingement and disability depending on location and extent of diseased bone. 90% of all skeletal burden is present by mid adolescence and fracture rate peaks in childhood although high skeletal burden and young age at first fracture are associated with high risk of recurrent fractures throughout life.[2]

FD can occur as part of MAS, a syndrome defined by the constellation of skin manifestations, hyperfunctioning endocrinopathies and FD. To date there are no approved disease modifying therapies. Recommended main stay of treatments are supportive care, treatment of phosphate deficiency and endocrinopathies, physical therapies, selective orthopaedic procedures, analgesia, and parenteral bisphosphonate therapy.[3] It is recognised that those with MAS have limited response to bisphosphonates likely due to high skeletal burden of disease. [4]

However, there is hope on the horizon with mouse-models and biomarkers improving the understanding of the pathogenesis of fibrous dysplasia. [5] Receptor-activating-nuclear- kappa-B ligand (RANK-L) has been implicated in the disease pathogenesis and therefore anti-RANK-L therapy (denosumab) is a plausible therapeutic option.[6, 7] The first case reported from a decade ago demonstrated striking reduction in tumour growth and related pain in a child with severe FD treated with denosumab, however, cessation of therapy led to severe hypercalcaemia and rebound elevation in BTM.[8] Observational data from adults with FD has demonstrated that even after non-response to bisphosphonate therapy, denosumab reduces BTM, pain and disease burden. [9-11] Frequent dosing interval (3 months versus 6 months) was supported, and higher dose (120mg) may be required for those with more severe disease.[11] Reassuringly, severe rebound hypercalcaemia has not been reported in adult cohorts. Despite the overall heterogeneity and non-standardised outcomes this is promising data, although many questions remain. The optimal time to start denosumab is unclear- presumably children would benefit prior to onset of advanced skeletal disease but safety concerns remain. Regression of bone lesions has been seen in adults and whether adults with high disease burden, such as with our patient, derive greater benefit is unclear. The optimal dose and frequency of dosing needs to be refined and monitoring of adverse events undertaken. Further trials are underway.

Other therapy modalities are under investigation. IL-6 has also been implicated in the pathogenesis of FD, but a recent randomised controlled trial of IL-6 inhibitor tocilizumab did not show reduction in pain or BTM compared to placebo.[12]

KEY POINTS*:*

- Polyostotic Fibrous Dysplasia/MAS is a rare, debilitating condition with no known cure
- This case highlights the difficulties in treating FD/MAS
- RANK-L has been demonstrated to have a role in pathogenesis and the use of anti-RANK-L therapy denosumab has shown promise in case series
- The exact benefit, timing of use, dose, frequency, safety profile and issues around cessation need to be further delineated
- Other treatments such as IL-6 inhibitors have not shown improved outcomes in recent trials.

An unusual cause of hypercalcemia in two siblings

Lucy Collins[1], Emma Boehm[1, 2], Catherine Luxford[3], Roderick Clifton-Bligh[3, 4], Vivian Grill[1, 2]

1. Department of Endocrinology and Diabetes, Western Health, Melbourne, IC

2. University of Melbourne, Melbourne, VIC

3. Kolling Institute, Royal North Shore Hospital, Sydney, NSW

4. Department of Endocrinology, Royal North Shore Hospital, Sydney, NSW

A 53 year old man was investigated for symptomatic hypercalcemia. His medical history included hypertrophic cardiomyopathy with previous septal myomectomy, paroxysmal atrial fibrillation, ischaemic heart disease and obstructive sleep apnoea. He denied previous nephrolithiasis and minimal trauma fractures. Corrected calcium was 3.08 mmol/L (2.15-2.65), Parathyroid hormone (PTH) 2.5 pmol/L (1.5-7.6), Phosphate 1.0 mmol/L (0.8-1.4), Creatinine 102 umol/L (45-90), 25-hydroxyvitamin D (25(OH)D) 52 nmol/L (> 50) and 1,25-dihydroxyvitamin D (1,25(OH)2D) 330 pmol/L (78-190). Urine Calcium excretion was 15.9 mmol/24h (2.0-7.5). Serum Angiotensin-Converting Enzyme (ACE) was normal, serum and urine monoclonal proteins were absent. Chest, renal imaging and whole-body bone scan were unremarkable. A parathyroid 99Tc-MIBI uptake study led to a focused left upper parathyroidectomy (180mg adenoma).

Hypercalcemia, hypercalciuria with low normal PTH levels persisted post-operatively. An 18FDG-PET/CT study was negative. A repeat parathyroid 99Tc-MIBI uptake study led to a right inferior parathyroidectomy (170mg adenoma). After the second parathyroidectomy, hypercalcemia (2.86 mmol/L), hypercalciuria (8.3 mmol/24hour) persisted but PTH became undetectable (< 0.3 pmol/L) and 1,25(OH)2D was 130 pmol/L.

A new presentation with PTH-independent hypercalcemia in a sibling (Case 2) signalled the underlying cause.

Case 2

A 62 year old woman presented with PTH-independent hypercalcemia during hospitalisation for a subarachnoid hemorrhage. Her medical history included diet-controlled T2DM, fibromyalgia, anxiety and depression. She had a distant history of nephrolithiasis and a family history of hypercalcemia in her brother (Case 1). Corrected calcium was 2.96 mmol/L (2.15-2.65), PTH 0.5 pmol/L (1.5-7.6), Phosphate 1.02 mmol/L (0.75-1.5), Creatinine 61 umol/L (40-90), 25(OH)D 76 nmol/L (> 50) and 1,25(OH)2D 179 pmol/L (50-190). Urinary calcium excretion was 10.3 mmol/24h (2.0-7.5). Serum ACE, PTH-related Protein (PTHrP), serum and urine monoclonal proteins were absent. Chest, renal imaging and whole-body bone scan were unremarkable. Bone Mineral Density (BMD) measurement showed the following: total lumbar spine (L1-L4) T score -3.6, femoral neck T score -1.8 and distal radius T score -4.1 (Hologic Horizon).

In the absence of available assays for 24,25-dihydroxyvitamin D (24,25(OH)2) levels, Sanger sequencing found her to be homozygous for the pathogenic variant c.1186C>T, p.Arg396Trp (R396W) of *CYP24A1*(NM_000782.4).

Cascade testing identified the same mutation in her brother (Case 1).

Discussion

Hypervitaminosis D as a cause of hypercalcemia may be due to vitamin D intoxication, granulomatous diseases or abnormalities of vitamin D metabolism. *CYP24A1* gene encodes the 24-hydroxylase enzyme responsible for the catabolism of 25(OH)D and 1,25(OH)2D (1). Loss-of-function mutations in *CYP24A1* can result in elevated concentrations of 1,25(OH)2D causing hypercalcemia, hypercalciuria, low/undetectable PTH, nephrolithiasis and nephrocalcinosis in children and adults. *CYP24A1* loss-of-function mutations were first reported as an underlying cause of idiopathic infantile hypercalcemia in ten paediatric patients presenting with failure to thrive, vomiting, dehydration and nephrolithiasis/nephrocalcinosis (2). Whilst the majority of documented cases in the literature are consistent with an autosomal recessive inheritance, an autosomal dominant inheritance pattern with incomplete penetrance has been postulated (3).

In clinical practice *CYP24A1* loss-of-function mutations should be considered in patients presenting with PTH-independent hypercalcemia, hypercalciuria and 1,25(OH)2D levels in the upper normal or elevated range. Whilst in our case assays of 24,25(OH)2D were not available, calculation of the 25(OH)D:24,25(OH)2D ratio can assist in the diagnostic process. In unaffected individuals, the levels of 25(OH)D and 24,25(OH)2D are proportional, and the ratio is typically less than 25 (4, 5). However, in individuals harbouring a *CYP24A1* loss-of-function mutation, 25(OH)D is elevated in comparison to 24,25(OH)2D, leading to an increased ratio, typically greater than 80 (4, 5).

Other isolated case reports have identified both hyperplastic parathyroid glands and discrete parathyroid adenomas in patients also harbouring *CYP24A1* loss-of-function mutations. It is not clear whether there is an underlying association between these two conditions, or merely a random coincidence (6, 7).

Possible treatments to manage the risk of hypercalcemia in patients with *CYP24A1* loss-of-function mutations include avoidance of vitamin D over-supplementation and excessive sun exposure, hydration and bisphosphonate therapy. Treatment with ketoconazole, fluconazole and rifampicin have also been described as potential therapeutic options, but their long-term efficacy and safety for this purpose requires further evaluation (3, 8).

Take Home Messages

- A loss-of-function mutation of *CYP24A1* should be considered in cases of unexplained hypercalcemia with inappropriately normal or elevated 1,25(OH)2D.
- Concurrent Primary Hyperparathyroidism and a *CYP24A1* loss-of-function mutation is very rare and of unclear mechanistic association.
- Future possible treatment options include ketoconazole, fluconazole and rifampicin.

1. Miller WL. Genetic disorders of vitamin D biosynthesis and degradation. J Steroid Biochem Mol Biol 2017; 165(Pt A): 101–108.
2. Schlingmann KP. Mutations in CYP24A1 and idiopathic infantile hypercalcemia. N Engl J Med 2011; 365(5): 410-421.
3. Tebben PJ, Milliner DS, Horst RL et al. Hypercalcemia, hypercalciuria, and elevated calcitriol concentrations with autosomal dominant transmission due to cyp24a1mutations: Effects of ketoconazole therapy. J Clin Endocrinol Metab 2012; 97(3): 423-427.
4. Kaufmann M, Gallagher JC, Peacock M et al. Clinical utility of simultaneous quantitation of 25-hydroxyvitamin D and 24,25-dihydroxyvitamin D by LC-MS/ms involving derivatization with DMEQ-tad. J Clin Endocrinol Metab 2014; 99(7): 2567–2574.
5. Molin A, Baudoin R, Kaufmann M et al. CYP24A1Mutations in a Cohort of Hypercalcemic Patients: Evidence for a Recessive Trait. J Clin Endocrinol Metab 2015; 100(10): 1343-1352.
6. David K, Khalil R, Hannon H et al. Therapy-Resistant Hypercalcemia in a Patient with Inactivating CYP24A1 Mutation and Recurrent Nephrolithiasis: Beware of Concomitant Hyperparathyroidism. Calcif Tissue Int 2020; 107(5): 524-528.
7. Loyer C, Leroy C, Molin A et al. Hyperparathyroidism complicating CYP 24A1 mutations. Ann Endocrinol (Paris) 2016; 77(5): 615-619.
8. Hawkes C, Li D, Hakonarson H et al. CYP3A4 Induction by Rifampin: An Alternative Pathway for Vitamin D Inactivation in Patients with CYP24A1 Mutations. J Clin Endocrinol Metab 2017; 102(5): 1440-1446.

Multiple vertebral fractures in a patient with severe COVID-19 treated with lung transplantation

Louise S Goodall[1], Weiwen Chen[1], Jackie Center[1]

1. St Vincent's Hospital Sydney, Darlinghurst, NSW, Australia

We present a case of a 46-year-old male who underwent a bilateral single sequential lung transplant (BSSLTX) for severe COVID pneumonitis complicated by multiple vertebral fractures and evidence of bony demineralisation.

His background was significant for type-2 diabetes treated with insulin and Empagliflozin; previous lumbar surgery; and an unprovoked deep vein thrombosis. He was a non-smoker and did not consume alcohol. There was no previous history of fracture, nor a family history of osteoporosis. At the time of infection, he had received 2 doses of COVID vaccination.

He presented to hospital with respiratory distress and tested positive for COVID-19 on admission. Despite treatment with a dexamethasone, remdesivir and tocilizumab he was intubated for hypoxic respiratory failure and was commenced on venous-venous extracorporeal membrane oxygenation.

He received a BSSLTX on day 68 of his admission. Post-transplantation, his course was complicated by critical illness neuropathy, anuric renal failure requiring dialysis, worsening type 2 respiratory failure, left pleural effusion requiring drainage, fluid overload and right sided phrenic nerve palsy requiring re-intubation for worsening respiratory distress.

A CT of his chest/abdomen/pelvis demonstrated bony demineralisation as well as new compression fractures of the T7 endplate with 25% height loss, T8 vertebral body with 20% loss of height and reduced height of the T9 and T11 superior and inferior endplates. A subsequent CT two weeks later showed progressive height loss of multiple thoracic and lumbar vertebral bodies as well as generalised increased density of both femoral heads suspicious for the development of osteonecrosis.

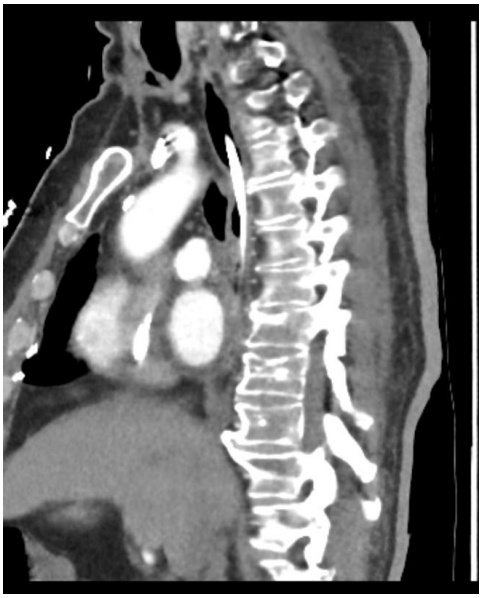

Figure 1; CT chest/abdomen/pelvis demonstrating generalised bony demineralisation, compression fracture of T7 and T8 vertebra

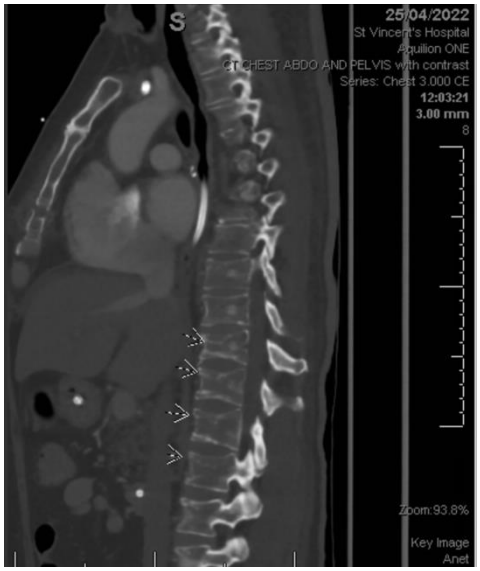

Figure 2; repeat CT demonstrating progressive height loss of multiple thoracic and lumbar vertebral bodies

His biochemistry demonstrated an eGFR of 22 ml/min/1.73m2 and creatinine of 297 umol/L. Corrected calcium was initially normal but became elevated to a peak of 3.17 mmol/L (2.10-2.60) with PTH of 1.5 pmol/L (2.0-9.0), phosphate 0.76 mmol/L (0.70-1.50) and magnesium 0.80 mmol/L (0.70-1.10). Bone turnover markers were elevated with CTX 2010 ng/L (100-600), P1NP 635 ug/L (18-80) and bone-specific ALP 45.1 ug/l (4.4-24.6). His 25-OH vitamin D was normal on replacement at 99 nmol/L. TSH was 1.67 mU/L. His myeloma screen was negative and there was no evidence of malignancy CT imaging.

A bone densitometry was unable to be performed due to immobility requiring hoist transfer. He was managed with a dose of renally-adjusted Zoledronic acid 2 mg with normalisation of his hypercalcaemia by day 3.

Unfortunately he had ongoing worsening type 2 respiratory failure and renal failure and succumbed to his illness after haemodialysis was ceased.

Discussion

Vertebral fractures (VFs) have been shown to be common in patients admitted with COVID19, and are associated with increased requirement for non-invasive ventilation and poorer respiratory outcomes including decreased pulmonary vital capacity, restrictive pulmonary dysfunction, and increased mortality.[i]

Our case had evidence of rapid and progressive bone loss resulting in multiple vertebral fractures. The bone loss was likely contributed to by immobility and bone unloading. In rodent models of immobility, changes in bone markers occur within 15-21 days.[ii] Bed rest alone in humans has been shown to result in significant early spinal bone density loss of 3.6% at 27 days. Reambulation resulted in restoration of lumbar spine mineral content by 4 months.[iii] Patients with spinal cord injuries have lower limb bone mineral density decreases of 4% per month below the level of the injury.[v]

Apart from immobility, other possible contributors to bone loss in this case may include the release of inflammatory cytokines such as IL6, TNFa, IL1 and IL2 resulting in osteoclastogenesis, high-dose corticosteroid use, acidaemia, and hypoxia.[vi]

Prolonged ventilation in itself has been hypothesised to lead to injury of the lung leading to the release of inflammatory agents including TLR4, NOD like receptor P3 and IL1, in turn accelerating bone resorption via accelerated osteoclastogenesis via RANKL.[vi]

Additionally, vertebral fractures may also exacerbate respiratory function with evidence that vertebral fractures result in reduced forced vital capacity (FVC) and vital capacity, which may suggest a complex bidirectional interaction between respiratory dysfunction and bone status.[vii]

Conclusions

We highlight a case of severe COVID infection requiring lung transplantation resulting in significant bony demineralisation and multiple vertebral compression fractures. Patients with acute critical illness demonstrate early rapid bone demineralisation with an associated increase in fracture risk. Patients with severe COVID-19 have been shown to have a high prevalence of thoracic vertebral fractures with consequences including possible influences on respiratory function. Early detection and management of fractures may prevent subsequent fractures and improve respiratory status in patients with COVID and other respiratory distress syndromes.

[i] di Filippo L, Formenti AM, Doga M, Pedone E, Rovere-Querini P, Giustina A. Radiological Thoracic Vertebral Fractures are Highly Prevalent in COVID-19 and Predict Disease Outcomes. J Clin Endocrinol Metab. 2021 Jan 23;106(2):e602-e614. doi: 10.1210/clinem/dgaa738. PMID: 33159451; PMCID: PMC7797741.

[ii] Zhang B, Cory E, Bhattacharya R, Sah R, Hargens AR. Fifteen days of microgravity causes growth in calvaria of mice. Bone. 2013 Oct;56(2):290-5. doi: 10.1016/j.bone.2013.06.009. Epub 2013 Jun 20. PMID: 23791778; PMCID: PMC4110898.

[iii] Krølner B, Toft B. Vertebral bone loss: an unheeded side effect of therapeutic bed rest. Clin Sci (Lond). 1983 May;64(5):537-40. doi: 10.1042/cs0640537. PMID: 6831837

[iv] Martin CT, Niewoehner CB, Burmeister LA. Significant Loss of Areal Bone Mineral Density Following Prolonged Bed Rest During Treatment With Teriparatide. J Endocr Soc. 2017 Apr 24;1(6):609-614. doi: 10.1210/js.2017-00049. PMID: 29264514; PMCID: PMC5686584.

[v] Martin CT, Niewoehner CB, Burmeister LA. Significant Loss of Areal Bone Mineral Density Following Prolonged Bed Rest During Treatment With Teriparatide. J Endocr Soc. 2017 Apr 24;1(6):609-614. doi: 10.1210/js.2017-00049. PMID: 29264514; PMCID: PMC5686584

[vi] Watanabe R, Shiraki M, Saito M, Okazaki R, Inoue D. Restrictive pulmonary dysfunction is associated with vertebral fractures and bone loss in elderly postmenopausal women. Osteoporos Int. 2018 Mar;29(3):625-633. doi: 10.1007/s00198-017-4337-0. Epub 2017 Dec 7. PMID: 29218382.

[vii] Gugala Z, Cacciani N, Klein GL, Larsson L. Acute and severe trabecular bone loss in a rat model of critical illness myopathy. J Orthop Res. 2021 Aug 11. doi: 10.1002/jor.25161. Epub ahead of print. PMID: 34379332.

55

Diagnostic dilemma: progressive femoral lesion in a young woman

Christopher Preston[1]

1. St Vincent's Hospital, Melbourne, VIC, Australia

Title

Diagnostic dilemma: progressive femoral lesion in a young woman

Clinical case detail

A 21-year-old Lithuanian-born woman presented with a 3-year history of progressive, severe right thigh pain. The pain was worse at the end of the day and exacerbated by prolonged standing or walking, despite regular paracetamol and ibuprofen, as well as PRN oxycodone. She did not have any associated rash, arthralgia, unintentional weight loss, or systemic features of infection. Her medical history is otherwise significant for a microprolactinoma diagnosed three years earlier on weekly Cabergoline, a benign tectal plate glioma, mild vitamin D deficiency and pityriasis versicolour. She was a smoker and worked as a beauty therapist. She did not have any previous fractures or any family history of bone disorders.

Laboratory and medical imaging findings

Plain film radiography demonstrated extensive cortical bone thickening of the right femoral shaft with no malignant ossification or cortical erosion. Magnetic resonance imaging showed abnormal bone marrow signal distal to this region. Bone scan revealed significantly increased uptake in the distal femur, consistent with abnormal osteoblastic activity.

Initial biochemistry revealed normal serum alkaline phosphatase, albumin-adjusted calcium and phosphate; low 1,25-dihydroxyvitamin D of 46 nmol/L; and elevated procollagen type 1 amino-terminal propeptide (P1NP) of 116 ug/L (normal range 15-90 ug/L) with normal C-telopeptide (CTX) of 341 ng/L (normal range 150-800 ng/L). Parathyroid hormone, serum protein electrophoresis, insulin-like growth factor-1 and anti-nuclear antibody testing were all within normal limits, as were c-reactive protein, erythrocyte sedimentation rate and tryptase levels. DEXA scan revealed bone mineral density of 1.090 g/cm2 with Z-score of +0.6 at the femoral neck, and 1.207 g/cm2 with Z-score of 0 at the lumbar spine.

CT-guided bone biopsy of the femoral lesion demonstrated only focal lymphocytic infiltrate with no evidence of malignancy, granulomas or plasma cells. Gram stain revealed no polymorphs or organisms and there was no growth on tissue culture. Repeat CT-guided biopsy showed benign trabecular osseous tissue with some architectural disorder and focal areas of degeneration with again no growth on culture.

Given ongoing pain and investigations suggestive of an osteoblastic lesion, a dose of 5mg intravenous zoledronic acid was administered. Despite reduction of bone turnover markers (P1NP 32 ug/L, CTX 185 ng/L), pain relief was only transient, with significant nocturnal pain returning after three months.

Repeat imaging twelve months post zoledronic acid revealed progression in size of the lesion with persistent periostitis and marrow oedema, and localised change in morphology, as well as a new site of increased activity on bone scan suspicious for sternoclavicular joint involvement. Repeat open biopsy of the femoral lesion demonstrated areas of osteosclerotic bone and patchy osteonecrosis.

A provisional diagnosis of a SAPHO-CRMO spectrum syndrome is considered.

Brief outline of the literature

SAPHO syndrome, named for its typical features of synovitis, acne, pustulosis, hyperostosis and osteitis, is a rare condition characterised by chronic, sterile inflammation of the bones, often with associated autoimmune and inflammatory conditions of the skin and joints, although this is not always present1. Chronic recurrent multifocal osteomyelitis (CRMO) is a similar condition with many shared features, although age of onset is typically in childhood as opposed to adulthood in SAPHO, and indeed both conditions may exist on the same spectrum of disease, although the exact relationship between the two is not fully understood2.

Clinical presentation of either condition typically involves unifocal or multifocal bone pain of insidious onset, most commonly affecting the metaphysis of the long bones of the legs, although any bone may be affected, and sternoclavicular joint involvement is also particularly common in SAPHO syndrome, as was suggested on bone scan in our patient1-2.

Disease course is variable, ranging from mild, intermittent episodes or flares of pain, to persistent and progressive inflammation, which may potentially lead to significant morbidity, including bone deformities, fractures, arthritis, and nerve entrapment syndromes3.

Initial evaluation typically demonstrates normal inflammatory markers and negative blood cultures, with bone turnover markers reflecting disease activity4. Plain film radiography may demonstrate lytic lesions, sclerosis, hyperostosis and periostitis at sites of disease, whilst magnetic resonance imaging reveals bone marrow oedema, and bone scintigraphy typically demonstrates increased osteoblastic activity, and frequently identifies extra sites of asymptomatic disease5.

Bone biopsy is often required to exclude malignancy, and commonly demonstrates a mixture of fibrosis and inflammation, however pathological findings are indistinguishable from infectious osteomyelitis6. Diagnosis therefore remains clinical, incorporating history, laboratory and imaging findings, and histology results if available, and whilst validated diagnostic criteria are currently lacking, multiple have been proposed7-8.

Whilst the exact pathogenesis of SAPHO syndrome and CRMO remains unknown, both conditions appear largely autoinflammatory, and most likely osteoclast-mediated9. Treatment options therefore include standard dose non-steroidal anti-inflammatory drugs (NSAIDs) as first line, with up to half of patients achieving clinical remission, defined as resolution of pain with or without resolution of activity on bone scan, within one year, whilst additional treatment options also include bisphosphonates, tumour necrosis factor (TNF) inhibitors, and disease-modifying anti-rheumatic drugs (DMARDs)10.

3-5 take home messages (dot points)

- SAPHO syndrome and CRMO are rare bone disorders characterised by sterile bone inflammation and fibrosis, with or without associated inflammatory conditions of the skin and joints.

- Diagnosis of SAPHO syndrome and CRMO is often delayed, likely due to a lack of awareness of these conditions as well as the absence of validated diagnostic criteria.

- Early diagnosis and treatment of SAPHO syndrome and CRMO is important as it may prevent or ameliorate disease complications.

- Further research is required to fully elucidate SAPHO syndrome and CRMO disease pathogenesis and optimal treatment options.

1. Cianci F, Zoli A, Gremese E, Ferraccioli G. Clinical heterogeneity of SAPHO syndrome: challenging diagnose and treatment. Clin Rheumatol 2017; 36:2151.

2. Costa-Reis P, Sullivan KE. Chronic recurrent multifocal osteomyelitis. J Clin Immunol 2013; 33:1043.

3. Zhao Y, Dedeoglu F, Ferguson PJ, et al. Physicians' Perspectives on the Diagnosis and Treatment of Chronic Nonbacterial Osteomyelitis. Int J Rheumatol 2017; 2017:7694942.

4. Roderick MR, Shah R, Rogers V, et al. Chronic recurrent multifocal osteomyelitis (CRMO) – Advancing the diagnosis. Pediatr Rheumatol 2016; 14:47.

5. Probst FP, Björksten B, Gustavson KH. Radiological aspect of chronic recurrent multifocal osteomyelitis. Ann Radiol (Paris) 1978; 21:115.

6. Björksten B, Boquist L. Histopathological aspects of chronic recurrent multifocal osteomyelitis. J Bone Joint Surg Br 1980; 62:376.

7. Jansson A, Renner ED, Ramser J, et al. Classification of non-bacterial osteitis: Retrospective study of clinical, immunological and genetic aspects in 89 patients. Rheumatology (Oxford) 2007; 46(1):154-60.

8. Roderick MR, Sen ES, Ramanan AV. Chronic recurrent multifocal osteomyelitis in children and adults: current understanding and areas for development. Rheumatology (Oxford) 2018; 57:41.

9. Cox AJ, Zhao Y, Ferguson PJ. Chronic Recurrent Multifocal Osteomyelitis and Related Diseases-Update on Pathogenesis. Curr Rheumatol Rep 2017; 19:18.

10. Zhao Y, Wu EY, Oliver MS, et al. Consensus Treatment Plans for Chronic Nonbacterial Osteomyelitis Refractory to Nonsteroidal Antiinflammatory Drugs and/or With Active Spinal Lesions. Arthritis Care Res (Hoboken) 2018; 70:1228.

A RUNX1 germline mutation as a novel cause of previously unexplained severe osteoporosis in a young male

Tomasz J Block[1, 2], Cat Shore-Lorenti[3], Roger Zebaze[4], Peter Kerr[5], Anna Kalff[6], Andrew Perkins[6], Peter R Ebeling[1, 4], Frances Milat[1, 3, 4]

1. Department of Endocrinology, Monash Health, Melbourne VIC, Australia

2. Department of Diabetes, Monash University, Melbourne, VIC, Australia

3. Centre for Endocrinology and Metabolism, Hudson Institute of Medical Research, Melbourne, VIC, Australia

4. Department of Medicine, Nursing & Health Sciences, Monash University, Melbourne, VIC, Australia

5. Department of Nephrology, Monash Health, Melbourne, VIC, Australia

6. Department of Haematology, Monash Health, Melbourne, VIC, Australia

A 44-year-old male presented for review of osteoporosis in the setting of several fractures including clavicle (high-impact) at age 16 as well as minimal trauma ankle and wrist fractures in his early twenties. Following a vertebral and elbow fracture sustained from a skateboarding fall at age 38, severe osteoporosis was diagnosed on dual energy x-ray absorptiometry (DXA) with a bone mineral density (BMD) Z-score of -3.6 at the spine and -2.3 at the hip. Family history for osteoporosis was positive for in his mother who had had a minimal trauma ankle fracture in her fifties. He had no glucocorticoid exposure or chronic illness. A spine MRI in July 2017 showed T6 and T7 vertebral fractures. He had also undergone jaw surgery for idiopathic condylysis in the past. He was a non-smoker with minimal alcohol intake.

An extensive screen for secondary causes of osteoporosis was negative, apart from mild vitamin D deficiency, which was promptly treated. Investigations revealed a normal serum tryptase and full blood count. The bone formation marker, serum P1NP, was 56 µg/L (N 15-80 µg/L) (1) and serum CTX was 388 ng/L (N 100-600 ng/L); his serum 25-hydroxyvitamin D had increased to 88 nmol/L. Serum calcium, phosphate, PTH, thyroid function tests, glucose, kidney (eGFR >90 ml/min/1.73m^2) and liver function tests were all normal, and his testosterone was normal, as was the ESR. Coeliac disease autoantibodies were negative, as was serum and urine electrophoresis and urine calcium excretion. In addition, a radionuclide bone scan did not demonstrate any abnormal uptake.

Treatment comprised optimising dietary calcium and initiating regular progressive resistance training exercise and commencing weekly 35 mg risedronate. His BMD improved, with a spinal Z-score of -2.8 and -1.9 at the hip within 2 years. In 2021, he had increased lethargy and malaise with associated weight loss of 8 kg over several months, with the diagnosis of a new normochromic and normocytic anaemia with a Hb of 95 g/L (baseline 130 g/L). General examination was unremarkable, he was normotensive with a standing blood pressure of 114/75 mmHg and there were no rashes or arthropathies. Further investigations revealed microscopic haematuria with glomerular RBCs and an elevated creatinine of 117 µmol/L (baseline 78 µmol/L) and mild proteinuria with an albumin/creatinine ratio (ACR) of 4.3. ANCA, a further myeloma screen, ANA, dsDNA, RF and hepatitis serology were negative, and an abdominal ultrasound was normal.

A subsequent renal biopsy confirmed mild IgA nephropathy and he was commenced on candesartan 16 mg daily for long-term renal protection. However, given his ongoing unexplained mild normochromic normocytic anaemia, a haematology review in 2022 recommended a bone marrow biopsy which demonstrated a hypocellular marrow and, in addition, a germline RUNX1 single nucleotide variant mutation (Arg250His) was identified. As this mutation affects osteoblasts and bone formation, risedronate was ceased and the anabolic agent, teriparatide, was commenced. A recent HRpQCT at the tibia and left radius prior to teriparatide commencement demonstrated profound reductions in trabecular vBMD (Tb.vBMD), trabecular number (Tb.N) (<2nd centile for age), as well as increased intra cortical porosity (Ct.Po) (< 2nd centile for age).

A previous high throughput genetic screening study has revealed that RUNX1 is one of the most frequently mutated genes in myelodysplastic syndromes (MDS), found in approximately 10% of cases (2). The patient's haemoglobin remain has remained stable, with no evidence of neutropenia or thrombocytopenia. The patient will have close clinical follow-up with haematology, as well as ongoing renal and endocrinology review. His response to teriparatide will be monitored with repeat DXA and HRpQCT at 12 months.

Literature review

Runt-related transcription factor 1 (Runx1) and other Runx family proteins including Runx2 and Runx3 play critical roles in cellular differentiation (3) including definitive haematopoiesis during embryonic development (4) and fracture healing (5, 6). A broad range of both germline and somatic RUNX1 mutations have been associated with various myeloid and lymphoblastic malignancies (7, 8). From a bone viewpoint, Runx1 induces mesenchymal stem cells into early stages of chondrogenesis (9, 10), whilst Runx2 in involved in osteoblast differentiation and skeletal development (11) with interactions with multiple co-regulators and transcription factors involved in the osteoblastic lineage (12). The expression of Runx1 has been detected in osteoblast progenitors, pre-osteoblasts, and mature osteoblasts, and our understanding of the role of Runx1 in bone formation is evolving.

A recent study involving Runx1 conditional knockout mice has revealed that Runx1 enhances osteoblast lineage commitment thereby promoting bone formation and inhibiting adipogenesis by up-regulating the Bmp7/Alk3/Smad1/5/8/Runx2/ATF4 and WNT/β-catenin signalling pathways, which are involved in bone formation to maintain postnatal and adult bone homeostasis (13). Specifically, it was shown that Runx1 deficiency impaired both BMP and TGF-β signalling in the femur, tibia and calvarial cells of the knockout mice, in addition to a down-regulation of active β-catenin protein levels in the trabecular bone due to impaired β-catenin signalling. Interestingly, in an ovariectomised animal model to simulate estrogen depletion-induced osteoporosis, Runx1 overexpression via adeno-associated virus (AAV)-mediated gene expression through calvaria adjacent subcutaneous injection, significantly increased bone volume.

Given the role of Runx1 as a central regulator of osteogenesis, we suggest that the RUNX1 mutation identified in this patient with a normochromic normocytic anaemia and severe osteoporosis is pathogenic. In addition, Runx1 may represent a potential therapeutic pathway for novel treatment strategies for osteoporosis and a range of degenerative bone diseases.

Take Home Points

- In a young patient with multiple/unusual minimal trauma fractures, it is imperative to consider rarer causes especially when appearing in a constellation with other clinical signs and symptoms.
- In young patients with fragility fractures, especially multiple ones, impaired bone formation should also be considered.
- A multidisciplinary approach is often required from a diagnostic and management perspective.
- In the context of a condition adversely affecting bone formation, together with profound reductions in BMD, an anabolic agent would be the initial treatment of choice.
- Runx1 has been recently shown to play a key role in the regulation of osteogenesis mediated by the BMP and WNT signalling pathways.
- The Runx family of proteins represent potential therapeutic targets for novel osteoporosis therapies.

1. Vasikaran SD, Chubb SP, Ebeling PR, Jenkins N, Jones GR, Kotowicz MA, et al. Harmonised Australian Reference Intervals for Serum PINP and CTX in Adults. Clin Biochem Rev. 2014;35(4):237-42.
2. Haferlach T, Nagata Y, Grossmann V, Okuno Y, Bacher U, Nagae G, et al. Landscape of genetic lesions in 944 patients with myelodysplastic syndromes. Leukemia. 2014;28(2):241-7.
3. Komori T. Regulation of skeletal development by the Runx family of transcription factors. J Cell Biochem. 2005;95(3):445-53.
4. Okuda T, Nishimura M, Nakao M, Fujita Y. RUNX1/AML1: a central player in hematopoiesis. Int J Hematol. 2001;74(3):252-7.
5. Kimura A, Inose H, Yano F, Fujita K, Ikeda T, Sato S, et al. Runx1 and Runx2 cooperate during sternal morphogenesis. Development. 2010;137(7):1159-67.
6. Liakhovitskaia A, Lana-Elola E, Stamateris E, Rice DP, van 't Hof RJ, Medvinsky A. The essential requirement for Runx1 in the development of the sternum. Dev Biol. 2010;340(2):539-46.
7. Grossmann V, Kern W, Harbich S, Alpermann T, Jeromin S, Schnittger S, et al. Prognostic relevance of RUNX1 mutations in T-cell acute lymphoblastic leukemia. Haematologica. 2011;96(12):1874-7.
8. Sood R, Kamikubo Y, Liu P. Role of RUNX1 in hematological malignancies. Blood. 2017;129(15):2070-82.
9. Wang Y, Belflower RM, Dong YF, Schwarz EM, O'Keefe RJ, Drissi H. Runx1/AML1/Cbfa2 mediates onset of mesenchymal cell differentiation toward chondrogenesis. J Bone Miner Res. 2005;20(9):1624-36.
10. Soung do Y, Talebian L, Matheny CJ, Guzzo R, Speck ME, Lieberman JR, et al. Runx1 dose-dependently regulates endochondral ossification during skeletal development and fracture healing. J Bone Miner Res. 2012;27(7):1585-97.
11. Muruganandan S, Roman AA, Sinal CJ. Adipocyte differentiation of bone marrow-derived mesenchymal stem cells: cross talk with the osteoblastogenic program. Cell Mol Life Sci. 2009;66(2):236-53.
12. Soltanoff CS, Yang S, Chen W, Li YP. Signaling networks that control the lineage commitment and differentiation of bone cells. Crit Rev Eukaryot Gene Expr. 2009;19(1):1-46.
13. Tang CY, Wu M, Zhao D, Edwards D, McVicar A, Luo Y, et al. Runx1 is a central regulator of osteogenesis for bone homeostasis by orchestrating BMP and WNT signaling pathways. PLoS Genet. 2021;17(1):e1009233.

Ex vivo assessment of surgically repaired tibial plateau fracture displacement under axial load using large-volume micro-CT

Kieran J Bennett[2, 1], Stuart A Callary[1, 3], Gerald J Atkins[1], Saulo Martelli[4], Egon Perilli[2], Bogdan Solomon[1, 3], Dominic Thewlis[1, 3]

1. Centre for Orthopaedic and Trauma Research, The University of Adelaide, Adelaide

2. Medical Devices Research Institute, Flinders University, Tonsley

3. Department of Orthopaedics and Trauma, Royal Adelaide Hospital, Adelaide

4. Queensland University of Technology, Brisbane

Postoperative weight bearing has the potential to generate fragmental motion of surgically repaired tibial plateau fractures (TPFs), which may contribute to loss of fracture reduction. The effect of loading on the internal distribution of fragmentary displacements is currently unknown. The aim of this study was to determine the internal displacements of surgically repaired split TPFs due to a three-bodyweight load, using large-volume micro-CT imaging and image correlation.

Fractures were generated and surgically repaired for two cadaveric specimens. Load was applied to the specimens inside a large-volume micro-CT system and scanned at 0.046 mm isotropic voxel size. Pre- and post-loading images were paired, co-registered, and internal fragmentary displacements quantified. Internal fragmental displacements of the cadaveric bones were compared to in vivo displacements measured in the lateral split fragments of TPFs in a clinical cohort of patients who had similar surgical repair and were prescribed pain tolerated postoperative weight bearing.

The split fragments of cadaveric specimens displaced, on average, less than 0.3 mm, consistent with in vivo measurements (Figure 1). Specimen one rotated around the mediolateral axis, while specimen two displaced consistently caudally. Specimen two also had varying displacements along the mediolateral axis where, at the fracture site, the fragment displaced caudally and laterally, while the most lateral edge of the tibial plateau displaced caudally and medially. The methods applied in this study can be used to measure internal fragmental motion within other TPFs.

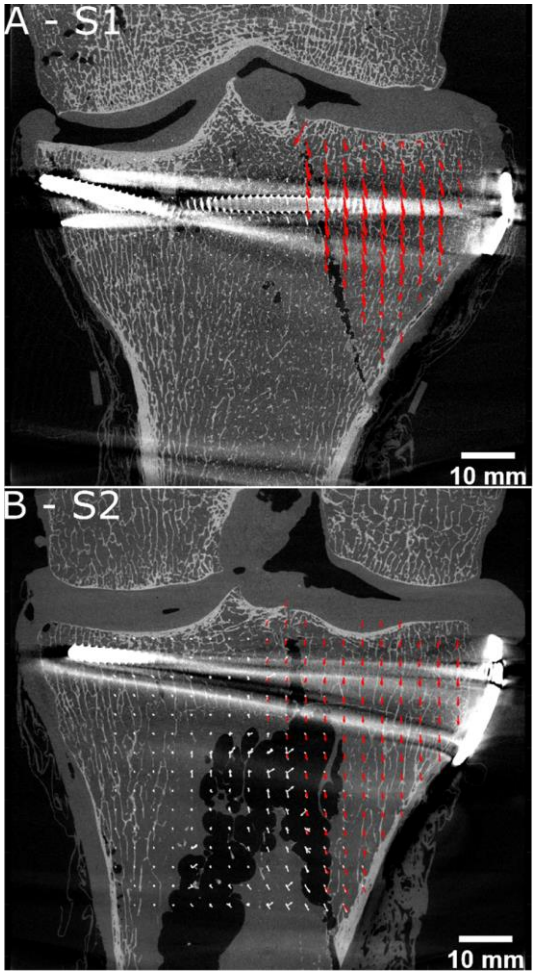

Figure 1 Fragment (red) and intact tibia (white) displacements from every slice of (A) specimen one, and (B) specimen two overlaid onto the coronal micro-CT reconstructions at Figure Legends 20 mm from the anterior edge. The vectors displayed are from all ten slices analysed, resulting in some appearing within the gaps in the bone. Displacement vectors were multiplied by a factor of five for emphasis

Development of predictive statistical shape models for paediatric lower limb bones

Beichen Shi[2, 1], Martina Barzan[2, 1], Azadeh Nasseri[2, 1], Christopher Carty[1, 3], David Lloyd[2, 1, 4], Giorgio Davico[6, 5], Jayishni Maharaj[2, 1], Laura Diamond[2, 1], David Saxby[2, 1]

1. Griffith Centre of Biomedical and Rehabilitation Engineering, Menzies Health Institute Queensland, Gold Coast, QLD, Australia

2. School of Health Sciences and Social Work, Griffith University, Gold Coast, QLD, Australia

3. Department of Orthopaedic Surgery, Children's Health Queensland Hospital and Health Service, Brisbane, QLD, Australia

4. Queensland and Advanced Design and Prototyping Technologies Institute, Griffith University, Gold Coast, QLD, Australia

5. Department of Industrial Engineering, Alma Mater Studiorum , University of Bologna, Bologna, Italy

6. Medical Technology Lab, IRCCS Istituto Ortopedico Rizzoli, Bologna, Italy

Background and Objective: Accurate representation of bone shape is important for subject-specific musculoskeletal models as it may influence modelling of joint kinematics, kinetics, and muscle dynamics. Statistical shape modelling is a method to estimate bone shape from minimal information, such as sparse anatomical landmarks, and to avoid the time and cost associated with reconstructing bone shapes from comprehensive medical imaging. Statistical shape models (SSM) of lower limb bones have been developed and validated for adult populations but have limited applicability to paediatric populations. This study aimed to develop SSM for paediatric lower limb bones and evaluate their reconstruction accuracy using sparse anatomical landmarks.

Methods: The SSM for femur, pelvis, tibia, fibula, patella, haunch (i.e., combined femur and pelvis), and shank (i.e., combined tibia and fibula) were generated from manual segmentation of comprehensive magnetic resonance images of 29 typically developing children (15 females; 13±3.5 years) to describe the shape variance of the cohort. We implemented a leave-one-out cross-validation method wherein SSM were used to reconstruct novel bones (i.e., those not included in SSM generation) using sparse-input (i.e., anatomical landmarks), and then compared these reconstructions against bones segmented from magnetic resonance imaging. Reconstruction performance was evaluated using root mean squared errors (RMSE, mm), Jaccard index (0-1), Dice similarity coefficient (DSC) (0-1), and Hausdorff distance (mm). All results reported in this abstract are mean±standard deviation.

Results: Femurs, pelves, tibias, fibulas, and patellae reconstructed via SSM using sparse-input had RMSE ranging from 1.26±0.39 mm (patella) to 3.41±0.95 mm (pelvis), Jaccard indices ranging from 0.61±0.09 (pelvis) to 0.83±0.03 (tibia), DSC ranging from 0.75±0.08 (pelvis) to 0.91±0.02 (tibia), and Hausdorff distances ranging from 3.05±0.90 mm (patella) to 12.41±3.18 mm (pelvis).

Conclusions: The SSM of paediatric lower limb bones showed reconstruction accuracy consistent with previously developed SSM and outperformed adult-based SSM when used to reconstruct paediatric bones.

Anterior lift-off of implanted press-fit tibial tray during deep knee bend: a time-elapsed micro-CT and digital volume correlation analysis.

Lauren S Wearne[1], Sophie Rapagna[1], Maged Awadalla[1], Greg Keene[2], Mark Taylor[1], Egon Perilli[1]

1. Medical Device Research Institute, College of Science and Engineering, Flinders University, Adelaide, SA, Australia

2. Orthopaedic Division, sportsmed, Adelaide, SA, Australia

Achieving primary stability of press-fit tibial implants is important for their long-term success. Deep knee bending (DKB) exposes the implant to posterior loading that may jeopardise this stability[1]. Here, time-elapsed micro-CT imaging and digital volume correlation (DVC) is undertaken on a cadaveric human tibia implanted with a titanium tibial tray, while under a mechanical loading sequence replicating DKB, with the aim of quantifying the internal strain field under progressive load.

One cadaveric proximal tibia (male: 42yr, 67kg) was implanted with a titanium tibial tray. Step-wise uniaxial loads (0.0–3.5 x body weight (BW)) were applied through two contact points replicating the medial and lateral condyle of the femur on the tray during DKB. Micro-CT scans (46µm/pixel) were performed at each load step. Loaded scans were co-registered to the 0.0BW scan and DVC analysis performed (DaVis, LaVision). The minimum principal strains (P_{min}) of subvolumes in direct contact with the tray, and then moving radially outwards, were extracted, and their 10th percentile analysed (Fig.1a). For five volumes of interest (VOIs; pegs: anterior-lateral (AL), anterior-medial (AM), posterior-lateral (PL), posterior-medial (PM) and Tray), the strain values were normalised to the final load step.

Increased compressive strains reflected the progressive compressive loads applied, while bone strain dissipated radially from the implant. Interestingly, at 1.5BW there was a reduction of P_{min} across the anterior pegs (AL, AM) (Fig.1b), which coincided with an anterior lift-off of the tray, observed from the micro-CT images.

This ongoing study presents a novel method to analyse the internal strain of an implanted proximal tibia under progressive load, which will improve the understanding of primary implant stability.

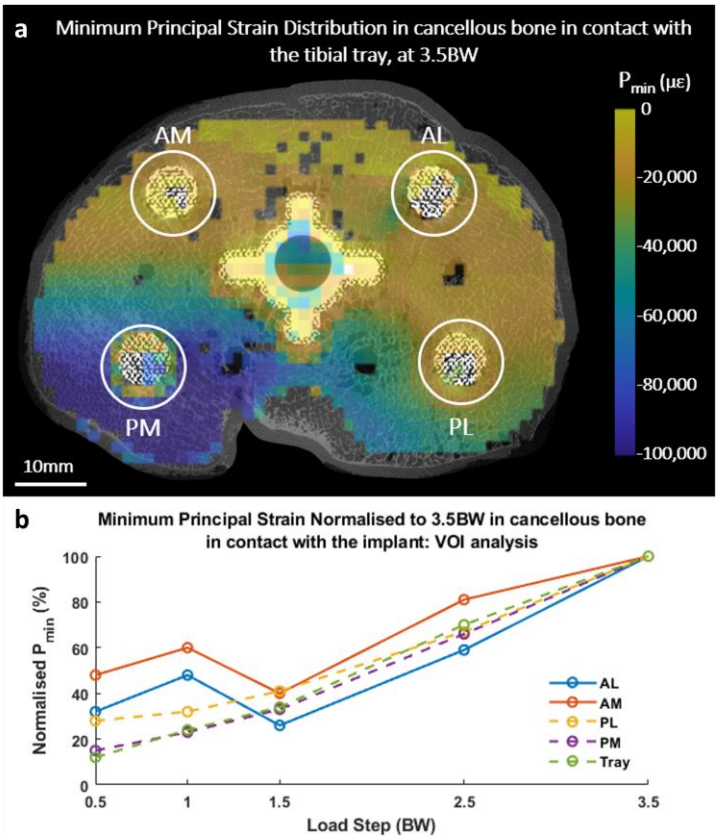

Fig.1a) Minimum principal strain P_{min} (με) distribution at 3.5BW; b) Normalised P_{min} (%, normalised to the 3.5BW load step) in each volume of interest (VOI).

1. Taylor et al., J Orthop Res, 30:1362-1368, 2012

Histological characterisation of different tendons of the human hand

Samantha A Hefferan[1, 2], Dylan M Ashton[1, 2], Carina L Blaker[1, 2], David Chang[3], Richard Lawson[3], Christopher B Little[2, 4], Elizabeth C Clarke[1, 2]

1. Murray Maxwell Biomechanics Laboratory, Kolling Institute, Institute of Bone and Joint Research, Royal North Shore Hospital, Sydney, NSW, Australia

2. Faculty of Medicine and Health, The University of Sydney , Sydney, NSW, Australia

3. Department of Hand Surgery, Royal North Shore Hospital, Northern Sydney Local Health District, Sydney, NSW, Australia

4. Raymond Purves Bone and Joint Research Laboratories, Kolling Institute, Institute of Bone and Joint Research, Royal North Shore Hospital, Sydney, NSW, Australia

Tendons play an important role in the musculoskeletal system, however, they are prone to injury, pathology or disease which can impede normal functioning. Hand tendons are no exception, and highly prevalent in soft-tissue injuries[1-2]. Currently there is little known about structural variations between different tendons and what implications such variability has on clinical outcomes. This study aims to histologically characterise and compare a range of different human hand/wrist tendons.

Formalin-fixed paraffin-embedded samples from 17 different hand/wrist tendons (Figure 1a) (6 human cadavers; fresh-frozen; 3 males, 3 females; 49-62 years; no history of musculoskeletal disease or injury) were sectioned and stained with either Haematoxylin and Eosin (HE), Toluidine Blue (TB) or Picrosirius Red (PSR). Scores assessed cellularity and cell-morphology (H&E), proteoglycan content (TB), and collagen alignment and crimp wavelength (PSR). Outcomes between functionally pooled tendon groups (Figure 1a) were analysed using a Kruskal-Wallis test with Dunn's correction for multiple comparisons.

A total of n=102 specimens were included for analysis. There were significantly more rounded cell nuclei (Figure 1b) in Deep Digital Flexors versus Wrist Flexors (p=0.0016) and Digital Extensors (p=0.0003); and Superficial Digital Flexors versus Wrist Flexors (p<0.0001) and Digital Extensors (p<0.0001). Proteoglycan staining in Wrist Flexors was significantly less than Deep Digital Flexors (p=0.0059) and Superficial Digital Flexors (p=0.0340). Collagen structure was less aligned in Deep Digital Flexors versus Wrist Flexors (p=0.0333) and Digital Extensors (p=0.0002); and Superficial Digital Flexors versus Digital Extensors (p=0.0268).

These results highlight important previously unidentified differences between human hand/wrist tendons. Future investigations will seek to identify further cellular, molecular and biomechanical variations and facilitate research on tendon structure-function relationships. With injury of the hand a serious and prevalent health condition, better characterisation of tendon similarities/differences could aid understanding of tendon injury and healing, and provide design targets for engineered tissues.

a

Tendon Name	Tendon Group
Flexor Carpi Radialis	Wrist Flexors
Palmaris Longus	
Flexor Carpi Ulnaris	
Flexor Pollicis Longus	Thumb Flexor
Flexor Digitorum Profundus (Index finger)	Deep Digital Flexors
Flexor Digitorum Profundus (Middle finger)	
Flexor Digitorum Profundus (Ring finger)	
Flexor Digitorum Profundus (Little finger)	
Flexor Digitorum Superficialis (Index finger)	Superficial Digital Flexors
Flexor Digitorum Superficialis (Middle finger)	
Flexor Digitorum Superficialis (Ring finger)	
Flexor Digitorum Superficialis (Little finger)	
Extensor Digitorum Communis (Index finger)	Digital Extensors
Extensor Digitorum Communis (Middle finger)	
Extensor Digitorum Communis (Ring finger)	
Extensor Digitorum Communis (Little finger)	
Extensor Digiti Minimi	

b

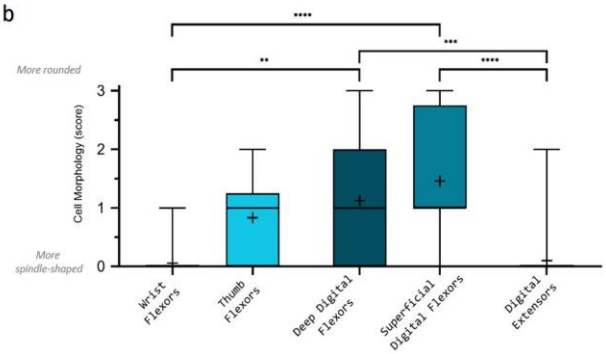

Figure 1. a) List of hand/wrist tendons (and designated functional groups) used in this study. **b)** Cell Morphology (Score) for tendon groups. Box and whisker plots with 95% confidence interval and mean indicated by the cross (+). Asterisks (*) indicate significant difference: *p<0.05, **P<0.01, ***P<0.001, ****P<0.0001.

1. Clayton R. and Court-Brown C., Injury, 2008. 39(12), 1338-1344
2. Colzani G. et al., J Hand Microsurg, 2016. 8(1), 2-12

61

Examination of the interaction of autophagy and antibiotics in *Staphylococcus aureus* persistent infection of osteocytes

Nicholas J Gunn[1], Anja Zelmer[1], Dongqing Yang[1], Lucian B Solomon[1, 2], Stephen P Kidd[3, 4], Eugene Roscioli[5, 6], Gerald J Atkins[1]

1. Centre for Orthopaedic and trauma research, University of Adelaide, Adelaide, SA, Australia

2. Department of Orthopaedics and Trauma, Royal Adelaide Hospital, Adelaide, SA, Australia

3. Research Centre for Infectious Disease, University of Adelaide, Adelaide, SA, Australia

4. Australian Centre for Antimicrobial Resistance Ecology, University of Adelaide, Adelaide, SA, Australia

5. Department of Thoracic Medicine, Royal Adelaide Hospital, Adelaide, SA Australia

6. Department of Medicine, Faculty of Health and Medical Sciences, University of Adelaide, Adelaide, SA, Australia

We and others have postulated that the intracellular persistence of *Staphylococcus aureus* (1) may underlie the high failure rate of current gold-standard treatments for Periprosthetic Joint Infection (PJI) associated with joint replacement surgery. As such, the characterisation of the interactions between *S. aureus* and osteocytes, the most abundant cell type in bone, is of primary importance for understanding not only mechanisms of treatment failure and the development of chronic infection but also new modalities through which clinical cure can be achieved. An additional axis requiring consideration is how antibiotics influence this relationship, as chronic or high dose antibiotic treatments are known to cause adverse host cell effects. Autophagy, the physiological process by which intracellular material is targeted for phagolysosomal degradation, is a first-line innate immune mechanism against intracellular pathogens. In this study, the effects of modulation of autophagy on the clearance or persistence of intracellular *S. aureus* in a human osteocyte model (2) were assessed. Additionally, we examined the influence of clinically used antibiotics on this relationship. Interestingly, whilst both promotion and blockade of autophagic flux affected intracellular bacterial culturability in both an acute and chronic infection model, neither of these treatments affected bacterial burden in terms of DNA levels. Concerningly, treatment with vancomycin or rifampicin resulted in a modest but significant blockade of autophagic flux and an increase in intracellular viable bacterial DNA quantity. In conclusion, whilst autophagic flux was demonstrated to have a significant impact on the growth phenotype of the resident bacteria, its modulation was not capable of affecting the number of viable bacteria. Additionally, whilst antibiotics were capable of blocking autophagy, the paradoxical increase in the number of viable bacteria inside host osteocytes suggests the involvement of additional host or bacterial mechanisms resulting in failure to clear these *S. aureus* intracellular infections.

1. D. Yang, A. R. Wijenayaka, L. B. Solomon, S. M. Pederson, D. M. Findlay, S. P. Kidd and G. J. Atkins: Novel Insights into Staphylococcus aureus Deep Bone Infections: the Involvement of Osteocytes. MBio, 9(2) (2018) doi:10.1128/mBio.00415-18
2. N. J. Gunn, A. R. Zelmer, S. P. Kidd, L. B. Solomon, E. Roscioli, D. Yang and G. J. Atkins: A Human Osteocyte Cell Line Model for Studying Staphylococcus aureus Persistence in Osteomyelitis. Front Cell Infect Microbiol, 11, 781022 (2021) doi:10.3389/fcimb.2021.781022

62

Bone microenvironment regulation of tumour outgrowth

Michelle M McDonald[1]

1. Garvan Institute of Medical Research, Darlinghurst, NSW, Australia

Bone is one of the most common sites for metastatic disease. Virtually incurable, bone cancers are destructive and have a high risk of disease recurrence and increased mortality. Anti-resorptive agents, such as bisphosphonates and Denosumab, are mainstay treatment for bone metastatic disease, reducing further bone loss and fracture. Remarkably, anti-resorptive agents have been shown to improve disease free survival and reduce disease recurrence, suggesting that anti-resorptives could also modify early disease stages.

Our work is focused on determining the cellular mechanisms within the bone micro-environment which may be driving this clinical finding. The bone microenvironment provides a fertile soil which supports tumour cell engraftment and survival. We pioneered a novel intravital imaging technique in bone which revealed for the first time that long lived chemo-resistant dormant tumour cells reside in a niche in bone and can be reactivated through osteoclastic bone resorption to drive disease recurrence. Further, this imaging technique allowed us to define novel osteoclast biology, a finding which is likely to have implications in control of tumour cell reactivation. Through visualising tumour cell and osteoclast interactions in real time *in vivo* we are revealing new insight into how modifying this interaction, with anti-resorptive agents, may supress tumour growth in the skeleton, and therefore limit further metastatic outgrowth. The outcomes of this work may lead to improvements in the application of bone modifying agents in the clinic to prevent the outgrowth of cancers in bone, thereby impacting significantly on cancer survivorship and quality of life.

63

Bioengineering solutions for articular cartilage regeneration

Claudia Di Bella[1, 2, 3]

1. Department of Surgery, The University of Melbourne, Melbourne, Victoria, Australia

2. BioFab3D, Aikenhead Centre for Medical Discovery, Melbourne, Victoria, Australia

3. Department of Orthopaedic Surgery, St Vincent's Hospital, Melbourne, Victoria, Australia

Three-dimensional (3D) printing of acellular, non biological material, is already widely used in surgery. In the biomedical field, this technology is in fact increasingly used to create custom-made implants, precise cutting guides, anatomic or models, and can greatly help surgeons in i) identifying specific anatomic variations in complex cases, ii) assisting in the planning of the surgery, or iii) performing precise cuts for bone removal.

In recent years, the possibility to print biological materials (Bioprinting), including cells, has gained increasing interest in surgery. Bioprinting has the potential to fabricate living tissues and organs, by delivering biologic elements (not only cells, but also growth factors, drugs, cytokines) within a biomaterial scaffold in a pre-determined way [1]. Bioprinting is typically performed using bench-based sophisticated 3D printers, often in a sterile environment, and allow for the creation of multi-layered scaffolds with cell-to-cell interactions and matrix production [2]. Furthermore, new studies have described the design and applicability of surgical bioprinters, which can deliver, at the time and point of need, a biomaterial that can be deployed during surgery to repair or regenerate human tissues. Ideally handheld directly by the surgeon, this approach can potentially solve some of the difficulties encountered with bench-based constructs [3].

3D printing and bioprinting now carry huge expectations from the surgical community, because it promises the potential regeneration of entire living organs and tissues.

In this talk I will discuss the current state of the art in bioprinting from a surgical prospective, focusing on its application in the musculoskeletal field and, more specifically, for the regeneration of articular cartilage. I will highlight the current roadblocks for the application of this technique in clinical practice, as well as the expectations and the promises for the future seen with the eyes of the final user.

ACKNOWLEDGEMENTS: Financial support was received from NHMRC-MRFF, Viertel Foundation, Australian Orthopaedic Association, Victorian Medical Acceleration Research Fund, SVHM REF Grants

1. Ravnic DJ, Leberfinger AN, Koduru SV, et al. Ann Surg. 266:48–58. 2017
2. Wu Z, Su X, Xu W, et al. Sci Rep. 6: 24474. 2016
3. Duchi S, Onofrillo C, O'Connell C, et al. Sci Rep 7: 5837. 2017

64

The ATP-P2X7 signalling axis in graft-versus-host disease: Recent insights from humanised mouse studies

Peter Cuthbertson[1, 2], Amal Elhage[1, 2], Amy Button[1, 2], Chloe Sligar[1, 2], Nicholas J Geraghty[1, 2], Sam R Adhikary[1, 2], Ellen M Reilly[1, 2], Nicolas R Tomasiello[1, 2], Katrina Bird[1, 2], Kara L Vine-Perrow[1, 2], Debbie Watson[1, 2], Ronald Sluyter[1, 2]

1. University of Wollongong, Wollongong, NSW, Australia

2. Illawarra Health and Medical Research Institute, Wollongong, NSW, Australia

Allogeneic blood stem cell transplantation is used for the treatment of leukaemia through the generation of life-saving graft-versus-tumour (GVT) immunity. However, this treatment can also result in graft-versus-host disease (GVHD), an often fatal inflammatory response mediated by donor T cells targeting tissues of recipients. Studies in allogeneic mouse models of GVHD indicate a role for the ATP-P2X7 signalling axis in the development of this disease. In this model, ATP is released from damaged tissues to activate P2X7 on host antigen presenting cells to drive T cell-mediated GVHD. However the relevance of this signalling axis to human GVHD and the role of P2X7 donor immune cells remains to be fully elucidated. To address these and other questions, our groups study a humanised mouse model of GVHD, in which NOD-*scid* IL2Rg^{null} (NSG) mice are injected with human peripheral blood mononuclear cells (PBMCs) and develop lethal GVHD from 3 weeks. Injection of the human/mouse P2X7 antagonist, Brilliant Blue G (BBG; 50 mg/kg, Days 0-10), into humanised mice reduced clinical and liver GVHD. This effect was associated with a reduction in circulating human IFNg and an increase in human T regulatory cells (Tregs). Injection of a human-specific neutralising anti-P2X7 monoclonal antibody (mAb; 0.1 mg/mouse, Days 0,2,4,6,8,) into humanised mice reduced also clinical and liver GVHD, which was similarly associated with an increase in human Tregs. Use of either inhibitor in cultures of serum-starved human PBMCs prevented the loss Tregs, suggesting that BBG and the anti-P2X7 mAb can prevent the ATP-induced death of these cells, providing a possible mechanism of action of these treatments in mice to reduce GVHD development. Notably, use of BBG (as above) with the clinical treatment post-transplant cyclophosphamide (PtCy; 33 mg/kg, Days 3,4) in humanised mice also reduced clinical and liver GVHD and increased human CD39^{+} Tregs but did not reduce GVT immunity to human THP-1 myeloid leukaemia cells. Collectively, this data indicates a role for P2X7 activation on donor Tregs and the subsequent loss of these cells in the development of GVHD. Moreover, inhibition of P2X7 does not compromise GVT immunity.

Transient lipodystrophy protects against high-fat diet-induced bone volume loss in male mice

Emma J Buckels[1, 2], Randall F D'Souza[2, 3], Troy L Merry[2, 3], Brya G Matthews[1, 2]

1. Department of Molecular Medicine and Pathology, The University of Auckland, Auckland, New Zealand

2. Maurice Wilkins Centre for Molecular Biodiscovery, University of Auckland, Auckland, New Zealand

3. Department of Nutrition, University of Auckland, Auckland, New Zealand

Adipose tissue is a key regulator of glucose homeostasis and interacts with the skeleton locally and systemically. Recent severe murine lipodystrophy models, where white and brown adipose tissue (WAT and BAT) are eliminated, demonstrated massive increases in trabecular and cortical bone when mice were fed a chow diet, despite marked metabolic dysfunction. A high-fat diet (HFD) has repeatedly been shown to have adverse effects on bone in rodents. Our study aimed to determine whether an HFD would affect trabecular or cortical bone microarchitecture in a model of inducible transient lipodystrophy.

Male Adiponectin-CreER/IR$^{flox/flox}$ (Adipo-IR-KO) mice were treated with tamoxifen at 8-weeks of age. Adiponectin-CreER primarily targets mature adipocytes. Signalling through the insulin receptor (IR) is critical for adipocyte survival in WAT and BAT. Therefore, tamoxifen-induced deletion of IR in adiponectin-expressing cells leads to marked but transient depletion of adipose depots that are gradually replenished by IR+ progenitors.

Following a 12-week recovery period, Adipo-IR-KO or wild-type (WT) control mice were switched to an HFD (60% kcal from fat). Tissues were collected from a subset of animals prior to HFD-feeding or after 20-weeks of HFD. Metabolic phenotypes were evaluated throughout the study, and bone phenotypes were evaluated by microCT.

Adipo-IR-KO mice experienced marked hyperglycemia in the days following adipocyte-specific IR knockout (Figure 1). WT and Adipo-IR-KO had similar blood glucose concentrations and trabecular bone volume by 4-weeks post IR depletion. After 20-weeks of HFD, trabecular bone volume was 25% higher (p=0.03), and trabecular number was increased 18% (p=0.04) in Adipo-IR-KO vs. WT mice. Cortical bone was similar between groups.

This study demonstrated that transient lipodystrophy 12-weeks before the induction of HFD prevented HFD-induced bone loss in male mice. Following this novel finding, work is underway to understand the crosstalk between adipose tissue and the skeleton.

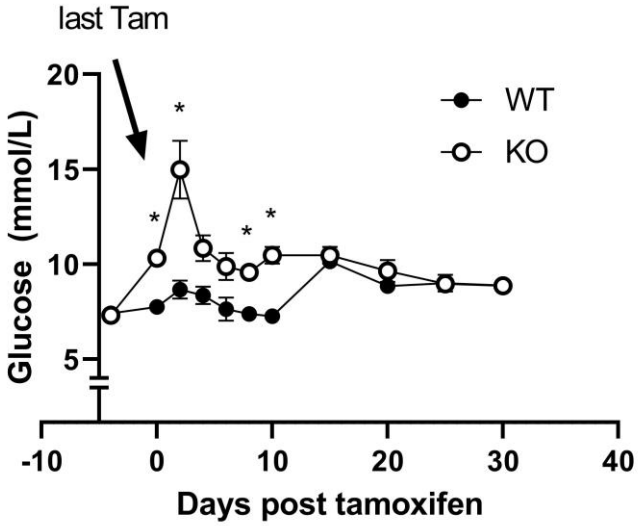

Figure 1: Fed blood glucose measurements in Adipo-IR-KO mice (KO) compared to Wild-type (WT) controls following 5 daily doses of tamoxifen (Tam). * p<0.05

Multimorbidity compounds excess mortality following proximal fractures: A nationwide cohort study

Thach Tran[2, 1], Dana Bliuc[2, 1], Le Phuong Thao Ho[3], Bo Abrahamsen[4, 5], Joop P van den Bergh[6, 7], Weiwen Chen[2], John A Eisman[2, 1, 8], Piet Geusens[9, 10], Louise Hansen[11], Peter Vestergaard[12, 13, 14], Tuan V Nguyen[8, 15], Robert Blank[2], Jackie Center[2, 1, 8]

1. Faculty of Medicine, University of New South Wales, Sydney, Australia

2. Garvan Institute of Medical Research, Darlinghurst, NSW, Australia

3. Ha Tinh University, Ha Tinh, Vietnam

4. Department of Medicine, Holbak Hospital, Holbak , Denmark

5. Department of Clinical Research, Odense Patient Data Explorative Network, University of Southern Denmark, Odense, Denmark

6. Department of Internal Medicine, Maastricht University Medical Centre, Research school Nutrim, Maastricht, Netherlands

7. Department of Internal Medicine, VieCuri Medical Centre of Noord-Limburg, Venlo, The Netherlands

8. School of Medicine Sydney, University of Notre Dame Australia, Sydney, Australia

9. Department of Family Medicine, Maastricht University, Research School CAPHRI, Maastricht, The Netherlands

10. University Hasselt, Biomedical Research Institute, Hasselt, Belgium

11. Kontraktenheden, North Denmark Region, Aalborg, Denmark

12. Department of Clinical Endocrinology, Aalborg University Hospital, Aalborg, Denmark

13. Steno Diabetes Center , North Jutland, Denmark

14. Department of Endocrinology, Aalborg University Hospital, Aalborg, Denmark

15. School of Biomedical Engineering, Centre of Health and Technologies, University of Technology Sydney, Sydney, NSW, Australia

Multimorbidity, the presence of 2 or more chronic diseases, poses a major challenge to public health though its contribution to post-fracture mortality remains unclear. We sought to identify the pattern of multimorbidity and its relationship to post-fracture excess mortality.

This nationwide population-based cohort study involved 307,870 adults in Denmark born on or before 1/1/1950 with an incident low-trauma fracture between 2001 and 2014 who were followed through 2016. Fracture and 32 predefined chronic diseases recorded within 5 years prior to the index fracture were identified using ICD-10 codes from the Danish National Hospital Discharge Register. Because most diseases are correlated, we conducted to identify clusters of comorbidities, and relative survival analysis to quantify excess mortality attributable to the combination of multimorbidity and specific fracture sites.

There were 95,372 men (age at fracture: 72±11 years) and 212,498 women (75±11) with incident fractures followed by 41,017 and 81,727 deaths, respectively. Almost half of fracture patients had multimorbidity. Comorbidities at fracture grouped into a low-multimorbidity (60.5% in men, 66.5% in women), cardiovascular (23.7%, 23.5%), diabetic (5.6%, 5.0%), malignant (5.1%, 5.0%) and mixed hepatic/inflammatory clusters (5.1%, men only). These clusters distinguished individuals with advanced, complex, or late-stage disease from those having earlier stage disease. Multimorbidity and proximal or lower leg fractures were associated with significantly increased mortality risk, with the highest excess mortality found in hip fracture patients in the malignant cluster. Importantly, the combination of multimorbidity and fracture compounded mortality, conferring much greater risk than either alone (Figure).

Concomitant illnesses were common and clustered into distinct multimorbidity clusters that imparted excess mortality post-fracture. The compound contribution of multimorbidity to post-fracture excess mortality highlights the need for more

comprehensive approaches in these high-risk patients. The analytical approach we have applied to fracture could be also used

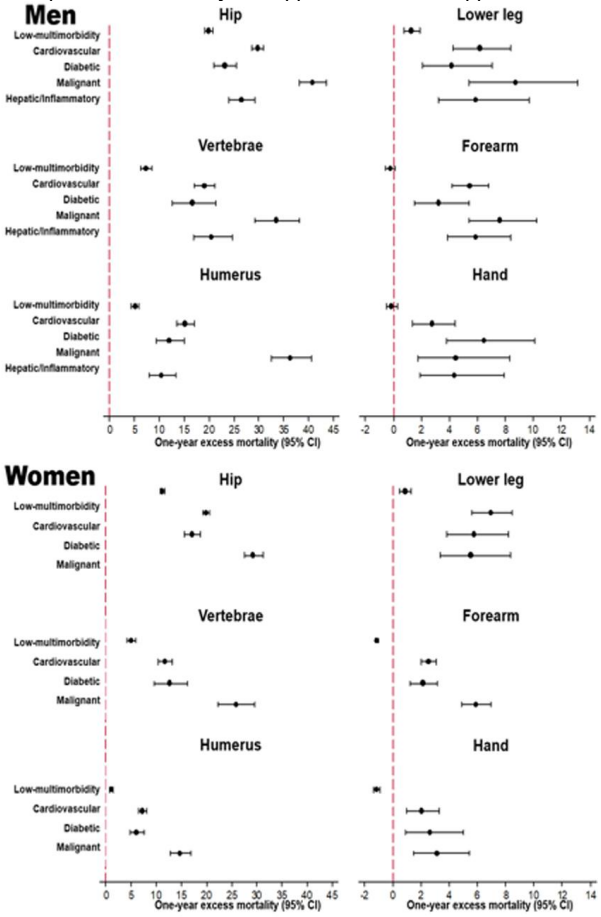

to examine other sentinel health events.

1. Figure: Excess mortality 1 year following selected fracture sites by specific multimorbidity clusters and genders

Osteocytes regulate organismal senescence of bone and bone marrow

Peng Ding[1], Chuan Gao[1], Youshui Gao[1], Delin Liu[2, 3], Hao Li[1], Jun Xu[1], Xiaoyi Chen[4], Yigang Huang[1], Changqing Zhang[1], Ming-Hao Zheng[2, 3], Junjie Gao[5, 1]

1. Department of Orthopaedics, Shanghai Jiao Tong University Affiliated Sixth People's Hospital, Shanghai, 200233, China

2. Centre for Orthopaedic Translational Research, Medical School, University of Western Australia, Nedlands, Western Australia 6009, Australia

3. Perron Institute for Neurological and Translational Science, Nedlands, Western Australia 6009, Australia

4. Ningbo Institute of Life and Health Industry, University of Chinese Academy of Sciences, Ningbo, Zhejiang, China

5. Institute of Microsurgery on Extremities, Shanghai Jiao Tong University Affiliated Sixth People's Hospital, Shanghai, 200233, China

The skeletal system contains a series of sophisticated cellular lineages arisen from the mesenchymal stem cells (MSC) and hematopoietic stem cells (HSC), that determine the homeostasis of bone and bone marrow. Here we reasoned that osteocyte may exert a function in regulation of these lineage cell specifications and tissue homeostasis. Using a mouse model of conditional deletion of osteocytes, we demonstrated that partial ablation of DMP-1 positive osteocytes caused severe sarcopenia, osteoporosis and degenerative kyphosis and led to shorter lifespan in these animals. Osteocyte reduction altered mesenchymal lineage commitment resulting in impairment of osteogenesis and induction of osteoclastogensis. Single cell RNA sequencing further revealed that hematopoietic lineage was mobilized towards myeloid lineage differentiation with expanded myeloid progenitors, neutrophils and monocytes, while the lymphopoiesis was impaired with reduced B cells in osteocyte ablation mice. The acquisition of a senescence-associated secretory phenotype (SASP) in both osteoprogenic and myeloid lineage cells was the underlying cause. Together, we showed that osteocytes play critical roles in regulating of lineage cell specifications in bone through mediation of organismal senescence.

Spatially resolving the bone marrow microenvironment in MGUS and multiple myeloma

Melissa D Cantley[1, 2], Laura Trainor[1, 2], Nicholas West[3], Duncan Hewett[1, 2], Andrew C.W Zannettino[1, 2, 4], Kate Vandyke[1, 2]

1. Myeloma Research Laboratory, School of Biomedicine, Faculty of Health and Medical Sciences, The University of Adelaide, Adelaide, South Australia, Australia

2. Precision Cancer Medicine Theme, South Australian Health and Medical Research Institute, Adelaide, South Australia, Australia

3. Central Facility for Genomics, Griffith University, Gold Coast, Queensland, Australia

4. Central Adelaide Local Health Network (CALHN), Adelaide, South Australia, Australia

Multiple myeloma (MM) is a haematological malignancy characterised by proliferation of clonal plasma cells (PCs) in the bone marrow (BM) and is proceeded by an asymptomatic stage known as monoclonal gammopathy of undetermined significance (MGUS). BM microenvironment cells support proliferation and survival of MMPCs and may play a role in MGUS-to-MM progression. Here, we aimed to characterise BM microenvironment changes with MGUS-to-MM progression in trephine biopsies.

Nanostring GeoMx Digital Spatial Protein profiling was performed on paraffin embedded decalcified BM trephine biopsies from 3 patients with matched samples at MGUS and subsequent MM diagnosis. Tissues were stained with immunofluorescent CD138 and CD45 antibodies, Syto13 nuclear stain and 68 barcoded antibodies (Nanostring immune-oncology panel). Regions of interest (ROI) (4/tissue section) were selected representing low (0-40%) to high (70%-100%) CD138+ PC% (Figure 1A-C) and barcoded antibodies were quantitated using the nCounter system. Affymetrix microarray gene expression analysis was conducted on sorted PCs ($CD138^{+}CD38^{+}CD45^{low}CD19^{-}$) from BM aspirates (n=5 matched MGUS/MM diagnosis) to identify PC expression of markers included in the spatial analysis.

Results demonstrated significant positive correlations (Pearson) between tumour cell infiltration (PC%) as assessed by CD138 immunostaining and expression of CD56, BAD, BCL2, and BCL-XL, reflective of expression of these markers by myeloma PCs, as shown by microarray analysis. Interestingly, microenvironment cell markers CD127 and SMA, which are not expressed by MM PCs, significantly positively correlated with PC% whilst ARG1 expression was inversely correlated with PC% (Figure 1D). SMA expression was significantly increased in myeloma samples compared to MGUS in 2/3 patients ($p<0.05$; 2way ANOVA).

This study optimised Digital Spatial Protein Profiling of trephine biopsies revealing correlations of PC% with tumour markers and with microenvironment markers. Future studies will utilise this method on additional matched MGUS and MM samples, to increase our understanding of how the BM microenvironment changes with MGUS-to-MM progression.

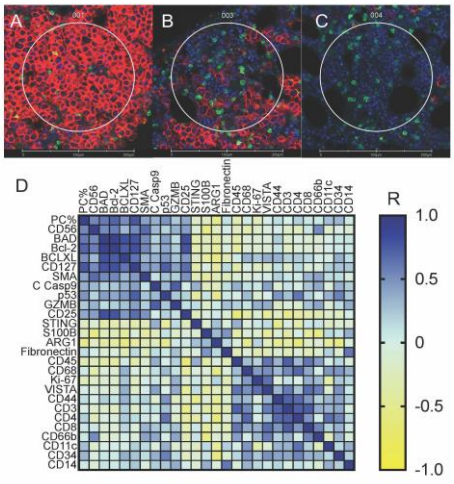

Figure 1: A-C) Representative ROIs: A) high CD138+ cells, B) intermediate CD138+ and C) low CD138+ infiltrate. red:CD138, green:CD45, blue:nuclei D) Pearson's correlation matrix revealing associations between tumour cell infiltration (PC%) and tumour markers CD56 (r=0.55, p=0.005), BAD (r=0.62, p=0.001), BCL2 (r=0.71, p<0.001) and BCL-XL (r=0.53, p=0.008) and with microenvironment markers CD127 (r=0.77, p<0.001), SMA (r=0.43, p=0.04) and ARG1 (r= -0.50, p=0.013).

69

Transitioning adolescents with Osteogenesis Imperfecta to adult care: challenges and opportunities

Jenny Harrington[1]

1. Women's and Children's Hospital, Adelaide, North Adelaide, SA, Australia

Osteogenesis imperfecta (OI) is the most common form of primary osteoporosis, with an estimated prevalence of 1 in 12,000 to 1 in 15,000 children. It has a broad clinical phenotype, from significant bone deformities, multiple fractures and short stature to mild clinical forms without fractures. There is an expanding list of pathogenic genetic variants found to be associated with OI with increased understanding about phenotypic and treatment responsive differences by genotype.

The management of children with OI aims to maximise mobility and daily life competencies, decrease bone pain and fragility and monitor for known associated skeletal and non-skeletal clinical features of OI. This ideally involves multi-disciplinary teams to help provide rehabilitation, surgical and pharmacological treatments. In children with OI with recurrent fractures, bisphosphonate therapy is often initiated and usually continued until the end of linear growth.

Transitioning to adult care can present challenges with navigating new health systems and taking more ownership and independence with personal health care. As youth with OI pass puberty and enter adulthood, there is most commonly a decline in the rate of peripheral fractures. Other non-skeletal clinical features of OI, can however increase over time.

In this session we will discuss some of the management considerations, unanswered questions and challenges in transitioning youth with OI to adult care.

70

Transition services for bone health in adolescents and young adults

Anne Trinh[1]

1. Hudson Institute of Medical Research, Melbourne, Victoria, Australia

Education of the young adult and empowering them to manage their own health is at the core of successful transition from paediatric to adult health services. The model of care at Monash Health is presented with examples of patients attending our service. The challenges of rare genetic bone diseases, chronic diseases of childhood such as cerebral palsy, and disorders of puberty are discussed.

Geometry and bone mineral density determinants of femoral neck strength changes following exercise

Dermot O'Rourke[1], Belinda R Beck[3, 2, 4], Amy T Harding[3, 2], Steven L Watson[5], Peter Pivonka[1], Saulo Martelli[1]

1. Queensland University of Technology, Brisbane, QLD, Australia

2. Griffith University, Gold Coast, QLD, Australia

3. Menzies Health Institute Queensland, Gold Coast, QLD, Australia

4. The Bone Clinic, Brisbane, QLD, Australia

5. Gold Coast University Hospital, Gold Coast, QLD, Australia

INTRODUCTION Physical exercise elicits spatially heterogeneous adaptation in bone to mitigate bone loss and improve strength [1]. The aim of the study was to determine the principal changes in geometry and BMD induced by exercise with the greatest relation to femoral neck strength.

METHODS Pre- and post-intervention proximal femur DXA scans were obtained (Medix DR) from 92 male participants (67 ± 7 years) in an exercise trial [2]. The 3D shape and BMD distribution of the femur was reconstructed from the planar DXA images with a statistical shape and appearance model and converted into volume meshes with element-by-element correspondence [3]. Femoral neck strength under single-leg stance and sideways fall was estimated using a maximum principal strain criterion [4]. Partial Least Squares (PLS) regression models were developed with predictor variables: (1) geometry changes and (2) BMD changes.

RESULTS The BMD-model required 4 PLS components and the geometry-model 8 components to account for 90% of the strength variance. BMD changes in PLS 1 were related to cortical bone density in the calcar region, greater trochanter, and femoral neck (Fig. 1a). Geometry changes in PLS 1 were related to scaling changes in the trochanteric and femoral head regions. VIP scores indicated that changes in the femoral neck were important for single-leg stance strength and in the lateral-superior neck and greater trochanter for sideways fall (Fig. 1b).

DISCUSSION Changes in femoral neck strength were primarily governed by changes in BMD distribution. The superior neck and distal cortex were most important for single-leg stance. The superior neck, medial head, and lateral trochanter were most important for sideways fall. BMD changes in the calcar region, superior neck, and greater trochanter regions accounted for the greatest strength changes.

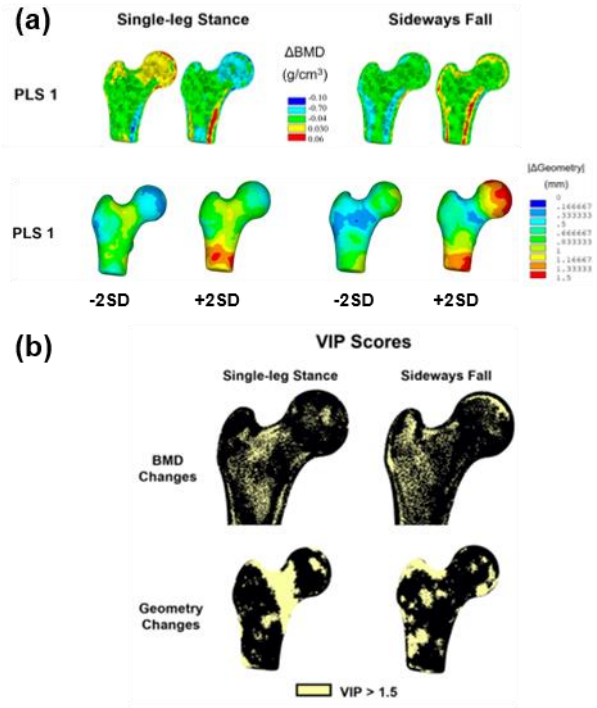

Fig 1: (a) ± 2SD along the first PLS component of the BMD-only and geometry-only models; (b) VIP scores indicating the spatial and geometry changes important in the PLS regression model for their relationship to strength

1. Rubin et al., Calcif. Tissue Int 1985 37(4): 411-417
2. Harding, et al. J Bone Miner Res 2020 35(8):1404–1414
3. O'Rourke, et al., J Biomech, 2021. 119: 110315
4. Schileo, et al., J Biomech, 2008. 41(2): 356-367.

72

What impact have therapeutic advances for musculoskeletal health had on mortality risk – do we see differential relationships for muscle and bone?

Faidra Laskou[1], Leo Westbury[1], Harnish Patel[1], Cyrus Cooper[1, 2], Elaine M Dennison[3, 1]

1. MRC Lifecourse Epidemiology Centre, Southampton University, Southampton, UK

2. NIHR Oxford Biomedical Research Centre, Oxford, UK

3. Victoria University of Wellington, Wellington, NZ

Objectives

Historically, several studies have reported associations between either low bone mineral density (BMD) or low grip strength (GS) and mortality risk. However, therapeutic advances in management of osteoporosis (OP) and sarcopenia have occurred at different rates over the last two decades; in this study, we examined relationships between BMD and GS and subsequent all-cause and cause-specific mortality in a UK community-dwelling cohort, considering whether relationships differ between mortality risk and either muscle or bone health.

Material and Methods

Data on GS and mortality were available for 2987 Hertfordshire Cohort Study participants (47% women). Femoral neck BMD was ascertained in 992 participants using DXA; GS was assessed by grip dynamometry in the whole group and deaths were recorded from baseline (1998-2004) until 31st December 2018. Medication use was recorded. Associations between BMD and GS in relation to mortality (all-cause, cardiovascular-related, cancer-related, and other) were examined using sex-specific Cox regression models with adjustment for age.

Results

Mean (SD) baseline age of participants was 65.7 (2.9) years in men and 66.6 (2.7) years in women. Lower GS at baseline was associated with higher all-cause mortality in men (hazard ratio per SD lower grip strength: 1.22 (1.12,1.33), p<0.001) and in women (1.29 (1.17,1.43), p<0.001). Lower GS was associated with increased risk of cardiovascular (1.30 (1.11,1.52), p=0.001 in men; 1.61 (1.30,1.99), p<0.001 in women) and other mortality (1.33 (1.14,1.55), p<0.001 in men; 1.39 (1.18,1.63), p<0.001 in women) in both sexes, but no association was found with cancer mortality (p>0.25). However, lower BMD was not associated with increased risk of all-cause or cause-specific mortality (p>0.09 for all associations).

Conclusions

We report strong relationships between GS and mortality in both sexes after adjustment for age in comparison with BMD. We hypothesize this may reflect better recognition and treatment of low BMD. Further longitudinal studies are required.

73

Association Between Lifestyle Factor and Bone Loss in Elderly Women

Ngoc Huynh[1], Krisel De Dios[1], Thach S Tran[2], Tuan v Nguyen[3, 1]

1. School of Biomedical Engineering, University of Technology Sydney, Sydney, NSW, Australia

2. Garvan Institute of Medical Research, Sydney, NSW, Australia

3. School of Population Health, UNSW Medicine, UNSW Sydney, Sydney, NSW, Australia

Background:

Risk factors for age-related bone loss have not been well documented. The present study examined the relationship between femoral neck bone loss and lifestyle factors in elderly women.

Methods:

We analysed the data from the Study of Osteoporosis Fractures that included 9704 Caucasian women aged 65 years and above. Bone mineral density (BMD) at the femoral neck was measured by DXA (Hologic QDR 1000 and QDR 2000) at baseline and subsequent visits. We limited the analysis to those with at least 3 BMD measurements (n=4903). For each woman, the rate of change in BMD was estimated by the linear regression model. Smoking was classified as "never smoking", "ex-smoking", and "current smoking". Alcohol use was classified as "drinking" vs "non-drinking". Physical activity was quantified as total calories burned by activity and walking per week. Dietary calcium intake (mg/week) and dietary protein intake (mg/week) were ascertained based on self-reports.

Results:

The annual rate of loss in FNBMD progressively increased with age: −0.8±1.7, −1.1±2.4, and −1.7±2.7 (mean±SD) among those aged 65–69, 70–79, and ≥80 years, respectively (p<0.001). Women smokers suffered a greater rate of bone loss (-1.3±1.9% per year) than ex-smokers/non-smokers (-0.9±2.2% per year, p=0.002). However, alcohol users were associated with a lower bone loss (-0.9±2.1% per year) than abstainers (-1.0±1.9% per year; p=0.024). The calories burned from activity and walking was adversely associated with a higher rate of bone loss after adjustment for age (p<0.001). Greater dietary calcium intakes were associated with a lower rate of bone femoral neck bone loss (p=0.01). However, there was no statistically significant association between dietary protein intakes and bone loss. Collectively, these lifestyle factors explained approximately 2% of the variance in bone loss.

Conclusion:

These data suggest that post-menopausal bone loss is increased with advancing age, and that the loss can be reduced by modifying lifestyle factors.

A 6-month digital health osteoporosis self-management intervention delivered via Amazon Alexa improved osteoporosis knowledge and falls self-efficacy in postmenopausal women with osteoporosis

David Scott[1], Paul Jansons[1], Belinda De Ross[1], Nicole Kiss[1], Peter R Ebeling[2], Robin M Daly[1]

1. Deakin University, Burwood, VIC, Australia

2. Monash University, Clayton, VIC, Australia

Background: Emerging digital health tools may support self-management of osteoporosis. We aimed to determine whether a 6-month digital health intervention could improve osteoporosis knowledge, medication behaviours, health-related quality of life and falls efficacy in postmenopausal women with osteoporosis.

Methods: Fifty postmenopausal women currently prescribed anti-osteoporosis medication were randomised to receive 6 months of automated education sessions (video/audio/text) on medication, nutrition, and exercise (including 3 sessions/week home-based strength, balance and impact training) for osteoporosis, broadcast via a provided voice-activated Amazon Alexa Echo Show (Alexa) device located in their home (Figure), or automated monthly emails only (control). Outcomes included changes in Osteoporosis Knowledge Assessment Tool (OKAT), Adherence Evaluation of Osteoporosis Treatment Questionnaire (ADEOS), EQ-5D-5L, and Modified Falls Efficacy Scale (MFES) scores.

Results: Forty-seven (94%) women (mean±SD age 64.3±6.1 years) completed follow-up (23 Alexa group; 24 control group). The Alexa group completed 68±25 of 72 (94%) prescribed education/exercise sessions and demonstrated significantly greater (between-group difference: P=0.038) improvements in osteoporosis knowledge (OKAT; out of 20) compared with controls (Alexa: 10.4±2.6 baseline vs 13.0±3.1 6-months; P<0.001; controls: 10.8±3.0 baseline vs 11.9±2.8 6-months; P=0.06). Change in adherence to osteoporosis treatment (ADEOS) scores did not differ between groups (P=0.114), but improved within the Alexa group only (18.7±3.3 baseline vs 19.9±2.0 6-months; P=0.041). There were no differences between groups for most quality of life (EQ-5D-5L) domains, but the proportion of women experiencing no problems performing usual activities at 6-months was significantly greater for the Alexa group compared with controls (83% vs 54%; P=0.023). Average falls efficacy (MFES; out of 10) scores improved significantly (P=0.032) for the Alexa group (9.70±0.70 baseline vs 9.94±0.20 6-months) compared with controls (9.37±1.67 baseline vs 9.26±1.77 6-months).

Conclusions: A 6-month, remotely-delivered digital health intervention, supporting osteoporosis self-management and including home-based exercise, significantly improved osteoporosis knowledge and falls efficacy in postmenopausal women with
osteoporosis.

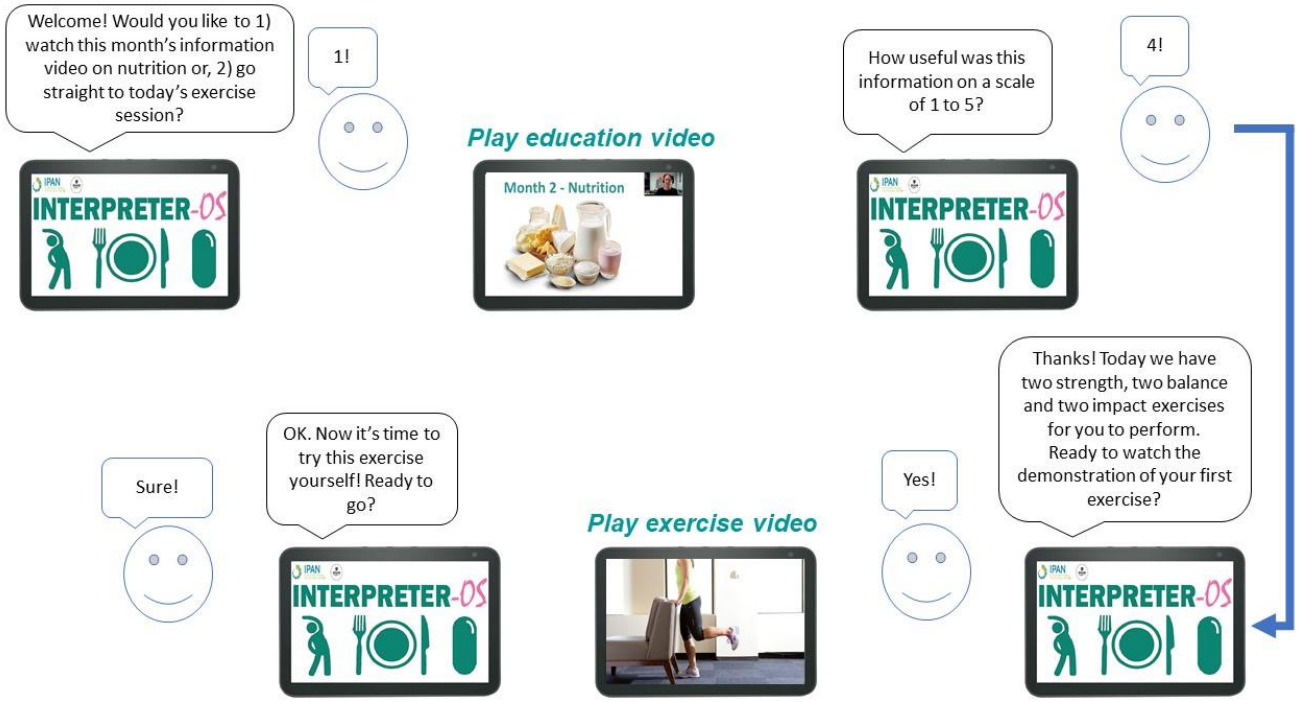

75

An individualized approach for assessing change in bone mineral density

Tuan V Nguyen[1]

1. University of Technology Sydney, Sydney, NEW SOUTH WALES, Australia

Background: The assessment of BMD change is currently based on the “least significant change” (LSC) rule, but this rule has many methodological deficiencies, and often generates wrong decisions. Here, I propose a new approach for assessing BMD change tailored to each individual.

Methods: For each individual, I estimated the 'true' average and standard deviation of BMD change, using the individual's measured change, the mean change in the population, and the intrasubject and intersubject variance. This approach implicitly removes the impact of regression-toward-the-mean effect. The probability of a real change in BMD is then estimated for each individual.

The longitudinal data from the Study of Osteoporotic Fracture (SOF) were used to test the utility of the new approach. Femoral neck BMD (FNBMD) was measured at baseline and subsequent visits using a densitometer (Hologic QDR1000 or QDR2000). From a published analysis, the measurement error of FNBMD on QDR1000 was 0.022 g/cm^2, and the LSC threshold was 6.36%.

Results: The analysis was based on 5797 women aged 65 yr and older at baseline. The average (SD) baseline FNBMD was 0.65 (0.108) g/cm^2. During an average duration of 3.5 years (range: 1.8 to 5.1) of follow-up, the annual rate of FNBMD change was -1.01% (SD 2.2%), but the adjusted average was 0.93%. Using the LSC rule, only 68 women (1.2%) were classified as 'decrease', and the rest was either 'unchanged' (98.3%) or 'increase' (0.5%). The new approach detected significant BMD change in 91% (n=5282) of women; of which, 42% (n=2447) showed a loss of at least 1% per year.

Conclusion: The approach introduced here allows the assessment of bone loss to be individualised rather than the one-size-fits-all LSC approach, and helps clinicians better identify people at high-risk of osteoporosis and fracture.

76

All models are wrong, but some are useful: The challenge of model complexity for orthopaedic application

Thor Besier[1]

1. University of Auckland, Auckland, New Zealand

Computational modelling of biomechanical systems has experienced exponential growth over the last two decades (of the authors academic career at least). Technological advancements in medical imaging and computational power has fuelled this growth and we are at an interesting cross-roads, where the traditional methods of biological and clinical science are giving way to disciplines of mathematics and engineering in order to further our understanding of biological systems and the form-function relationship of our musculoskeletal system. Few would argue the impact that mathematical modelling and engineering disciplines has had on our lives when they happily travel to the other side of the planet (pre-COVID) on an airplane that was designed and tested entirely *in silico*. The same scientific approach lures us into realm of personalised medicine and data-driven healthcare. However, our clinical colleagues remind us that ‘all models are wrong’ and we argue that ‘some are useful’. Herein lies the challenge for the computational modeller. As the statistician, George Box, stated, “Remember that all models are wrong; the practical question is how wrong do they have to be to not be useful”. This talk will touch on a few real-world examples within orthopaedic research, to encourage debate and discussion on how ‘personal’ our personalised models really need to be.

Finite element modelling to predict femoral fractures in transfemoral amputees with osseointegrated implants

Ryan Tiew[1], Hans A Gray[1], Dale L Robinson[1], David Ackland[1], Peter Lee[1]

1. Department of Biomedical Engineering, The University of Melbourne, Melbourne, VIC, Australia

The use of osseointegrated implants for lower limb amputees has gained popularity over the past few decades, particularly as an alternative to conventional socket-based prostheses. Unfortunately, up to 5.5% of these implanted femurs fail within the first year of surgery [1]. The ability to predict these fractures and the external loading conditions that cause them may help design better implants and improve surgical procedure. Thus, the aim of this study was to investigate whether computational modelling can accurately predict fractures that occurred in osseointegrated femurs. A finite element (FE) model of a composite femur with an osseointegrated implant was generated using a set of QCT images. Over 15,000 combinations of unique external loads (force and moment directions) were applied individually to the implant while the nodes on the proximal femur were fixed. Each of the loads was gradually increased until the femur fractured, defined by the point in which the volume of contiguous failed elements reached 350 mm^3 [2]. We compared the fracture sites predicted by the FE model to in vivo fracture data reported in literature. Our analysis predicted that 99.3% of the 15,056 fractures occurred at two distinct regions, the superior trochanteric region, and adjacent to the proximal tip of the implant (Fig. 1(b)). These findings are consistent with those of Hoellwarth et al [1] who reported that 20 out of 22 femoral fractures in osseointegrated patients occurred in the trochanteric region and that 19 out of 22 occurred within 2 cm of the proximal tip of the implant. This preliminary work demonstrates that FE analysis can predict the location of in vivo fractures in femurs with osseointegrated implants. Future work will focus on validating specimen specific finite element models and using them to study the effect of implant positioning on femoral fractures.

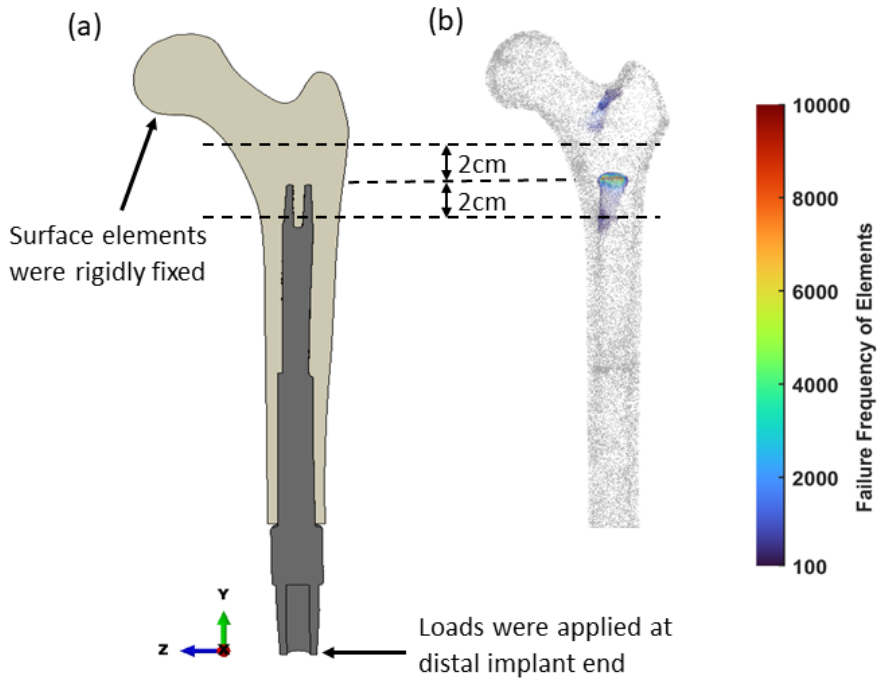

Figure 1: Position of osseointegrated implant in finite element model and fracture sites. (a) Finite element model of composite bone fitted with implant. The femoral head was clamped rigidly While the forces and moments were applied at the distal end of the implant. (b) Failure frequency of elements in the finite element model. Each finite element is represented by a dot. The colour of each dot denotes the number of unique loading combinations (out of the 15,056 combinations) under which the respective element failed. Elements that failed in less than 100 loading combinations are represented by grey dots.

1. J. S. Hoellwarth et al., "Periprosthetic osseointegration fractures are infrequent and management is familiar," Bone and Joint Journal, vol. 102 B, no. 2, pp. 162–169, 2020, doi: 10.1302/0301-620X.102B2.BJJ-2019-0697.R2.
2. W. B. Edwards and K. L. Troy, "Finite element prediction of surface strain and fracture strength at the distal radius," Medical Engineering and Physics, vol. 34, no. 3, pp. 290–298, Apr. 2012, doi: 10.1016/j.medengphy.2011.07.016.

Three-dimensional kinematics of the jaw following unilateral and bilateral prosthetic TMJ surgery

Sarah Woodford[1], Dale Robinson[1], Peter VS Lee[1], Jaafar Abduo[2], George Dimitroulis[3], David Ackland[1]

1. Department of Biomedical Engineering, The University of Melbourne, Melbourne, Victoria, Australia

2. Melbourne Dental School, The University of Melbourne, Melbourne, Victoria, Australia

3. Department of Surgery, St Vincent's Hospital, Melbourne, Victoria, Australia

OBJECTIVE

Total temporomandibular joint (TMJ) replacements reduce pain and improve quality of life in patients suffering from end-stage TMJ disorders, such as osteoarthritis and trauma. Jaw kinematics measurements following TMJ arthroplasty provide a basis for evaluating implant performance and jaw function. The aim of this study is to provide the first measurements of three-dimensional kinematics of the jaw in patients following unilateral and bilateral prosthetic TMJ surgeries.

METHODS

Jaw motion tracking experiments were performed on 7 healthy control participants, 3 unilateral and 1 bilateral TMJ replacement patients. Custom-made mouthpieces were manufactured for each participant's mandibular and maxillary teeth, with each supporting three retroreflective markers anterior to the participant's lip line. Participants performed 15 trials each of maximum jaw opening, lateral and protrusive movements. Marker trajectories were simultaneously measured using an optoelectronic tracking system. Laser scans taken of each dental plate, together with CT scans of each patient, were used to register the plate position to each participant's jaw geometry, allowing 3D condylar motion to be quantified from the marker trajectories.

RESULTS

The maximum mouth opening capacity of joint replacement patients was comparable to healthy controls with average incisal inferior translations of 37.5mm, 38.4mm and 33.6mm for the controls, unilateral and bilateral joint replacement patients respectively. During mouth opening the maximum anterior translation of prosthetic condyles was 2.4mm, compared to 10.6mm for controls (Fig-1). Prosthetic condyles had limited anterior motion compared to natural condyles, in unilateral patients this resulted in asymmetric opening and protrusive movements and the capacity to laterally move their jaw towards their pathological side only. For the bilateral patient, protrusive and lateral jaw movement capacity was minimal.

CONCLUSIONS

Total TMJ replacement surgery facilitates normal mouth opening capacity and lateral and inferior condylar movements but limits anterior condylar motion. This study provides future direction for TMJ implant design.

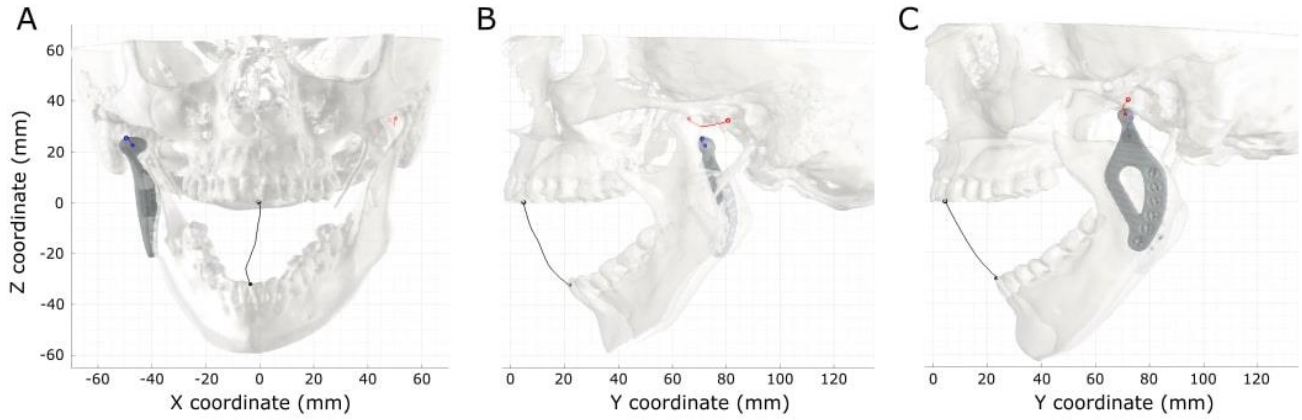

Figure 1) Asymmetric mouth opening for a unilateral joint replacement patient in the frontal (A) and sagittal (B) planes. Mouth opening for a bilateral joint replacement patient in the sagittal plane (C). Black, red and blue lines represent the movement trajectories for the incisal point, left condyle and right condyle respectively. Unfilled circles represent the initial starting position for each landmark, filled circles represent the final landmark positions.

Overload-induced extracellular mitochondria releasing from tendon organoid leads to inflammation

Ziming Chen[1], Peilin Chen[1], Andrew Tai[1], Euphemie Bassonga[1], Christopher Mitchell[1], Allan Wang[1], Ming-Hao Zheng[1]

1. The University of Western Australia, Perth, Western Australia, Australia

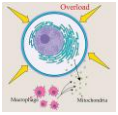

Objectives: Tendinopathy is the most frequent musculoskeletal disease that requires medical attention. Mechanical overload has been considered as a key driver of its pathology. However, the underlying mechanism on how overload induces tendinopathy and inflammation is unclear. Extracellular mitochondria (EM) are newly identified as cell-to-cell communicators. The aim of this study is to elucidate the role of mitochondria in overload-induced inflammation.

Methods: We performed three-dimensional uniaxial stretching to mouse tendon organoid in bioreactors. Cyclic strain of uniaxial loadings included underload, normal load, and overload, according to previous work. We then harvested microvesicles including EM, from the bioreactor by differential centrifugation and evaluated their characteristics by flow cytometry and super-resolution confocal microscopy. Raw 264.7 mouse macrophage cell line was used for chemotaxis assay in a Boyden Chamber System with Magnetic-Activated Cell Sorting Technology. EM induced cytokines secretion by macrophages was analyzed by a bead-based multiplex assay panel. N-Acetyl-L-cysteine (NAC) was used as the antioxidant to tendon organoid to regulate mitochondrial fitness.

Results: We showed mechanical load induced tendon organoid to release microvesicles including mitochondria. The size of microvesicles is mainly in the range from 220nm to 880nm. More than 75% of microvesicles could be stained by PKH26, confirming they were with lipophilic membrane. Super-resolution confocal microscopy identified two forms of mitochondria, including mitochondria encapsulated in vesicles and free mitochondria. Overload led to the degeneration of the organoid and induced microvesicles release containing most EM. Chemotaxis assay showed that EM from overloaded tendon organoid induced macrophages chemotaxis. In addition, microvesicles extracted from overloaded tendon organoid induced the production of proinflammatory cytokines including IL-6, KC (Keratinocyte-Derived Chemokine) and IL-18. NAC treatment to tendon cells could attenuate overload-induced macrophage chemotaxis.

Conclusions: Overload induces EM releasing from tendon cells, which leads to chemotaxis of macrophages toward tendon, resulting in induction of inflammation.

Lumbar spinal canal occlusion due to bulging of intervertebral disc

Dale L Robinson[1], Melanie Franklyn[2], David C Ackland[1], Peter Vee Sin Lee[1]

1. University of Melbourne, Parkville, VIC, Australia

2. Defence Science and Technology Group, Melbourne, VIC, Australia

During spinal fractures, occlusion of the spinal canal presents a high risk of neurological deficit due to bone fragments being retropulsed into the canal. There is evidence that bulging of the intervertebral disc can also result in neurological compression [1], yet no previous studies have examined how this alternative mechanism in detail. For example, it is unclear to what extent the spinal canal may be occluded by the disc or whether occlusion is influenced by morphometric variation. These questions are relevant to understanding spinal injuries encountered in military scenarios, where there are disproportionately high rates of spinal injuries below the thoracolumbar junction. The aim of this study was to quantify how lumbar spine canal occlusion induced by disc bulging is influenced by vertebral fracture or morphometic variation between different spinal positions.

Twenty sets of three-vertebra specimens with centre vertebra encompassing L1 to L5 were compressed at 1m/s. Canal occlusion was measured optically with a high-speed camera (Figure 1). The compression test was repeated with incremental increases in displacement until a bone fracture was identified using acoustic emission sensors and computed tomographic imaging. For axial compression prior to fracture, the peak occlusion was 29.9+/-10.0%, which was deduced to result from posterior bulging of the intervertebral disc. The maximum occlusion correlated significantly with lumbar spinal level ($p<.001$) and the cross-sectional area of the vertebra ($p=.031$). It may be concluded that disc bulging can cause significant amounts of lumbar spinal canal occlusion, which is more severe at distal levels. This finding is of clinical relevance because occlusion from disc bulging may not be apparent radiographically. Further, the lower lumbar spine's greater susceptibility to occlusion suggests that this location ought to be the focus of new injury mitigation technologies in situations at risk of high-rate axial compression.

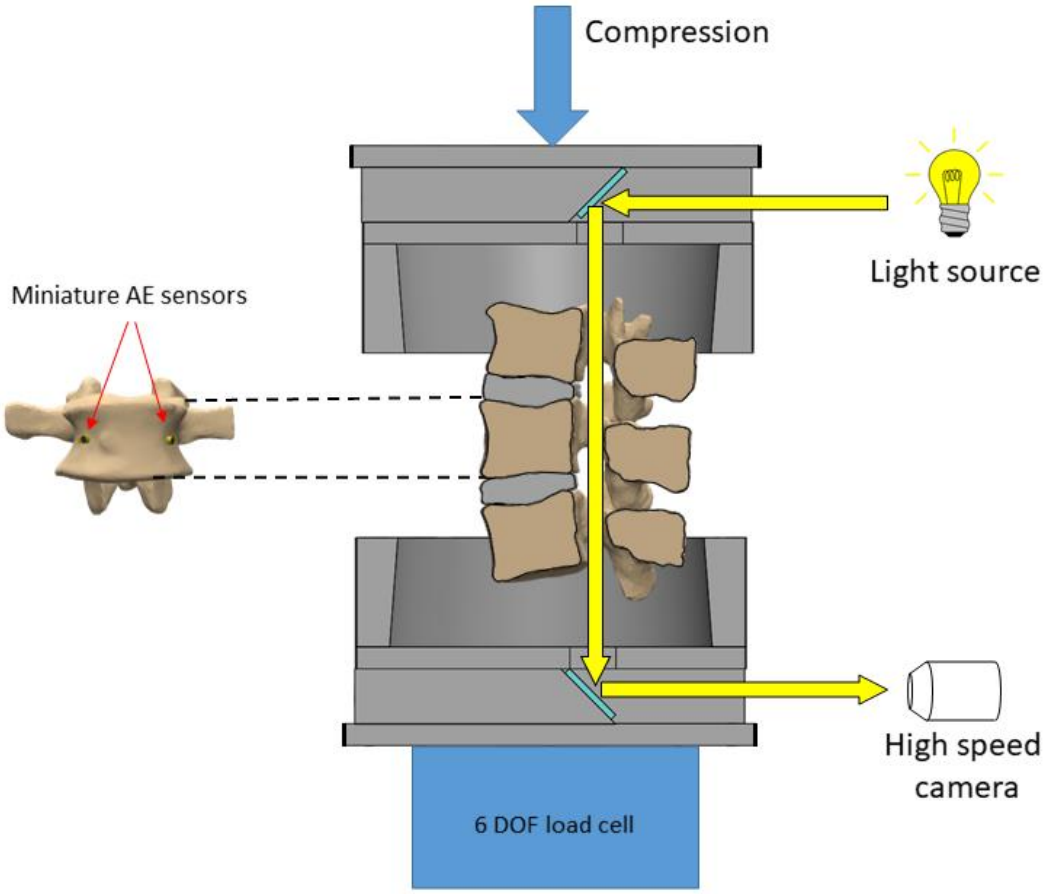

Figure 1: Experimental setup

1. [1] Fredericson M, et al. Spine J 2001;1(1):10–7.

A pipeline to morph the finite element model of lumbar spine

Yihang Yu[1], Dale L Robinson[1], David C Ackland[1], Peter V.S. Lee[1]

1. University of Melbourne, Melbourne, VICTORIA, Australia

Preoperative planning of spinal surgery involving biomechanical analysis provides the possibility for implant customization. However, the implant customization process has been limited by excessive time or cost requirements involved in verifying implant designs using patient-specific finite element (FE) models [1]. Therefore, our project aims to build an automated pipeline to generate patient-specific FE models of the lumbar spine. A template lumbar spine FE model was established in ABAQUS 2017 based on an average-sized healthy male. A statistical shape model (SSM) was developed using a training set of 46 lumbar spines. The surface geometry of the template model was non-rigidly aligned to each spine with radial basis functions, then a principal component analysis was performed. Hence, by choosing the weightings of these principal components, the surface geometry of the template model could be fitted to a new spine [2]. Once fitted, the full FE model could be adapted to the new spine by the following steps: (a) changing the surface mesh node positions of the template FE model to match the new spine, (b) generation of solid meshes from updated surface meshes, (c) assigning material properties to generated solid meshes and (d) updating solid meshes and centre of rotations of each lumbar level in the template FE model. To evaluate the performance of FE models, lateral bending and torsion range of motion (ROM) were simulated for the template model, and for the model morphed to a representative patient (Figure-1). In each case, the simulated ROM compared reasonably to the upper and lower range to published data [3]. In conclusion, the pipeline can reduce the manual efforts of spinal surgery planning and benefit spinal implant customization. The pipeline will be further validated in other ROMs and facet joint forces, and enriched by adding spinal implant generation function.

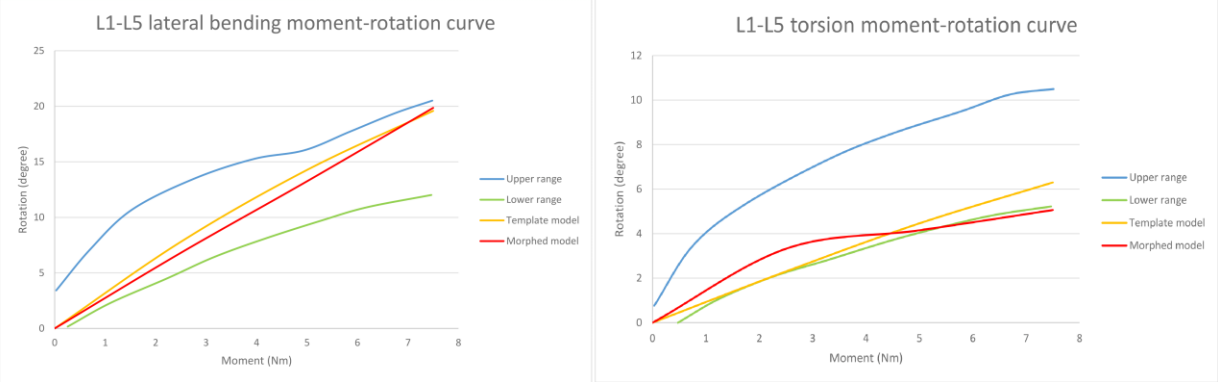

Figure 1.

1. Tong Y, Kaplan DJ, Spivak JM, Bendo JA. Three-dimensional printing in spine surgery: a review of current applications. The Spine Journal. 2020 Jun 1;20(6):833-46.
2. Zhang J, Hislop-Jambrich J, Besier TF. Predictive statistical models of baseline variations in 3-D femoral cortex morphology. Medical engineering & physics. 2016 May 1;38(5):450-7.
3. Dreischarf M, Zander T, Shirazi-Adl A, Puttlitz CM, Adam CJ, Chen CS, Goel VK, Kiapour A, Kim YH, Labus KM, Little JP. Comparison of eight published static finite element models of the intact lumbar spine: predictive power of models improves when combined together. Journal of biomechanics. 2014 Jun 3;47(8):1757-66.

82

A nonlinear controller algorithm to design a self-paced treadmill based on the real-time center of mass data

Hossein Mokhtarzadeh[1, 2], Rosie Richards[1], Thomas Geijtenbeek[3]

1. Research Business Unit, Motek Medical B.V. (DIH Brand), Houten, Netherlands

2. Biomedical Engineering, The University of Melbourne, Parkville, VIC, Australia

3. Goatstream / Delft University of Technology, Delft, Netherlands

The gold standard to study gait and balance is in the field but is challenging for those with impaired neuromuscular conditions. Using treadmills can be an alternative with some benefits including experiments in a safe and controllable environment. Most treadmill studies use a fixed speed that may not adequately represent a participant's normal walking speed. Several studies have compared treadmill and overground walking with conflicting biomechanical outcomes. Self-paced (SP) treadmills were designed to allow participants to walk at their own comfortable gait speed. Many algorithms have been developed to design SP based on various data sources including ground reaction forces, markers, marker-less, and 3D depth cameras. In this novel controller design, we present a non-linear algorithm that implements a self-paced procedure integrated with instrumented treadmills [1]. The algorithm attempts to prevent the subject from reaching the front and back of the treadmill via minimal treadmill acceleration. Our algorithm uses real-time data from the center of mass relative to the front and back ends of the treadmill. The controller adjusts the treadmill's belt speed via belt acceleration at every time step. Numerous studies (with over 410 participants from different populations) have been conducted using this method in the safe environment of a lab with instrumented treadmills. Moreover, we provided a simulation of the SP algorithm in different controlled conditions in MATLAB. The treadmill's belt speed calculated by the simulated algorithm matched well with the experimental belt speed in a Gait Realtime Analysis Interactive Lab (GRAIL) system. The algorithm works in real-time with the other multi-sensory systems integrated with the treadmill via D-Flow software. This SP algorithm can be used in several biomechanical scenarios of gait and balance and is a step toward a more standardized algorithm in biomechanics across various instrumented treadmills with different populations.

1. Geijtenbeek, T., Steenbrink, F., Otten, B., Even-Zohar, O., 2011. D-flow: immersive virtual reality and real-time feedback for rehabilitation, in: Proceedings of the 10th International Conference on Virtual Reality Continuum and Its Applications in Industry. pp. 201–208.

83

Surgical outcomes following tibialis anterior tendon transfer for recurrent congenital talipes equinovarus (CTEV).

Alexis Brierty[1, 2], Sean Horan[2], Claudia Giacomozzi[3], Liam Johnson[1], David Bade[1], Christopher P Carty[1, 2]

1. Children's Health Queensland, South Brisbane, QLD, Australia

2. Griffith University, QLD

3. Istituto Superiore di Sanità, Rome

The tibialis anterior tendon transfer (TATT) is a common surgical intervention aimed at correcting dynamic varus deformity in patients with congenital talipes equinovarus (CTEV). In our previous work (Brierty et al 2022) we identified two clear subgroups within a CTEV cohort being considered for TATT surgery, one group more impacted by hindfoot inversion (varus) and one more impacted by hindfoot adduction. To date, no studies have compared outcomes between differing kinematic presentations of CTEV following TATT surgery. The aim of this research was to determine whether differences in surgical outcomes were evident between these two groups.

Of the 17 participants (23 feet) who underwent gait analysis pre-operatively, 13 participants (19 feet) progressed to having tendon transfer surgery, and 11 of the 13 participants (15 feet) attended post-operative gait analysis at the Queensland Children's Motion Analysis Service (QCMAS). Post-operative Plug-in-Gait and Oxford Foot Model kinematics and kinetics were collected. Data analysis was performed using Vicon Nexus and dedicated Mathworks Matlab codes. Statistical analysis included Statistical Parametric Mapping (SPM) for time-series comparisons between cohorts.

In subgroup one, there were no significant differences pre- to post-operatively, however there was a trend towards a decrease in hindfoot and forefoot inversion during swing, and decreased variability, supporting the efficacy of tendon transfer surgery for this subgroup. In subgroup two, we observed decreases in the two most affected variables, hindfoot adduction/abduction and forefoot dorsiflexion/plantarflexion, falling within the typical bands across the majority of the gait cycle. Evaluation of individual traces showed that despite positive results in hindfoot adduction, inversion/eversion results were unpredictable following tendon transfer surgery.

Patients who presented with a predominate hindfoot inversion deformity at baseline appeared to have predictably positive results, whereas patients who presented with a predominate hindfoot adduction deformity at baseline had less convincing outcomes that should be considered in future investigations.

1. Alexis Brierty, Sean Horan, Claudia Giacomozzi, Liam Johnson, David Bade, Christopher P Carty, Kinematic differences in the presentation of recurrent congenital talipes equinovarus (clubfoot), Gait & Posture, 2022

84

Mucosal protein-based vaccination with a TLR2-stimulating adjuvant induces potent local immunity against SARS-CoV-2 in mice

Anneliese s Ashhurst[1, 2, 3], Matt D Johansen[4], Joshua WC Maxwell[1, 5], Caroline L Ashley[3], Anupriya Aggarwal[6], Rezwan Siddiquee[7, 8], Joel P Mackay[7], Claudio Counoupas[2, 3], Scott N Byrne[3], Stuart Turville[6], Megan Steain[3], Jamie A Triccas[3], Philip M Hansbro[4], Richard J Payne[1, 5], Warwick J Britton[2, 9]

1. School of Chemistry, University of Sydney, Sydney, NSW, Australia

2. Tuberculosis Research Program, Centenary Institute, Sydney, NSW, Australia

3. Infection, Immunity and Inflammation Theme, School of Medical Sciences, Faculty of Medicine and Health, University of Sydney, Sydney, New South Wales, Australia

4. Centre for Inflammation, Centenary Institute and Faculty of Science, School of Life Sciences, University of Technology, Sydney, NSW, Australia

5. Australian Research Council Centre of Excellence for Innovations in Peptide and Protein Science, University of Sydney, Sydney, New South Wales, Australia

6. Kirby Institute, Sydney, NSW, Australia

7. School of Life and Environmental Sciences, The University of Sydney, Sydney, NSW, Australia

8. Sydney Analytical, The University of Sydney, Sydney, NSW, Australia

9. Department of Clinical Immunology, Royal Prince Alfred Hospital, Sydney, NSW, Australia

The development of vaccines against SARS-CoV-2 has provided critical opportunities to reduce the morbidity and mortality associated with COVID-19. While current vaccines can reduce the risk of transmission, enhancing mucosal immunity to provide a barrier against infection may further increase protection, and importantly, minimise viral spread. Mucosal vaccination, including protein-based vaccines with the inclusion of appropriate adjuvants, have proven advantageous in vaccine studies for multiple respiratory pathogens. We tested a novel subunit vaccine, consisting of SARS-CoV-2 Spike protein with a TLR2-stimulating adjuvant, delivered peripherally (sub-cutaneously) or mucosally (intra-nasally) to mice. Vaccination by either route led to substantial serum anti-Spike IgG titres, and high neutralising titres when tested against a lentivirus expressing SARS-CoV-2 Spike, or SARS-CoV-2 virus. Importantly, mucosal vaccination generated anti-Spike IgA, as well as increased neutralising antibodies in both the serum and airways. Additionally, mucosal vaccination facilitated increased lung Spike-specific $CD4^+$ T-cell responses. In the pulmonary environment, TLR2 is expressed by both respiratory epithelia and immune cells. Using TLR2 deficient chimeric mice, we determined that TLR2 expression in either compartment facilitated early innate responses to mucosal vaccination. By contrast, TLR2 on hematopoietic cells was essential for optimal lung-localised, antigen-specific responses. In K18-hACE2 mice, vaccination provided complete protection against disease and sterilising lung immunity against SARS-CoV-2 challenge. Mucosal vaccines may therefore provide a powerful strategy to generate local protective responses against SARS-CoV-2 and other respiratory viruses, with potential to reduce risk of infection and transmission.

85

High-dimensional spatial analysis of the tumour-microenvironment to determine metastatic disease progression and response and resistance to therapy.

Angela L Ferguson[1]

1. Infection, Immunity and Inflammation theme, School of Medical Sciences, Faculty of Medicine and Health, The University of Sydney , Sydney, NSW, Australia

Content unavailable at time of print.

86

Tuft cells regulate inflammation in the lung during influenzaA virus infection

Jacqueline Marshall[1], Gang Liu[1], Ridhima Wadhwa[1], Angelica Katsifis[1], Elinor Hortle[1], Shatarupa Das[1], Scott N Byrne[2, 3], Michael Buchert[4], Gabrielle Belz[5], Philip M Hansbro[1]

1. Centre for Inflammation, Centenary Institute and University of Technology Sydney, School of Life Sciences, Faculty of Science, Sydney, NSW 2007, Australia

2. School of Medical Sciences, Faculty of Medicine and Health, The University of Sydney, Sydney, New South Wales, Australia

3. Westmead Institute for Medical Research, Centre for Immunology and Allergy Research, Sydney, New South Wales, Australia

4. Olivia Newton-John Cancer Research Institute, School of Cancer Medicine, La Trobe University, Melbourne, Australia

5. The University of Queensland Diamantina Institute, Woolloongabba, Brisbane, Queensland, Australia

Tuft cells are rare, solitary, specialised epithelial cells found in most mucosal tissues. They have important roles in initiating and propagating immune responses in the gastrointestinal tract. However, the role of tuft cells in the respiratory tract has not been extensively studied, and their potential roles in respiratory inflammation during lung infection remains unclear. In this study, we investigate the role of airway tuft cells during inflammation in a mouse model of influenza A virus (IAV) infection. Double cortin-like kinase 1 (DCLK1) is a widely used marker of murine tuft cells. We used a tamoxifen inducible DCLK1 deleter mouse to deplete DCLK1+ cells from C57BL/6 mice, then infected them with 33 p.f.u. of A/PR8 H1N1 IAV or sham. At day 7 post infection, DCLK1 deleter mice had significantly reduced numbers of total leukocytes in bronchoalveolar lavage fluid, particularly a significant decrease in total numbers of neutrophils compared to WT controls in cytospins. IAV infected DCLK1 deleter mice also had no changes in neutrophil numbers in the lung tissues but significantly increased total numbers of neutrophils in the blood compared to WT controls by flow cytometry. Infected deleter mice had increased mRNA expression of IL-1b, IL-6, CXCL-1 and IFN-Y in the lungs after 7 days post infection compared to WT controls. Our data indicate that airway tuft cells contribute to inflammation in the lung during flu infection.

87

Local and systemic effects of narrowband UVB irradiation in mice

Rachael A Ireland[1, 2], Benita CY Tse[1], Anneliese S Ashhurst[1], Anthony S Don[1], Scott N Byrne[1, 2]

1. University of Sydney, Camperdown, NSW, Australia

2. Westmead Institute of Medical Research, Westmead, NSW, Australia

Ultraviolet radiation stimulates local and systemic immunomodulatory effects in a wavelength-dependant manner. Narrowband UVB (NBUVB) phototherapy is a common and effective treatment for inflammatory skin diseases including psoriasis, but its mechanism of action is not fully understood. This study aims to characterise local and systemic changes in mice following NBUVB irradiation. In a model of contact hypersensitivity, a single exposure to 3 J/cm^2 NBUVB suppressed the response to an irritant applied at an unirradiated site. Like exposure to solar simulated UV (ssUV), this immune suppressive dose of NBUVB resulted in Langerhans cell depletion and dermal neutrophil infiltration. Mast cells are a key mediator of ssUV-induced immune suppression, but dermal mast cell frequency was not altered by single or repeated exposure to NBUVB. NBUVB irradiation also generated fewer changes in both the plasma lipidome and lymphocyte recirculation compared to ssUV. However, NBUVB suppressed antigen-specific T cell cytolytic activity *in vivo*. NBUVB is a potent local immunomodulator that appears to suppress systemic immunity through different mechanisms to ssUV. Understanding the immunomodulatory effects of NBUVB will help identify the forms of phototherapy most likely to be effective for treating a wider range of diseases.

Artificial Intelligence Based Diagnostic Software for Atypical Femur Fractures

Hanh H Nguyen[1], Duy T Le[1], Cat Shore-Lorenti[1], Hengcan Shi[2], Roger Zebaze[1], Frances Milat[3], Shoshana Sztal-Mazer[4], Vivian Grill[5], Roderick Clifton-Bligh[6], Jianfei Cai[2], Peter R Ebeling[1]

1. Department of Medicine, Monash University, Clayton, Victoria, Australia

2. Department of Information Technology, Monash University, Clayton, Victoria, Australia

3. Department of Endocrinology, Monash Health, Clayton, Victoria, Australia

4. Department of Endocrinology and Diabetes, Alfred Health, Melbourne, Victoria

5. Department of Endocrinology and Diabetes, Western Health, Footscray, Victoria

6. Department of Endocrinology, Royal North Shore Hospital, Sydney, New South Wales

Background

Despite well-defined criteria for radiographic diagnosis of atypical femur fractures (AFFs)[1], misdiagnosis is common. An AFF diagnostic software could provide timely AFF detection to improve their management and prevent progression of incomplete/contralateral AFFs.

Objective

Develop a semi-supervised artificial intelligence (AI)-based application using deep learning models (DLMs) to train algorithms to diagnose AFFs from femur X-rays.

Methods

Pre-operative complete AFF(cAFF), incomplete AFF(iAFF), typical femoral shaft fracture(TFF), and non-fractured femoral(NFF) X-ray images in anterior-posterior view were used. AFFs were defined as per 2014 ASBMR case definition[1]. Fractures were labelled using bounding boxes in Conda. All images were used to train and test the model using a 5-fold cross validation approach. Convolutional neural networks (CNNs) were trained to identify AFF diagnostic features. The DLMs were built using a pretrained (ImageNet dataset) ResNet backbone with the proposed Box Attention Guide (BAG) module. The model's attention beta was visualised. Precision (result relevancy), recall (prediction performance within a category), and F1 score (precision-recall, overall prediction performance) were measured.

Results

The dataset included 2015 radiographs from 1014 patients. The number of cAFF, iAFF, TFF and NFF radiograph labels were 213, 49, 394 and 1359, respectively. The model achieved high precision, recall and F1-score for classifying cAFF X-rays (96%, 94%, and 95%, respectively), while iAFFs were detected with 86% precision, 82% recall and an F1-score of 83%. High precision, recall and F1-scores were also achieved for classifying TFFs (96%, 97%, 97%, respectively) and NFFs (99%, 99%, 99%, respectively).

Conclusion

A DLM trained on femoral X-rays was able to classify cAFF, TFF, and NFF X-rays with excellent precision and accuracy. Accurate AI-based AFF diagnostic software has the potential to improve AFF diagnosis, reduce radiologist error, and allow urgent intervention, thus improving patient outcomes. Further research to validate this model in a larger, well-phenotyped dataset is underway.

1. Shane E, Burr D, et al. Atypical subtrochanteric and diaphyseal femoral fractures: second report of a task force of the American Society for Bone and Mineral Research. JBMR 29(1)(2014)1-23.

Variance in Estimated Strength Along the Femoral Neck and Radius is Accounted for Differences in Macro- and Micro-architecture, not Bone Mass

Ali Ghasem-Zadeh[1], Naghmeh Firouzi[2], Olga Panagiotopoulou[3], Phil Salmon[4], Narelle McGregor[5], Rita Hardiman[6], Natalie Sims[5], Ego Seeman[1]

1. Departments of Endocrinology and Medicine , Austin Health, the University of Melbourne, Heidelberg, VIC, Australia

2. Preclinical Laboratory, Department of Medicine , Tehran University of Medical Sciences, Tehran, Iran

3. Monash Biomedicine Discovery Institute, Department of Anatomy & Developmental Biology, Monash University, Melbourne, VIC, Australia

4. Bruker Micro-CT, Kontich, Belgium

5. Bone Cell Biology & Disease Unit, St. , Vincent's Institute of Medical Research, Melbourne, VIC, Australia

6. Melbourne Dental School, Faculty of Medicine, Dentistry and Health Sciences, , The University of Melbourne, Melbourne, VIC, Australia

Introduction Resistance to fracture is achieved by modelling and remodelling adding bone to, or removing bone from, its periosteal (external) and three (endocortical, intracortical, trabecular) components of its endosteal (internal) surfaces. These cellular events modify the spatial distribution and mineral content of the volume of bone without necessarily altering its mass. For example, similar amounts of bone are used to assemble adjacent cross sections differing in size, shape and microarchitecture along a tubular bone.[1,2] As these studies were confined to regions only ~36 mm in length, we hypothesized that, if this observation is confirmed in whole post-mortem specimens, the variance within a cross-section, and from cross-section to cross-section along a bone will be accounted for by focal differences in macro- and micro-architecture, not mass.

Methods We quantified macro-structure of the cross-sections of 5 radii and 5 femora from human post-mortem specimens using CT-Scan (300 microns), and micro-structure of the cross-sections of the distal and proximal metaphyseal-diaphyseal regions (1/3 of bone length) of 18 radii and 5 femora using HR-pQCT (82 micron). Bone cross sectional area, moment of inertia and cortical thickness were measured using Bone J and 3Matic software for CT images. Finite element analysis (FEA) was used to estimate bone strength.

Results Bone mass was constant along diaphyseal regions of radii, femoral neck and distal femur (figure). Along the metaphyseal regions, the constant mass was fashioned with a large void volume and high surface area/matrix volume forming mainly trabecular bone. At the mid-diaphyseal regions the same mass was fashioned with small intracortical and medullary void volumes and low surface area/matrix volume forming cortical bone. Preliminary FEA showed a reduction in strains in areas with greater cortical thickness and moment of inertia.

Conclusion Maintaining optimal focal strain is achieved by diversity in structure more than mass.

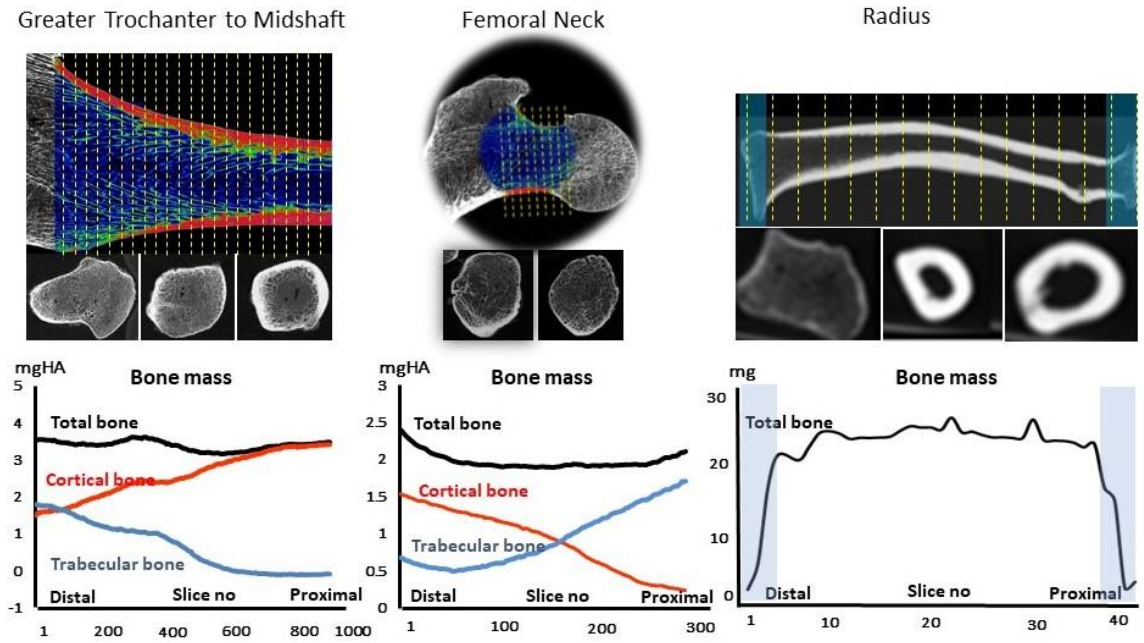

Fig. Coronal section and axial images of cross sections along the greater trochanter to midshaft, femoral neck, and radius. For each region, the same amount of bone mass is used to assemble each cross-section using different void volumes thereby achieving different size, shape and proportions of cortical and trabecular bone.

1. Ghasem-Zadeh A, et al. Bone. 2017 Aug; 101:206-213. PMID: 28502884 2.Zebaze RM, et al. J Bone Miner Res. 2007 Jul;1055-61. PMID: 17501625.

90

Association between automated abdominal aortic calcification 24 scoring obtained from lateral spine images with long-term fracture risk: the Perth Longitudinal Study of Ageing Women

Marc Sim[1], Naeha Sharif[2], Zulqarnain Gilani[2], John T Schousboe [3], Doug Kiel[4], Richard L Prince[5, 1], David Suter[2], Joshua R Lewis[1]

1. School of Medical & Health Sciences, Edith Cowan University, Joondalup, Western Australia, Australia

2. School of Science, Edith Cowan University, Joondalup, Western Australia, Australia

3. Park Nicollet Clinic and HealthPartners Institute, University of Minnesota, Minnesota, United States

4. Marcus Institute for Aging Research, Harvard Medical School, Boston, MA, United States

5. Medical School, The University Western Australia, Perth, Western Australia, Australia

Publish consent withheld

1. Lewis JR, Eggermont CJ, Schousboe JT, Lim WH, Wong G, Khoo B, Sim M, Yu M, Ueland T, Bollerslev J, Hodgson JM. Association between abdominal aortic calcification, bone mineral density, and fracture in older women. Journal of Bone and Mineral Research. 2019 Nov;34(11):2052-60.

91

Agreement and associations between bone variables assessed via standard and high-resolution peripheral quantitative computed tomography

Jakub Mesinovic[1, 2], David Scott[1, 2], Cat Shore-Lorenti[2], Roger Zebaze[2], Mícheál Ó Breasail[3], Camelia Lim[2], Zihui Ling[2], Peter Ebeling[2], Ayse Zengin[2]

1. Institute for Physical Activity and Nutrition (IPAN), Deakin University, Burwood

2. Department of Medicine, Monash University, Clayton

3. Population health Sciences, University of Bristol, Bristol

Introduction: Comparisons of bone variables measured by two commonly used three-dimensional imaging modalities, peripheral quantitative computed tomography (pQCT) and second-generation high-resolution pQCT (HR-pQCTII), are limited. We assessed agreement and associations between volumetric bone mineral density (vBMD) and bone strength parameters at the radius and tibia via pQCT and HR-pQCTII.

Methods: Thirty older adults aged >50 years were recruited. Total, trabecular and cortical vBMD assessed at the radius and tibia by pQCT (both: 4%; radius: 33%; tibia: 38%) and HR-pQCTII (both: 4% and 30%). Stress-strain index (SSI) and bone stiffness were assessed at the proximal radius and tibia via pQCT and HR-pQCTII, respectively. Bland-Altman plots assessed agreement between pQCT and HR-pQCTII parameters. Pearson correlations and linear regression explored relationships between bone variables and proportional bias, respectively.

Results:

Outcome	pQCT mean ± SD	HR-pQCT mean ± SD	Correlation Coefficient	Mean Difference (95%CI)	Limits of Agreement	P-value*	β-coefficient	P-value**
Radius								
Total vBMD (g/cm^3)	283.7 ± 57.6	236.3 ± 66.8	0.86 (<.001)	47.4 (34.3, 60.6)	-19.1, 114.0	<.001	-0.16	0.15
Trabecular vBMD (g/cm^3)	191.4 ± 39.6	149.3 ± 40.6	0.95 (<.001)	42.1 (37.0, 47.1)	16.6, 67.5	<.001	-0.03	0.70
Cortical vBMD (g/cm^3)	1179.0 ± 30.7	1081.3 ± 29	0.84 (<.001)	97.7 (90.8, 104.7)	64.8, 130.7	<.001	0.06	0.62
Tibia								
Total vBMD (g/cm^3)	281.4 ± 42.7	226.2 ± 42.8	0.99 (<.001)	55.2 (52.7, 57.7)	42.2, 68.2	<.001	0.00	0.94
Trabecular vBMD (g/cm^3)	240.7 ± 39.0	191.9 ± 37.7	0.94 (<.001)	48.8 (43.8, 53.7)	23.3, 74.2	<.001	0.03	0.62
Cortical vBMD (g/cm^3)	1152.6 ± 30.8	1004.1 ± 32.9	0.84 (<.001)	148.5 (141.6, 155.5)	113.5, 183.5	<.001	-0.07	0.55

* - one-sample t-test; **- linear regression

There was systematic bias (range: 9-26%) between pQCT and HR-pQCTII vBMD variables at the radius and tibia (all P<0.001; Table). Proportional bias was not observed between absolute vBMD measures at any site (all P>0.05) but was observed for percentage mean differences in total and trabecular vBMD at the distal radius and tibia (all P<0.05); participants with lower vBMD had higher percentage mean differences. pQCT- and HR-pQCTII-determined total, trabecular and cortical vBMD at the radius were strongly correlated (all r>0.8 and P<0.001). SSI was strongly correlated with bone stiffness at the proximal radius (r=0.93) and tibia (r=0.93).

Conclusion: Systematic bias exists between pQCT- and second-generation HR-pQCT-determined vBMD measurements at the radius and tibia, so these imaging modalities cannot be used interchangeably. Proportional bias in total and trabecular vBMD percentage mean differences suggests bias is more pronounced in those with poorer bone health. Although there was poor agreement between pQCT and HR-pQCTII, bone density and strength estimates derived via both imaging modalities were strongly correlated and likely have similar fracture prediction capabilities.

92

Contribution of local density variation to micro-finite element analysis in pediatric HR-pQCT

Andrew J Burghardt[1], Jin Long[2], Tandy Aye[2], Kyla Kent[2], Ariana Strickland[2], Mary B Leonard[2]

1. University of California San Francisco, San Francisco, CA, United States

2. Stanford University, Stanford, CA, USA

Micro-finite element analysis (μFEA) of HR-pQCT images typically assumes homogenous material properties. This approach does not account for variability in tissue density, which is high during periods of rapid growth. Alternatively, material properties can be assigned proportional to each element's BMD. Our objective was to evaluate the contribution of local density by comparing stiffness derived from homogenous and density-scaled μFEA in pediatric HR-pQCT.

The density-modulus relation was fit to a power function:

$E(x,y,z)=E_t*[BMD(x,y,z)/BMD_t]^{\gamma}$

HR-pQCT scans from a cohort of young adults (n=42;age:21-30) were assumed to approximate homogenous properties (Fig1a). Therefore, in this population, optimization of the power equation coefficients should minimize the RMS difference between stiffness derived by scaled and homogenous models. We assumed the maximal density of fully mineralized bone (BMD_t) to be 1200mg/cm^3. To investigate how the optimized density-modulus function impacts μFEA outcomes in pediatric HR-pQCT, we applied this model to tibia and radius scans from a pediatric cohort (n=214;age=5-20). Differences were calculated by tanner stage. Regression analysis was used to evaluate the association with cortical bone features.

In young adults, minimization of RMSD of homogenous and density-scaled μFEA stiffness yielded power coefficient γ=2.25 and maximal modulus E_t=15,974MPa (RMSD=7.9%;Fig1b). In the pediatric cohort, homogenous μFEA stiffness was, on average, significantly higher than density-scaled stiffness (RMSD=13.8%,p<0.01,Fig1c). Differences tended to increase by Tanner stage and were negatively associated with Ct.TMD (tibia:r^2=0.48;radius:r^2=0.73;p<0.0001).

In pediatric subjects, numerically higher μFEA-derived stiffness computed using homogenous tissue property assumptions likely reflects overestimation of the material properties themselves as well as a sub-optimal fine-structure segmentation that systematically overestimates bone volume. This differential increases with maturation. By accounting for tissue heterogeneity and providing threshold independence, density-scaled material properties likely improve the accuracy of μFEA for pediatric HR-pQCT, particularly across maturational stages and in the context of mineralization abnormalities.

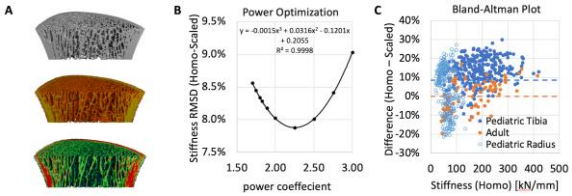

Fig. 1 (a) 3D visualization of homogenous model (top), density-scaled model (middle), with von Mises stress distribution of the density-scaled model (bottom); (b) Minimization of stiffness RMSD by homogenous vs scaled μFEA yields optimal value of power coefficient γ=2.25; (c) Bland-Altman Plot of Homogenous vs. Scaled μFEA Stiffness for adult (orange) and pediatric (blue) cohorts.

93

Translational Orthopaedics from the Perspective of an Academic Surgeon

Ross Crawford[1]

1. Queensland University of Technology, Chermside, QUEENSLAND, Australia

Universities are desperate to turn academic outputs into technologies that are used to deliver better outcomes for patients and to drive an income for the university. Unfortunately this has been rarely successful and in this talk I will explain my thoughts on why the current structure of universities is not likely to change this success rate. I will also explore the contribution of research to the advancement of orthopaedic surgery to date, address the challenges/barriers for translating orthopaedic research into clinical practice. Finally we will look at current/future technologies that can best facilitate translation of research into clinical practice.

Development of a patient specific workflow for the corroboration of FE models with clinical migration data: A case study of the implanted acetabulum

Stuart Callary[1, 2], Khosro Fallahnezhad[3], John Arnold[4], Jasvir Bahl[2], Dominic Thewlis[2], Bogdan Solomon[1, 2], Mark Taylor[3]

1. Orthopaedics and Trauma, Royal Adelaide Hospital, Adelaide, SA, Australia

2. Centre for Orthopaedic and Trauma Research, The University of Adelaide, Adelaide, SA, Australia

3. Medical Device Research Institute, Flinders University, Adelaide, SA, Australia

4. Sport & Exercise Science, University of South Australia, Adelaide, SA, Australia

While Finite Element (FE) studies have made valuable contributions to the understanding of the acetabular component mechanical environment, there is a lack of direct comparison between FE predictions and the actual performance of the implant *in vivo*. Radiostereometric Analysis (RSA) has been widely used to accurately monitor implant migration *in vivo*. The aims of this study were to 1) develop an improved FE modelling work flow, that includes musculoskeletal modelling to estimate the patient specific forces, to predict acetabular component stability; and 2) validate FE model predictions against patient-matched in vivo measurements of acetabular component stability using RSA.

Eight patients underwent primary THR and received an uncemented acetabular component. Postoperative CT scans and RSA exams were performed on day three; and gait analysis and RSA exams were performed at six weeks, three months, one and two years post-surgery. Patient-specific hemi-pelvis FE models[1] were developed to calculate the mean elastic modulus (MEM) of cancellous bone, composite peak micromotion (CPM) and implant contact area during a complete level gait walking cycle. *In vivo* RSA 3D translation and rotation of the acetabular component were calculated using UmRSA software.

There was good conformity between predicted CPM and MEM and the *in vivo* 3D RSA migration at six weeks. The two cases with the largest predicted MEM (>920MPa) and lowest CPM (<20µm) were confirmed to have the lowest *in vivo* RSA 3D migration (<0.14mm). The two cases with the largest predicted CPM (>80µm) and least MEM (>480MPa) were confirmed to have the largest *in vivo* RSA 3D migration (>0.78mm).

The results of this study are the first patient-matched *in vivo* validation of FE predictions of implant stability. While the sample size of this pilot study was low, using prospectively matched CT, gait and RSA examinations may allow further improvements of FE model predictions.

1. O'Rourke D, Al-Dirini R, Taylor M, J Orthop Res 2018.36(3):1012-23.

Sex differences in a pre-clinical model of injury-induced osteoarthritis

Sasha Gonzales-malcolm[1], Carina Blaker[2], Christopher Little[2], Sanaa Zaki[1]

1. Sydney School of Veterinary Science, University of Sydney, Camperdown, NSW, Australia

2. The Kolling Institute of Medical Research, St Leonards, NSW, Australia

Figure 1a: Pain behaviour response following ACLR or sub-critical injury in C57BL female (a, c) and male (b, d) mice. Tactile allodynia = von frey test; Hindlimb weight bearing = forceplate right:left hindlimb weight distribution. Graphs depict individual replicates with connecting line set at mean.

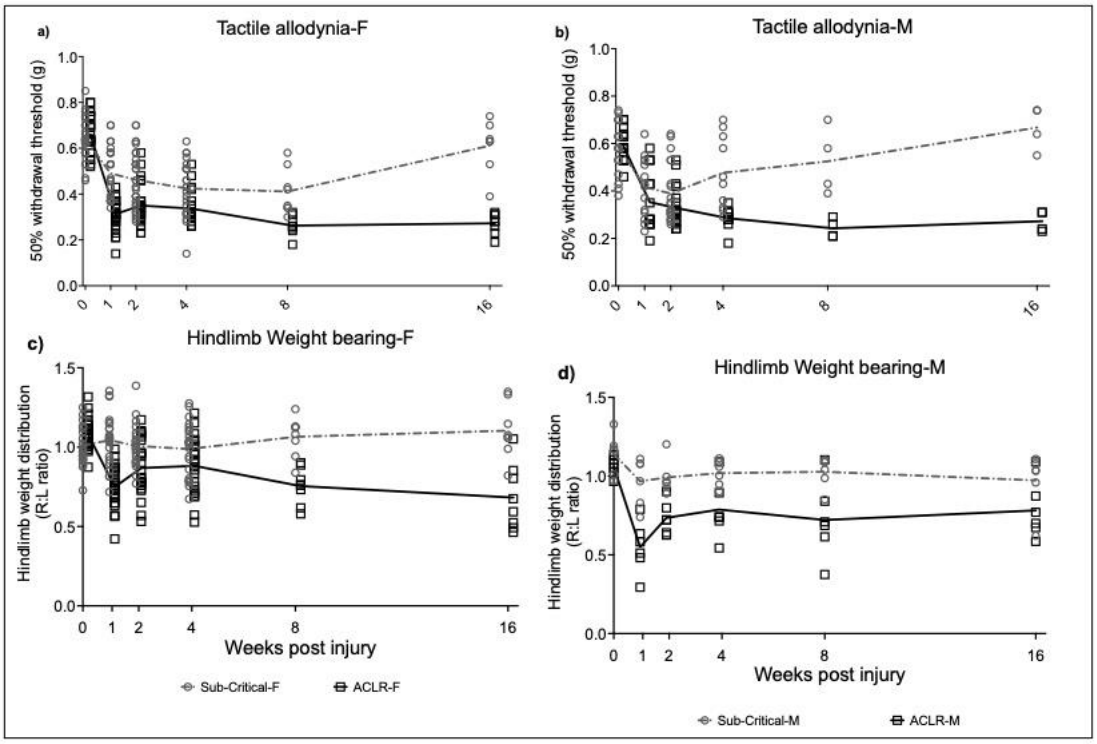

Figure 1b: Knee joint tissue histopathology scores for articular cartilage structural damage (a) and proteoglycan loss (b) at 8- and 16-weeks post ACLR or sub-critical injury in male and female C57BL mice.

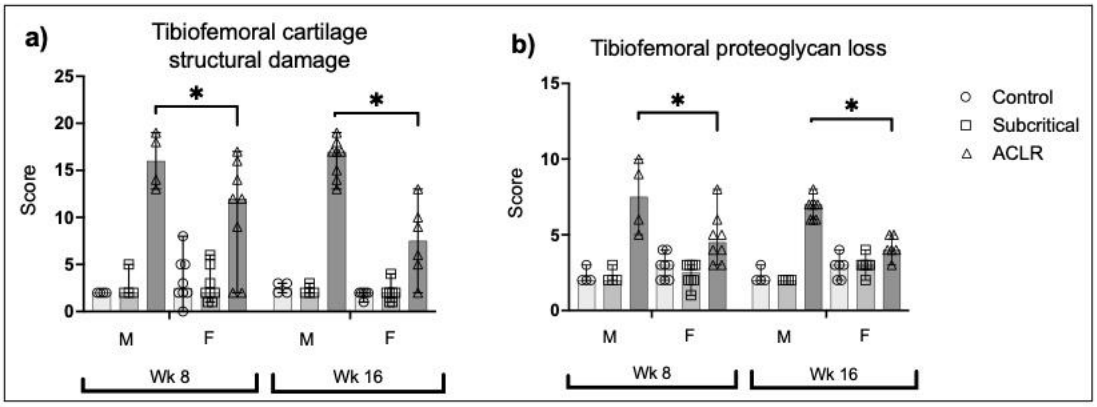

Background: Osteoarthritis (OA) is a complex heterogeneous joint disease. Prevalence is higher in women who also suffer worse symptoms than men. However, despite well-established sex differences most pre-clinical research is conducted in males. Consequently, the female OA animal model phenotype is poorly defined. We investigated differences in male and female OA severity and progression in a well-established murine model of post-injury OA to better characterise the female phenotype in this model.

Methods: Male and female 10-week C57BL6 mice had unilateral anterior cruciate ligament rupture (ACLR) to induce knee OA or sub-critical injury. Tactile allodynia, local hyperalgesia and hindlimb weight distribution (HLWD) were measured at baseline and week-1/-2/-4/-8/-16. Joints were harvested week-4/-8/-16 post-injury. Joint-wide histopathology was quantified by scoring articular cartilage (AC), synovium, subchondral bone (SCB), menisci & osteophyte/enthesophyte pathology. Associations between different histology scores were determined using Kendall's tau-b partial correlation coefficients.

Results: Both males and females developed allodynia, mechanical-hyperalgesia and altered HLWD. Sex differences were only observed in sub-critical injury mice. Despite similar pain, sex differences were identified in the measured histopathology outcomes in ACLR mice. Males had worse OA pathology than females for AC damage and proteoglycan loss at week-8 and 16. Osteochondral and meniscus damage was worse in males. In contrast, females demonstrated greater anterior meniscus bone formation (week-8) and posterior pannus (week-16). There were no significant sex differences for SBC sclerosis, osteophyte and enthesophyte formation. Sex-specific tissue pathology correlations were observed predominantly in females; positive correlations between posterior joint fibrosis and proteoglycan loss (r=0.52) and SCB sclerosis (r=0.60), whole joint AC damage and pannus (r=0.55), and posterior joint AC damage and SCB sclerosis (r=0.77).

Conclusions:These findings define the female phenotype of an established OA model and suggest the mechanisms driving OA joint pathology are sex-specific, thus highlighting the current 'sex' gap in pre-clinical OA research.

96

Can RSA measurements predict long-term acetabular implant loosening earlier than the current two-year time point?

Chan Hee Cho[1], John Abrahams[1, 2], Raissa Katembwe[1], Andrew Baker[1], Stuart Callary[1, 2]

1. Centre for Orthopaedic and Trauma, The University of Adelaide, Adelaide, South Australia, Australia

2. Department of Orthopaedics and Trauma, Royal Adelaide Hospital, Adelaide, SA, Australia

Radiostereometric analysis (RSA) is the most accurate method to measure acetabular migration in vivo. RSA migration measurements at two years have been shown to predict long term loosening [1]. New implant designs now require clinical evidence to gain CE marking due to changes to European Union Medical Device Regulations in 2021. It would be optimal to have the shortest validated clinical surrogate measure for long term success. Hence the aim of this meta-analysis was to investigate if RSA migration measurements earlier than two years can predict later loosening.

A systematic review of all RSA acetabular migration studies was performed in accordance with PRISMA guidelines (PubMed, Scopus and Embase databases). Migration results of each reported cohort were analysed at all early timepoints including three months, six months, one year and two years. Implant type, fixation method and additional screw fixation were investigated as independent factors that may influence the pattern of early migration.

61 RSA studies (including 1579 acetabular components) reported two year migration results of 33 different implants. There was no difference in the median migration of cemented (0.16mm) and uncemented (0.14mm) components at two years (p=0.36). The migration of uncemented components with additional screw fixation (0.157mm) was not significantly different to components without screws (0.161mm, p=0.94). RSA migration was reported at both one and two years for only 25 cohorts and 11 of these cohorts had mean migration above the recommended threshold of 0.2mm at two years. One year migration data correctly identified 10 of these 11 cohorts having a mean migration above the threshold at one year.

This meta-analysis provides the first evidence that RSA migration measurements at one year may be used to predict long-term loosening of acetabular components. This is significant for orthopaedic companies requiring the earliest clinical evidence available to introduce new implants.

1. Pijls B, et al. Acta Orthop. 2012;83(6):583-91.

97

Evaluating the effectivity of treatment options for intracellular *S. aureus* infections in osteomyelitis

Anja R Zelmer[1], Nicholas J Gunn[1], Renjy Nelson[2, 3], Bogdan L Solomon[2, 1], Stephen P Kidd[4], Katharina Richter[5], Gerald J Atkins[1]

1. Centre for Orthopaedic and Trauma Research, Faculty of Health and Medical Sciences, University of Adelaide, Adelaide, SA, Australia

2. Royal Adelaide Hospital, Adelaide, SA

3. Department of Infectious Diseases, Central Adelaide Local Health Network, Adelaide, SA, Australia

4. Australian Centre for Antimicrobial Resistance Ecology, and Research Centre for Infectious Disease, University of Adelaide, Adelaide, SA, Australia

5. Richter Lab, Department of Surgery, Basil Hetzel Institute for Translational Health Research, University of Adelaide, Adelaide, SA, Australia

Staphylococcus aureus (SA), the predominant pathogen in human osteomyelitis, is known to persist by forming intracellular reservoirs, including in bone cells, promoting decreased antibiotic susceptibility. However, there are no evidence-based treatment guidelines for intracellular SA infections in osteomyelitis. We addressed this by systematically reviewing the literature and testing candidate antibiotics in a clinically relevant *in vitro* assay.

A systematic review was conducted for the efficacy of antibiotics against intracellular SA infections relevant to osteomyelitis. Mostly, osteoblasts and macrophages have been used to test immediate short-term activity against intracellular SA, with a high variability in methodologies. Some extant evidence supports that rifampicin, oritavancin, linezolid, moxifloxacin and oxacillin may be effective intracellular treatments. For potentially useful antibiotics identified, the minimal inhibitory concentration (MIC) against 11 clinical osteomyelitis SA-isolates was determined. We tested those further, which are reported to reach a higher concentration in bone than their respective MIC. Thus, rifampicin, oxacillin, linezolid, levofloxacin, oritavancin and doxycycline were tested in human SaOS2-osteocyte infection models of acute (1d) or chronic (14d) infection for the ability to reduce intracellular SA numbers at 1x/4x/10x the MIC for 1d or 7d in each model.

Of the antibiotics tested to date, rifampicin linezolid and levofloxacin showed to be effective treatments for osteomyelitic intracellular SA infection, while oxacillin and doxycycline have proved ineffective. The combined approach of a systematic review and disease-relevant *in vitro* screening will potentially inform as to the best approach for treating osteomyelitis where intracellular SA infection is confirmed or suspected.

98

The Increased Hospital Cost of Treating Septic Revision Total Hip Arthroplasty

Aaron Hammat[1], Chan Hee Cho[1], Bogdan Solomon[1, 2], Stuart Callary[1, 2]

1. Centre for Orthopaedic and Trauma Research, The University of Adelaide, Adelaide, SA, Australia

2. Department of Orthopaedics and Trauma, Royal Adelaide Hospital, Adelaide, SA, Australia

Revision Total Hip Arthroplasty (THA) are complex procedures with varying diagnoses and treatment methods that have historically been difficult to code and cost appropriately. The aim of this study was to perform a meta-analysis of revision THA hospital costs by 1) diagnosis, 2) treatment and 3) hospital costing mechanism used.

A meta-analysis investigated the effect of diagnosis (infection, fracture, dislocation, and loosening); treatment method (DAIR, partial revision, 1-stage revision, 2-stage revision); and the reported costing mechanism calculation (Diagnosis Related Group (DRG) costing, International Classification of Diseases (ICD), US Medicare Estimated (USME) and independent cost modelling (ICM)) on reported revision THA hospital costs. All costs were adjusted for inflation and converted to AUD for statistical analysis.

The review identified 54 studies from 13 different countries. Only 14 studies reported revision THA costs by diagnosis. Six individual studies reported septic revisions to cost 69% to 193% more than aseptic revision THAs. The unadjusted pooled reported mean cost for septic revision THA was $AU94,313 (range $18,429 to $215,162) in 12 studies compared to $39,922 for aseptic revisions ($7,454 to $120,409) in 11 studies. Only one study separated aseptic revisions by diagnosis and reported the mean cost of fracture ($42,437), loosening ($33,438), and dislocation ($29,607). The cost of different treatment methods was only investigated in one study. 12 studies used USME; 11 ICM; 3 DRG, 1 ICD, and 24 studies did not report the costing mechanism calculation used.

This meta-analysis found septic revision THA costs to be on average 136% more than aseptic revisions. The large variation in reported revision THA costs is likely due to the different costing mechanism used, however the method was not reported in over half of the studies in this review. Revision THA costs need further detailed investigation to enable overburdened healthcare systems to budget appropriately.

99

Making personalization of cancer treatment a reality with Spatial transcriptomics

Jazmina L Gonzalez-Cruz[1], Andrew Causer[2], Debottam Sinha[1], Min Teoh[2], Jerry Tay[1], Rahul Ladwa[3, 4], Christopher Perry[4, 5], Ian Frazer[1], Benedict Panizza[4, 5], Quan Nguyen[2]

1. The University of Queensland Diamantina Institute, Brisbane, QLD, Australia

2. Institute of Molecular Biology, The University of Queensland, Brisbane, QLD, Australia

3. Department of Medical Oncology, Princess Alexandra Hospital, Brisbane, QLD, Australia

4. Faculty of Medicine, , The University of Queensland, Brisbane, QLD, Australia

5. Department of Otolaryngology, Princess Alexandra Hospital, Brisbane, QLD, Australia

Human Papillomavirus (HPV) is responsible of >70% of all Oropharyngeal Squamous cell carcinoma (OPSCC). Immune checkpoint inhibitors (ICI) are available to treat recurrent metastatic OPSCC patients. Unfortunately, only a <20% of OPSCC patients benefits from this approach.

We postulate that the tumour microenvironment plays a critical role in determining ICI therapy outcome. Therefore, we performed spatial transcriptomics (ST) on tumour tissue isolated from a patient diagnosed with metastatic HPV^+ OPSCC.

The patient's primary OPSCC tumour responded to chemo-radio therapy, followed by Nivolumab (anti-PD-1) therapy to target lung metastasis. After Nivolumab, new OPSCC soft pallet tumours resurged, and Pembrolizumab (a-PD-1) and Lenvatinib (VEGFR inhibitor) were given. This approach initially regressed the secondary OPSCC. However, Lenvatinib's dose was reduced, and OPSCCs recurred.

We performed ST on the OPSCC soft palate tumours and healthy tissue, after Nivolumab treatment. We observed unbiased clustering, based on differentially expressed genes (DEG) of ST array spots, that recapitulated the H&E tissue annotations (i.e., epithelium *vs* muscle). Interestingly, only one cluster, cluster 6, was identified as Oropharyngeal cancer cells, with most of the cells in S and G2M cell cycle phases, indicating that this cluster was the proliferative tumour. The profile of upregulated genes in cluster 6 (49 genes, $\log_2$>1.5, adj.p-value <0.001) included oncogenes (18.4%); poor prognosis biomarkers (24.5%); drug resistance genes (20.40%); known targets (18.4%) including *EGFR* and *VEGFA*; and experimentally-druggable-targets (20.4%). We didn't find PD-1 or PD-L1 expression in the tumour, suggesting that Lenvatinib was mainly responsible for the OPSCC regression, likely due to the high VEGFA levels in cluster 6.

ST data accurately predicted disease evolution in this patient and could be used to generate a list of clinically relevant therapeutic candidates. We foresee that this technology will allow oncologist to accurately personalize cancer management, and open new approaches to drug discovery.

100

Development of a novel compound for the treatment of SCC in organ transplant recipients

James W Wells[1], Margaret Veitch[1], Kim Beaumont[2], Rebecca Pouwer[2], Brian Dymock[2], Andrew Harvey[2], Terrie-Anne Cock[2]

1. The University of Queensland Diamantina Institute, Faculty of Medicine, The University of Queensland, Translational Research Institute, Woolloongabba, QLD, Australia

2. Queensland Emory Drug Discovery Initiative (QEDDI), UniQuest, The University of Queensland, St Lucia, QLD, Australia

Australia has the highest incidence of skin cancer in the world, causing considerable social and economic burden. Indeed, two out of every three Australians are likely to be diagnosed with skin cancer by the age of 70. Organ transplant recipients suffer a greatly increased risk of cutaneous squamous cell carcinoma (SCC) development due to impaired immune surveillance as a consequence of their lifelong regime of prescribed immunosuppressive drugs. We proposed to develop a first in class, topically applied, small molecule for the treatment of SCC in organ transplant recipients receiving immunosuppressive therapy. We found that Compound 1 is able to reverse the anti-proliferative effects of immune suppressing agents in both mouse and human T cells *in vitro*. To investigate whether Compound 1 has an effect on T cell activation and tumour regression *in vivo*, we used a mouse model in which an SCC cell line was derived from UV-irradiated HPV38E6E7-FVB mice. The cell line forms SCCs when injected into immuno-suppressed mice, and regresses when immunosuppression is removed. Twice-daily intratumoural injections of Compound 1 significantly reduced tumour growth in immuno-suppressed mice, compared to Vehicle treated tumours. Treatment with Compound 1 also significantly increased the percentage of activated CD8 T cells within tumours, and their expression of IFN-gamma and TNF-alpha. Furthermore, when CD8 T cells were depleted *in vivo*, Compound 1 was no longer able to reduce tumour growth. In summary, we have demonstrated the efficacy of Compound 1 *in vivo*, and established a key role of CD8 T cells in Compound 1 mediated SCC regression.

101

Is there a role for regulatory T cells in the establishment of Cutaneous Squamous Cell Carcinoma?

Shoaib Anwaar[1], Marcela Montes de Oca[1], Jazmina-Libertad Gonzalez-Cruz[1], James Wells[1]

1. The University of Queensland Diamantina Institute, Faculty of Medicine, The University of Queensland, Brisbane, QUEENSLAND, Australia

Cutaneous squamous cell carcinoma (cSCC) is one of the most prevalent cancers in Caucasian populations, and its aggressive form poses a high risk of metastasis resulting in increased rates of mortality and morbidity. Recurrent and chronic exposure to ultraviolet (UV) radiation from the sun plays a crucial role in the initiation, development, and perpetuation of cSCC. Accumulating evidence suggests that regulatory T (Treg) cells are associated with UV-induced immunosuppression, however, their direct contribution to the establishment of cSCC remains elusive. When mice were exposed to 5 consecutive days of UVB (dose rate 150mJ/cm^2), they showed reduced ear swelling in response to ovalbumin challenge in a contact hypersensitivity assay, suggesting that functional antigen-specific Tregs were induced. Ear swelling responses did not show signs of suppression however, when mice were treated with an anti-CTLA-4 antibody following the cessation of UV treatment. Phenotypically, the expression of Foxp3, FR4, GITR, CTLA-4 and TIGIT on Tregs in the inguinal lymph nodes and spleen of UV-exposed mice did not differ from those in non-UV-exposed mice. Following the treatment of mice with UVB 5 days per week for different time periods (2w, 4w, 6w, 8w), it was determined that only UVB treatment for eight weeks consistently allowed the establishment and growth of tumours following the adoptive transfer of cSCC tumour fragments from donor mice. We aim to target Tregs in these tumour models in our future studies to determine whether Treg depletion or manipulation will reverse the capacity of UV to enable cSCC tumour establishment. Overall, this study will examine the plausibility of Treg manipulation as a preventative strategy to prevent UV-induced cSCC tumour establishment.

102

Physical determinants of vitamin D synthesis

Antony R Young[1]

1. King's College London, London, United Kingdom

Vitamin D synthesis is initiated by conversion of cutaneous 7-dehydrocholesterol (7-DHC) to previtamin D after exposure to solar ultraviolet radiation (UVR). Thereafter, previtamin D undergoes non-photobiological steps to become biologically active vitamin D. The whole process, which is the only well-established benefit of solar UVR exposure, depends on many factors including genetics, age, health, and behaviour. However, the most important factor is the quantity and spectral quality of UVR reaching 7-DHC in skin. Vitamin D synthesis specifically requires ultraviolet B (UVB) radiation (~295-315nm in sunlight) that is the minority component (<5%) of solar UVR. This waveband is also the most important for the adverse effects of solar exposure, including sunburn (erythema) and epidermal DNA damage that is a prerequisite for most skin cancers. The properties of UVB at the Earth's surface depend on many physical and temporal factors such as latitude, altitude, season, time of day and weather. The quantity and spectral quality of UVB reaching 7-DHC also depend on personal, cultural, and behavioural factors. These include epidermal thickness, skin melanin, clothing, body surface area (BSA) exposed, holiday habits, and sunscreen use. There is considerable disagreement in the literature about the role of most of these factors. New recently published data on these controversies will be presented including wavelength dependence (action spectroscopy), BSA, melanin and sunscreen use. Accurate action spectroscopy is essential for risk-benefit analyses from solar exposure. It can be argued that vitamin D supplementation obviates the need for solar exposure, but many studies have shown little benefit from this approach for a wide range of health outcomes. In any case, public health advice must optimize risk versus benefit for solar exposure. It is therefore fortunate that the individual UVB doses necessary for maintaining optimal vitamin D status are much lower than those for sunburn, irrespective of skin melanin.

103

Vitamin D and Health – where is the research heading?

Robert Scragg[1]

1. School of Population Health, University of Auckland, Auckland, NEW ZEALAND, New Zealand

Epidemiological studies over the last 10 years have greatly increased our understanding about the role vitamin D in health. During this time, a tension has arisen between the results from observational studies and randomised controlled trials of vitamin D supplementation. Several cohort studies have reported non-linear inverse associations between vitamin D status, as measured by circulating 25-hydroxyvitamin D concentrations (25(OH)D), and risk of some outcomes such as cardiovascular disease and all-cause mortality, with the increased disease risk being observed in people with 25(OH)D less than 50 nmol/L. In contrast, recent large-scale trials have reported no effect of vitamin D supplementation on major disease outcomes such as cardiovascular disease, cancer, diabetes and mortality, even in subgroup analyses of participants with baseline 25(OH)D levels less than 50 nmol/L. The latter results have been confirmed by mendelian randomisation studies which mostly have not found an association between genetically predicted 25(OH)D and disease outcome. Until now, the inconsistency between observational studies and trials has been assumed to be due to residual confounding leading to spurious inverse associations in the former. However, a major limitation of most mendelian randomisation studies is that they have assumed a linear association between genetically predicted vitamin D status and disease. Recent mendelian studies which have investigated possible non-linear associations have found that disease risk is increased in people with 25(OH)D less than 25-40 nmol/L, confirming the findings of the earlier cohort studies. These new findings and their implications will be discussed.

104

Delayed cortical bone healing due to inactivated Nrf2 signaling pathway in COPD mice

Takayuki Nabeshima[1], Manabu Tsukamoto[1], Yosuke Mano[1], Daisuke Arakawa[1], Ke-Yong Wang[2], Takafumi Tajima[1], Yoshiaki Yamanaka[1], Eiichiro Nakamura[1], Akinori Sakai[1]

1. Department of Orthopaedic Surgery, School of Medicine, University of Occupational and Environmental Health, Kitakyushu, Fukuoka, Japan

2. Shared-Use Research Center, School of Medicine, University of Occupational and Environmental Health, Kitakyusyu, Fukuoka, Japan

Introduction: The influence of bone fracture healing in patients with chronic obstructive pulmonary disease (COPD) is unknown. It has been suggested that the pathogenesis of COPD may involve a dysfunction of the NF-E2-related factor 2 (Nrf2) signaling pathway, a defense mechanism against oxidative stress. We investigated the process of cortical bone remodeling in COPD mice by focusing on Nrf2 and the effect of sulforaphane (SFN), an Nrf2 activator, on delayed cortical bone repair.

Methods: Twelve-week-old male C57BL/6J mice were intratracheally injected with saline (C group) or PPE 0.1U (P group), and a 1.0 mm diameter drill hole was made in the distal femur at 12 weeks after the administration. All mice were sacrificed at day 14 after surgery, and the bone histomorphometry of the generating bone at the drill hole was measured, and the expression levels of Nrf2 and NQO-1 in the same area were evaluated by immunostaining. Next, half of each of the C and P groups were treated with SFN (CS, PS group) subcutaneously 5 times a week, sacrificed at day 14 after surgery, and bone tissue samples were evaluated with the same procedure.

Results: Bone histomorphometry of the generating bone at the drill hole on day 14 showed that bone volume (BV/TV), osteoblast surface (Ob.S/BS), and number of osteoblasts (Ob.N/BS) were significantly lower in the P group than in the C group, but all values were significantly higher in the PS group than in the P groups. Immunostaining showed that Nrf2 and NQO-1 protein expression was decreased in the P group compared to the C group, while the PS group showed protein expression comparable to the C group.

Conclusion: In COPD mice, there was the delayed cortical bone repair due to the impaired bone formation associated with inactivated Nrf2 signaling pathway, and SFN may improve this condition.

105

Can alternative bone measures improve prediction of fracture in individuals with osteopenia or normal BMD?

Kara B Anderson[1], Mohammadreza Mohebbi[1], Pamela Rufus-Membere[1], Natalie K Hyde[1], Didier Hans[2], Lana J Williams[1], Julie A Pasco[1, 3, 4, 5], Mark A Kotowicz[1, 3, 5], Kara L Holloway-Kew[1]

1. Deakin University, Geelong, VIC, Australia

2. Bone & Joint Department, Centre of Bone Diseases, Lausanne University, Lausanne, Switzerland

3. Barwon Health, Geelong, Victoria, Australia

4. Department of Epidemiology and Preventative Medicine, Monash University, Melbourne, Victoria, Australia

5. Department of Medicine-Western Health, Melbourne Medical School, The University of Melbourne, Melbourne, VIC, Australia

Background

Many individuals who sustain a fracture have normal/moderate deficits in bone mineral density (BMD). Recent technologies for assessing fracture risk (trabecular bone score [TBS], advanced hip analysis [AHA] and quantitative ultrasound [QUS])may improve prediction but have not yet been assessed in concert. We aimed to develop a best-fit model of these tools and to assess if this model improves fracture risk prediction over femoral neck BMD alone in those with BMD above diagnostic threshold for osteoporosis.

Methods

Participants (613 men, 395 women, aged 40-92yr) from the Geelong Osteoporosis Study (GOS) were followed from date of assessment to first fracture, death or end of study. BMD was measured at hip and lumbar spine (GE Lunar Prodigy Pro, Madison, WI), TBS was calculated from lumbar spine scans (TBS iNsight V2.2) and AHA was measured from hip scans (GE Lunar, Madison WI). QUS was performed on the left heel using a Lunar Achilles ultrasonometer. Incident fractures were self-reported and verified via radiological report. Cox-proportional hazards and logistic regressions were used to evaluate predictive accuracy, with Harrell's C and area under the Receiver Operating Curve (AUROC) values respectively.

Results

There were 74 fractures in 63 participants (fracture rate: 1.1/1000 person years; 95%CI 0.8-1.4) over a median follow up time of 8.0 (IQR 6.8-8.7) years for men and 4.7 (IQR 3.9-5.3) years for women. Multivariable Cox-proportional hazards modelling for any fracture, including bone parameters of femoral neck BMD, AHA buckling ratio, TBS and QUS stiffness index adjusted for confounders showed a small improvement over adjusted femoral neck BMD alone (Harrell's C: 0.696 vs 0.709; AUROC: 0.682 [95%CI:0.614-0.751] vs 0.696 [95%CI:0.629-0.763]).

Conclusion

Novel techniques for measuring bone showed modest improvements over femoral neck BMD as measured by DXA. Further studies are needed to assess if potential sex related differences exist.

Plant-derived soybean peroxidase stimulates osteoblast collagen biosynthesis, matrix mineralization, and accelerates bone regeneration in a sheep model

Vasilios Panagopoulos[1, 2, 3], Alexandra J Barker[4], Agnieszka Arthur[3, 5], Mark O DeNichilo[6], Romana Panagopoulos[2], Stan Gronthos[3, 5], Peter J Anderson[3, 5, 7, 8], Andrew CW Zannettino[1, 3, 8, 9], Andreas Evdokiou[2]

1. Myeloma Research Laboratory, Adelaide Medical School, Faculty of Health and Medical Sciences, University of Adelaide, Adelaide, SA, Australia

2. Breast Cancer Research Unit, School of Medicine, Discipline of Surgery and Orthopaedics, Basil Hetzel Institute, University of Adelaide, Adelaide, SA, Australia

3. Precision Medicine Theme, South Australian Health and Medical Research Institute, Adelaide, SA, Australia

4. Musculoskeletal Biology Research Laboratory, Clinical and Health Sciences, University of South Australia, Adelaide, SA, Australia

5. Mesenchymal Stem Cell Laboratory, Adelaide Medical School, Faculty of Health and Medical Sciences, University of Adelaide, Adelaide, SA, Australia

6. Centre for Cancer Biology, University of South Australia, Adelaide, SA, Australia

7. Australian Craniofacial Unit, Women's and Children's Hospital and Department of Paediatrics and Dentistry, University of Adelaide, Adelaide, SA, Australia

8. Central Adelaide Local Health Network, Adelaide, SA, Australia

9. Department of Haematology, Royal Adelaide Hospital, Adelaide, SA, Australia

Bone defects arising from fractures or disease represent a significant problem for surgeons to manage and are a substantial economic burden on the healthcare economy. Recent advances in the development of biomaterial substitutes provides an attractive alternative to the current "gold standard" autologous bone grafting. Despite on-going research, we are yet to identify cost effective biocompatible, osteo-inductive factors that stimulate controlled, accelerated bone regeneration.We have recently reported that enzymes with peroxidase activity possess previously unrecognised roles in extracellular matrix biosynthesis, angiogenesis and osteoclastogenesis, which are essential processes in bone remodelling and repair. Here, we report for the first time, that plant-derived soybean peroxidase (SBP) possesses pro-osteogenic ability by promoting collagen I biosynthesis and matrix mineralization of human osteoblasts in vitro. Mechanistically, SBP regulates osteogenic genes responsible for inflammation, extracellular matrix remodelling and ossification, which are necessary for normal bone healing. Furthermore, SBP was shown to have osteo-inductive properties, that when combined with commercially available biphasic calcium phosphate (BCP) granules can accelerate bone repair in a critical size long bone defect ovine model. Micro-CT analysis showed that SBP treated BCP granules significantly increased bone formation within the defects as early as 4 weeks compared to BCP alone. Histomorphometric assessment demonstrated accelerated bone formation prominent at the defect margins and surrounding individual BCP granules, with evidence of intramembranous ossification. These results highlight the capacity of SBP to be an effective regulator of osteoblastic function and may be beneficial as a new and cost effective osteo-inductive agent to accelerate repair of large bone defects.

107

Ankle fractures increase subsequent fracture risk and mortality: The 45 and Up study, a population-based cohort study of New South Wales, Australia

Weiwen Chen[1, 2], Thach Tran[2], Dana Bliuc[2], Robert Blank[2], Fiona Blyth[3], Lyn March[4, 5], Jackie Center[1, 2]

1. St Vincent's Hospital, St Vincent's Hospital Clinical School, Darlinghurst, NSW, Australia

2. Garvan Institute, Darlinghurst, NSW, Australia

3. University of Sydney, Camperdown, NSW

4. Kolling Insitute of Medical Research, Sydney

5. Royal North Shore Hospital, Sydney

Background: Ankle fractures are common but are often not considered to be osteoporotic fractures as they occur in patients with higher bone density.

Objectives: To examine the risk of subsequent fracture and mortality following ankle fractures

Methods: Baseline questionnaire data from the 45 and Up Study (143,070 women and 128,818 men) were linked to the Emergency Department Data Collection (EDDC), Admitted Patient Data Collection (ADPC), Registry of Births, Marriages and Death (RBDM). Fractures were identified from the EDDC and ADPC using the ICD 9, 10, SNOMED and procedure codes. Participants were followed from recruitment (2005-2009) until death or 1/4/2017. Relative survival analysis and Cox proportional hazards regression with fracture as a time-dependent variable were used to quantify the contribution of ankle fracture to subsequent fracture and mortality, respectively.

Results: During a mean follow-up of 8.4± 1.9 years, 1,579 women and 519 men sustained an ankle fracture. Participants who experienced ankle fractures were younger, had higher body weight and fewer co-morbidities than those who experienced other fractures. Ankle fracture patients sustained a subsequent fracture after an average of 2.6± 2.1 years. Following ankle fracture, there was a 5% increased risk of a subsequent fracture in both sexes compared to the overall initial fracture risk. Proximal fractures accounted for 56% of the subsequent fractures Ankle fractures were associated with increased mortality in men (HR: 1.34; 95% CI: 1.02-1.77). Similar trend was seen in women but did not reach significance (HR: 1.10; 95% CI: 0.85-1.42). The presence of diabetes and a subsequent proximal fracture were predictive of the increased mortality in men.

Conclusion: In this healthy cohort, ankle fractures were associated with a modestly increased risk of further fractures and increased mortality in men. Ankle fractures should be considered as an indication for fracture prevention.

Identifying Adult Human Skeletal Stem/Progenitor Cells in the Periosteum

Ye Cao[1], Scott Bolam[1], Helen Murray[1], Anna Brooks[1], Brya Matthews[1]

1. University of Auckland, Auckland, -, New Zealand

Tissue-resident skeletal stem and progenitor cells (SSPCs) support homeostasis and regeneration. The periosteum is critical for fracture healing and mouse periosteum is enriched for SSPCs. Recently human SSCs have been characterized in fetal tissue, but adult human SSCs remain elusive. The aim of this study was to evaluate hSSPC populations in different tissue compartments.

We compared marker expression in human skeletal tissues with a 21-colour flow cytometry panel. Femoral heads were used to isolate matched tissue from 21 patients; specifically bone marrow (BM), trabecular endosteum (or bone-associated cells), femoral neck periosteum, and articular chondrocytes. Markers enriched in the periosteum included CD90, CD34, CD51, and CD26; while CD24 was primarily in the endosteum/BM. Cartilage showed high expression for markers including ALP, CD105, and PDPN and was the only tissue that showed a clear hSSC population as defined previously (1).

Sorted Lin- cells from the periosteum and cartilage formed more fibroblastic colonies (CFU-Fs) than endosteum; while BM Lin- cells did not form colonies. CD90 is one of the SSPC markers that significantly enriched in the periosteum (20.7%), compared with cartilage (11.8%), and endosteum (2.0%). Histologically, CD90 expression was restricted to perivascular cells in the periosteum. After sorting, CD90+ but not CD90- cells from the endosteum and BM formed CFU-Fs. Similar CFU-Fs formed from CD90+ and CD90- cartilage.

We subdivided the CD90+ periosteal population with CD73, CD34, and CD26. CD90+CD34+, the majority of which resided on the periosteum layer, showed the highest CFU-Fs. Single CD90+CD34+ colonies reached confluence faster than any other populations sorted, and 100% showed tri-lineage (osteogenic, chondrogenic, adipogenic) differentiation. Surprisingly, colonies from CD90-CD73+ and CD90+CD34- formed adipocytes spontaneously.

Using cell surface markers, we found that adult hSSC populations vary in different skeletal compartments (Figure). In the periosteum, CD90+CD34+ cells show characteristics of hSSCs in vitro.

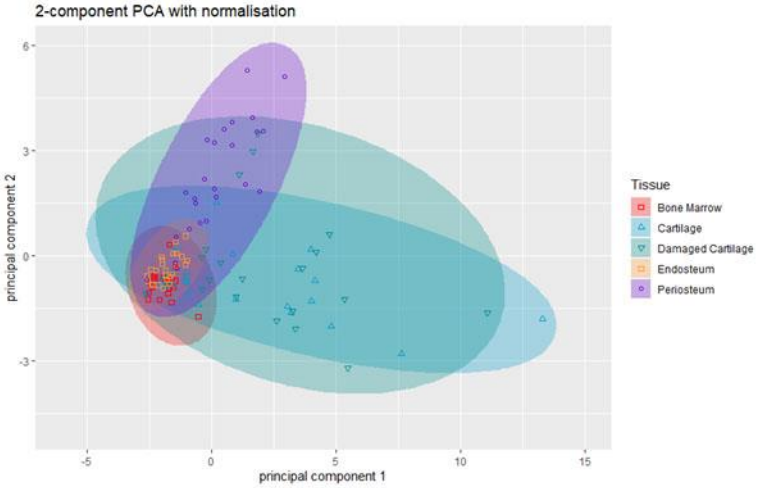

Figure: Principal component analysis visualisation of cell surface marker expression in the Lin- cells from four skeletal tissues (cartilage tissues were split into damaged and undamaged).

1. Chan et al 2018, Cell 175:43

109

Is chronic peripheral vestibular dysfunction associated with bone-related and fall-related indices of fracture risk in community-dwelling older women?

Jayde A Collier[1], Belinda R Beck[1], Benjamin K Weeks[1]

1. Griffith University, Southport, QLD, Australia

Purpose

Peripheral vestibular dysfunction (PVD) is prevalent in older adults, particularly post-menopausal women. PVD greatly increases the risk of falling due to impaired balance and dizziness. Our aim was to investigate whether post-menopausal women with PVD, were at greater risk of fracture by also exhibiting poorer bone-related indices of fracture risk, than healthy post-menopausal women.

Methods

Healthy community-dwelling post-menopausal women (> 60 years) and those with clinically diagnosed PVD were recruited. DXA and pQCT-derived indices of bone and muscle strength and clinical measures of strength and balance, were used to characterise bone-related and fall-related indices of fracture risk. Univariate analyses were used to examine differences in indices of fracture risk between PVD and healthy participants. Correlation analyses were undertaken to investigate relationships between variables within each group.

Results

Women with PVD had lower FN BMD than healthy women (0.74 ± 0.13 g/cm^2 versus 0.83 ± 0.10 g/cm^2, p = 0.027). There were no between-group differences for any pQCT-derived indices of bone or muscle strength. Whilst PVD participants had lower scores on the Dynamic Gait Index compared to their healthy counterparts (18.9 ± 5.4, 22.4 ± 2.24, p < 0.001), there were no between-group differences for any other fall-related measure.

Conclusions

Post-menopausal women with PVD may be at particularly high risk of minimal trauma fracture due to a combination of lower BMD and increased risk of falling. These findings suggest that screening for osteoporosis in PVD populations and for PVD in osteoporotic populations, may be indicated given the high treatability of both conditions.

110

The Regulatory Effect of Macrophages on Osteocytes

Yinghong Zhou[1], Shengfang Wang[2], Yin Xiao[2]

1. The University of Queensland, Brisbane, QLD, Australia

2. Queensland University of Technology, Brisbane, QLD, Australia

It is well-known that both macrophages and osteocytes are critical regulators of bone remodelling, yet there is limited understanding of the macrophage-osteocyte interaction, and how their crosstalk could affect mineralisation. This research aims to investigate the effects of macrophage polarisation on osteocyte maturation and mineralisation process. Indirect co-culture using conditioned medium was applied to investigate the impact of macrophages on osteocyte maturation and mineralisation. Our results identified that osteocytes were confined in an immature stage after the M1 macrophage stimulation, showing a more rounded morphology, higher expression of early osteocyte marker E11, and significantly lower expression of mature osteocyte marker DMP1. Surgically induced osteoarthritis (OA) rat model was used to investigate the macrophage-osteocyte interaction in inflammatory bone remodelling, as well as the involvement of the Notch signalling pathway in the mineralisation process. Immature osteocytes were found in inflammatory bone remodelling areas, showing altered morphology and mineralised structures similar to those observed under the stimulation of M1 macrophages *in vitro*, suggesting that M1 macrophages negatively affect osteocyte maturation, leading to abnormal mineralisation. The Notch signalling pathway was found to be down regulated in M1 macrophage-stimulated osteocytes as well as osteocytes in inflammatory bone. Overexpression of the Notch signalling pathway in osteocytes showed a significant circumvention on the negative effects from M1 macrophage. Taken together, our findings provide valuable insights into the mechanisms involved in abnormal bone mineralisation under inflammatory conditions.

A multi-scale mechanobiological model of skeletal muscle regeneration in typical and pathological conditions

Stephanie Khuu[1], Justin W Fernandez[1, 2], Geoffrey G Handsfield[1]

1. Auckland Bioengineering Institute, Auckland, New Zealand

2. Department of Engineering Science, The University of Auckland, Auckland, New Zealand

Skeletal muscle is an adaptable tissue with the potential to repair in response to injury. Muscle fibres and surrounding cells carry the repair process within and around skeletal muscle fibres. The cytokine and chemokine environment in skeletal muscle and surrounding extracellular matrix are crucial to guiding cell activity for efficient repair. Exercise can induce focal or segmental muscle fibre damage and elicits the muscle repair cascade. Surrounding cells migrate towards the damage and begin the repair process that results in well-organised contractile units that form muscle fibres[1]. While this complex process is essential for understanding muscle regeneration and repair in disease, post-surgery, and regenerative medicine applications; few models exist that integrate mechanical and physiological cues to simulate skeletal muscle regeneration. Here we use agent-based modelling to explore the role of the molecular and mechanical environment in typical and pathological skeletal muscle repair following simulated exercise-induced muscle damage.

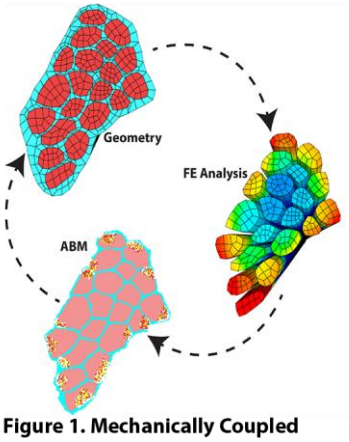

Figure 1. Mechanically Coupled ABM-FEM workflow

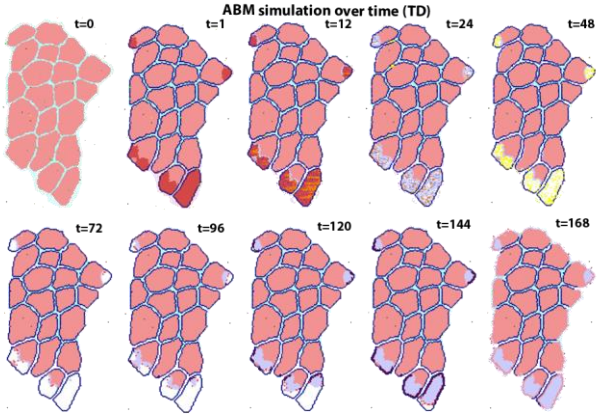

Figure 2. Agent-based model of skeletal muscle regeneration over time.

Agent-based modelling is well-positioned to connect macroscale muscle adaptation to its cellular level causes [2]. To investigate the cellular level interactions that give rise to muscle degeneration in pathological scenarios, we created a mechanically coupled agent-based model (Figure 1) that aims to explore cycles of muscle regeneration and degeneration in typically developing muscle and muscle affected by cerebral palsy or inflammatory myopathies, over time. We created a finite element (FE) model of a muscle fibre bundle with active contraction using FEBio, and models of cytokine and chemokine behaviour to represent the effect of HGF, IGF-1, TNF-α, IL-10, IL-6, IL-15 and TGF-β levels on muscle repair. The FE model was used to determine locations of high strain following active muscle lengthening, which indicate locations of mechanical damage (Figure 2). The molecular models acted as bottom-up cell-guidance cues. These in silico models may be used in the future for regenerative medicine and modelling post-surgery outcomes.

1. M. N. Wosczyna and T. A. Rando, A Muscle Stem Cell Support Group: Coordinated Cellular Responses in Muscle Regeneration, vol. 46, no. 2. Cell Press, 2018, pp. 135–143. doi: 10.1016/j.devcel.2018.06.018.
2. T. E. Gorochowski, “Agent-based modelling in synthetic biology,” Essays In Biochemistry, vol. 60, no. 4, pp. 325–336, 2016, doi: 10.1042/EBC20160037.

112

The effect of saturated fatty acid exposure on tenocyte health

Subhajit Konar[1], Chris Hedges[1], Karen Callon[1], Scott Bolam[1], Sophia Leung[1], Dorit Naot[1], Jillian Cornish[1], David Musson[1]

1. University of Auckland, Auckland, AUCKLAND, New Zealand

Dyslipidemia negatively affects several tissues, and is associated with increased BMI. Clinical studies have established a strong correlation between increased BMI and risk of tendinopathy. However, the underlying mechanisms are not well understood. We hypothesised that increased saturated fatty acid levels, which are found in dyslipidemia, would have a negative effect on tenocyte health, and this would be driven by mitochondrial processes.

Rat-tail tenocytes were isolated and treated with stearic and palmitic acid (SA and PA, 10µg/ml). Cell viability was assessed using AlamarBlue™ assay (24hr and 48hr). Cell deposited collagen was assessed using sirius red assay (72hr), and tenocyte gene expression was quantified using RT-PCR. Cell respiration and reactive oxygen species production was measured by oxygraphy and MitoSox staining. To assess whether effects were driven by mitochondrial processes, fatty acid transport into the mitochondria was blocked by pre-treatment with 50µM etomoxir.

Treatment with SA and PA decreased tenocyte viability ($p<0.05$). PA treatment decreased collagen deposition ($p<0.05$) and the expression of tendon markers scleraxis ($p=0.004$) and tenomodulin ($p=0.0054$), and increased MMP-3 ($p=0.036$), MMP-13 ($p=0.0059$) and cox-2 ($p=0.0075$) gene expression. Cell respiration, as measured by an oxygraphy, increased after PA treatment ($p<0.0001$), and there was increased ROS production with PA treatment ($p<0.0001$). Pre-treatment with 50µM etomoxir partially rescued cell death ($p=0.02$), inhibited PA-induced MMP-3 expression, reduced ROS staining and partially reduced cell respiration, but did not affect PA-induced scleraxis or tenomodullin expression.

Our study indicates that increased saturated fatty acid concentrations in the cellular microenvironment can lead to cell death and altered tenocyte behaviour, which are indicative of tendinopathy. Blocking PA transport into mitochondria partially rescues some of the negative effects of PA, but not all of them, suggesting other pathways are involved. Overall, increased saturated fatty acid levels, which are observed with dyslipidemia, may contribute to poor tendon health.

113

Comparative analysis of human migratory and fibronectin adhesion assay derived chondroprogenitors to assess superiority for cartilage repair

Elizabeth Vinod[1], Noel Naveen Johnson[1], Sanjay Kumar[1], Soosai Manickam Amirtham[1], Jithu James Varghese[2], Abel Livingston[1], Grace Rebekah[1], Alfred Job Daniel [1], Boopalan Ramasamy [3], Solomon Sathishkumar[1]

1. Christian Medical College, VELLORE, TAMIL NADU, India

2. Department of Diabetes, School of Life Course Sciences, King's College London, London, UK

3. Department of Orthopaedics and Trauma,, Royal Adelaide Hospital, Adelaide,, Adelaide,, Australia

Purpose:

Cell-based therapies for the regeneration of hyaline-like cartilage predominantly involve the use of chondrocytes and mesenchymal stem cells. However, the repair response is impeded by the nature of regenerated tissue, which comprises a mixture of hyaline and fibrocartilage, thus resulting in suboptimal long-term functional outcomes. Current preclinical research demonstrates that cartilage-derived chondroprogenitors display inherent potential for chondrogenesis and appear to be a viable option for cartilage regeneration. Isolation of these progenitors commonly employs the subjection of chondrocytes to fibronectin adhesion assay or strategic use of cartilage explants to obtain chondroprogenitors based on their migratory potential. Although both types of progenitor cells possess characteristics conducive to neocartilage formation, they are isolated using different protocols. A direct comparison between the two cell-types would provide valuable information on the better-suited contender for cartilage repair. The study aimed to compare human migratory and fibronectin adhesion assay-derived chondroprogenitors; to evaluate differences in their biological characteristics and repair potential.

Methods:

Chondroprogenitors were obtained from three human-osteoarthritic knee joints using either explant cultures to obtain migratory chondroprogenitors(MCP) or fibronectin adhesion assay(FAA-CP). Assessment parameters included immunophenotyping, growth kinetics, multilineage differentiation potential with particular attention to assessing chondrogenic potential using mRNA expression for markers of chondrogenesis and hypertrophy, GAG/DNA, and histological staining under normoxia and hypoxia culture conditions.

Results:

Normoxia and hypoxia MCPs displayed significantly lower levels of the hypertrophy marker RUNX2 and fibrocartilage marker COL1A1 compared to the FAA counterparts. Concerning their chondrogenic potential, normoxia-MCPs exhibited significantly higher levels of the chondrogenic gene Aggrecan and COL2A1/COL1A1 ratio. Additionally, normoxia-MCPs displayed efficient histological staining and total GAG/DNA, reiterating its better chondrogenic potential.

Conclusion:

Normoxia-MCPs displayed superior regenerative potential for cartilage repair, owing to their higher chondrogenic and limited hypertrophic ability. Focused investigations to study its regenerative potential using in-vivo models are warranted to understand its therapeutic potential.

114

A high-fat diet has negative effects on tendon resident cells in an in vivo rat model

Scott M Bolam[1], Subhajit Konar[1], Young Eun Park[1], Karen E Callon[1], Josh Workman[1], Paul Monk[1], Brendan Coleman[2], Jillian Cornish[1], Mark H Vickers[3], Jacob T Munro[1], David S Musson[1]

1. University of Auckland, Grafton, AUCKLAND, New Zealand

2. Orthopaedics, Counties Manukau DHB, Auckland, New Zealand

3. Liggins Institute, University of Auckland, Auckland, New Zealand

Background: Tendinopathy is a major complication of diet-induced obesity. However, the effects of a high-fat diet (HFD) on tendon have not been well characterized. We aimed to determine: [1] the impact of a HFD on tendon properties and gene expression; and [2] if dietary transition to a control diet (CD) could restore normal tendon health.

Methods: Sprague-Dawley rats were randomised into three groups from weaning, and fed either a: CD, HFD or HFD for 12 weeks, then CD thereafter (HF-CD). Biomechanical, histological and structural evaluation of the Achilles tendon was performed at 17 and 27 weeks of age. Tail tenocytes were isolated with growth rate and collagen production determined. Tenocytes and activated THP-1 cells were exposed to conditioned media (CM) of visceral adipose tissue explants and gene expression was analysed.

Results: There were no differences in the biomechanical, histological or structural tendon properties between groups. However, tenocyte growth and collagen production were increased in the HFD group at 27 weeks. There was lower SOX-9 expression in the HFD and HF-CD groups at 17 weeks and higher expression of collagen-Iα1 and matrix metalloproteinase-13 in the HFD group at 27 weeks. THP-1 cells exposed to adipose tissue CM from animals fed a HFD or HF-CD had lower expression of Il-10 and higher expression of Il-1β.

Conclusions: In this rodent model, a HFD negatively altered tendon cell characteristics. Dietary intervention restored some gene expression changes, however, adipose tissue secretions from the HF-CD group promoted an increased inflammatory state in macrophages. These changes may predispose tendon to injury and adverse events later in life.

115

A Novel Material Evidences a Great Potential in Future Orthopaedic Implant

Rachel W. R Li[1], Paul N. P Smith[2]

1. Australian National University, Canberra City, ACT, Australia

2. Clinical Orthopaedic Surgery , ACT Health, Canberra, ACT , Australia

Introduction: Device-associated bacterial infections are a major and costly clinical challenge. This project aims to develop a smart new "biomaterial" for implants that helps to protects against infection and inflammation, promotes bone growth, and is biodegradable.

Methods: Pure Mg as a model biodegradable material was coated with gallium doped strontium-phosphate through a chemical conversion process. Gallium was distributed in a graduated manner throughout the strontium-phosphate coating, with a compact structure and a gallium-rich surface. The sample was exposed to Gram-positive *Staphylococcus aureus* and *Gram-negative E. coli* - two major strains causing clinical infections, for its effects of antibacterial and bone cells growth promotion.

Results: Ga was distributed in a gradient way throughout the entire strontium-phosphate coating with a compact structure and a gallium-rich surface. The Ga coating protected the underlying Mg from substantial degradation in minimal essential media at physiological conditions over 9 day. The liberated Ga ions from the coatings upon Mg specimens inhibited the growth of Gram-positive *Staphylococcus aureus*, and Gram-negative *Escherichia coli* – key strains causing infection and early failure of the surgical implantations in orthopaedics and trauma. More importantly, the gallium dopants displayed minimal interferences with the strontium-phosphate based coating, which boosted osteoblasts and undermined osteoclasts in *in vitro* co-cultures. This work provides a new strategy to prevent bacterial infection and control the degradation behaviour of Mg-based orthopaedic implants, while preserving osteogenic features of the devices.

Conclusion/Clinical Significance/Potential Commercialization: This work provides a new biocompatible strategy to prevent bacterial infection and control the degradation behaviour of Mg-based orthopaedic implants. The results provides great evidence for the great potential to attract biomaterial industry for further development of orthopaedic Implant.

116

ADR3, a next generation i-body to human RANKL, inhibits osteoclast formation and bone resorption

Heng Qiu[1], Christopher Hosking[2], Ariela Samantha[3], Kai Chen[3], Vincent Kuek[1], Alice Vrielink[3], Kevin Lim[2], Mick Foley[2], Jiake Xu[1]

1. School of Biomedical Sciences, University of Western Australia, Perth, WA, Australia

2. Department of Biochemistry and Genetics, La Trobe University, La Trobe , Victoria, Australia

3. School of Molecular Sciences, University of Western Australia, Perth, WA, Australia

Osteoporosis is a chronic skeletal condition characterized by low bone mass and deteriorated microarchitecture of bone tissue, putting tens of millions of people at high risk of fractures. New therapeutic agents like i-body, a class of next-generation single-domain antibody, are needed to overcome some limitations of conventional treatments. An i-body is a human immunoglobulin scaffold with two long binding loops that mimic the shape and position of those found in shark antibodies the variable new antigen receptors (V_{NARs}) of sharks. Its small size (~12kDa) and long binding loops provide access to drug targets which are undruggable by traditional monoclonal antibodies. We have successfully identified a human Receptor activator of nuclear-factor kappa B (RANK) ligand (hRANKL) i-body, ADR3, which demonstrated high binding affinity to hRANKL with no adverse effect on the survival or proliferation of bone marrow-derived macrophages (BMMs). A differential scanning fluorimetry assay suggested that ADR3 was stable and able to tolerate a wide range of physical environments (temperature and pH). *In vitro* studies showed a dose-dependent inhibitory effect of ADR3 on osteoclast differentiation, podosome belt formation and bone resorption activity. Further investigation on mechanism of action of ADR3 revealed that it could block RANKL-mediated signalling pathways, supporting the *in vitro* functional observations. Collectively, these data indicate that RANKL antagonist ADR3, a next generation i-body attenuates osteoclast differentiation and bone resorption, representative of a novel therapeutic to protect bone loss such as osteoporosis and orthopaedic implant loosening.

Long-term Effect of Denosumab on Bone Microarchitecture as Assessed by Tissue Thickness–Adjusted Trabecular Bone Score (TBS) in Postmenopausal Women with Osteoporosis: Results from the FREEDOM and Open-Label Extension (OLE)

Didier Hans[1], Jeff Hassall[2], Michelle McDermott[3], Shuang Huang[3], Min Kim[3], Enisa Shevroja[1], Michael McClung[4, 5]

1. Lausanne University Hospital and Lausanne University, Lausanne, Switzerland

2. Amgen Australia, Sydney, NSW, Australia

3. Amgen Inc, Thousand Oaks, CA, USA

4. Oregon Osteoporosis Center, Portland, USA

5. Mary MacKillop Institute for Health Research, Australian Catholic University, Melbourne, VIC, Australia

Figure. Percentage change from baseline by visit and treatment group for tissue thickness–adjusted trabecular bone score.

Data are presented as least-squares mean and 95% CI. n = number of subjects with observed data. *$P < 0.05$ compared with OLE baseline; **$P < 0.0001$ compared with baseline; ***$P < 0.0001$ compared with OLE baseline; ‡$P < 0.0001$ compared with placebo. BL, baseline; OLE, open-label extension.

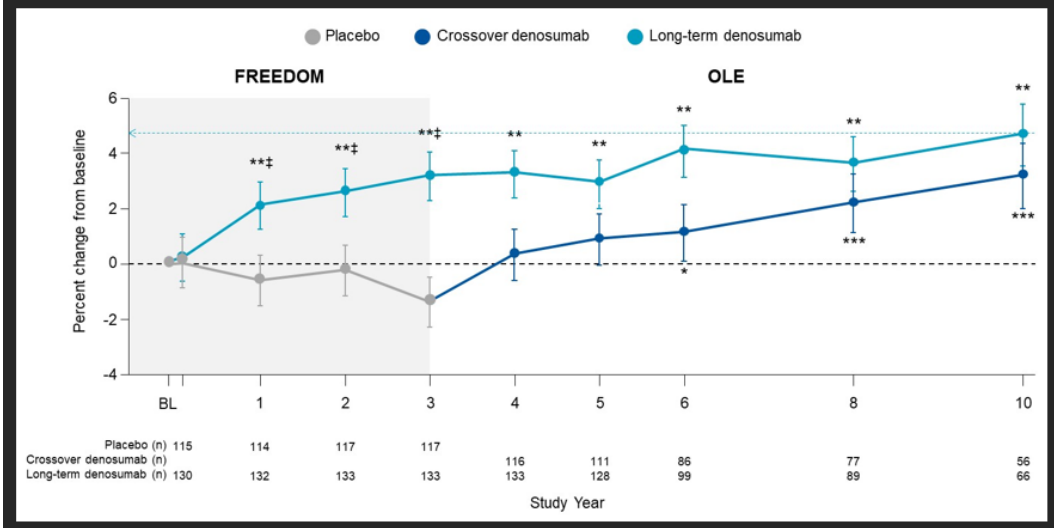

Objective:
This retrospective analysis applied updated built-in tissue thickness–adjusted TBS algorithm to investigate the long-term effect of denosumab on bone microarchitecture in FREEDOM and OLE.

Material and Methods:
This analysis included 279 postmenopausal women with LS or total hip BMD T-score <−2.5 and ≥−4.0 who completed the FREEDOM DXA substudy and continued in the OLE study: 150 women received denosumab 60 mg SC Q6M for 3 years and open-label denosumab for 7 years (long-term group); 129 women received placebo for 3 years and open-label denosumab for 7 years (crossover group). BMD and TBS were assessed on LS DXA scans.

Results:
Baseline characteristics were similar between groups. Long-term denosumab led to significant and progressive increases in TBS over 10 years of treatment (Figure). A similar trend was observed in the crossover group during 7 years of denosumab therapy. In the long-term denosumab group, % of patients with normal microarchitecture (TBS >1.074) increased from 26.1% at baseline to 53.2% up to Year 10, and % of patients with degraded (TBS ≤1.027) or partially degraded (1.027<TBS≤1.074) microarchitecture decreased from 48.6% to 29.1% and from 25.4% to 17.7%, respectively ($P < 0.0001$; TBS thresholds equivalent to 1.230 and 1.310 for the classical TBS algorithm corrected for body mass index). A similar improvement in bone microarchitecture was observed in the crossover group from OLE baseline up to OLE Year 7 ($P < 0.0001$). Over the course of long-term denosumab treatment, TBS changes were largely unrelated to LS BMD changes: $r^2$was 0.05 from baseline to Year 10 in the long-term group and 0.28 from OLE baseline to OLE Year 7 in the crossover group.

Conclusion:
Up to 10 years of denosumab treatment significantly and progressively improved TBS assessment of bone microarchitecture independently of BMD in postmenopausal women with osteoporosis.

118

Osteoblast precursor or osteoblast? Tracking cell differentiation *in vivo* and *in vitro*

Natalie Wee[1], Narelle McGregor[1], Natalie Sims[1, 2]

1. Bone Cell Biology and Disease, St Vincent's Institute of Medical Research, Fitzroy, Victoria, Australia

2. Department of Medicine, The University of Melbourne, Melbourne, VIC, Australia

To define how bone formation is controlled, we need to identify transitions from stem/progenitor cells to osteoblasts. Osteoblast precursors first commit to the lineage by expressing *Sp7* (osterix) and when differentiated into osteoblasts, express high levels of *Col1a1*.

To define stages of osteoblast differentiation, we studied 12 week old (young adult) mice with fluorescence targeted to the osteoblast lineage (*OsxCherry*) or to mature osteoblasts (*Col1a1GFP*). Additionally, we generated an osteoblast lineage dual-reporter (DR) mouse that distinguishes osteoblasts from osteoblast precursors by these fluorescent markers, and assessed distribution of these cells on bone surfaces by cryohistology.

In *Col1a1GFP* mice, *Col1a1GFP*+ cells covered ~30% of all bone surfaces, which were almost entirely active bone forming surfaces (identified by Alizarin Red labelling). In contrast, in *OsxCherry* mice, >90% of periosteal and endocortical surfaces, and 52% of trabecular bone surfaces had *OsxCherry*+ cells. Within *OsxCherry*+ cells, 78% and 92% were on active bone forming surfaces (calcein-labelled) on endocortical and trabecular bone, respectively. However, on the periosteal surface only 29% of *OsxCherry*+ cells resided on actively forming bone. By flow cytometry, periosteal *OsxCherry*+ cells had a 3-5x greater proportion of cells expressing progenitor markers (Sca1+CD51+) than bone marrow *OsxCherry*+ cells.

By crossing *OsxCherry* and *Col1a1GFP* mice to generate DR mice, we could distinguish osteoblast precursor cells (*OsxCherry+Col1a1GFP-*) from osteoblasts (*OsxCherry+Col1a1GFP*^{hi}). This confirmed the distinct distributions of cell populations on bone surfaces: the periosteum was lined predominantly by *OsxCherry+Col1a1GFP-* cells whilst other surfaces were covered by *OsxCherry+Col1a1GFP*^{hi} cells. Furthermore, periosteal and bone marrow stromal cells from DR mice expressed changes in fluorescence as they differentiated *in vitro*.

We have developed a model that distinguishes between osteoblast precursors and osteoblasts *in vivo* and *in vitro*. We also identified osteoblast precursors are the predominant cell type residing on periosteal, but not trabecular and endocortical, surfaces under physiological conditions.

119

Zoledronate Reduces Height Loss Independently of Vertebral Fracture Occurrence in a Randomized Trial in Osteopenic Older Women

Ian Reid[1], Sonja Sonja Bastin[1], Anne Horne[1], Borislav Mihov[1], Gregory Gamble[1], Mark Bolland[1]

1. University of Auckland, Auckland, New Zealand

Vertebral fractures are associated with height loss, reduced quality of life and increased mortality, and are an important endpoint for osteoporosis trials. However, height loss is associated with quality of life and mortality independent of associations with fracture.

We have used data from a recent 6-year trial of zoledronate in 2000 osteopenic women aged >65 years to assess the impact of the semi-quantitative and quantitative components of the definition of vertebral fracture on the outcome of that trial, to determine what factors impacted on height loss, and to test whether height loss can be used as a surrogate for vertebral fracture incidence.

In the trial protocol, an incident vertebral fracture was defined as a change in Genant grade plus both a 20% and 4 mm decrease in a vertebral height. The addition of the quantitative criteria reduced the number of fractures detected but did not change the size of the anti-fracture effect (odds ratios of 0.49 versus 0.45) nor the width of the confidence intervals for the odds ratios. Multivariate analysis of baseline predictors of height change showed that age accelerated height loss ($P < 0.0001$) and zoledronate reduced it ($P = 0.0001$). Incident vertebral fracture increased height loss ($P = 0.0005$) but accounted for only 0.7% of the variance in height change, so fracture could not be reliably inferred from height loss. In women without incident vertebral fractures, height loss was still reduced by zoledronate (height change: zoledronate, -1.23; placebo -1.51 mm/year, $P < 0.0001$). This likely indicates that zoledronate prevents a subtle but widespread loss of vertebral body heights not detected by vertebral morphometry. Since height loss is associated with quality of life and mortality independent of associations with fracture, it is possible that zoledronate impacts on these endpoints via its effects on vertebral body integrity.

120

Assessment of strategies for safe drug discontinuation and transition of denosumab treatment in PMO - insights from a mechanistic PK/PD model of bone turnover

Javier Dr Martinez-Reina[1], Jose L. Dr Calvo-Gallego[1], Madge Dr Martin[2], Peter Dr Pivonka[3]

1. Department of Mechanical Engineering and Manufacturing, University of Seville, Seville, Spain

2. Multiscale Modeling and Simulation, University of Paris-Est Creteil, Paris, Creteil, France

3. Queensland University of Technology, Brisbane, QLD, Australia

Denosumab (Dmab) treatment against postmenopausal osteoporosis (PMO) has proven very efficient in increasing bone mineral density (BMD) and reducing the risk of bone fractures[1]. However, concerns have been recently raised regarding safety when drug treatment is discontinued[2]. Mechanistic pharmacokinetic-pharmacodynamic (PK-PD) models are the most sophisticated tools to develop patient specific drug treatments of PMO to restore bone mass. However, only a few PK-PD models have addressed the effect of Dmab drug holidays on changes in BMD[3].

Here, we show that using a standard bone cell population model (BCPM) of bone remodelling it is not possible to account for the spike in osteoclast numbers observed after Dmab discontinuation[4]. We demonstrate that inclusion of a variable osteoclast precursor pool in BCPMs is essential to predict the experimentally observed rapid rise in osteoclast numbers and the associated increases in bone resorption. This new model also showed that Dmab withdrawal leads to a rapid increase of damage in the bone matrix, which in turn decreases the local safety factor for fatigue failure.

Furthermore, we studied how to safely discontinue Dmab treatment by exploring several transitional and combined drug treatment strategies. Our simulation results indicate that using transitional reduced Dmab doses are not effective in reducing rapid bone loss. However, we identify that use of a bisphosphonate (BP) is highly effective in avoiding rapid bone loss and increase in bone tissue damage compared to abrupt withdrawal of Dmab. Also, the final BMD and damage values were not sensitive to the time of administration of the BP.

1. Cummings S, San Martin J, McClung M, Siris E, Eastell R, Reid I, et al. Denosumab for prevention of fractures in postmenopausal women with osteoporosis. N Engl J Med 2009;361(8):756{65. doi:10.1056/NEJMoa0809493.
2. Anastasilakis A, Makras P, Yavropoulou M, Tabacco G, Naciu A, Palermo A. Denosumab discontinuation and the rebound phenomenon: A narrative review. J Clin Med 2021, 10(1):152. doi:10.3390/jcm10010152.
3. Martinez-Reina J., Calvo-Gallego J.L., Pivonka P. Are drug holidays a safe option in treatment of osteoporosis? - Insights from an in silico mechanistic PK-PD model of denosumab treatment of postmenopausal osteoporosis. J Mech Behav Biomed Mater, 2021, 113:104140. doi:10.1016/j.jmbbm.2020.104140.
4. Martinez-Reina J., Calvo-Gallego J.L., Martin M., Pivonka P. Assessment of strategies for safe drug discontinuation and transition of denosumab treatment in PMO - Insights from a mechanistic PK/PD model of bone turnover, Frontiers in Bioengineering and Biotechnology, 2022. (In Print)

121

A *in vivo* microCT imaging protocol for reproducible quantitative morphometric analysis of joint structures

Kathryn S Stok[1]

1. The University of Melbourne, Parkville, VIC, Australia

Micro-computed tomography (microCT) offers a three-dimensional (3D), high-resolution technique for the visualisation and analysis of bone microstructure. With carefully designed longitudinal studies, it can be expanded to capture time-lapse changes in microstructure (4D) and using contrast-enhanced microCT also capture cartilage morphometry and whole joint measures - known together as quantitative morphometric analysis (QMA). However, one of the main challenges in quantitative analysis of joint images is sensitivity to joint pose and alignment, which may influence measures related to both joint space and joint biomechanics. This challenge requires reproducible protocols in both the data acquisition and image processing stages of the study workflow.

In this presentation, I present a comprehensive microCT imaging protocol for reproducible and efficient QMA of *in situ* mouse tibio-femoral joint. This work consists of a diffusion kinetics study for a known cationic iodinated contrast agent (CA4+) for QMA of the cartilage, and a joint positioning and image processing workflow for whole joint QMA. Secondly, I demonstrate a novel automatic, efficient, and model-invariant image preprocessing pipeline that allows for highly reproducible 3D QMA of the joint.

The joint positioning and image processing workflow was established by developing a novel positioning device to control joint pose during scanning, and a spherical harmonics-based image processing workflow to ensure consistent alignment during image processing. The pipeline addresses the joint pose problem by deploying two modules: an alignment module and a subdivision module. Alignment is achieved by representing the tibia in its basic form using lower degree spherical harmonic basis functions and aligning using principal component analysis. The second module subdivides the joint into lateral and medial VOIs via a watershedding approach based on persistence homology. Joint QMA evaluation of the workflow showed excellent reproducibility; intraclass correlation coefficients ranged from 0.794 to 0.930, confirming that the imaging protocol enables reproducible and efficient QMA of joint structures in preclinical models, and that contrast agent injection did not cause significant alteration to the measured parameters. Furthermore, processing time and technical requirements were reduced compared to manual processing in previous studies.

Time-elapsed micro-CT imaging of humeral implant failure in reverser shoulder replacement

Xiaolong Fan[1], Egon Perilli[2], Sophie Rapagna[2], Ashish Gupta[1], Saulo Martelli[1]

1. Queensland University of Technology, Brisbane City, QLD , Australia

2. Medical Device Research Institute, College of Science and Engineering, Flinders University, , Adelaide, South Australia, Australia

Abstract

Reverse total shoulder arthroplasties can have complications due to adverse scenarios including mechanical failure of the humeral component[1], resulting in the need for exploring the bone-implant interface. This study presents a novel time-elapsed microstructural imaging protocol for observing the volumetric deformation of a humerus implanted with a common reverse shoulder implant subjected to physiological loading, increased until fracture occurred.

Method

A left humerus from a male donor (age: 75 years) was used. The load applied on the proximal humerus head was based on the physiological glenohumeral joint force[2]. The specimen was mounted in a compressive stage described previously[3] and scanned in a large-volume micro-CT (45µm/pixel). Micro-CT scans were performed for two scenarios: 1. pre-implantation: at 50N pre-load and after application of physiological load (650N); 2. implanted with an Aequalis reversed II stem (inlay technique): scanned at pre-load, physiological load (650N) and after load increased to fracture.

Results

A vertical displacement of the actuator by 1.5mm generated 650N compressive force. By increasing the displacement to 3mm, the force reached 2000 N, before dropping to 1000N (fracture). At 650N compression, most deformation occurred in the peri-prosthetic bone (Fig. 1c). A longitudinal fracture was accompanied by a significant distal migration of the implant stem with respect to the hosting bone (Fig. 1e).

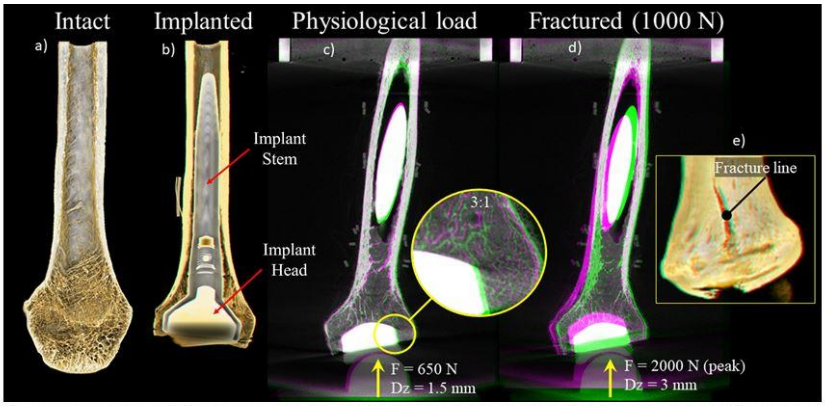

Figure 1. Frontal micro-CT cross-section of intact humerus (a) and implanted (b); under physiological load (in purple colour), compared to pre-load (in green colour) (c); after fracture (d) and the fracture line (e).

CONCLUSIONS

The protocol successfully displayed the relative displacement of the implant and the bone while under physiological load and after a fracture with micrometric detail. In this first test, the trabecular bone appears to mostly provide support for implant stability, while fracture likely occurred due to increased circumferential strain, caused by the implant migrating distally. The study is ongoing. The protocol can be used to study and optimize the effect on implant stability of different surgical procedures, and implant designs for maximal stability of the implant in the future.

1. Shah, Roche, Sullivan, et al. JSES Int. 2021;5(1):121. 2. Orthoload database, 2020 (https://orthoload.com). 3. Martelli, Perilli. J M. Behav Biomed Mater. 2018;84:265-272.

Muscle and Fascia Structural Changes Following Ankle Sprain Injury and Immobilization

Meeghage R Perera[1], Samantha Holdsworth[2], Geoffrey Handsfield[1]

1. Auckland Bioengineering Institute, Auckland, AUCKLAND, New Zealand

2. Matai Medical Research Institute, Gisborne, New Zealand

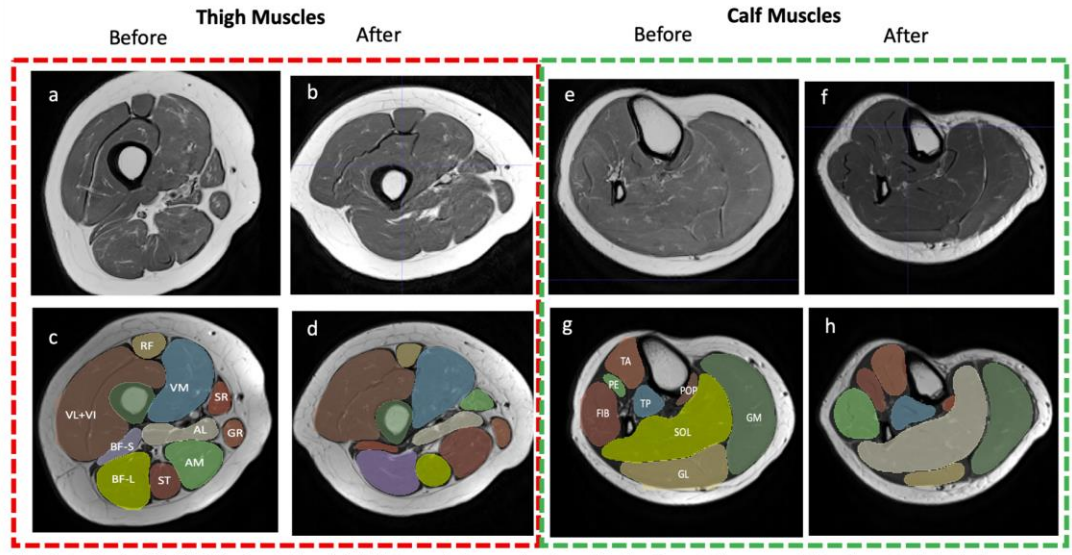

Fig.1 Proton Density MRI of Thigh(a-d) and calf region(e-h) before and after moonboot immobilization. Segmentation were made based on a standard atlas by a trained individual. Quadriceps femoris consisted of the rectus femoris (RF), vastus lateralis+ vastus intermedius (VL+VI) and vastus medialis (VM). Hamstring consisted of bicep femoris short head (BF-S), long head(BF-L) & semitendinosus (ST) muscles. Adductor compartment consisted of the sartorius (SR), Gracilis(GR), Adductor Magnus(AM) & Adductor Longus(AL). The anterior compartment of calf consisted of tibialis anterior(TA),Phalangeal Extensors(PE). The lateral compartment consisted of the fibulari (FIB). The deep posterior calf consisted of the tibial posterior (TP), Popliteus(POP) muscles. The superficial posterior consisted of the soleus (SOL) and gastrocnemius medial head and lateral head (MG and LG) muscles.

Introduction

Ankle sprains are common injuries [1,2] and muscle atrophy is common after immobilization [3]. This may contribute to poor recovery leading to long term ankle instabilities [2]. There is a limited understanding of the extent of muscle atrophy post-injury and a complete dearth of knowledge on how soft tissues like fascia respond to such injury. Here, we use advanced MRI to investigate skeletal muscle and fascia structural changes during recovery period of one patient.

Method

Our participant (female, age: 33 years, mass 54 kg, height 1.69 m) volunteered for MRI scan as a part of a separate project. Three days after initial scan the participant suffered an ankle sprain suddenly and was put into an immobilization boot for 18 days. The participant agreed to an MRI scan 3 days after removing the boot. MRI was conducted on 3T Siemens Skyra scanner over two-thirds of the right shank below the knee. Muscle imaging was done using a Proton Density sequence; fascia imaging used 2D stack of spirals non-Cartesian sequence [4]. Spatial resolution was 1x1x3 mm^3. Muscles and fascia were segmented in images to determine volume and thickness, respectively.

Results

We observed atrophy of most shank muscles and hypertrophy of some muscles after injury and immobilization. Muscle loss ranged from no change in the lateral gastrocnemius to 19.5% in flexor hallucis longus. The soleus displayed a 12% loss of volume. Hypertrophy occurred in the hamstrings, quadriceps, tibialis anterior, and the adductor magnus. Fascia thickness increased from 2.37mm to 2.6mm post-injury.

Discussion

We demonstrate variable responses of muscles to immobilization after ankle sprain injury, implying some increased loading of muscles during recovery. We quantify changes to the deep fascia using novel imaging, demonstrating a significant thickening in response to sprain injury and immobilization [5,6].

Acknowledgement

Funding provided by RSNZ Marsden Fast-Start Grant.

1. Hootman et al. (2007), J Athl Train.42:311–319.
2. Kobayashi. et al.(2014), Foot Ankle Spec;7(4):298–326.
3. Boonyarom, O et al.(2017), Acta Physiol (Oxf). 2006;188(2):77–89.
4. Qian et al.(2008), Magn Reson Med.60:135–145.
5. Pavan et al.[2020],. Int. J. Mol. Sci.21:3992.
6. Carmelo et al. [2021], Diagnostics.11:21.

124

Current challenges of 3D-printing spinal orthoses

Rachel Chalmers[1], Marie-Luise Wille[2], J. Paige Little[1]

1. Biomechanics and Spine Research Group, Queensland University of Technology, Brisbane, QLD

2. ARC ITTC for Multiscale 3D Imaging, Modelling and Manufacturing, Queensland University of Technology, Brisbane, QLD

INTRODUCTION: Thoracic-lumbar-sacral orthoses (TLSO) are the current gold-standard for conservatively managing the scoliotic deformity for idiopathic adolescent patients with a major curve Cobb angle between 20°-45°. Early detection and well-timed bracing are key factors in the treatment's success. Scoliotic deformity can rapidly progress during the pubescent growth spurt. Current manufacturing methods for TLSO are labour-intensive with an approximate manufacturing time of 8-12 weeks. New time-efficient and cost-effective manufacturing methods are crucial to improve patient outcome and satisfaction. The research aimed to evaluate the reliability of 3D-printing for spinal orthoses.

METHODS: Four spinal orthoses were 3D-printed using an existing database of 3D surface scans from Queensland Children's Hospital Spine Clinic (QCH-HREC-LNR/21/QCHQ/75249). The traditional manufacturing methods conducted by an orthotist were virtually replicated through 3D surface scanning and computer-aided-design modelling. The orthoses were 3D-printed using a Delta WASP Industrial X 4070 3D-printer and thermoplastic filament. Establishing suitable print settings to achieve a successful print was an iterative process. The constrained print settings, as well as, print time, print completion, print quality, print reliability, material waste and require post-processing for each orthosis was recorded.

RESULTS: Constraining the raster angle, infill pattern, infill density, print orientation and perimeter layers were important for improving print quality and reliability. Although an independent factor, bed adhesion had the most significant influence on print completion. Some patients were currently receiving bracing treatment through QCH. This allowed the fit, feel and cosmesis of the 3D-printed orthosis to be directly compared to a traditional orthosis.

DISCUSSION and CONCLUSION: Current challenges surrounding 3D-printing TLSO includes the complexity of 3D-printing thin-walled structures and selecting suitable material filament. This novel research shows promise for reducing manufacturing time, cost, and single-use material waste during spinal orthoses fabrication.

125

Linking the Ultrastructure and Micromechanics of Articular Cartilage

Jingrui Hu[1], Keke Zheng[1], Eve Nebbiolo[1], Jessica Mansfield[1], Ellen Green[1], Peter Winlove[1], Ben Sherlock[1], Junning Chen[1]

1. University of Exeter, Exeter, DEVON, United Kingdom

Articular cartilage, as the connective tissue of diarthrodial joints, plays a crucial role in load-bearing and mobility. Its extracellular matrix (ECM), consisting of a collagenous network interacting with interstitial fluid rich in proteoglycans, largely determines the biomechanical properties [1]. Polarisation-resolved second-harmonic generation (pSHG) is a recently developed optical technique, which could investigate the intrafibrillar organisation of fresh, unlabelled, and thick collagenous tissues at sub-diffraction length scales [2, 3]. The fast-scanning speed also provided the ability to visualise the dynamic response to external loads. However, a quantitative correlation between collagen organisation and its mechanical function still lacking. Cartilage in the anterior and posterior regions of the joint found more shear force than the apex, which is subjected to the compression force [4]. Therefore, we hypothesise that the collagen organisation is tailored to its local biomechanical environment at different anatomical locations, and such organisational variation is also manifested in their susceptibility to injury and degenerative disease.

The overarching aim of our study is to establish a framework quantitative of the relationship between the ultrastructure of articular cartilage and its biomechanics. Four bovine metacarpophalangeal (MCP) joints were acquired from a local abattoir, and 48 explants in cuboid shapes were harvested from the anterior, apex and posterior regions of trochlear surfaces and condyles. We first mapped the longitudinal cross-section of the explants with pSHG and evaluated the structural variations among three zones quantifying the principal angles and degrees of dispersion of collagen. Next, the same specimens were loaded on a custom-built rig integrated with our pSHG microscope, to visualise structural responses under two levels of tissue strains applied at 8% and 16%. These two strain levels present a medium and an extreme case in normal activities, respectively. The structural responses were evaluated in terms of the re-orientation and re-alignment of the collagen fibrils.

1. Inamdar, S.R., et al., The secret life of collagen: temporal changes in nanoscale fibrillar pre-strain and molecular organization during physiological loading of cartilage. ACS nano, 2017. 11(10): p. 9728-9737.
2. Mansfield, J.C., J.S. Bell, and C.P. Winlove, The micromechanics of the superficial zone of articular cartilage. Osteoarthritis and cartilage, 2015. 23(10): p. 1806-1816.
3. Mansfield, J.C., et al., Collagen reorganization in cartilage under strain probed by polarization sensitive second harmonic generation microscopy. Journal of the Royal Society Interface, 2019. 16(150): p. 20180611.
4. Moger, C., et al., Regional variations of collagen orientation in normal and diseased articular cartilage and subchondral bone determined using small angle X-ray scattering (SAXS). Osteoarthritis and cartilage, 2007. 15(6): p. 682-687.

126

Mammary-specific ablation of Cyp24a1 reduces mammary density and inhibits tumour development in MMTV-PyMT breast cancer mice

Jiarong Li[1], Lei Sheng[2], Richard Kremer[1], Paul H Anderson[3]

1. Department of Medicine, McGill University, Montreal, QC, Canada

2. University of Adelaide, Adelaide, SA, Australia

3. University of South Australia, Adelaide, SA, Australia

Active vitamin D (1,25(OH)2D) has been shown to regulate numerous cell processes in mammary cells. Degradation of 1,25(OH)2D is initiated by the mitochondrial enzyme, 25-hydroxyvitamin D 24-hydroxylase (CYP24 A1), and provides local control of 1,25(OH)2D bioactivity. CYP24A1 is coamplified with a known oncogene in human breast cancer tissue and thus CYP24A1 may be an important player in contributing to the dysregulation of cell growth through lowering local cellular 1,25(OH)2D production. To assess the role of CYP24A1 activity in normal mammary development, we used mammary epithelial-specific Cyp24a1 knockout mice to demonstrate reduced terminal end bud number, ductal outgrowth and branching during puberty and alveologenesis during early pregnancy (1). These mice were then used to create mammary epithelial-specific Cyp24a1 knockout in PyMT mouse breast cancer model (KO) to examine its role in tumour progression. Specific CYP24A1 ablation was confirmed by histology and qPCR analysis. Breast tumour initiation was significantly delayed with palpable tumours occurring at 10 weeks in KO animals (mean=0.140 cm^3, SD=0.061 N=17) compared to 7 weeks (mean= 0.385 cm^3, SD=0014, N=17) in control animals (CYP24A1 flox/flox Cre- and CYP24A1wt/wt Cre+). At 13 weeks, tumour volume in KO mice was 75% smaller than in control mice ($p < 0.0001$). Furthermore, tumour size at endpoint in KO (6 cm^3) was observed at age 18 weeks (mean= 5.6 cm^3 SD=0.42 N=19) compared to 13 weeks in control animals (mean= 6.5 cm^3 SD=0.22 N=17). Breast tumour number in KO mice (4.6 ± 0.5 N=20) was significantly decreased at death (17- 18 weeks) compared to 13-14 weeks control mice (7.9 ± 0.3 N=20). Finally, CYP24A1 knockout animals showed a dramatic reduction in lung metastasis development compared to control animals (2/10 Vs 9/10, $P<0.001$ N=10). These data suggest inhibiting CYP24A1 is a potential approach to activating the vitamin D pathway in breast cancer prevention and therapy.

1. Sheng L, Turner AG, Barratt K, Kremer R, Morris HA, Callen DF, Anderson PH, Tarulli GA. Mammary-specific ablation of Cyp24a1 inhibits development, reduces proliferation and increases sensitivity to vitamin D. J Steroid Biochem Mol Biol. 2019 May;189:240-247. doi: 10.1016/j.jsbmb.2019.01.005. Epub 2019 Jan 14. PMID: 30654105.

127

Defining how vitamin D promotes tolerogenic dendritic cells to enable its use in combined therapy for multiple sclerosis and other autoimmune diseases.

Grant P Parnell[1, 2], Stephen D Schibeci[2], Samantha Law[2], David R Booth[2]

1. School of Medical Sciences, The University of Sydney, Sydney, NSW, Australia

2. Centre for Immunology and Allergy Research, The Westmead Institute for Medical Research, Sydney, NSW, Australia

Background:

There is compelling genetic, laboratory and environmental evidence that vitamin D contributes to MS pathogenesis, but the inactive forms currently used in clinical trials have failed to provide benefit. This is because of genetic and epigenetic bottlenecks to vitamin D response.

Objective:

An improved approach is needed to obtain benefit from the vitamin D pathway. The objective of this study was to define how vitamin D promotes a tolerogenic phenotype in the immunological context most likely to underpin its benefit: control of dendritic cells.

Methods:

We identified how the chromatin is remodelled using ATACseq (Assay for Transposase-Accessible Chromatin using *sequencing)* and global gene expression changes using RNAseq in response to treatment with calcipotriol (active vitamin D analogue) for monocyte-derived dendritic cells with a tolerogenic or inflammatory phenotype. We also characterised the effect of co-treatment with vitamin D and a novel bromodomain inhibitor, i-BRD9.

Results:

ATACseq revealed distinct chromatin accessibility changes in response to calcipotriol with over 4,000 genomic locations affected, accounting for approximately 8% of the variation in the ATACseq dataset. Transcriptomic analysis also showed a clear vitamin D response signature, with a far larger number of genes dysregulated in response to calcipotriol the inflammatory cells compared to the tolerogenic cells. Pathway analysis indicated a reduced inflammatory state in cells treated with calcipotriol.

Conclusions:

Calcipotriol treatment revealed a distinct a shift away from the inflammatory phenotype to a more immunosuppressive/tolerogenic phenotype. Work is ongoing to assess alternative strategies, including co-treatment with i-BRD9, to upregulate the vitamin D response and bypass the body's homeostatic setpoint.

128

Photoprotection by vitamin D compounds: finding the missing pieces to the photocarcinogenesis puzzle.

Katie M Dixon[1], Furkan A Ince[1], Artur Shariev[1], Julianne C Nayar[1], Mark S Rybchyn[2], W.G. Manori De Silva[1], Bianca Y McCarthy[1], Chen Yang[1], Rebecca S Mason[3]

1. School of Medical Sciences, Faculty of Medicine and Health, University of Sydney, NSW, Australia

2. School of Chemical Engineering, University of New South Wales, Sydney, NSW, Australia

3. School of Life and Environmental Sciences, Faculty of Science, University of Sydney, NSW, Australia

Skin cancers are the most common cancer in Australia, and also the most costly to treat. The key initiating events in ultraviolet radiation (UV)-induced skin carcinogenesis are UV-induced DNA damage, some of which is inadequately repaired, resulting in mutations, and UV-induced immune suppression, which results in developing skin tumours not being recognised and eliminated by immune surveillance. Vitamin D and its active metabolite, 1,25-dihydroxyvitamin D3 (1,25D), are synthesised in skin cells following exposure to ultraviolet radiation. Our studies showed that 1,25D, when applied immediately after UV, can inhibit UV-induced DNA damage, immune suppression as well as skin carcinogenesis in a well accepted 40 week murine model of photocarcinogenesis. We further tested low calcemic vitamin D analogs and vitamin D-like compounds and demonstrated similar protective effects with 1,25-dihydroxylumisterol and tetrahydrocurcumin. Yet several of the potentially photoprotective agents we have examined in acute and chronic UV studies have reduced UV-generated DNA damage and UV-induced immune suppression, but have not reduced photocarcinogenesis in the long term murine model. Therefore, our studies show that reductions in UV-induced DNA damage and immune suppression alone are not necessarily predictive of potential for photoprotective agents to prevent skin carcinogenesis in the long term, and thus, there is a need to find more reliable markers. If there were early markers to indicate whether photoprotective agents were likely to reduce tumours in a long term photocarcinogenesis model, this would make for a more time- and cost-efficient process for identifying suitable agents for this lengthy testing.

129

Photoprotection by vitamin D compounds: uncovering markers that predict efficacy in reducing photocarcinogenesis.

Furkan A. Ince[1], Julianne C. Nayar[1], Artur Shariev[1], Mark S. Rybchyn[2], Manori De Silva[1], Bianca Y. McCarthy[1], Chen Yang[1], Myriam Abboud[3], Rebecca S. Mason[4], Katie M. Dixon[1]

1. School of Medical Sciences, Faculty of Medicine and Health, The University of Sydney, Sydney, NSW, Australia

2. School of Chemical Engineering, University of New South Wales, Sydney, NSW, Australia

3. College of Natural and Health Sciences, Zayed University, Dubai, ., United Arab Emirates

4. School of Life and Environmental Sciences, The University of Sydney, Sydney, NSW, Australia

The primary factors leading to development of ultraviolet radiation (UVR)-induced skin tumours are DNA damage and immunosuppression. The active metabolite of vitamin D, 1,25-dihydroxyvitamin D (1,25D) reduces UVR-induced DNA damage, immunosuppression and skin tumours. Similar effects on DNA damage and immunosuppression were also observed using vitamin D-like compounds 1,25-dihydroxylumisterol and tetrahydrocurcumin, though reductions in skin tumours were not observed in a long term murine model. Therefore, it is important to uncover markers measurable in acute studies that can reliably identify agents that have potential to reduce UVR-induced skin tumours in a longer term model.

Phosphatase and tensin homolog (PTEN) and N-myc downstream regulated gene-1 (NDRG1) are suppressed in photocarcinogenesis. Following UVR exposure, we have shown that the levels of both markers are depleted in primary human melanocytes and Skh:hr1 mouse skin. Additionally, treatment with 1,25D immediately after UVR lead to increases in the levels of both proteins. Phosphorylation of cyclic AMP response element binding protein (CREB) was shown to increase in skin cells following UVR and is linked to carcinogenesis. Our preliminary data demonstrated a 1,25D-induced reduction in pCREB following UVR. The cytokine interleukin-6 (IL-6) is also increased following UVR. IL-10 was also observed to increase after UVR and is involved in immunosuppression. Both cytokines are reduced with 1,25D treatment.

Using the vitamin D-like compounds, we performed further studies in primary human skin cells, Skh:hr1 mice and *ex vivo* human skin. The aim of these studies was to develop a matrix to determine which markers could best predict the efficacy of the compounds to reduce UVR-induced skin tumours.

Testing for efficacy against UVR-induced skin tumours, while essential, is a long and expensive process. If early markers were identified to reliably predict which agents were likely to reduce tumours, this could streamline selection of candidates for this testing.

1. Dixon, K.M., et al., 1alpha,25(OH)2-Vitamin D and a Nongenomic Vitamin D Analogue Inhibit Ultraviolet Radiation-Induced Skin Carcinogenesis. Cancer Prevention Research, 2011. 4(9): p. 1485-94
2. Tongkao-On, W., Role of Vitamin D and Other Compounds in the Protection of Skin Cells from UV, in Physiology, School of Medical Sciences, University of Sydney, 2015 [PhD Thesis]
3. Rybchyn, M.S., et al., Enhanced Repair of UV-Induced DNA Damage by 1,25-Dihydroxyvitamin D3 in Skin Is Linked to Pathways that Control Cellular Energy. J Invest Dermatol, 2018. 138(5): p. 1146-1156

130

Mass spectrometry imaging spatially identifies complex-type *N*-glycans as putative cartilage degradation markers in human knee osteoarthritis tissue

Yea Rin Olivia Lee[1, 2, 3], Matthew Briggs[3], Julia Kuliwaba[1], Peter Hoffmann[3], Jakub Jagiello[4], Paul Anderson[2]

1. School of Medicine, The University of Adelaide, Adelaide, SA, Australia

2. Clinical and Health Sciences, Health and Biomedical Innovation, University of South Australia, Adelaide, SA, Australia

3. Clinical and Health Sciences, University of South Australia, Adelaide, SA, Australia

4. Department of Orthopaedics Surgery, Royal Adelaide Hospital, Adelaide, SA, Australia

Publish consent withheld

131

A meta-analysis examining the impact of wait time for orthopaedic consultation on pain levels in individuals with osteoarthritis

Rhiannon Patten[1], Alexander Tacey[1], Matthew Bourke[1], Cassandra Smith[1, 2], Michaela Pascoe[1], Sara Vogrin[3], Alexandra Parker[1], Michael McKenna[1], Phong Tran[1, 4], Mary De Gori[5], Catherine Said[6], Vasso Apostolopoulos[1], Rebecca Lane[1], Mary Woessner[1], Itamar Levinger[1]

1. Institute for Health and Sport, Victoria University, Footscray, Victoria, Australia

2. School of Medical and Health Sciences, Edith Cowan University, Perth, Western Australia, Australia

3. Department of Medicine, The University of Melbourne, Melbourne, Victoria, Australia

4. Department of Orthopaedic Surgery, Western Health, Melbourne, Victoria, Australia

5. Department of Physiotherapy, Western Health, Melbourne, Victoria, Australia

6. Physiotherapy, Melbourne School of Health Sciences, University of Melbourne, Melbourne, Victoria, Australia

Objective

Time spent waiting for access to orthopaedic specialist health services has been suggested to result in increased pain in individuals with osteoarthritis (OA). We assessed whether time spent on an orthopaedic waiting list resulted in a detrimental effect on pain outcome measures in patients with knee or hip OA.

Methods

We searched Ovid MEDLINE, EMBASE and EBSCOhost databases from inception until September 2021. Eligible articles included individuals with OA on an orthopaedic waitlist and not receiving active treatment, and reported pain outcome measures at two or more time points. Random-effects meta-analysis was used to estimate the pooled effect of time on pain outcome measures. Meta-regression was used to determine predictors of effect size.

Results

Thirty-three articles were included (n = 2,490 participants, 67 ± 3 years and 62% female). The range of waiting time was 2 weeks to 2 years (20.8 ± 18.8 weeks). There was no significant longitudinal change in pain (effect size = 0.082, 95% CI = -0.009, 0.172), nor was the length of time associated with longitudinal changes in pain (β = 0.004, 95% CI = -0.005, 0.012). Body mass index was a significant predictor of pain (β = -0.043, 95% CI = -0.079, 0.006), whereas age and sex were not.

Conclusions

Patients with OA who were on an orthopaedic waitlist did not report a change in pain levels for up to 2 years. As such, this presents an opportune time to deliver non-surgical, interventions to improve patient wellbeing and reduce the burden on the healthcare system.

132

Compromised Osteocyte Viability and Connectivity: a Key Contributor to the Pathogenesis of Human Hip Osteoarthritis.

Dzenita Muratovic[1], Micaela J Quinn[2], David M Findlay[1], Gerald J Atkins[1]

1. Centre for Orthopaedic & Trauma Research, The University of Adelaide, Adelaide, South Australia, Australia

2. Bone and Joint Osteoimmunology Laboratory , The University of Adelaide, Adelaide, SA, Australia

Introduction: Structural, cellular, and molecular changes within subchondral bone are causal of osteoarthritis initiation and progression. Despite osteocytes being the most abundant cell type within the bone, their association in OA pathogenesis, particularly hip OA, remains unknown. Overall, hip OA's osteocyte viability, density, and connectivity are largely unexplored. This study aimed to comprehensively characterise osteocyte metabolic and functional state in human subchondral bone of hip OA.

Method: Femoral heads were collected from 8 patients undergoing total hip replacement surgery (4 females, aged 69 14 years) and 8 human cadavers (5 females, 64 12 years). Two bone core biopsies were sampled per subject, imaged by synchrotron micro-CT to obtain osteocyte lacunar properties, and then processed for histological assessment and evaluation of osteocyte density, viability, and connectivity.

Results: Compared to control, subchondral bone in OA tissue were characterised by larger ($p=0.0003$) and more spheric ($p=0.03$) osteocyte lacunae, decreased osteocyte cell density ($p=0.020$, $p<0.0001$), decreased canalicular number ($p=0.003$, $p=0.002$) and decreased canalicular length ($p=0.01$, $p=0.003$) but significantly increased percentage of empty lacunae ($p=0.0009$, $p<0.0001$) and apoptotic osteocytes ($p=0.02$, $p=0.04$) in both plate and trabeculae respectively. Osteocyte senescence assessed by Sudan Black B staining was not significantly different between control and OA.

Discussion: These data demonstrate that osteocyte viability and connectivity is compromised within OA subchondral bone implicating a direct role for osteocytes in hip OA pathogenesis. The results from this study have the potential to identify a specific target for the development of effective therapies to prevent OA progression in suffering patients. However, further investigation is necessary to identify osteocyte molecular mechanisms involved in the pathogenesis in hip OA.

133

Loss of body mass index (BMI) reduces the need for knee replacement: a multi-cohort survival analysis

Zubeyir Salis[1], Amanda Sainsbury-Salis[2]

1. University of NSW, Centre for Big Data Research in Health, Kensington, NSW, Australia

2. University of WA, School of Human Sciences, Crawley, WA, Australia

Introduction: The annual healthcare cost of total knee replacement surgery due to osteoarthritis in Australia is expected to reach A$3.40 billion by 2030. While osteoarthritis is clearly associated with obesity, and inter/national osteoarthritis guidelines recommend patients with overweight/obesity lose weight for symptom reduction, the effect of weight loss on progression to knee replacement is unclear.

Materials and methods: Using data from 3 cohorts of people with or at risk of clinically significant knee osteoarthritis (the Osteoarthritis Initiative (OAI) and the Multicenter Osteoarthritis Study (MOST) from the USA, and the Cohort Hip and Cohort Knee (CHECK) study from the Netherlands), we conducted a time-to-event survival analysis with clustering of both knees per person to determine the association between change in BMI (as a proxy for weight) and the incidence of primary knee replacement over 7 to 10 years' follow-up.

Results: A total of 16,362 knees from 8181 participants (61.5 % female), aged 45-79 years, with mean ± SD baseline BMI of 29.1 ± 5.3 kg/m^2, were included in the analysis. Mean follow up was 6.9 years.

Change in BMI had a positive, dose-responsive association with the risk of knee replacement (adjusted hazard ratio 1.03; 95% confidence interval 1.00–1.06). There were no significant interactions between change in BMI and baseline BMI in the association with knee replacement. Thus, regardless of baseline BMI, every 1-unit reduction in BMI was associated with a 3% reduced risk of knee replacement. Calculation of the population attributable fraction (PAF) suggested that if people with or at risk of clinically significant knee osteoarthritis and with BMI ≥ 25 kg/m^2 lost 1 BMI unit, then 3.2% (range: 0.3-5.9%) of knee replacements would be avoided.

Conclusion: Public health strategies that incorporate weight loss interventions could potentially reduce the burden of knee replacement surgery.

134

Unveiling the role of microRNA-1 in chondrocytes and osteoarthritis

Jiao Jiao Li[1, 2], Yang Yang[3], Yawei Wang[3], Haobo Jia[3], Bing Li[3], Dan Xing[4]

1. University of Technology Sydney, Ultimo, NSW, Australia

2. Kolling Institute, St Leonards, NSW, Australia

3. Tianjin Hospital, Tianjin, China

4. Peking University People's Hospital, Beijing, China

Publish consent withheld

1. Swingler TE, Wheeler G, Carmont V, Elliott HR, Barter MJ, Abu-Elmagd M, Donell ST, Boot-Handford RP, Hajihosseini MK, Münsterberg A, Dalmay T, Young DA, Clark IM. The expression and function of microRNAs in chondrogenesis andmosteoarthritis. Arthritis Rheum. 2012;64(6):1909-19.
2. Hong E, Reddi AH. MicroRNAs in chondrogenesis, articular cartilage, and osteoarthritis: implications for tissue engineering. Tissue Eng, Part B. 2012;18(6):445-53.
3. Sumiyoshi K, Kubota S, Ohgawara T, Kawata K, Nishida T, Shimo T, Yamashiro T, Takigawa M. Identification of miR-1 as a micro RNA that supports late-stage differentiation of growth cartilage cells. Biochem Biophys Res Commun. 2010;402(2):286-90.
4. Lu T-Y, Lin B, Li Y, Arora A, Han L, Cui C, Coronnello C, Sheng Y, Benos PV, Yang L. Overexpression of microRNA-1 promotes cardiomyocyte commitment from human cardiovascular progenitors via suppressing WNT and FGF signaling pathways. J Mol Cell Cardiol. 2013;63:146-54.

Fracture risk assessment: does competing risk adjustment make a difference?

Thach Tran[1, 2], **Tuan V Nguyen**[3, 4]

1. Garvan Institute of Medical Research, Darlinghurst, NSW, Australia

2. Faculty of Medicine, University of New South Wales, Sydney, Australia

3. School of Medicine Sydney, University of Notre Dame Australia, Sydney, Australia

4. School of Biomedical Engineering, Centre of Health and Technologies, University of Technology Sydney, Sydney, NSW, Australia

The estimate of fracture risk can be compromised by the competing event of mortality, in which individuals die during a period of time without sustaining a fracture, resulting in the current suboptimal prediction of fracture risk and contributing to the global crisis of osteoporosis management. We hypothesized that the multistate model (MSM) could predict the risk fracture more accurately than the currently used competing risks models.

We used data from the Dubbo Osteoporosis Epidemiology Study that monitored bone health and mortality of 3,035 elderly individuals for more than 20 years. Fragility fracture was ascertained by X-ray reports. Mortality was ascertained from the NSW Registry of Births, Deaths and Marriages. We considered 4 statistical models for estimating an individual's risk of fracture: (i) standard Cox's proportional hazards (conventional); (ii) cause-specific (CS); (iii) Fine-Gray subdistribution (FG); and (iv) MSM. These models were fitted and validated in the development (60% of the original sample) and validation (40%) cohort, respectively. Accuracy of fracture risk prediction was assessed using discrimination and calibration analysis.

During a median of 11.3 years, 628 (34.5%) individuals in the development cohort had sustained a fracture, and 630 (34.6%) had died without a fracture. All models had comparable discrimination performance (C index ~ 0.73 and 0.69 at 5 and 10-year prediction, respectively). All models had little difference in the 5-year predicted risk, though the conventional model tended to overestimate the fracture risk. For 10-year risk prediction, the MSM (calibration-in-the-large index = -0.05), CS (-0.23) and FG (-0.31) models outperformed the conventional Cox's model (-0.54) which over-estimated fracture risk (Figure).

The multistate model produces the most accurate estimate of fracture risk, especially for long-term prediction and practically superior to the currently used models. The multistate model should be considered as the optimal competing risks approach in development of a prediction model.

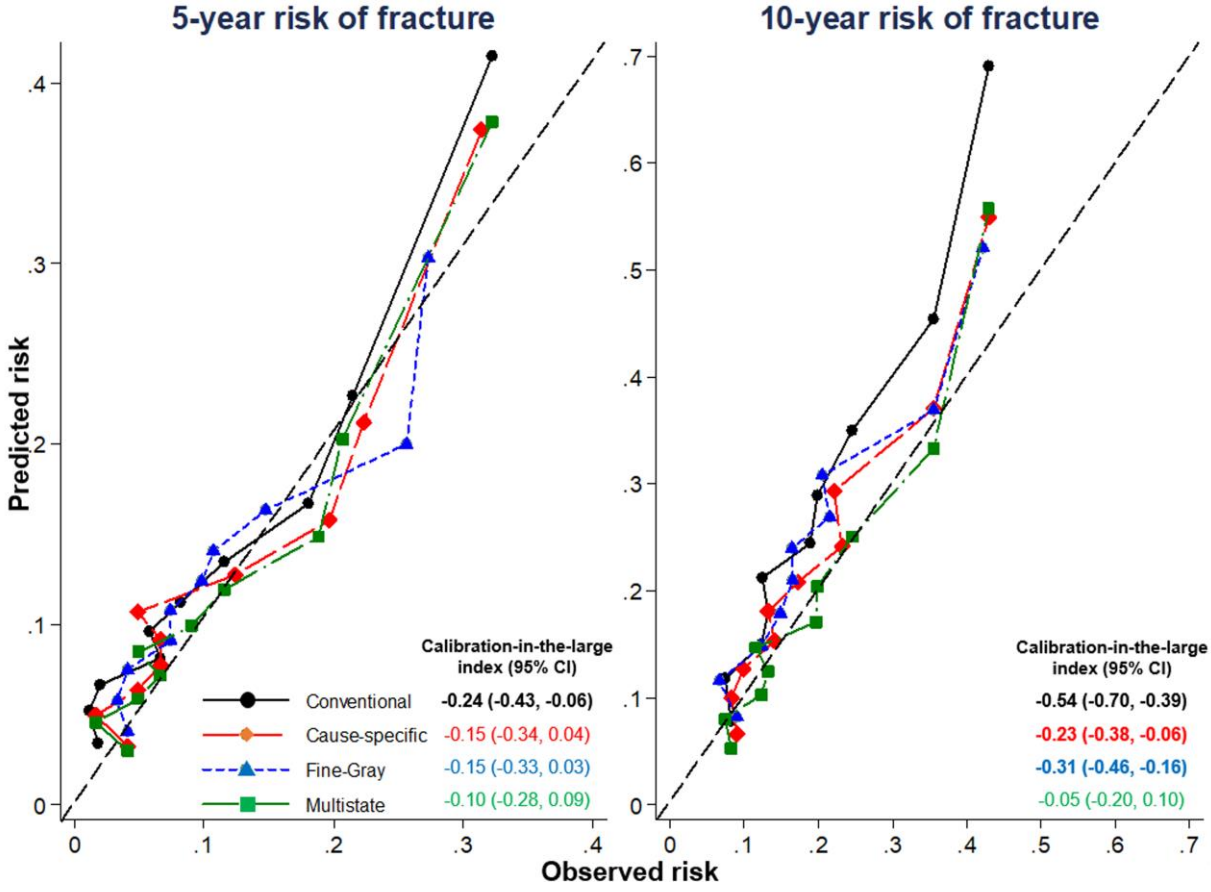

1. Figure: Accuracy of the conventional and different competing risks model for predicting fracture risk

136

Advanced Mass Spectrometry imaging technique provides novel approaches to understanding the lipid fingerprinting of osteoarthritis progression

Xiwei Fan[1], Brett Hamilton[2], Stephen Blanksby[3], Ross Crawford[1, 4], Indira Prasadam[1]

1. Queensland University of Technology, Kelvin Grove, QLD, Australia

2. Centre for Microscopy and Microanalysis, University of Queensland, St Lucia, QLD, Australia

3. Central Analytical Research Facility, QUT, Kelvin Grove, QLD, Australia

4. The Prince Charles Hospital, Brisbane, QLD, Australia

The spatial changes of lipids and lipid-related proteins play a vital role in the reflection of osteoarthritis. Due to sample preparation difficulties, the hallmark of spatial changes in lipids and proteins remains less well known. The aim of this study is to use advanced mass spectrometry imaging techniques to discover the proteins, and lipids and their functionality change at a spatial level. We collected osteochondral tissue samples stratified according to disease severity, from 10 knee OA patients who underwent knee replacement surgery. We defined the lipid and related protein changes using the spatial multi-omics technique, including spatial proteomics, spatial lipidomics and functional mass spectrometry imaging technique. We confirmed our results using immunohistochemistry and laser-microdissection guided lipidomics and proteomics. Our results find a characteristic distribution of lipids and lipid-related proteins in the osteochondral unit. We also demonstrated that the functionality of phospholipase A2 was reactivated on the surface of the cartilage surface. In conclusion, our results suggest that the multiple lipids and lipid-related protein changes can reflect the disease progression.

137

Observational and genetic relationships between hip shape and hip osteoarthritis: findings from UK Biobank

Monika Frysz[1, 2], B G Faber[1, 2], R Ebsim[3], F R Saunders[4], J S Gergory[4], N C Harvey[5], C Linder[4], T Cootes[4], J P Kemp[1, 6, 7], J H Tobias[1, 5]

1. Musculoskeletal Research Unit, University of Bristol, UK

2. Medical Research Council Integrative Epidemiology Unit at the University of Bristol, UK

3. Division of Informatics, Imaging and Data Science, The University of Manchester, UK

4. Centre for Arthritis and Musculoskeletal Health, University of Aberdeen, UK

5. Medical Research Council Lifecourse Epidemiology Centre , University of Southampton, UK

6. Diamantina Institute, University of Queensland, Woolloongabba, Australia

7. Institute for Molecular Bioscience, University of Queensland, St Lucia, Australia

Background

Hip shape is an important risk factor for hip osteoarthritis (HOA). In the present study, we used statistical shape modelling (SSM) to evaluate observational relationships between hip shape and HOA, and genetic associations with hip shape using UK Biobank (UKB) dual-energy X-ray absorptiometry (DXA) images.

Methods

Statistical shape modelling (SSM) was used to quantify hip shape (BoneFinder, University of Manchester) from DXA images and generate orthogonal modes of variation (hip shape modes (HSMs)). The first ten HSMs were analysed for associations with HOA outcomes (hospital diagnosed HOA, and grade 2 and ≥3 radiographic HOA (rHOA)) using logistic regression and total hip replacement (THR) using Cox proportional hazards regression. Genome-wide association (GWA) analyses were adjusted for age, sex, genotyping chip and 20 ancestry principal components. GCTA-COJO was implemented to identify conditionally independent SNPs at each genome-wide significant HSM-associated locus.

Results

A total of 40,311 individuals were included in observational analyses (mean 63.7 years, 47.8% male), of whom 5.7% had grade 2 rHOA, 1.7% grade ≥3 rHOA, 1.3% hospital diagnosed HOA, and 0.6% underwent THR. Combined results for grade 2 rHOA revealed femoral neck widening, increased acetabular coverage, and enlarged lesser and greater trochanters. In contrast, grade ≥3 rHOA, hospital diagnosed HOA and THR were suggestive of cam morphology and reduced acetabular coverage. Genetic analyses in 38,175 individuals identified a total of 233 conditionally independent signals associated with the first ten HSMs at genome-wide significance ($p<5x10^{-8}$) which mapped to 201 loci (based on a 1mb sliding window).

Conclusions

Observational relationships between hip shape and HOA differed according to severity. Notably, cam morphology and acetabular dysplasia were features of severe HOA, but unrelated to moderate disease, suggesting possible prognostic utility. Genetic analyses revealed several loci not previously found to associate with hip shape.

200

Parental fracture in early life predicts early life fracture risk in offspring

Kara Anderson[1], Mia Percival[1], Julie Pasco[1], Sarah Hosking[1], Natalie Hyde[1]

1. Deakin University, Geelong

Aims Fractures during childhood and adolescence are common as peak bone mass has not yet been accrued; previous studies have reported that offspring are at higher risk of a fracture if one or both parents has experienced a fracture. However, it is not known if parental fracture demonstrates differential risk profiles across the sexes. Therefore, this study aimed to determine the associations between maternal and paternal fracture history and offspring fracture risk in early life.

Methods Women (n=1,336) and men (n=1,174) enrolled in the Geelong Osteoporosis Study were included. Parental and personal fracture history from birth until 20 years of age was determined through self-report at the baseline visit (women: 1993-97; men: 2001-06). Univariate logistic regression models were used to assess the odds of fracture. Exposures of paternal, maternal or any parent fracture were tested.

Results In total, 208 (15.6%) women and 292 (24.9%) men experienced a fracture at 20 years of age or younger. In women, 48 mothers and 59 fathers had experienced a fracture before the age of 20 and in men 18 mothers and 43 fathers, respectively. Maternal fracture, paternal fracture and either parental fracture were associated with an increased odds of fracture in women (OR 2.32, 1.22-4.41, p=0.010, OR 1.91, 1.04-3.51, p=0.036, and OR 2.25, 2.41-3.57, p=0.001, respectively). Paternal fracture was associated with an increased odds of fracture in men (OR 2.04, 1.09-3.81, p=0.026). There were no other associations in men.

Conclusion Parental fracture history appears to be sex-specific, whereby both maternal and paternal fracture history increases the risk of fracture in girls, while only paternal fracture history in boys. Paternal, rather than maternal, history of early life fracture appears to be a more consistent predictor of early-life fractures across the sexes.

201

The effect of astaxanthin on the structural alterations in muscles of elastase-induced emphysema mouse models

Yosuke Mano[1], Manabu Tsukamoto[1], Ke-Yong Wang[2], Takayuki Nabeshima[1], Takafumi Tajima[1], Yoshiaki Yamanaka[1], Eiichiro Nakamura[1], Akinori Sakai[1]

1. Department of Orthopaedic Surgery, School of Medicine, University of occupational and environmental health, Japan, Kitakyushu, Fukuoka, Japan

2. Shared-Use Research Center, School of Medicine, University of occupational and environmental health, Japan, Kitakyushu, Fukuoka, Japan

Background: Sarcopenia is a complication of chronic obstructive pulmonary disease (COPD) that negatively affects physical activity and quality of life. However, the underlying mechanism by which COPD affects skeletal muscles remains to be elucidated. Therefore, we investigated the association between oxidative stress and structural alterations in muscles of COPD mouse models and verified the effect of astaxanthin on the structural alterations in muscles.

Methods: Twelve-week-old male C57BL/6J mice were treated with intratracheal porcine pancreatic elastase (PPE) dissolved in saline or saline alone. The mice were euthanized 12 weeks after administration, and the lungs and leg muscles were obtained for protein analysis of oxidative stress and p38 mitogen-activated protein kinase (p38 MAPK) signaling pathway, muscle atrophy signaling pathway related with oxidative stress. Furthermore, C57BL/6J mice treated with PPE or saline were investigated with the effects of oral administration of astaxanthin.

Results: The weight of the soleus muscle, proportion of type I muscle fibers, and cross-sectional areas of muscle fibers in the COPD mice were lower than those in the control mice. In the mouse model, oxidative stress marker levels were elevated in skeletal muscles. The p38 mitogen-activated protein kinase signaling pathway was activated in the soleus muscles, leading to the activation of the ubiquitin-proteasome system. Astaxanthin attenuated alterations in muscle structure by deactivation of the p38 mitogen-activated protein kinase signaling pathway.

Conclusions: This study provides evidence that oxidative stress induced by COPD triggers a series of muscle structural changes.

202

Associations of body mass index, body fat percentage and sarcopenia components with bone health estimated by second-generation high-resolution peripheral quantitative computed tomography in older adults with obesity

Anoohya Gandham[1], Jakub Mesinovic[1, 2], Mavil May Cervo[1], Costas Glavas[2], Paul Jansons[2], Carrie-Anne Ng[1], Juan Rodriguez[1], Ayse Zengin[1], Maxine Bonham[1], Peter Ebeling[1], David Scott[1, 2]

1. Monash University, Clayton, VICTORIA, Australia

2. Institute for Physical Activity and Nutrition (IPAN), School of Exercise and Nutrition Sciences, Deakin University, Geelong , Victoria, Australia

Purpose: To investigate associations between body mass index (BMI), body fat percentage, and components of sarcopenia (muscle mass and muscle strength/power), with bone microarchitecture measured by high-resolution peripheral computed tomography (HR-pQCT) in older adults with obesity.

Methods: Seventy-four adults aged ≥55 years with body fat percentage ≥30% (men) or ≥40% (women) were included. Fat mass, lean mass and total hip, femoral neck, and lumbar spine areal bone mineral density (aBMD) were measured by dual-energy X-ray absorptiometry. Appendicular lean mass (ALM) was calculated as the sum of lean mass in the upper- and lower-limbs. BMI was calculated and participants completed physical function assessments including stair climb power test. Distal tibial bone microarchitecture was assessed using HR-pQCT. Linear regression (β-coefficients and 95% confidence intervals) analyses were performed with adjustment for confounders including age, sex, smoking status, vitamin D and self-reported moderate to vigorous physical activity.

Results: BMI and ALM were both positively associated with total hip, femoral neck and lumbar spine aBMD and trabecular bone parameters including bone volume fraction and volumetric BMD (vBMD) after adjusting for confounders (all $p<0.05$). Body fat percentage was not associated with aBMD or any trabecular bone parameters but was negatively associated with cortical area (-1.647mm^2; -3.127, -0.167). Stair climb power (indicating better performance) was positively associated with cortical area and bone stiffness (both $p<0.05$).

Conclusion: Higher BMI, ALM and muscle power were associated with more favourable bone microarchitecture, but higher body fat percentage was negatively associated with cortical bone area. These findings suggest the protective effect of high BMI for fractures is attributable to higher muscle mass and/or forces, but that higher relative body fat is not associated with/beneficial for bone health in older adults with obesity.

203

Development of Optimised Sintered Bovine Bone Block for Oral Grafting: Physio-chemical, mechanical and biological characterisation

Asrar Elahi[1], Warwick Duncan[1], Kai Chun Li[1], J Neil Waddell[1], Carla Meledandri[2], Dawn Coates[1]

1. FACULTY OF DENTISTRY, UNIVERSITY OF OTAGO, DUNEDIN, OTAGO, NEW ZEALAND

2. DEPARTMENT OF CHEMISTRY, UNIVERSITY OF OTAGO, DUNEDIN, OTAGO, NEW ZEALAND

Objectives: Oral bone defects require bone grafts that are biocompatible, osteoconductive and physically robust to withstand clinical handling. Bovine bone is accepted as a source of suitable grafting material (xenografting). However, the manufacturing process reduces its biological properties and mechanical strength. Therefore, the aim of our study was to develop optimised bovine bone blocks while assessing the effects of different sintering temperatures on their physio-chemical properties, biocompatibility and clinically-relevant mechanical strength.

Methods: Bone blocks/disks (5x5x5 mm/5x2 mm) were divided into four groups; Gp1: Control/Untreated, Gp2: Initial boil (6 hours), Gp3: Sintered at 550°C (6 hours), Gp4: Sintered at 1100°C (6 hours). Samples were tested for purity (thermogravimetric analysis), crystallinity (X-ray diffraction), mechanical strength (compression testing), surface morphology and chemical composition (SEM/EDS). Biocompatibility was tested with human osteoblasts *in vitro* by measuring viability (PrestoBlue™) and cellular adhesion (phalloidin). Clinical handling was tested by placing a 10x1.5 mm diameter cross-head bone-block screw into blocks drilled at 800 RPM. Statistical analysis was performed using GraphPad PRISM software and Tukey's multiple comparison test based on one-way ANOVA. P value <0.05 was considered as significant.

Results: Higher temperature sintering (Gp4) removed all organic components but increased crystallinity (95.33%). All test groups (Gp2-4) showed decreased mechanical strength (MPa: 4.21 ± 1.97, 3.07 ± 1.21, 5.14 ± 1.86, respectively) compared with raw bone (Gp1) (MPa: 23.22 ± 5.24, p <0.05), with micro-cracks seen under SEM. However, Gp4 had highest biocompatibility as compared to control (p <0.05). Clinically-relevant bench-top testing showed that Gp4 samples could better withstand drilling and screw placement, but demonstrated high brittleness compared to Gp1.

Conclusion: Bovine bone blocks sintered at higher temperatures resulted in highly pure bone with better biocompatibility and reduced but acceptable mechanical strength and clinical handling. Further animal model studies will demonstrate the suitability of this construct for bone grafting applications.

Gender-related differences in bone architecture in Vietnamese

Duy K. Hoang[1, 2, 3], Huy G. Nguyen[1, 2, 3], Thach Tran[1, 4], Lan T. Ho-Pham[2, 3], Tuan Nguyen[1]

1. University of Technology Sydney, Ultimo, NSW, Australia

2. Ton Duc Thang University, Faculty of Applied Sciences, Ho Chi Minh, Vietnam

3. Ton Duc Thang University, Bone and Muscle Research Group, Ho Chi Minh, Vietnam

4. Garvan Institute of Medical Research, Osteoporosis and Bone Biology, Sydney, NSW

Objective

It is commonly assumed that for given body size, Caucasian men have larger skeletal size and higher bone mass than women. We revisit this assumption by examining gender-related differences in bone size, geometry and density after controlling for body size.

Methods

The study involved 4196 women and men aged 20 years and older who were recruited from the general population of Ho Chi Minh City (Vietnam). Tibia and cortical bone volumetric BMD were measured at 4%, 38%, and 66% sites using a peripheral quantitative computed tomography XCT2000 (Stratec, Germany). Bone mineral density (BMD) was measured at the lumbar spine and femoral neck by DXA (Hologic Horizon). For each woman, we randomly matched with a man of similar age, height, and weight. The difference in bone parameters between both genders was tested by the paired t-test.

Results

The matching algorithm resulted in 325 pairs of men and women with identical age (48 years), height (160 cm), and weight (57 kg). Averagely, women had 12% more fat mass than men ($P < 0.001$). Men had higher lean mass (40.3±4.0 vs 33.5±3.8 kg, $P < 0.001$) but lower fat mass (17.2±4.1 vs 24.1±4.4 kg, $P < 0.001$) than women. Areal BMD at femoral neck and total hip was consistently higher in men than women ($P < 0.001$). Furthermore, men had greater bone area and volumetric BMD than women at either the radius or tibia regardless of at 4% or 66% sites. The force required to break the radius or tibia in men was about 1.5 times ($P < 0.001$) higher than in women.

Conclusion

These results show that for the same age, height and weight, men have greater bone size, volumetric BMD, and breaking force than women, and these differences may explain why men have a lower risk of fracture than women.

Bayesian Network Meta-Analysis of Cancer Events in Trials of Osteoporosis Therapies

Alexander H Seeto[1], Joshua Long[1], Kevin Leow[2], Mina Tadrous[3], Abadi Kahsu Gebre[4], Joshua R Lewis[4], Howard A Fink[5], Peter R Ebeling[6], Alexander J Rodriguez[6]

1. Griffith University, Southport, QLD, Australia

2. The Canberra Hospital, Canberra

3. Leslie Dan Faculty of Pharmacy, University of Toronto, Toronto

4. Institute for Nutrition Research, School of Medical and Health Sciences, Edith Cowan University, Joondalup

5. Geriatric Research Education and Clinical Center, VA Health Care System, Minneapolis

6. Bone and Muscle Health Research Group, Monash University, Clayton

Anti-resorptive drugs reduce skeletal-related events in cancer. However, little is known about the effects of these and other osteoporosis therapies on incident cancer in postmenopausal women. Therefore, we conducted a network meta-analysis (NMA) examining cancer adverse event data from randomised trials of osteoporosis therapies in postmenopausal women.

Trials were identified from recent NMAs of osteoporosis therapies for fracture reduction, updated to December 2020. Included trials enrolled >100 postmenopausal women per study without cancer at baseline, randomised to placebo or an active comparator (bisphosphonate, denosumab, parathyroid [PTH] analogue, romosozumab, or menopausal hormone therapy [MHT] such as selective estrogen receptor modulators or direct estrogen and/or progesterone supplementation), and reported primary skeletal outcomes. We extracted incident cancer diagnoses from reported trial adverse events. Outcomes of interest were breast cancer, and a composite comprising all cancer events. Data were synthesized into a random-effects model using Bayesian principles. Relative to placebo, point estimates for the odds ratio with 95% credible intervals were generated. Probabilistic ranking of treatment safety in relation to cancer diagnoses was performed.

We identified 33 eligible trials, enrolling 54,617 women. During a mean follow-up of 24 months, 85 incident breast cancer events (0.16%) and 1229 incident all cancer events (2.25%) occurred. We found no significant difference in either cancer outcome between placebo or any osteoporosis therapy. In probabilistic ranking, MHT and bisphosphonates were less likely to have increased risk of breast cancer than placebo. Denosumab, romosozumab and PTH analogues ranked more likely to have increased risk of breast cancer than placebo. Probabilistic rankings were similar when considering all cancer events.

We found no pooled direct/indirect evidence that osteoporosis therapies significantly increased the risk of cancer relative to placebo. Equally, there was no convincing evidence that osteoporosis therapies reduced cancer risk in the setting of fracture reduction in postmenopausal women.

Probablistic Ranking

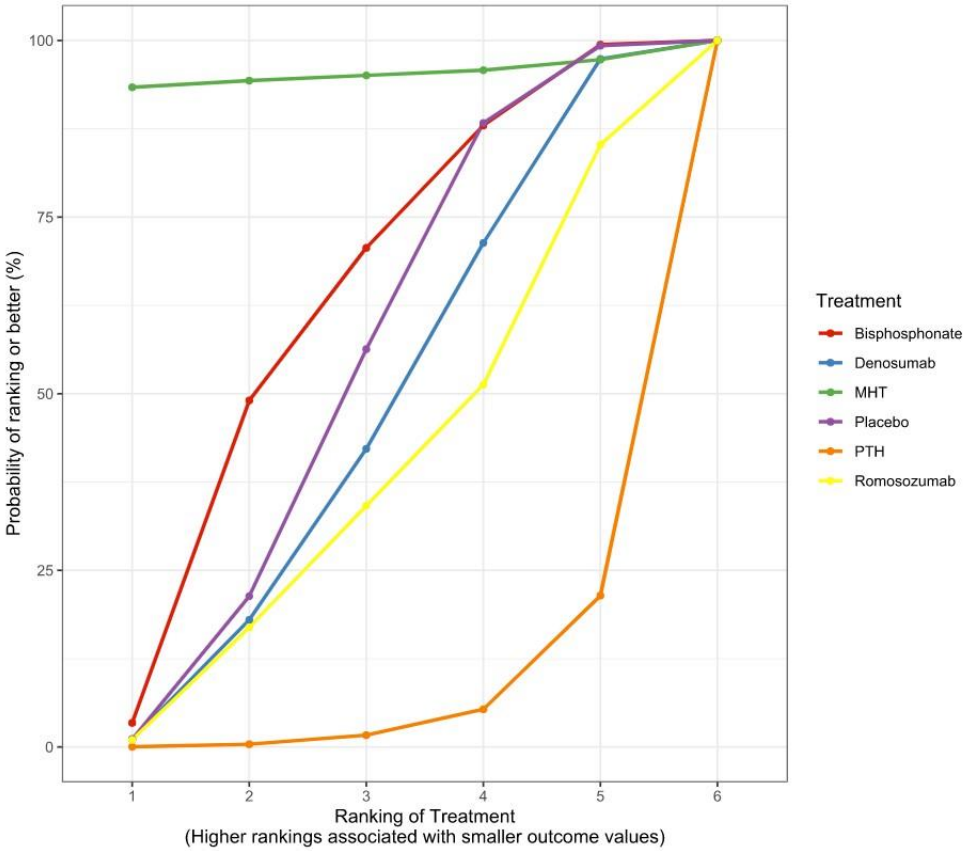

Discordance in paretic and non-paretic hips bone density in hemiplegic stroke patients – a cross-sectional multicenter retrospective study

Hoo Young Lee[1], Byung-Mo Oh[1], Jungeun Son[2], Seung Don Yoo[2]

1. Seoul National University Hospital/National Traffic Injury Rehabilitation Hospital, Yangpyeong-Eub, Yangpyeong-Gun, GYEONGGI-DO, South Korea

2. Dept. of Rehabilitation Medicine, KYUNG HEE UNIVERSITY HOSPITAL AT GANGDONG, Seoul, South Korea

Background

The diagnosis of osteoporosis is determined based on the lowest bone mineral density (BMD) T-score at the lumbar spine (LS) and hip. Bone loss after stroke escalates the risk of fractures, mainly in the hip, leading to further disability in individuals with stroke. However, there are occasional marked discordances between the T-score of paretic hip and LS or T-scores of paretic and non-paretic hips. We aimed to compare the BMD between the paretic and non-paretic hips and spine and each hip, and elucidate the relationship between the discordance and BMD of paretic hip.

Methods

The 753 hemiplegic stroke patients (360 male, 393 female) above 20 years of age with cerebral infarction or hemorrhage were analyzed. BMD in the lumbar, paretic, and non-paretic hip as well as the demographic variables were analyzed retrospectively.

Results

The concordance and discordance rates of the lowest T-score and BMD between both hips were evaluated. The BMDs of the femoral neck were different between both hips. There were also discrepancies between the T-scores of both femur neck and LS. The concordance rates were about 81% between bilateral femoral neck and 53.5% between paretic femur neck and LS.

Conclusions

Due to significant high discordance rate in BMD between both hips at the femoral neck and between paretic femoral neck and LS bilateral hip measurements using DEXA are recommended to avoid underestimating osteoporosis, to minimize subsequent bone loss and to prevent possible complications in patients who experience stroke.

Table 1. Demographic data

	Total (N=753)
age	74.56 (11.73)
duration	116.01 (259.44)
right hemiplegia (%)	400 (53.12)
infarction (%)	589 (78.2)
BMI	23.32 (4.36)
MMT total	20 (3.53)
MAS Hip	1
MAS Knee	1
MAS Ankle	1
MBI total	44 (27.19)
MBI stairs	0 (2.60)
MBI transfer	8 (4.72)
MBI ambulation	0 (5.05)
FAC	1 (1.14)
BBS	21 (18.15)
MMSE	21 (9.62)
NIHSS	8 (5.15)
mRS	4 (1.09)

Table 2. Concordance according to the T score of paretic and nonparetic femoral neck and lumbar spine

N=620	G1 PFN	G2 PFN	G3 PFN
G1 NPFN	**163 (27.4%)**	32 (5.4%)	1 (0.2%)
G2 NPFN	28 (4.7%)	**191 (32.2%)**	31 (5.2%)
G3 NPFN	0 (0.0%)	20 (3.4%)	**128 (21.5%)**

N=671	G1 PFN	G2 PFN	G3 PFN
G1 LS	**149 (22.2%)**	102 (15.2%)	31 (4.6%)
G2 LS	58 (8.6%)	**117 (17.4%)**	60 (8.9%)
G3 LS	6 (0.9%)	55 (8.2%)	**93 (13.9%)**

N=673	G1 NPFN	G2 NPFN	G3 NPFN
G1 LS	**158 (23.5%)**	99 (14.7%)	28 (4.2%)
G2 LS	59 (8.8%)	**114 (16.9%)**	54 (8.0%)
G3 LS	5 (0.7%)	68 (10.2%)	**88 (13.1%)**

PFN paretic femur neck, NPFN non-paretic femur neck, LS lumbar spine

Coronary stenosis scores in a cohort of osteoporosis medication users undergoing cardiac computed tomography at a single tertiary centre

Alexander J. Rodriguez[1], Rachel Hii[2], Nitesh Nerlekar[2], Peter R. Ebeling[1]

1. Monash University, Clayton, VIC, Australia

2. Monash Heart, Clayton, VIC, Australia

Introduction

Anti-resorptive medications are first-line treatments for osteoporosis. Additionally, patients with osteoporosis are at high cardiovascular risk, which may be partly due to extra-skeletal calcification such as in the coronary vessels. It is uncertain if anti-resorptive medication effects coronary calcification. We therefore measured the presence and severity of coronary stenosis in a cohort of patients with osteoporosis using anti-resorptive medications and in controls.

Methods

Individuals dispensed at least one script for an anti-resorptive medication (bisphosphonates or denosumab) at Monash Health between 2009-2022 were identified. Unique record numbers for these individuals were cross matched against the cardiac CT imaging service at Monash Heart (HREC#73603). Sex-matched controls not taking anti-resorptive medications were identified from the imaging database. Coronary calcification causing stenosis was reported using the standardised "Coronary Artery Disease - Reporting and Data System (CAD-RADS)". Moderate-severe stenosis was defined as CAD-RADS≥4 (stenosis ≥25%).

Results

Eighty-four patients (women=68 [81%], median age =66 years [range: 57-74]) were enrolled. Seventy-four (88%) individuals had evidence of coronary stenosis. Zoledronic acid (n=13 [31%]), alendronate (n=11 [26%]) and risedronate (n=11 [26%]) were the most dispensed medications. Additionally, there were five individuals dispensed denosumab (12%) and two dispensed pamidronate (5%). The frequency of moderate-severe stenosis was comparable between groups (n=13 [31%] in anti-resorptive users versus n=15 [36%] in controls). In age and sex adjusted models, anti-resorptive use was negatively associated with CAD-RADS stenosis score (β=0.47 [0.24 to 0.92]) and was associated with reduced odds for increasing stenosis grade (0.25 [0.10 to 0.75]). Analyses were not significant when restricted to those with CAD-RADS>0.

Interpretation

In this preliminary report, we describe that anti-resorptive medication users appear to have lower coronary stenosis scores. Analysis of the full cohort, including consideration of important cardiovascular and skeletal risk factors, is needed to validate this initial finding.

	Anti-resorptive (n=42)	Control (n=42)
CAD-RADS		
0 (no stenosis)	10 (24%)	0 (0%)
1 (1-24% stenosis)	6 (14%)	11 (26%)
2 (25-49% stenosis)	13 (31%)	16 (38%)
3 (50-70% stenosis)	4 (9%)	10 (24%)
4 (70-99% stenosis)	7 (17%)	3 (7%)
5 (complete stenosis)	2 (5%)	2 (5%)
Stenosis severity		
Low-moderate (CAD-RADS <4)	33 (79%)	37 (88%)
Severe (CAD-RADS ≥4)	9 (21%)	5 (12%)
Stenosis grade		
None (CAD-RADS = 0)	10 (24%)	0 (0%)
Mild (CAD-RADS >0 & <3)	19 (45%)	27 (64%)
Moderate-severe (CAD-RADS ≥3)	13 (31%)	15 (36%)

Fracture does not exist in isolation: What do commodities contribute to subsequent fracture and mortality risk?

Dana D Bliuc[1], Thach T Tran[1], Weiwen W Chen[1], Dunia D Alarkawi[1], Dima D Alajlouni[1], Fiona F Blyth[2], Lyn L March[3], Robert RD Blank[1], Jackie JR Center[1]

1. Osteoporosis and Bone Biology, Garvan Institute of Medical Research, Darlinghurst, NEW SOUTH WALES, Australia

2. Concord Clinical School, University of Sydney, Sydney, NSW, Australia

3. Institute of Bone & Joint Research, University of Sydney, Sydney, NSW, Australia

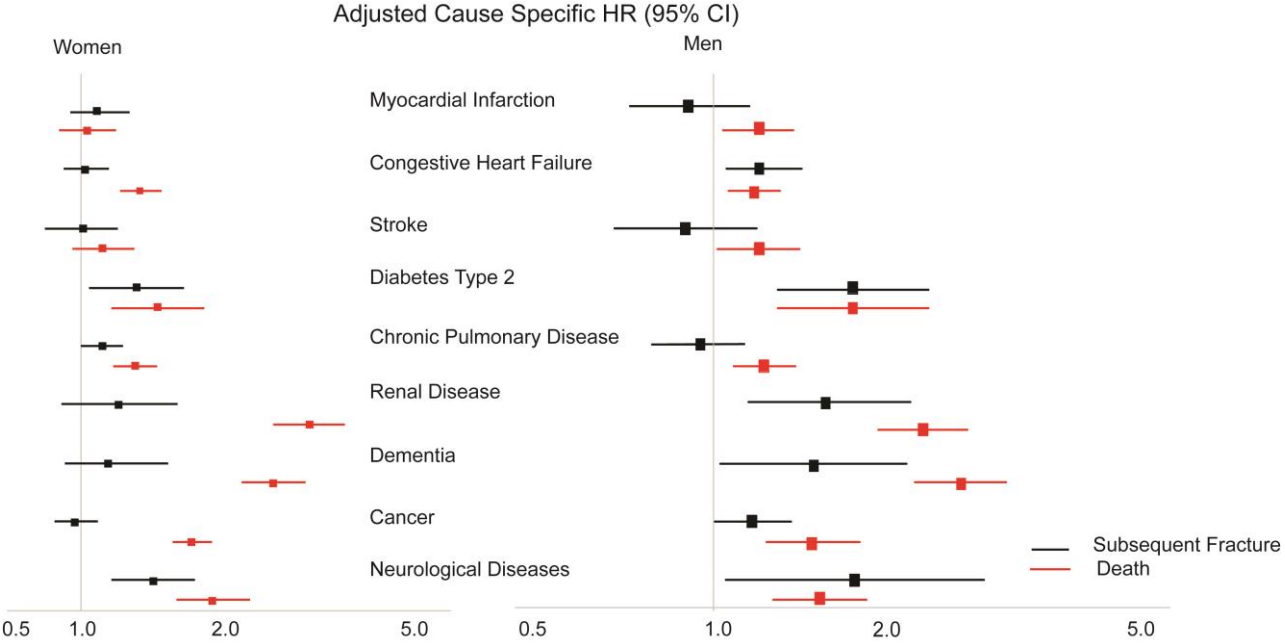

Multimorbidity is known to increase clinical management complexity promote osteoporosis treatment hesitancy, but its impact on post-fracture adverse events is unknown. This study aimed to determine the association between multimorbidity and risk of subsequent fracture and post-fracture mortality risk.

45 and Up is a prospective population-based cohort of 267,153 people with questionnaires linked to hospital (Admitted Patients Data Collection –APDC), emergency (Emergency Department Data Collection – EDDC)[1], Pharmaceutical Benefits Scheme (PBS) and Registry of Births, Deaths and Marriages (RBDM)[2] datasets. Fractures and Charlson Comorbidity Index (CCI) were identified from APDC and EDDC, and mortality from RBDM.

Association of comorbidities and post-fracture adverse events was determined using cause-specific Cox model; a competing risk model which produces simultaneous estimates of subsequent fracture and mortality and is recommended for etiological studies. The models were further adjusted for age, weight, prior fracture and falls.

Of the 25,000 persons with fracture, approximately 15% sustained subsequent fractures and 22% died during 8,460 person-years follow-up. Compared to a CCI <2, a CCI ≥ 2 was associated with increased risk of both subsequent fracture [HR 1.38 (95% CI, 1.16-1.64) and 1.59 (95% CI, 1.30 – 1.95) for women and men, respectively] and mortality [HR, 5.16 (95% CI, 4.57 – 5.84) and 4.02 (95%, 3.58 – 4.52) for women and men, respectively]. Of the individual chronic conditions, diabetes and neurological diseases were associated with increased subsequent fracture risk in both genders, while renal disease and dementia contributed to subsequent fracture risk in men only. All chronic conditions were associated with increased mortality risk in both genders (Figure).

The findings that multimorbidity is associated with poor fracture outcomes highlight the need for development of robust framework for fracture management in sicker patients.

1. Data was linked by the Centre for Health Record Linkage [2] MBS and PBS data sets were provided by Services Australia

Tracking of vitamin D status and its association with bone loss in middle-aged Australians: Busselton Healthy Ageing Study

Kun (Kathy) Zhu[2, 1], Michael Hunter[3, 4], Jennie Hui[3, 4, 5], Kevin Murray[4], Alan James[1, 6], Ee Mun Lim[2, 5], John Walsh[2, 1]

1. Medical School, University of Western Australia, Perth, WA, Australia

2. Department of Endocrinology and Diabetes, Sir Charles Gairdner Hospital, Perth, WA, Australia

3. Busselton Population Medical Research Institute, Busselton, WA, Australia

4. School of Population and Global Health, University of Western Australia, Perth, WA, Australia

5. Department of Clinical Biochemistry, PathWest Laboratory Medicine, Queen Elizabeth II Medical Centre, Perth, WA, Australia

6. Department of Pulmonary Physiology and Sleep Medicine, Sir Charles Gairdner Hospital, Perth, WA, Australia

Context: Little is known on the stability of vitamin D status in middle age and whether its tracking patterns associate with bone loss. We evaluated the tracking of serum 25-hydroxyvitamin D (25OHD) measured 6 years apart, and its association with bone mineral density (BMD) in participants of the Busselton Healthy Ageing study aged 46-70 years at baseline.

Methods: Out of the 5017 individuals recruited, 3386 (1871 females) who had serum 25OHD and DXA BMD assessments at both baseline and ~6 years were included in the analysis. The tracking patterns of serum 25OHD were defined as: low/decreasing (both measures <60 nmol/L or moved to lower category over time, n=1103), increasing (moved to higher category over time, n=549), medium (both measures 60-75 nmol/L, n=335) and high (both measures ≥75 nmol/L, n=1399).

Results: Mean season-corrected serum 25OHD was 81.3±22.7 and 78.8±23.1 nmol/L at baseline and 6 years, respectively, and showed moderate correlation (Pearson's correlation coefficient: 0.568; intraclass correlation coefficient: 0.724). Significant predictors of change in serum 25OHD concentration over 6 years included baseline 25OHD, sex, change in BMI and vitamin D supplement use at follow-up. The high vitamin D status group had significantly higher femoral neck and total hip BMD at baseline than the other three groups (by 0.011-0.018 g/cm^2). The low/decreasing vitamin D status group had significantly greater decline in femoral neck and total hip BMD (by 0.005-0.008 g/cm^2) over the follow-up period compared with the increasing, medium and high vitamin D status groups after adjustment for sex and baseline BMD values, age, BMI, vitamin D supplement and lifestyle factors (all P<0.05) **(Table 1)**.

Table 1 Estimated mean BMD at baseline and change over 6 years by vitamin D status tracking patterns

	Low/decreasing (n=1103)	Increasing (n=549)	Medium (n=335)	High (n=1399)	P value
Baseline BMD, g/cm^2					
Femoral neck	0.972 ± 0.004 [1]	0.967 ± 0.005 [1]	0.968 ± 0.007 [1]	0.985 ± 0.003	**0.010**
Total hip	1.034 ± 0.004 [1]	1.028 ± 0.006 [1]	1.029 ± 0.007 [1]	1.045 ± 0.004	**0.028**
Lumbar spine	1.218 ± 0.005	1.199 ± 0.008	1.205 ± 0.010	1.211 ± 0.005	0.217
Change over 6 years, g/cm^2					
Femoral neck	−0.036 ± 0.001	−0.028 ± 0.002 [2]	−0.027 ± 0.002 [2]	−0.031 ± 0.001 [2]	**0.003**
Total hip	−0.032 ± 0.001	−0.025 ± 0.002 [2]	−0.026 ± 0.002 [2]	−0.027 ± 0.001 [2]	**0.004**
Lumbar spine	−0.007 ± 0.002	−0.005 ± 0.003	0.000 ± 0.003	−0.006 ± 0.002	0.324

Values are estimated mean ± SEM. [1]P <0.05 vs High, [2]P < 0.05 vs Low/Decreasing, general linear model adjusted for sex, race and baseline age, BMI, physical activity, smoking, alcohol intake, osteoporosis medication, vitamin D supplement; models for change in BMD additionally adjusted baseline BMD values.

Conclusion: Serum 25OHD measured 6 years apart showed moderate tracking. Individuals with consistently low or declining vitamin D status had greater bone loss during the follow-up period and could be the target for intervention.

210

Targeting cancer cells through arginine starvation

Hui Yi Chew[1], Goran Cvetkovic[2], Slobodan Tepic[2], James W Wells[1]

1. The University of Queensland Diamantina Institute, Brisbane, Queensland

2. Hepius Biotech AG, Zurich, Switzerland

Cellular metabolism plays a crucial role in maintaining basic cell survival. It provides the necessary energy and building blocks to support the biosynthetic demands of cell proliferation and differentiation. Due to its importance, cellular metabolism is often hijacked by cancer cells to aid in tumourigenesis, proliferation and survival. Arginine is a semi-essential amino acid that serves as a precursor for polyamines and cells become dependent on extracellular sources during rapid growth. Some tumours, known as auxotrophic tumours, display defective arginine synthesis and this is a metabolic vulnerability that can be exploited in the development of antitumour therapeutic strategies. Arginase is an arginine-depleting enzyme that breaks down arginine into ornithine and urea, and is currently undergoing clinical trials as a potential anti-cancer therapeutic agent. Due to a lack of cell cycle checkpoint control, deprivation of arginine in arginine-auxotrophic tumours leads to growth inhibition or cell death whereas deprivation of arginine in healthy cells leads to cell cycle arrest and quiescence. We hypothesise that the combination of arginase along with insulin aids in the uptake of arginase into cancer cells thus preventing cancer cells from utilising both intracellular and extracellular sources of arginine. We showed that the combination therapy improved the uptake of arginase into cells and has a negative impact on the proliferation of cancer cells.

211

Association between genotypes of the fat mass and obesity-associated gene (FTO) and osteoporosis phenotypes

Krisel De Dios[1], Ngoc Huynh[1], Thach Tran[2], Jackie Center[2], Tuan Van Nguyen[1, 3]

1. School of Biomedical Engineering, University of Technology Sydney, Sydney, NSW, Australia

2. Bone Biology, Garvan Institute of Medical Research, Sydney, NSW, Australia

3. School of Population Health, University of New South Wales, Sydney, NSW, Australia

Common variants in the FTO gene are associated with body weight and obesity, which are known to be associated with osteoporosis. This study examined the association between FTO genotypes and osteoporosis phenotypes (e.g., bone mineral density (BMD), bone loss, and fracture risk) in post-menopausal women and elderly men.

The study involved 1277 women and 758 men aged 60 years and older who were part of the Dubbo Osteoporosis Epidemiology Study (since 1990). BMD at the femoral neck and lumbar spine was measured by DXA (GE-Lunar Prodigy) at baseline and every 2 years during the follow-up period (1990-2020). Fragility fractures was ascertained by X-ray report. Six single nucleotide polymorphisms (SNPs) (rs1421085, rs1558902, rs1121980, rs17817449, rs9939609 and rs9930506) of the FTO gene were genotyped using TaqMan assay. The mixed-effects model assessed the association between the SNPs and BMD or bone loss. The Cox's proportional hazards model determined the association between SNPs and fracture risk.

The distribution of all FTO genotypes was consistent with the Hardy-Weinberg disequilibrium law. In women, carriers of the minor homozygous CC genotype (rs1421085) had a greater rate of bone loss than carriers of TC and TT genotypes (-1.14 vs -0.52 mg/cm^2, P=0.001). Furthermore, carriers of the CC genotype also had a greater risk of hip fracture (hazard ratio [HR] = 1.70, 95% CI, 1.10-2.63) than those with TC and TT genotypes, and this association was independent of baseline BMD, age, and body mass index. The same associations were also observed for rs1558902, rs1121980, and rs17817449. In men, there was no statistically significant association between any SNP and bone phenotypes.

These data indicate that variants within the FTO gene is associated with bone loss and hip fracture risk in women, suggesting that the FTO gene is a potential candidate for the delineation of the relationship between obesity and osteoporosis.

212

Association Between Polymorphisms in the Collagen Type 1 Alpha 1 (*COLIA1*) Gene and Bone Phenotypes

Ngoc Huynh[1], Krisel De Dios[1], Thach S Tran[2], Jacqueline R Center[2], Tuan V Nguyen[3, 1]

1. School of Biomedical Engineering, University of Technology Sydney, Sydney, NSW, Australia

2. Garvan Institute of Medical Research, Sydney, NSW, Australia

3. School of Population Health, UNSW Medicine, UNSW Sydney, Sydney, NSW, Australia

Background:

Polymorphisms in the collagen type Iα1 (COLIA1) gene is associated with bone mineral density (BMD), but its association with bone loss remains unknown. This study sought to test the hypothesis that COLIA1 polymorphisms are associated with both bone loss and fracture risk.

Methods:

The study involved 809 postmenopausal women in the Dubbo Osteoporosis Epidemiology Study. The women's bone health has been monitored for up to 30 years. BMD at the lumbar spine (LSBMD) and femoral neck (FNBMD) was biennially measured by DXA (GE-Lunar Prodigy). Fragility fracture was ascertained by X-ray reports. The G->T polymorphism at the Sp1 binding site in the COLIA1 gene was determined by the PCR-based method. The association between COLIA1 genotypes and bone loss was analysed by the mixed-effects model. The contribution of COLIA1 genotypes to fracture risk was analysed by the Cox's regression model.

Results:

The distribution of COLIA1 genotypes was consistent with the Hardy-Weinberg's equilibrium law: TT (n=31; 3.8%), GT (n=256; 32%) and GG (n=522; 64.2%). The rate of bone loss was -0.85±2.03%, -0.58+1.55% and -0.56+1.39% per year for women with TT, GT and GG genotype, respectively (p=0.57). During a median follow-up of 18.3 years, there were 423 fragility fractures, including 120 hip fractures. Women with TT genotype were associated with an increased risk of any fracture (adjusted HR: 2.16; 95%CI: 1.40-3.32) and hip fracture (adjusted HR=3.73; 95%CI, 1.84-7.56) than women with GG/GT genotype.

Conclusion:

These data suggest that polymorphic variation at the COLIA1 gene is not associated with bone loss, but associated with fracture risk, independent of BMD. This finding suggests that the COLIA1 gene may be a useful predictor of osteoporotic fracture in the elderly population.

213

Osteocalcin and glucose regulation, show me the evidence

Cassandra Smith[1], Steve Lin[2], Lewan Parker[3], Itamar Levinger[1]

1. Victoria University, Institute for Health and Sport, Victoria University, Melbourne, VIC, Australia

2. Hudson Institute, Melbourne, VIC

3. Deakin University, Melbourne, VIC

Osteocalcin (OC) is the most abundant non-collagenous protein within the bone matrix. Since 2007, with evidence mostly from genetically modified mouse models, it was suggested that undercarboxylated form of OC (ucOC) acts as a hormone involved in energy metabolism, male fertility, muscle mass regulation, and cognition. However, several studies with alternative OC knockout (KO) rodent models did not support earlier findings. Herein, we investigated whether ucOC is linked to glucose regulation and insulin sensitivity by examining the observational evidence in humans, as well as the evidence obtained from exogenous ucOC treatment models (*in vivo*, *ex vivo* and *in vitro*), independent of data generated via genetically modified animal models. Overall, in humans, there is a substantial amount of evidence linking lower circulating ucOC levels with increased adiposity and increased risk of type 2 diabetes. Furthermore, there is an increasing body of evidence showing that exogenous treatment with ucOC improves whole-body and skeletal muscle glucose metabolism. Conflicting results reported may be related to methodological differences between studies, such as type/source of animal and cell culture models, source/origin of exogenous ucOC, dose and duration of ucOC treatment. However, whether the reported effects of ucOC on glucose regulation is clinically significant is yet to be determined.

The effects of GCSF in human and murine osteoclast differentiation and mature function models

Rouha MS Granfar[1], Nigel A Morrison[1]

1. Griffith University, Southport, QUEENSLAND, Australia

CSF3 or granulocyte colony stimulating factor (GCSF) has clinically documented effects on bone homeostasis in health, pathology, and accompanying therapeutic applications by either directly or indirectly acting on mature osteoclasts or precursors. GCSF appears to stimulate osteoclasts (OC), impair osteoblasts (OB), elevated in tissue and serology of periodontitis, mobilise haematopoetic stem cells (HSC) and alter tumour burden in particular by disrupting the CXCR4:CXCL12 axis [8,9,11,12,13,14,15,16,18].

Our research group detected 11.8-fold up-regulation of GCSF receptor in human osteoclasts derived from adherent Peripheral Blood Mononuclear Cells (PBMC) [1] and indicated increased expression and involvement of C-C chemokine receptors and ligands (CCR2/CCL2 & CCL5) within OC and monocyte derived multinuclear cell fusion [1,2,3,4,5]. The involvement of GCSF in modulating CCL2 in neutrophil differentiation, neuropathic pain pathways, and Craniocervical Instability (CCI) supports further investigation of GCSF in musculoskeletal biology, pathology, and the potential as a broader therapeutic target [9,10,17].

Initial results of GCSF-treatment in models of osteoclast differentiation and mature OC function will be presented, including gene expression, dentine resorption, and cell morphology profiles of osteoclast models derived from human peripheral blood and mouse bone marrow monocytes (wild type, CCL2 -/-; CCR2 -/-) with either "continuous", "early" (0h to pre-osteoclast or fused polykaryons), and "late" (polykaryon to activated/mature) treatment [1,2,3,4,5,6,7].

Cell Culture Models	
	Adherent PBMC
	CD14+ MACS Protocol using PBMC
	Pre-differentiated on collagen
	BMM (WT & CCR2 -/- CCL2 -/- C57/BL6 background)

Cytokine Treatments					
MCSF	•	•	•	•	
sRANKL		•		•	•
GCSF			•	•	•
Timing	Continuous, Early, Late				
Interference	CCR2 -/-, CCL2 -/-, 7ND				

Phenotypic Profiling	
Multinucleation	DAPI stain; 3-5, 6-10, 11-20, ≥21 nuclei per cell
Fusion Index	nuclei/cytoplasmic area µm²
Cell size	area/diameter/spread
TRAP+ Multinucl. cells	TRAP Stain & count (light microscopy)
Cathepsin K	Cathepsin K Sigma Kit (fluorescence)
F-actin Ring	F-actin stain (fluorescence microscopy)
Resorption function	Dentine slice resorption %. Light microscopy & SEM

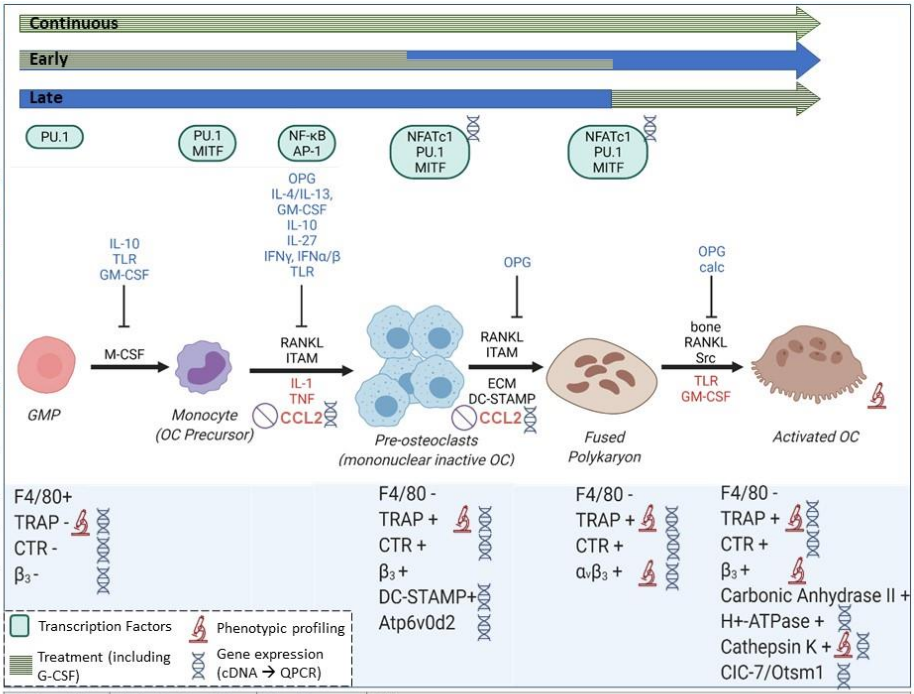

Protocol ID	Ethics Protocol #	Trim ID	Title
460	MSC/05/08/AEC	03/08/2303	Chemokines and human osteoclast differentiation (NHMRC 481946)
454	MSC/03/08/AEC	03/08/2298	Chemokines and bone cell phenotype.

1. Day CJ, Kim MS, Stephens SRJ, Simcock WE, Aitken CJ, Nicholson GC, & Morrison NA. (2004). Gene array identification of osteoclast genes: Differential inhibition of osteoclastogenesis by cyclosporin A and granulocyte macrophage colony stimulating factor. Journal of Cellular Biochemistry, 91(2), 303–315. https://doi.org/10.1002/jcb.10780
2. Day CJ, Kim MS, Lopez CM, Nicholson GC, & Morrison NA. (2005). NFAT expression in human osteoclasts. Journal of Cellular Biochemistry, 95(1), 17–23. https://doi.org/10.1002/jcb.20410
3. Granfar RMS, Day CJ, Kim MS, & Morrison NA. (2005). Optimised real-time quantitative PCR assays for RANKL regulated genes. Molecular and Cellular Probes, 19(2), 119–126. https://doi.org/10.1016/j.mcp.2004.10.003
4. Khan UA, Hashimi SM, Bakr MM, Forwood MR, & Morrison NA. (2016). CCL2 and CCR2 are Essential for the Formation of Osteoclasts and Foreign Body Giant Cells. Journal of Cellular Biochemistry, 117(2), 382–389. https://doi.org/10.1002/jcb.25282
5. Kim MS, Magno CL, Day CJ, & Morrison NA. (2006). Induction of chemokines and chemokine receptors CCR2b and CCR4 in authentic human osteoclasts differentiated with RANKL and osteoclast like cells differentiated by MCP-1 and RANTES. Journal of Cellular Biochemistry, 97(3), 512–518. https://doi.org/10.1002/jcb.20649
6. Selinger CI, Day CJ, & Morrison NA. (2005). Optimized transfection of diced siRNA into mature primary human osteoclasts: Inhibition of cathepsin K mediated bone resorption by siRNA. Journal of Cellular Biochemistry, 96(5), 996–1002. https://doi.org/10.1002/jcb.20575

7. Brazier H, Stephens S, Ory S, Fort P, Morrison N, & Blangy A. (2006). Expression Profile of RhoGTPases and RhoGEFs During RANKL-Stimulated Osteoclastogenesis: Identification of Essential Genes in Osteoclasts. Journal of Bone and Mineral Research, 21(9), 1387–1398. https://doi.org/10.1359/jbmr.060613
8. Yu H, Zhang T, Lu H, Ma Q, Zhao D, Sun J & Wang Z. (2021). Granulocyte colony-stimulating factor (G-CSF) mediates bone resorption in periodontitis. BMC Oral Health 21, 299. https://doi.org/10.1186/s12903-021-01658-1
9. Iida S, Kohro T, Kodama T, Nagata S, Fukunaga R. Identification of CCR2, flotillin, and gp49B genes as new G-CSF targets during neutrophilic differentiation. J Leukoc Biol. (2005) Aug;78(2):481-90. doi: 10.1189/jlb.0904515. Epub 2005 May 13. PMID: 15894583.
10. McRae JL, Vikstrom IB, Bongoni AK, Salvaris EJ, Fisicaro N, Ng M, Alhamdoosh M, Baz Morelli A, Cowan PJ, Pearse MJ. (2020). Blockade of the G-CSF Receptor Is Protective in a Mouse Model of Renal Ischemia-Reperfusion Injury. J Immunol. Sep 1;205(5):1433-1440. doi: 10.4049/jimmunol.2000390. Epub 2020 Jul 27. PMID: 32839213.
11. Hirbe AC, Rubin J, Uluçkan O, Morgan EA, Eagleton MC, Prior JL, Piwnica-Worms D, & Weilbaecher KN. (2007). Disruption of CXCR4 enhances osteoclastogenesis and tumor growth in bone. Proceedings of the National Academy of Sciences of the United States of America, 104(35), 14062–14067. https://doi.org/10.1073/pnas.0705203104
12. Amarasekara DS, Yun H, Kim S, Lee N, Kim H, & Rho J. (2018). Regulation of Osteoclast Differentiation by Cytokine Networks. Immune Network, 18(1), e8. https://doi.org/10.4110/in.2018.18.e8
13. Takamatsu Y, Simmons PJ, Moore RJ, Morris HA, To LB, & Lévesque JP. (1998). Osteoclast-mediated bone resorption is stimulated during short-term administration of granulocyte colony-stimulating factor but is not responsible for hematopoietic progenitor cell mobilization. Blood, 92(9), 3465–3473.
14. Soshi S, Takahashi HE, Tanizawa T, Endo N, Fujimoto R, & Murota, K. (1996). Effect of recombinant human granulocyte colony-stimulating factor (rh G-CSF) on rat bone: Inhibition of bone formation at the endosteal surface of vertebra and tibia. Calcified Tissue International, 58(5), 337–340. https://doi.org/10.1007/BF02509382
15. Lévesque J-P, Hendy J, Takamatsu Y, Simmons PJ, & Bendall LJ. (2003). Disruption of the CXCR4/CXCL12 chemotactic interaction during hematopoietic stem cell mobilization induced by GCSF or cyclophosphamide. The Journal of Clinical Investigation, 111(2), 187–196. https://doi.org/10.1172/JCI15994
16. Loi F, Córdova LA, Pajarinen J, Lin T, Yao Z, & Goodman SB. (2016). Inflammation, fracture and bone repair. Bone, 86, 119–130. https://doi.org/10.1016/j.bone.2016.02.020
17. Liao MF, Yeh SR, Lu KT, Hsu JL, Chao PK, Hsu HC, Peng CH, Lee YL, Hung YH, Ro LS. (2021). Interactions between Autophagy, Proinflammatory Cytokines, and Apoptosis in Neuropathic Pain: Granulocyte Colony Stimulating Factor as a Multipotent Therapy in Rats with Chronic Constriction Injury. Biomedicines. 2021 May 12;9(5):542. doi: 10.3390/biomedicines9050542. PMID: 34066206; PMCID: PMC8151381.
18. Brouard N, Driessen R, Short B, Simmons PJ. (2010). G-CSF increases mesenchymal precursor cell numbers in the bone marrow via an indirect mechanism involving osteoclast-mediated bone resorption. Stem Cell Res. 2010 Jul;5(1):65-75. doi: 10.1016/j.scr.2010.04.002. Epub 2010 Apr 21. PMID: 20537607.

Assessment of measures of bone distribution within DXA image cross sections improves prediction of femoral neck fracture independent of aBMD

Richard Prince[1], Ben Khoo[2], Joshua Lewis[3], Marc Sim[3], Keenan Brown [4]

1. University of Western Australia, Crawley, WA, Australia

2. Medical Technology and Physics, Sir Charles Gairdner Hospital, Nedlands, Western Australia, Australia

3. School of Medical and Health Sciences, Edith Cowan University, Joondalup, Western Australia, Australia

4. Mindways Software, , Austin, , Texas,, USA.

We have previously published on additional benefits of assessing geometric variables of bone distribution within cross sections of DXA images for hip fracture prediction in Chinese populations using Sigma, a measure of mineral mass distribution within the cross section and Delta, the inferior displacement of center of mass from the geometric center. We now report on role of these variables in the Perth Longitudinal Study of Aging in Women of 1,151 participants mean (SD) age 75(3) years with 15-years of follow up.

Baseline DXA structure in 1023 women who did not fracture were compared to 69 who sustained a femoral neck fracture (FNF), a median of 9.8 years after baseline.

The analytical approach focused on using Sigma and Delta in addition to common hip fracture prediction variables, age and Total Hip aBMD (THaBMD). In Cox analysis for FNF in which age and SD THaBMD were forced and SD Sigma and Delta entered in forward regression, the reported HRs (95% CI) were SD THaBMD 0.79 (0.61 – 1.03), age 1.13 (1.04–1.24) and SD Delta 1.70 (1.36-2.12). Interestingly in this model THaBMD was not significant. Effects of using tertiles of Delta in addition to age and Total hip aBMD are shown in Figure 1. Compared to lowest tertile of Delta, Tertile 2 HR was 2.21 (1.05–4.67), and Tertile 3 HR was 3.80 (1.88–7.69). The C statistic for age and THaBMD was 0.62, (0.55–0.69), the C statistic for FN Delta, age and THaBMD was improved at 0.69, (0.63–0.75) P for difference=0.01).

These data identify FN Delta in addition to aBMD as an important determinant of FNF prediction years before actual fracture. The larger the FN Delta the greater bone mass loss in the superior segment of FN compared to the inferior, related to fracture in buckling the biomechanical mechanism of FN fracture.

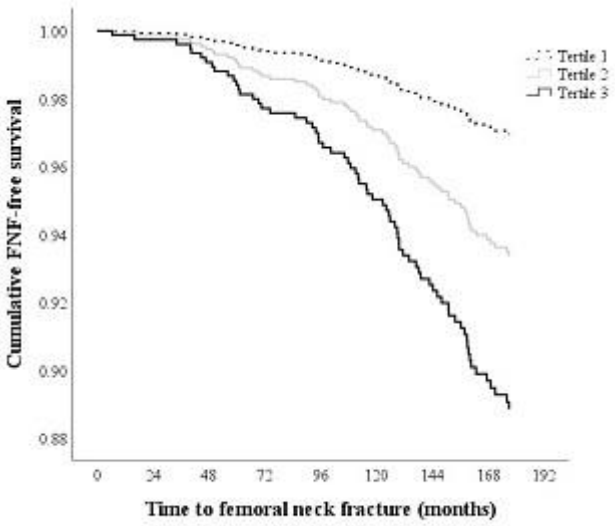

Figure 1 Effects of tertiles of Delta on FN fracture risk

217

Validation of a musculoskeletal human shoulder model using advanced computational modelling

Mélody Labrune[1], S.H. Hosseini Nasab[2], Danè Dabirrahmani[1], David T Axford[1, 3], Robert Potra[1, 4], Joseph Cadman[1], Louis M Ferreira[1, 3, 5], William R Taylor[2], Sumit Raniga[1], Richard Appleyard[1]

1. Faculty of Medicine, Health and Human Sciences, Macquarie University, Sydney, New South Wales, Australia

2. Institute for Biomechanics, ETH Zürich, Zürich, Switzerland

3. Dept of Mechanical and Materials Engineering, Western University, London, Ontario, Canada

4. Mathys Orthopaedics Pty Ltd, Sydney, New South Wales, Australia

5. School of Biomedical Engineering, Western University, London, Ontario, Canada

The shoulder joint is the most un-constrained joint in the human body and can present numerous clinical challenges including instability, soft tissues injuries and glenohumeral articulation degenerative diseases (1). Studying shoulder biomechanics provides better understanding of shoulder function and the impacts of pathologies and surgical interventions. Measuring joint biomechanics *in vivo* is challenging as it requires either invasive techniques or radiation imaging such as fluoroscopy. Non-invasive modelling tools have therefore been developed to predict shoulder mechanics. The goal of this study is to use computational modelling, specifically OpenSim, to develop a shoulder model. Concurrent Optimization of Muscles Activation and Kinematics (COMAK) algorithm is used to calculate muscle and joint reaction forces. The calibration and validation of the computational shoulder model will be achieved using data generated from our in-house 8 muscle-actuated, 6 degrees-of-freedom advanced *in-vitro* cadaveric shoulder simulator. Preliminary OpenSim simulations using passive laxity testing and simple arm motion have been performed with promising results. The development of the calibration model is currently in progress. Once validated, this model will be used to investigate the biomechanics of the shoulder for various clinical challenges along with surgical techniques.

1. Charalambous CP. The Shoulder Made Easy: Springer International Publishing; 2019. XXIII, 557 p.

218

Statistical Shape and Vector Field Model for Gastrocnemius Muscle Architecture Characterisation

Salim Bin Ghouth[1], Thor Besier[1, 2], Geoffrey Handsfield[1]

1. Auckland Bioengineering Institute, The University of Auckland, Auckland, New Zealand

2. Department of Engineering Science, Faculty of Engineering, The University of Auckland, Auckland , New Zealand

To understand the muscle architecture of healthy individuals in vivo, and in diseases such as cerebral palsy, structural and architectural parameters of skeletal muscles are often investigated using medical imaging. Diffusion tensor imaging, in particular, allows for in vivo determination of muscle fibre arrangement within a muscle. Common measurements taken are fascicle length and 2D pennation angle. However, muscle fibres are arranged 3-dimensionally, and cannot be fully described with a single or even multiple 2D pennation angles. Consequently, quantitative comparisons between individual muscle fibre arrangements are extremely limited, leaving a knowledge gap in understanding how fibre architecture varies between people and how it is impacted by pathologies such as cerebral palsy. In this abstract, we propose a new method to quantitatively and statistically assess fibre tracts arrangement in lower-limb muscles, focusing on the gastrocnemius muscle. Our method relies on the mathematical underpinnings of statistical shape modelling, but we add fibre directionality in the form of 3D vector fields in the muscle data. We obtained DTI data of healthy children from previous studies [1][2]. We constructed fibres using MRtrix and FSL software. We embedded vector fields obtained from DTI into volumetric meshes and ran Principal Component Analysis (PCA). Shape and vector field modes (i.e., principal components) were acquired. These weighted modes describe the dominant features of the muscle combined shape and vector field variations. Dominant features may reflect biomechanical variations in the functionality of gastrocnemius muscles. In short, a shape and vector field model was constructed to capture the dominant vector field features of fibre tract variations in gastrocnemius muscles. In future studies, differentiation of the shape and vector field dominant features between children with CP and healthy controls will be carried out; and the biomechanics behind the dominant features in a group of children with CP will be investigated.

1. G. G. Handsfield, C. H. Meyer, M. F. Abel, and S. S. Blemker, ‘Heterogeneity of muscle sizes in the lower limbs of children with cerebral palsy’, Muscle and Nerve, vol. 53, no. 6, pp. 933–945, 2016, doi: 10.1002/mus.24972.

2. S. Sahrmann, N. S. Stott, T. F. Besier, J. W. Fernandez, and G. G. Handsfield, ‘Soleus muscle weakness in cerebral palsy: Muscle architecture revealed with Diffusion Tensor Imaging’, PLoS One, vol. 14, no. 2, pp. 1–16, 2019, doi: 10.1371/journal.pone.0205944.

219

A retrospective analysis of obesity, fracture risk and overall survival in breast cancer bone metastasis

Michelle L Maugham-Macan[1], Huong Duong[1], Mia Schaumberg[1], Curtis Forbes[2], Meegan Walker[1], David Jenkins[1]

1. University of the Sunshine Coast, Sippy Downs, QLD, Australia

2. The Adem Crosby Centre, Sunshine Coast Hospital and Health Service, Sunshine Coast

Obesity is now recognised as a key risk factor for cancer with Breast Cancer one of thirteen obesity-driven cancers identified by the World Cancer Research Fund. Breast Cancer bone metastasis is a debilitating disease and recent research has demonstrated a link between obesity and poorer outcomes from bone metastatic breast cancer. The aim of this study is to investigate the impact of obesity on breast cancer bone metastases outcomes, specifically fracture risk and overall survival. We conducted a scoping review of existing literature to investigate the effect of obesity on fracture risk in bone metastatic breast cancer. At the time of review there was no literature examining this association. We therefore plan to conduct a retrospective analysis of female patients diagnosed with breast cancer bone metastases reviewed by a multidisciplinary team on the Sunshine Coast between 2008 and 2021. Patient BMI, evidence of fractures during the study period and survival 5 years and 10 years after diagnosis will be manually extracted from CHARM Oncology database. Anonymised data will then undergo correlation analysis. We hypothesise that there will be a correlation between body mass index and fracture risk as well as overall survival. The results of this study along with results of our scoping review will support future research into strategies that may reduce the impact of breast cancer bone metastases such as exercise physiologist-prescribed, personalised exercise plans to manage obesity and reduce bone loss that occurs with osteolytic lesions of bone metastatic breast cancer and therefore decrease bone pain and fracture risk and increase quality of life.

220

Prevalence of and risk factors for sarcopenia community-dwelling: Vietnam Osteoporosis Study

Khuong-Duy Hoang[1, 3, 2], Minh C. Doan[4, 3, 2], Nhan M. Le[3, 2], Huy G. Nguyen[1, 2], Lan T. Ho-Pham[3, 2], Tuan V. Nguyen[1, 2]

1. University of Technology Sydney, Ultimo, NSW, Australia

2. Ton Duc Thang University, Bone and Muscle Research Group, Ho Chi Minh, Vietnam

3. Ton Duc Thang University, Faculty of Applied Sciences, Ho Chi Minh, Vietnam

4. Pham Ngoc Thach University of Medicine, Department of Internal Medicine, Ho Chi Minh, Vietnam

Background: Sarcopenia is a geriatric syndrome characterized by the progressive and generalized loss of skeletal muscle mass and strength with age. This study sought to estimate the prevalence of and risk factors for sarcopenia in Vietnam.

Method: This cross-sectional study is part of the ongoing Vietnam Osteoporosis Study project. This study involved 1350 women and 617 men aged 50 years or above as at 2015 (study entry). Whole-body dual-energy X-ray absorptiometry was used to measure the appendicular skeletal muscle mass. Anthropometric and clinical data were collected using a structured questionnaire. Sarcopenia was defined according to the criteria proposed by the Asian Working Group for Sarcopenia (AWGS 2019). Logistic regression analysis was used to determine the association between potential risk factors and sarcopenia.

Results: Based on one the AWGS criteria, the prevalence of sarcopenia in women and men was 13.99% (n = 1350) and 14% (n = 617), respectively. In women, age (odds ratio [OR] per 10 years: 1.04; 95% CI 1.02 – 1.06), overweight (OR 0.24; 95% CI 0.16 - 0.34), and low physical activities (OR 1.5; 95%CI (1.1 – 2.15) were independently associated with increased risk of sarcopenia. In men, age (OR 1.12; 95% CI 0.12 – 1.15) and overweight (OR 0.28; 95% CI 0.15 - 0.5) were significant risk factors for sarcopenia.

Conclusion: Sarcopenia is common in community-dwelling Vietnamese adults, particularly among those with advancing age, overweight and low physical activity.

Acute ECG changes in patients receiving intravenous bisphosphonates: A systematic review and meta-analysis

Alex Shoung[1], Alexander J. Rodriguez[2]

1. Griffith Univeristy, Southport, Queensland

2. Monash University, Clayton, VIC, Australia

Objective: Bisphosphonates are the first-line treatment for several bone and mineral disorders. Randomised trials and cohort studies have reported increased rates of atrial fibrillation in patients receiving bisphosphonates. However, uncertainty remains as to whether other electrical disturbances are precipitated by bisphosphonates. We reviewed the literature for studies reporting ECG findings in patients receiving intravenous bisphosphonates for any indication.

Methods: We retrieved studies (June 2022) reporting ECG parameters following administration of intravenous bisphosphonates. We excluded studies that only reported atrial fibrillation, case reports and non-human studies. Continuous data were meta-analysed if reported in at least two studies. Random-effects models were fitted and reported as standardized mean difference (SMD) with 95%CI.

Results: 1123 records were retrieved. Six met our inclusion criteria, of which five had data for meta-analysis. Studies were of low to moderate quality. Five studies used zoledronic acid while one study used pamidronate. Most studies [n=4] were conducted in postmenopausal women with osteoporosis, one study was conducted in patients with bone metastases and one study was conducted in children with cerebral palsy and osteoporosis. Most studies [n=4] reported outcomes in the subacute (>24 h) phase. Study populations ranged from n=15 to n=116. There was a significant difference in QTc dispersion (SMD=-0.456 milliseconds [95%CI: -0.800 to -0.113]; I2=0%; n=67 patients; k=2 studies) but no differences in heart rate, P wave (maximum), P wave (minimum), P wave dispersion, PR interval, QRS duration QTc (maximum), QTc (minimum), or QTc. The correlation between pre- and post-infusion QTc dispersion was rho=0.981 (p=0.866). Results were unchanged when analysing studies reporting acute or subacute phase ECG changes.

Conclusion: Overall, there is insufficient and low-quality evidence to support an association between intravenous bisphosphonate administration and acute phase dysrhythmias. These data underscore the importance of performing a pre-infusion ECG to evaluate potentially unreported conduction abnormalities.

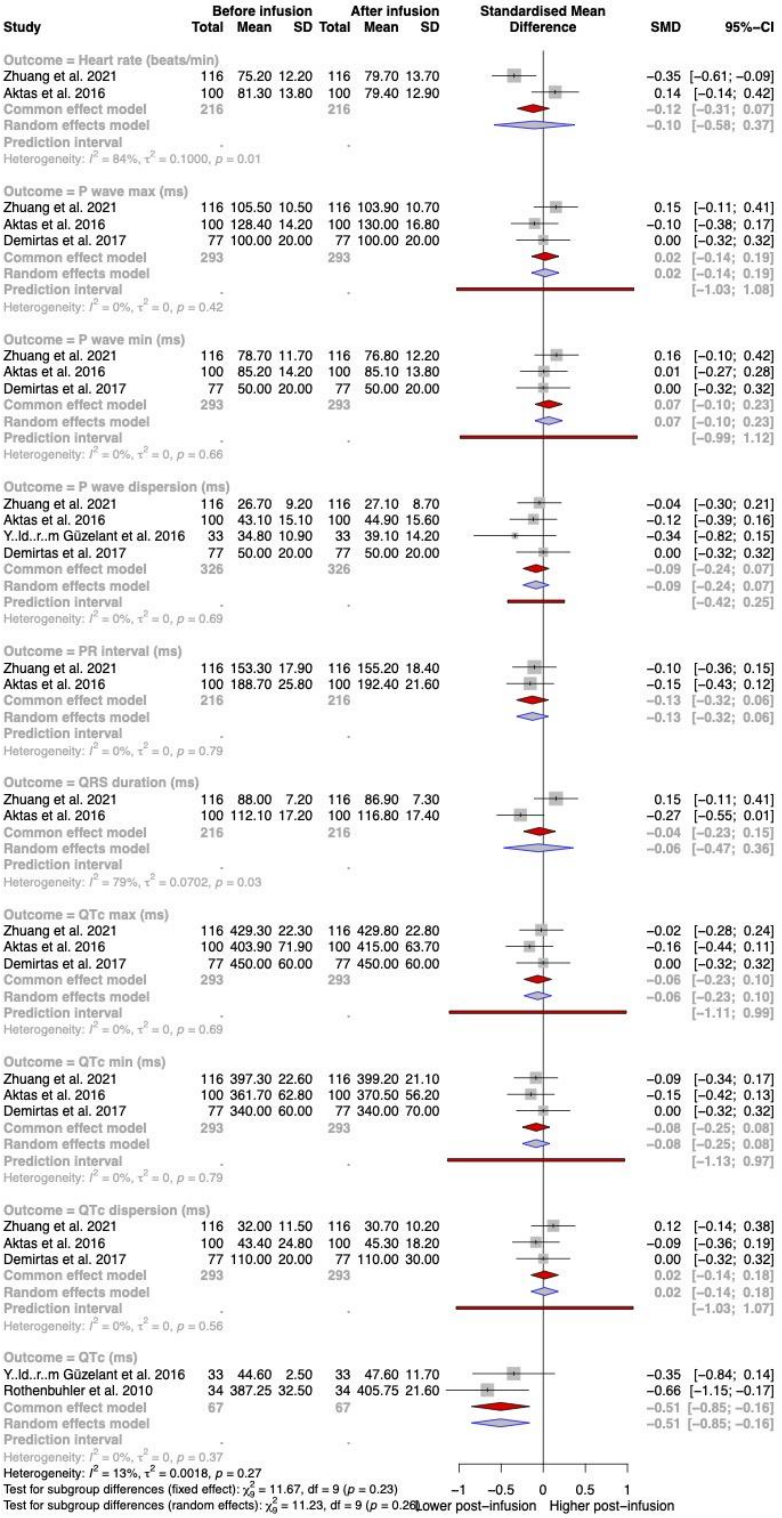
Study
Before infusion
Total Mean SD
After infusion
Total Mean SD
Standardised Mean Difference
SMD 95%−CI
Outcome = Heart rate (beats/min)
Zhuang et al. 2021 116 75.20 12.20 116 79.70 13.70 −0.35 [−0.61; −0.09]
Aktas et al. 2016 100 81.30 13.80 100 79.40 12.90 0.14 [−0.14; 0.42]
Common effect model 216 216 −0.12 [−0.31; 0.07]
Random effects model −0.10 [−0.58; 0.37]
Prediction interval [−1.03; 1.08]
Heterogeneity: I^2 = 84%, τ^2 = 0.1000, p = 0.01
Outcome = P wave max (ms)
Zhuang et al. 2021 116 105.50 10.50 116 103.90 10.70 0.15 [−0.11; 0.41]
Aktas et al. 2016 100 128.40 14.20 100 130.00 16.80 −0.10 [−0.38; 0.17]
Demirtas et al. 2017 77 100.00 20.00 77 100.00 20.00 0.00 [−0.32; 0.32]
Common effect model 293 293 0.02 [−0.14; 0.19]
Random effects model 0.02 [−0.14; 0.19]
Prediction interval [−1.03; 1.08]
Heterogeneity: I^2 = 0%, τ^2 = 0, p = 0.42
Outcome = P wave min (ms)
Zhuang et al. 2021 116 78.70 11.70 116 76.80 12.20 0.16 [−0.10; 0.42]
Aktas et al. 2016 100 85.20 14.20 100 85.10 13.80 0.01 [−0.27; 0.28]
Demirtas et al. 2017 77 50.00 20.00 77 50.00 20.00 0.00 [−0.32; 0.32]
Common effect model 293 293 0.07 [−0.10; 0.23]
Random effects model 0.07 [−0.10; 0.23]
Prediction interval [−0.99; 1.12]
Heterogeneity: I^2 = 0%, τ^2 = 0, p = 0.66
Outcome = P wave dispersion (ms)
Zhuang et al. 2021 116 26.70 9.20 116 27.10 8.70 −0.04 [−0.30; 0.21]
Aktas et al. 2016 100 43.10 15.10 100 44.90 15.60 −0.12 [−0.39; 0.16]
Y..ld..r..m Güzelant et al. 2016 33 34.80 10.90 33 39.10 14.20 −0.34 [−0.82; 0.15]
Demirtas et al. 2017 77 50.00 20.00 77 50.00 20.00 0.00 [−0.32; 0.32]
Common effect model 326 326 −0.09 [−0.24; 0.07]
Random effects model −0.09 [−0.24; 0.07]
Prediction interval [−0.42; 0.25]
Heterogeneity: I^2 = 0%, τ^2 = 0, p = 0.69
Outcome = PR interval (ms)
Zhuang et al. 2021 116 153.30 17.90 116 155.20 18.40 −0.10 [−0.36; 0.15]
Aktas et al. 2016 100 188.70 25.80 100 192.40 21.60 −0.15 [−0.43; 0.12]
Common effect model 216 216 −0.13 [−0.32; 0.06]
Random effects model −0.13 [−0.32; 0.06]
Prediction interval
Heterogeneity: I^2 = 0%, τ^2 = 0, p = 0.79
Outcome = QRS duration (ms)
Zhuang et al. 2021 116 88.00 7.20 116 86.90 7.30 0.15 [−0.11; 0.41]
Aktas et al. 2016 100 112.10 17.20 100 116.80 17.40 −0.27 [−0.55; 0.01]
Common effect model 216 216 −0.04 [−0.23; 0.15]
Random effects model −0.06 [−0.47; 0.36]
Prediction interval
Heterogeneity: I^2 = 79%, τ^2 = 0.0702, p = 0.03
Outcome = QTc max (ms)
Zhuang et al. 2021 116 429.30 22.30 116 429.80 22.80 −0.02 [−0.28; 0.24]
Aktas et al. 2016 100 403.90 71.90 100 415.00 63.70 −0.16 [−0.44; 0.11]
Demirtas et al. 2017 77 450.00 60.00 77 450.00 60.00 0.00 [−0.32; 0.32]
Common effect model 293 293 −0.06 [−0.23; 0.10]
Random effects model −0.06 [−0.23; 0.10]
Prediction interval [−1.11; 0.99]
Heterogeneity: I^2 = 0%, τ^2 = 0, p = 0.69
Outcome = QTc min (ms)
Zhuang et al. 2021 116 397.30 22.60 116 399.20 21.10 −0.09 [−0.34; 0.17]
Aktas et al. 2016 100 361.70 62.80 100 370.50 56.20 −0.15 [−0.42; 0.13]
Demirtas et al. 2017 77 340.00 60.00 77 340.00 70.00 0.00 [−0.32; 0.32]
Common effect model 293 293 −0.08 [−0.25; 0.08]
Random effects model −0.08 [−0.25; 0.08]
Prediction interval [−1.13; 0.97]
Heterogeneity: I^2 = 0%, τ^2 = 0, p = 0.79
Outcome = QTc dispersion (ms)
Zhuang et al. 2021 116 32.00 11.50 116 30.70 10.20 0.12 [−0.14; 0.38]
Aktas et al. 2016 100 43.40 24.80 100 45.30 18.20 −0.09 [−0.36; 0.19]
Demirtas et al. 2017 77 110.00 20.00 77 110.00 30.00 0.00 [−0.32; 0.32]
Common effect model 293 293 0.02 [−0.14; 0.18]
Random effects model 0.02 [−0.14; 0.18]
Prediction interval [−1.03; 1.07]
Heterogeneity: I^2 = 0%, τ^2 = 0, p = 0.56
Outcome = QTc (ms)
Y..ld..r..m Güzelant et al. 2016 33 44.60 2.50 33 47.60 11.70 −0.35 [−0.84; 0.14]
Rothenbuhler et al. 2010 34 387.25 32.50 34 405.75 21.60 −0.66 [−1.15; −0.17]
Common effect model 67 67 −0.51 [−0.85; −0.16]
Random effects model −0.51 [−0.85; −0.16]
Prediction interval
Heterogeneity: I^2 = 0%, τ^2 = 0, p = 0.37
Heterogeneity: I^2 = 13%, τ^2 = 0.0018, p = 0.27
Test for subgroup differences (fixed effect): χ^2_9 = 11.67, df = 9 (p = 0.23)
Test for subgroup differences (random effects): χ^2_9 = 11.23, df = 9 (p = 0.26)
−1 −0.5 0 0.5 1
Lower post−infusion
Higher post−infusion

IPN60130 for the treatment of fibrodysplasia ossificans progressiva: Methodology of the randomized, double-blind, placebo-controlled phase II FALKON trial

Shane Patella[1], Negar Karimian[2], Christine Powell[3], Fei Shih[3]

1. Ipsen, Melbourne, Australia

2. Ipsen, Montreal, Canada

3. Ipsen, Cambridge, MA, US

Objectives:

Fibrodysplasia ossificans progressiva (FOP) is an ultra-rare genetic disorder caused by *ALK2/ACVR1* mutation and characterized by heterotopic ossification (HO) and progressive disability. IPN60130 is a selective ALK2/ACVR1 inhibitor being investigated for FOP treatment.[1] Here, we describe methodology of the FALKON trial (NCT05039515) designed to compare efficacy and safety of IPN60130 with placebo in patients (pts) with FOP.

Methods:

Pts will be randomized to oral placebo, or low or high dose IPN60130 for 12 months; pts receiving placebo will then transition to IPN60130 for 12 months. Enrollment criteria include: ≥5 years old, FOP diagnosis with disease-causing mutation, and either a flare-up, new HO or joint ankylosis, or increase in Cumulative Analogue Joint Involvement Scale (CAJIS) score in the prior year. Recruitment is ongoing to enroll 90 pts. The primary efficacy outcome will be annualized change from Baseline in HO volume to Month 12, assessed by low-dose whole-body computed tomography (CT). Secondary efficacy outcomes are presented in the **Table**. Safety will be assessed via adverse event (AE) and serious AE incidence over 25 months.

Summary:

Results from FALKON will allow evaluation of IPN60130 in FOP.

References

1. Davis A et al. J Bone Miner Res 2019;34(Suppl 1):290

Funding: Sponsored by Ipsen.

Table: Secondary efficacy outcomes

Timeframe, months[a]	Outcome	Comparison
12	Change from Baseline (CfB) in volume of new heterotopic ossification (HO) lesions[b]	IPN60130 vs placebo
CfB in number of HO lesions[b]		
Flare-up rate; number of flare-up days		
Number of body regions with new HO		
CfB in pain intensity		
Proportion of patients with new HO		
24	CfB in HO volume[b]	IPN60130 vs placebo and untreated natural history study (NCT02322255) participants

[a]From Baseline up to the month given; [b]Assessed by low-dose whole-body computed tomography.

Disclosures: SP, NK, CP: Employees of Ipsen. FS: Employee and stockholder of Ipsen.

1. Davis A et al. J Bone Miner Res 2019;34(Suppl 1):290

Palovarotene for the treatment of Fibrodysplasia Ossificans Progressiva: Methodology of the phase III open-label PIVOINE rollover trial

Shane Patella[1], Alexander Artyomenko[2], Pascal Maisonobe[3], Kim Croskery[3]

1. Ipsen, Melbourne, Australia

2. Ipsen, Slough, UK

3. Ipsen, Boulogne-Billancourt, France

Objectives:

Fibrodysplasia ossificans progressiva (FOP) is an ultra-rare genetic disorder characterized by heterotopic ossification (HO) and progressive disability. Until the recent approval of palovarotene in Canada, no licensed disease-modifying treatments for FOP existed, but interim phase III trial (NCT03312634) results suggest marked efficacy for palovarotene (PVO).[1] Here, we describe methodology of the PIVOINE trial (NCT05027802) designed to allow treatment continuity and further evaluation of PVO safety and efficacy.

Methods:

Patients will receive 5 mg PVO once daily, or the parent study completion dose, for a maximum of 3 years. During flare-ups, patients will receive 20 mg daily for 4 weeks, then 10 mg daily for 8 weeks, in line with parent studies. Enrollment criteria: completion of a parent study (end of study/treatment visit of NCT03312634 or NCT02279095/NCT02979769), ≥14 years old, full skeletal maturity if aged <18 or deemed to be final height. PIVOINE aims to enroll 87 patients; recruitment began in March. Outcomes are presented in the **Table**.

Summary:

Results from PIVOINE, estimated to end in November 2024, will allow further evaluation of PVO in FOP.

Funding: Sponsored by Ipsen.

Table: Trial outcomes

Primary
Incidence of treatment-emergent adverse events[a]
Secondary[b]
Cumulative Analogue Joint Involvement Scale total score[c]
Use of aids, assistive devices and adaptations[c]
FOP-Physical Function Questionnaire % of worst score (total score; upper extremities/mobility sub-scores)[c]
Frequency/type of healthcare services utilization
Observed/percentage predicted (PP):[c] Forced vital capacity (FVC) Forced expiratory volume in 1 second (FEV_1) Diffusion capacity of the lung for carbon monoxide Absolute/PP:[c] FEV1/FVC ratio
Patient Reported Outcomes Measurement Information System physical and mental function scores[c]
Number of reported flare-ups, outcomes and duration[c]
% of patients with new bone growth[cd]

[a]Collected continuously over trial; [b]Collected every 6 months over trial; [c]Raw values and change from inclusion visit; [d]Not based on scans.

Disclosures: AA, PM, KC: Employees of Ipsen.

1. Pignolo R et al. JBMR 2020;35(Suppl 1):16–17

Joint function and quality of life in Fibrodysplasia Ossificans Progressiva: Results from an international burden of illness survey of patients and family members

Shane Patella[1], Mona A Mukaddam[2], Katherine S Toder[2], Michelle Davis[3], Kim Croskery[4], Anne-Sophie Grandoulier[5], Elaine A Boing[6], Frederick S Kaplan[2]

1. Ipsen, Melbourne, Australia

2. Departments of Orthopaedic Surgery and Medicine, The Center for Research in FOP and Related Disorders, Perelman School of Medicine, University of Pennsylvania, Philadelphia, PA, USA

3. International FOP Association, Kansas City, MO, USA

4. Ipsen, Slough, UK

5. Ipsen, Paris, France

6. Ipsen, Cambridge, MA, US

INTRODUCTION: Fibrodysplasia ossificans progressiva (FOP) is an ultra-rare genetic disorder of progressive heterotopic ossification, resulting in cumulative loss of joint function and severe disability. We present results from an international, cross-sectional FOP Burden of Illness Survey (NCT04665323) demonstrating the impact of loss of joint function on quality of life (QoL) for patients and their family members.

METHODS: Individuals with FOP (survey proxy-completed for patients aged <13 years), their primary caregivers, and other family members (aged ≥18 years) were eligible to participate. The survey was available online from 18Jan21–30Apr21 in 15 countries and 11 languages. The PatientReported Mobility Assessment (PRMA) evaluated range of motion across 12 joints and 3 body regions (higher scores reflect more severe limitations). To assess the impact of FOP on QoL, patients ≥13 years and their family members completed the EuroQoL health-related QoL questionnaire (EQ-5D-5L; index ranges from <0 [worst health] to 1 [full health]).

RESULTS: 463 survey responses were received from 405 individuals. Mean (standard deviation [SD]) EQ-5D-5L index score was 0.24 (0.36) for patients ≥13 years, 0.83 (0.22) for primary caregivers, and 0.85 (0.21) across all family members. There was a significant negative association between PRMA total score and EQ5D-5L index score for patients, such that for every 1-unit increase in the PRMA total score of the patient, there was a mean (standard error [SE]) decrease of 0.029 (0.003; $p<0.0001$) in EQ-5D-5L. For all family members, there was no significant association between EQ-5D-5L and the PRMA total score of the patient ($p=0.6737$).

DISCUSSION/CONCLUSION: Loss of joint function (as represented by PRMA Level) has a significant, detrimental impact on QoL for patients with FOP. These findings increase understanding of the impact of FOP on patients and their family members, and may help to improve quality of care and access to support for the FOP community.

Increased circulating levels of lipocalin-2 are associated with increased risk of metabolic syndrome the Perth longitudinal study of aging women

Carlie Bauer[1], Marc Sim[2, 3], Richard L Prince[4, 2], Kun (Kathy) Zhu[4, 2], Ee Mun M Lim[4, 5], Nathan Pavlos[6], Wai H Lim[7, 2], Germaine Wong[8], Joshua R Lewis[8, 2, 3], Itamar Levinger[1, 9]

1. Institute for Health and Sport, Victoria University, Footscray, Victoria, Australia

2. Medical School, University of Western Australia, Perth, WA, Australia

3. Nutrition & Health Innovation Research Institute, Edith Cowan University, Perth, WA, Australia

4. Department of Endocrinology and Diabetes, Sir Charles Gairdner Hospital, Perth, WA, Australia

5. Department of Clinical Biochemistry, PathWest Laboratory Medicine, Perth, WA, Australia

6. Biomedical School, University of Western Australia, Perth, WA, Australia

7. Department of Renal Medicine, Sir Charles Gairdner Hospital, Perth, WA, Australia

8. Centre for Kidney Research, Children's Hospital at Westmead School of Public Health, Sydney, NSW, Australia

9. Australian Institute for Musculoskeletal Science (AIMSS), Victoria University, University of Melbourne and Western Health, Melbourne, Victoria, Australia

Background: Lipocalin-2 (LCN2) is expressed by several tissues including osteoblasts, neutrophils and adipocytes. LCN2 is implicated in satiety control, energy regulation and cardio-metabolic health, suggesting a cross-talk between bone and other organs. However, it is unclear whether LCN2 is linked to metabolic syndrome (MetS) in older women.

Method: 781 community-dwelling older women were included in this cross-sectional study. Total circulating LCN2 levels was analysed in plasma using a two-step chemiluminescent microparticle monoclonal immunoassay on an automated platform (Abbott Diagnostics, Longford, Ireland). MetS was determined by a modified National Cholesterol Education Program (NCEP) Adult Treatment Panel (ATP) III classification. Women with diabetes were not included in MetS analysis. Multivariable-adjusted logistic regression was used to assess the association between quartiles of LCN2 and MetS (yes/no).

Results: Participants had a mean age of 75.1 ± 2.6 years and body mass index 26.9 ± 4.3 kg/m^2. Women in the highest LCN2 Quartile (Q4, median 115.8 mg/L) had approximately 3 times (OR 3.05; 95%CI 1.86-5.02) greater odds for MetS compared to women in Q1 (median 55.6 mg/L) . Higher LCN2 was correlated with increased MetS score (rho=0.24, p<0.001). Women with MetS (score 3+) and type 2 diabetes (n=76, median = 82.7 mg/L) had higher circulating levels of LCN2 compared to those with a MetS score of 0 (n=84) (p<0.05 for all).

Conclusion: Higher circulating levels of LCN2 are a risk factor for MetS in older women. Longitudinal studies are needed to determine whether LCN2 can be used in clinical practice to identify older women at risk of developing MetS.

Assessing the effect of Asian ethnicity on bone microarchitecture in patients with Atypical Femoral Fractures using 3D Dual X-Ray Absorptiometry (DXA)

Albert S Kim[3, 1, 2], Gareth Crouch[4], Nitesh D Dhanekula[4], Jean Doyle[5], Lillias Nairn[5], Liza M Nery[5], Andrew Ellis[6], Roderick Clifton-Bligh[4, 5], Christian M Girgis[3, 4, 5]

1. Bone Biology Division, Garvan Institute of Medical Research, Darlinghurst, NSW, Australia

2. St Vincent's Clinical School, Faculty of Medicine, University of New South Wales, Kensington, NSW, Australia

3. Department of Diabetes and Endocrinology, Westmead Hospital, Westmead, NSW, Australia

4. Faculty of Medicine & Health, University of Sydney, NSW 2600, Australia

5. Department of Endocrinology, Diabetes and Metabolism, Royal North Shore Hospital, St Leonards, NSW, Australia

6. Department of Orthopedic and Trauma Surgery, Royal North Shore Hospital, St Leonards, NSW, Australia

Introduction: Atypical femoral fractures(AFF) represent a rare, devastating complication related to long-term antiresorptive therapy. Asian ethnicity is an established risk factor for AFF but the mechanism for this is unclear. We utilised a 3D-DXA software algorithm (3DSHAPER, GalgoMedical, Spain) to generate quantitative computed tomography (QCT)-like models from DXA projections to assess the bone microarchitecture.

Methods: Retrospective review of areal BMD and 3D-DXA assessment of trabecular and cortical parameters at the contralateral hip and femoral shaft in patients on long-term antiresorptive therapy (>5years) who sustained AFFs and the left hip of those who did not.

Results: A total 54 femoral models were obtained using the 3D DXA algorithm including 17 AFF patients and 37 non-AFF patients. 9 of 17 AFF patients was Asian determined by country of birth. There was no difference in mean age(72.6 vs 74.2yrs), anthropometry, or duration of antiresorptive use between AFF and non-AFF patients(11.1 vs 11.1yrs).

There were no significant differences in the areal BMD in the femoral neck, trochanter, shaft and total hip. Total bone mineral content (BMC) was lower in AFF patients (23.4 vs 25.7g,p<0.05). Asian ethnicity was associated with significantly lower total BMC (21.5 vs 25.6g,p<0.01) and shaft BMC (14.2 vs 17.0g, p<0.05) in AFF patients. This was despite equivalent volumetric BMD and cortical volume. There was also no difference in mean cortical thickness. However, non-Asian AFF patients had higher total integral (71.3 vs 63.6cm3, p<0.001) and trabecular volume (55.9 vs 49.5cm3, p<0.01) compared to Asian AFF patients.

Conclusion: Lower BMC despite equivalent volumetric BMD and cortical volume was observed in AFF patients compared to patients on a similar duration of antiresorptive agents who did not sustain AFFs. Asian AFF patients had significantly lower BMC and trabecular volume compared to non-Asian AFF patients. Lower bone mineralisation in Asian individuals may increase AFF risk.

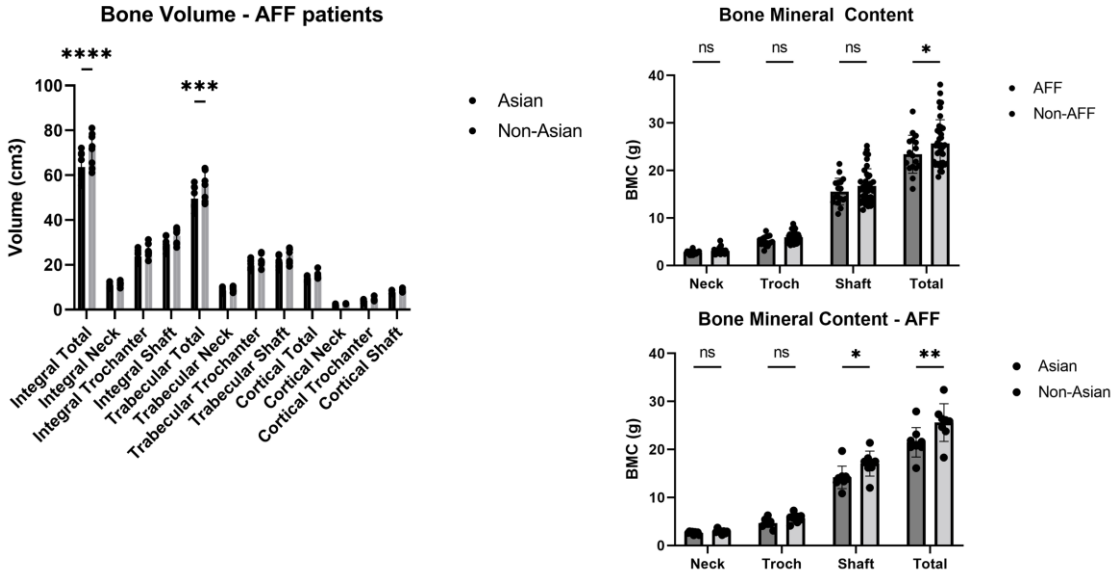

1. Girgis CM, Sher D, Seibel MJ. Atypical Femoral Fractures and Bisphosphonate Use. N Engl J Med. 2010 May 13;362(19):1848–9.
2. Dhanekula ND, Crouch G, Byth K, Lau SL, Kim A, Graham E, et al. Asian Ethnicity and Femoral Geometry in Atypical Femur Fractures: Independent or Interdependent Risk Factors? JBMR Plus. 2022;6(4):e10607.
3. Humbert L, Martelli Y, Fonolla R, Steghofer M, Di Gregorio S, Malouf J, et al. 3D-DXA: Assessing the Femoral Shape, the Trabecular Macrostructure and the Cortex in 3D from DXA images. IEEE Trans Med Imaging. 2017;36(1):27–39.

227

Healthy reference intervals for bone impact microindentation: a multi-centre international study.

Pamela Rufus-Membere[1], Kara L Holloway-Kew[1], Adolfo Diez-Perez[2], Natasha M Appelman-Dijkstra[3], Mary L Bouxsein[4], Erik F Eriksen[5], Joshua N Farr[6], Sundeep Khosla[6], Mark A Kotowicz[1], Xavier Nogues[7], Mishaela Rubin[8], Julie A Pasco[1]

1. IMPACT- Institute for Mental and Physical Health and Clinical Translation, School of Medicine,, Deakin University, Geelong, VIC, Australia

2. Department of Internal Medicine, Hospital del Mar-IMIM, Autonomous University of Barcelona and CIBERFES, , Instituto Carlos III, Barcelona, Spain

3. Department of Internal Medicine: division of Endocrinology and Center for Bone Quality, , Leiden University Medical Center, Leiden, Netherlands

4. . Center for Advanced Orthopedic Studies, Beth Israel Deaconess Medical Center and Department of Orthopedic Surgery,, Harvard Medical School, Boston, Massachusetts, USA

5. Spesialistsenteret Pilestredet Park and Faculty of Odontology, University of Oslo, Oslo Nor, Norway

6. Kogod Center on Aging and Division of Endocrinology, Mayo Clinic, Rochester, Minnesota, USA

7. Department of Internal Medicine, Hospital del Mar-IMIM, Pompeu Fabra University Barcelona- and CIBERFES, Instituto Carlos III,, Barcelona, Spain

8. Department of Medicine, Columbia University Vagelos College of Physicians & Surgeons, New York, USA

Publish consent withheld

228

Osteoporosis and fracture risk assessment in adults with ischaemic stroke

Basil Liu[1], Anne Trinh[3, 2], Paul Bao Duy La[2], Phillip Wong[3, 2], Peter R Ebeling[2, 1], Shaloo Singhal[2], Thanh Phan[2], Frances Milat[3, 2]

1. School of Clinical Sciences, Monash University, CLAYTON, VIC, Australia

2. Monash Health, Clayton, Victoria, Australia

3. Hudson Institute of Medical Research, Melbourne, Victoria, Australia

Background

Stroke is an important risk factor for minimal trauma fracture (MTF) due to immobilisation, gait disturbance and increased falls risk, yet it is neglected in guidelines worldwide.

Aim

To study the prevalence of osteoporosis, falls and fractures in adults with ischaemic stroke.

Methods

Retrospective cohort study of adults aged ≥50 years admitted with ischaemic stroke at Monash Health over a 6-month period in 2020. A subset of 50 patients had telephone interviews to ascertain falls and fracture 12 months post-stroke and to calculate a Fracture Risk After Ischaemic Stroke (FRAC-stroke) score.

Results

141 adults were admitted with stroke over a 6-month period; mean age was 74.7 ± 11.3 years and 39% were female. The modified Rankin Scale (mRS) on discharge was between 0-1 in 42.5%, 2-3 in 41.1% and 4-5 in 16.3%. Vitamin D levels were assessed in 26.2%, with a median vitamin D level of 55 nmol/L (IQR 40-76 nmol/L).

Of the 50 patients contacted for interviews: 26% (n=13) and 10% (n=5) had a FRAC-stroke score of ≥16 and ≥23 respectively, equating to a 5% and 10% risk of fracture in the year following stroke. Nine (18%) had a MTF prior to the stroke and eight (16%) had a history of known osteoporosis. 19 patients (38%) had a fall in the 12 months post-stroke with 9 (18%) having multiple falls. Only 7 patients (14%) had a history of falls prior to stroke. Two patients had a MTF in the 12 months post-stroke with a FRAC-stroke score of 22 and 26 (multisite fracture of hip/leg/radius and radius respectively).

Conclusion

The FRAC-stroke score is a simple clinical tool that can be used to identify patients at high risk of fracture post-stroke who would benefit most from osteoporosis therapy.

Reduced body mass index and reduced total lean mass but not cirrhosis are independent predictors of reduced bone mineral density and osteoporosis in chronic liver disease

Rachel Shingaki-Wells[1], Anne Trinh[2, 1], Nicholas Batt[3], Hannah Youn[1], Anouk Dev[1], Sally Bell[1], Suong Le[1], Frances Milat[2, 1]

1. Monash Health, Clayton, Victoria, Australia

2. Hudson Institute of Medical Research, Melbourne, Victoria, Australia

3. Eastern Health, Box Hill, VIC, Australia

Background and Aim:
The prevalence of osteoporosis in patients with chronic liver disease (CLD) varies from 12-55% but there is a paucity of data regarding risk factors for low bone mineral density (BMD) in this group. Our study investigated the determinants of low BMD and predictors of osteoporosis in an unselected CLD non-transplant population.

Methods:

Retrospective longitudinal observational study of 98 adult CLD patients at Monash Health. Serial BMD assessment was measured by DXA at the lumbar spine (LS), total hip (TH), and femoral neck (FN). Independent predictors for BMD and osteoporosis were determined by multivariate linear and logistic regression analysis.

Results:

98 CLD patients had 267 BMD measurements over a median follow-up of 6.9 years. Median age at first DXA was 32 years (interquartile range IQR: 27-59); 74 % had cirrhosis. The aetiology of CLD included hepatitis B (22 %), followed by alcohol (21%), Hepatitis C (16%), multiple aetiologies (19%) and NASH (9%).

The baseline prevalence of osteoporosis and osteopenia at index DXA was 70% and 30%, respectively. Baseline median TH and LS T-score was -1.9 (IQR: -2.4 to -1.1) and -2.1 (IQR: -2.8 to -1.2) respectively. Twenty-eight patients developed osteoporosis during follow-up. In total, 25 patients experienced a fracture: 20 (80%) were minimal trauma.

Independent predictors of reduced total hip BMD included age, female gender and reduced BMI. Independent predictors of osteoporosis included reduced BMI and total lean mass (TLM). The presence of cirrhosis, median stiffness score on fibro scan and heavy alcohol consumption were not independently associated with osteoporosis.

Conclusion:

Our study found that low BMI and total lean mass were independent predictors of reduced BMD and increased risk of osteoporosis in a general CLD non-transplant cohort. Identifying malnutrition and sarcopenia as modifiable risk factors may allow for proactive intervention for bone health optimisation in this group.

Atypical anecdotes: three cases of stress fracture associated with denosumab use for osteoporosis

Caitlin Corkhill[1], Sonia Stanton[1]

1. The Canberra Hospital, Garran, ACT, Australia

Atypical fractures are a rare adverse skeletal outcome of antiresorptive treatment and predominantly associated with long-term bisphosphonate use(1-3). Highest incidence occurs with long-term (>8yrs) alendronate use at ~13 per 10,000 patient-years, but drops by >50% one year and >80% three years after ceasing bisphosphonate(2). Published cases have been associated with denosumab, most with extensive prior bisphosphonate exposure(2-8), with fewer atypical fractures associated with denosumab involving very short-term bisphosphonate use(9,10). Five cases are reported in bisphosphonate-naïve patients taking denosumab(11-14).

The best characterised fracture type is atypical femur fracture (AFF) with specific radiological and clinical definition criteria(15). Atypical stress reactions of the femoral diaphysis and atypical or stress fractures at other sites, including periprosthetic, have also been associated with antiresorptives(4,16-18). Fractures meeting AFF criteria have additionally been reported in the absence of antiresorptive exposure(19-21), with additional risk factors including metabolic bone disorders, femur geometry (lateral bowing, varus hip alignment), inflammatory arthritis, glucocorticoid and proton-pump inhibitor (PPI) use(19).

We describe a series of three patients with minimal-trauma atypical or stress fractures in the setting of denosumab use for osteoporosis, two of which occurred in the absence of prior bisphosphonate exposure and one with previous bisphosphonate use (Table 1). Common across the cases is relatively young age at treatment onset and no prior fracture. Two patients were mobile and active throughout their treatment. Two had body mass index >32kg/m2, and one had asymmetrical antalgic gait, which possibly contributed to fracture site mechanical loading. All had significant improvement in bone mineral density (BMD) measured around the time of fracture, which may suggest an exaggerated response to denosumab. However, as post-fracture bone density was performed on the contralateral femur in two cases, another postulation is of pre-existing significant between-hip variation in BMD, with mechanical asymmetry predisposing to atypical fracture.

Table 1: Summary of key case characteristics

Case	Age at denosumab initiation (years)	Denosumab duration prior to fracture (years)	Lowest T-score	T-score within 6 months of fracture	Fracture site	Factors contributing to stress fracture risk
1	56	7	Femoral neck *(left)* -2.90	Femoral neck *(right)* *0.00*	Subtrochanteric femur, left *(meets AFF criteria)*	BMI 38kg/m^2 Asymmetric gait PPI use
2	56	5	Lumbar spine -2.95 Femoral neck *(left)* -2.13	Lumbar spine -2.16 Femoral neck *(right)* -0.30	Femoral neck, left	Active (runs) PPI use
3	60	4 (Alendronate for 14 years, ceased 5 years prior to fracture)	Femoral neck *(left)* -2.60	Femoral neck *(left)* -1.60	Intertrochanteric, right femur 4 months later subtrochanteric periprosthetic fracture	BMI 33.5 kg/m^2 Inflammatory arthritis Glucocorticoid use PPI use Active

1. Starr J, Tay YKD, Shane E. Current Understanding of Epidemiology, Pathophysiology, and Management of Atypical Femur Fractures. Curr Osteoporos Rep. 2018 Aug;16(4):519-529.
2. Reid IR, Billington EO. Drug therapy for osteoporosis in older adults. Lancet. 2022 Mar 12;399(10329):1080-1092.
3. Noble JA, McKenna MJ, Crowley RK. Should denosumab treatment for osteoporosis be continued indefinitely? Ther Adv Endocrinol Metab. 2021 Apr 22;12:20420188211010052.
4. Dupaix JP, Opanova MI, Lee LSK, Christensen K. Denosumab-Associated Peri-Implant Atypical Femur Fracture: A Case Report. Hawaii J Health Soc Welf. 2019 Nov;78(11 Suppl 2):47-51.
5. Drampalos E, Skarpas G, Barbounakis N, Michos I. Atypical femoral fractures bilaterally in a patient receiving denosumab. Acta Orthop. 2014 Feb;85(1):3-5.
6. Selga J, Nuñez JH, Minguell J, Lalanza M, Garrido M. Simultaneous bilateral atypical femoral fracture in a patient receiving denosumab: case report and literature review. Osteoporos Int. 2016 Feb;27(2):827-32.
7. Schilcher J, Aspenberg P. Atypical fracture of the femur in a patient using denosumab--a case report. Acta Orthop. 2014 Feb;85(1):6-7.

8. Thompson RN, Armstrong CL, Heyburn G. Bilateral atypical femoral fractures in a patient prescribed denosumab—a case report. Bone. 2014 Apr 1;61:44-7.
9. Khow KS, Yong TY. Atypical femoral fracture in a patient treated with denosumab. Journal of Bone and Mineral Metabolism. 2015 May;33(3):355-8.
10. Villiers J, Clark DW, Jeswani T, Webster S, Hepburn AL. An atraumatic femoral fracture in a patient with rheumatoid arthritis and osteoporosis treated with denosumab. Case Rep Rheumatol. 2013;2013:249872.
11. Hamahashi K, Noguchi T, Uchiyama Y, Sato M, Watanabe M. Clinical Features and Outcomes of Bilateral Atypical Femoral Fractures. Case Rep Orthop. 2020 Jul 23;2020:8824756.
12. Paparodis R, Buehring B, Pelley EM, Binkley N. A case of an unusual subtrochanteric fracture in a patient receiving denosumab. Endocr Pract. 2013 May-Jun;19(3):e64-8.
13. Saag KG, Wagman RB, Geusens P, et al. Denosumab versus risedronate in glucocorticoid-induced osteoporosis: a multicentre, randomised, double-blind, active-controlled, double-dummy, non-inferiority study. Lancet Diabetes Endocrinol. 2018;6(6):445–454.
14. Bone HG, Wagman RB, Brandi ML, Brown JP, Chapurlat R, Cummings SR, Czerwiński E, Fahrleitner-Pammer A, Kendler DL, Lippuner K, Reginster JY, Roux C, Malouf J, Bradley MN, Daizadeh NS, Wang A, Dakin P, Pannacciulli N, Dempster DW, Papapoulos S. 10 years of denosumab treatment in postmenopausal women with osteoporosis: results from the phase 3 randomised FREEDOM trial and open-label extension. Lancet Diabetes Endocrinol. 2017 Jul;5(7):513-523.
15. Shane E, Burr D, Abrahamsen B, Adler RA, Brown TD, Cheung AM, Cosman F, Curtis JR, Dell R, Dempster DW, Ebeling PR. Atypical subtrochanteric and diaphyseal femoral fractures: second report of a task force of the American Society for Bone and Mineral Research. Journal of bone and mineral research. 2014 Jan;29(1):1-23.
16. Binkley N, Goel H, Shives E, Krueger D, Hare K. A probable atypical ulnar fracture in a man receiving denosumab. Bone. 2021 Feb;143:115726.
17. Takahashi Y, Hatashita S, Shinden Y, Ito M, Kaneuchi Y, Hakozaki M, Konno S. Periprosthetic Fracture Resembling Atypical Femoral Fracture After Fixation With Retrograde Intramedullary Nail in Elderly Women: A Report of Two Cases. In Vivo. 2021 May-Jun;35(3):1837-1842.
18. Tan J, Sano H, Poole K. Antiresorptive-associated spontaneous fractures of both tibiae, followed by an atypical femur fracture during the sequential treatment with alendronate, denosumab then teriparatide. BMJ Case Rep. 2019 Jul 23;12(7):e229366.
19. Georgiadis GF, Begkas DG, Maniatis KA, Vasilakis AE, Chatzopoulos STD, Balanika AP. Atypical Femoral Fracture in a Patient without Bisphosphonate or Denosumab Exposure-A Case Report. J Orthop Case Rep. 2021 Oct;11(10):21-24.
20. Szolomayer LK, Izuchukwu KI, Lindskog DM. Bilateral atypical femur fractures without bisphosphonate exposure. Skeletal Radiol. 2017;46:241–7.
21. Tan SC, Koh SB, Goh SK, Howe TS. Atypical femoral stress fractures in bisphosphonate-free patients. Osteoporosis International. 2011 Jul;22(7):2211-2.

231

Extent of abdominal aortic calcification is associated with increased risk of rapid weight loss and cachexia: the Perth Longitudinal Study of Ageing Women

Cassandra Smith[1], Marc Sim[1], Jack Dalla Via[1], Abadi Gebre[1], Kun (Kathy) Zhu[2], Wai H Lim[2], Douglas P Kiel[3], John T Schousboe[4], Richard L Prince[2], Joshua R Lewis[1]

1. Nutrition and Health Innovation Research Institute, Edith Cowan University, Perth, Western Australia

2. Medical School, University of Western Australia, Perth, WA, Australia

3. Harvard Medical School, Boston, MA, USA

4. Univerity of Minnesota, Minneapolis, MN, USA

Publish consent withheld

232

Factors affecting pain management in adults with hypermobility-related multimorbidity

S. Jade Barclay[1]

1. University of Sydney, Broadway, NSW, Australia

Hypermobility-related conditions are a commonly overlooked cause of chronic pain, disability and multimorbidity; average diagnosis takes 16 years. Hypermobility-related conditions affect all bodily systems – neurological, gastrointestinal, immunological, vascular, skin, joints. Chronic multimorbidity is a priority area for the health system, affecting one in four young adults and three in four older adults. Working-age women are overrepresented, with a life expectancy that is 15.2 years shorter than healthy women, and 40% higher work absenteeism. Multimorbidity is commonly considered in paediatric and geriatric populations, but remains under-recognised in working-age adults. High clinical prevalence and impact of multimorbidity is not reflected in healthcare services or most clinical guidelines.

While exercise prescription, for example, is an important part of chronic pain management and musculoskeletal bone health, it is often treated as a panacea, even in patient populations with known contraindications. In these patients, evidence-based management of pain and other individual conditions can be iatrogenic, typically informed by guidelines based on research that explicitly excludes patients with multiple diagnoses, medications, or recent surgeries. This international Delphi study aims to identify what helps and harms and top priorities in the management of hEDS and related multimorbidity from patients and expert clinicians.

Consensus was established among patients and expert clinicians on many priorities. However this consensus is not reflected in the clinical guidelines that the majority of health professional use to guide management decisions for this patient population, indicating that unrecognised/unmanaged hypermobility may be contributing to the global burden of multimorbidity and chronic pain. These findings expose the gaps between clinical guidelines and clinical reality for patients and clinicians who are managing hypermobility-related multimorbidity and pain. They also highlight the need to embed hypermobility- and multimorbidity-informed evidence in pain management, guidelines, education, screening programs, and the importance of clinically-relevant representation in health data and research sampling.

1. Malek S, Reinhold EJ, Pearce GS. The Beighton Score as a measure of generalised joint hypermobility. Rheumatol Int. 2021 Oct;41(10):1707-1716. doi: 10.1007/s00296-021-04832-4. Epub 2021 Mar 18.
2. Gensemer C, Burks R, Kautz S, Judge DP, Lavallee M, Norris RA. Hypermobile Ehlers-Danlos syndromes: Complex phenotypes, challenging diagnoses, and poorly understood causes. Dev Dyn. 2021 Mar;250(3):318-344. doi: 10.1002/dvdy.220. Epub 2020 Aug 17.
3. Gazit Y, Jacob G, Grahame R. Ehlers-Danlos Syndrome-Hypermobility Type: A Much Neglected Multisystemic Disorder. Rambam Maimonides Med J. 2016 Oct 31;7(4):e0034. doi: 10.5041/RMMJ.10261.
4. Csecs JLL, Dowell NG, Savage GK, Iodice V, Mathias CJ, Critchley HD, Eccles JA. Variant connective tissue (joint hypermobility) and dysautonomia are associated with multimorbidity at the intersection between physical and psychological health. Am J Med Genet C Semin Med Genet. 2021 Dec;187(4):500-509. doi: 10.1002/ajmg.c.31957. Epub 2021 Nov 22.
5. Eller-Vainicher C, Bassotti A, Imeraj A, Cairoli E, Ulivieri FM, Cortini F, Dubini M, Marinelli B, Spada A, Chiodini I. Bone involvement in adult patients affected with Ehlers-Danlos syndrome. Osteoporos Int. 2016 Aug;27(8):2525-31. doi: 10.1007/s00198-016-3562-2. Epub 2016 Apr 15.
6. Krahe AM, Adams RD, Nicholson LL. Features that exacerbate fatigue severity in joint hypermobility syndrome/Ehlers-Danlos syndrome - hypermobility type. Disabil Rehabil. 2018 Aug;40(17):1989-1996. doi: 10.1080/09638288.2017.

Teriparatide used for bisphosphonate-associated atypical femoral fracture in multiple myeloma

Jessica M Del Gigante[1], Jessie Teng[1]

1. St Vincent's Hospital Melbourne, Melbourne, VIC, Australia

Clinical case

A 76 year old woman was referred to metabolic bone clinic for further management of bisphosphonate-associated right atypical femoral fracture (AFF). She initially presented in April 2020 with sudden, severe, atraumatic hip pain with imaging confirming markedly displaced transverse subtrochanteric fracture of the right femur. Magnetic resonance imaging (MRI) of the left hip excluded AFF on the contralateral side. Post-intramedullary (IM) nail insertion, she was mobilising with minimal pain using a 4-wheel frame.

Her medical history was significant for multiple myeloma (MM) diagnosed in 2007. Induction therapy comprised melphalan, prednisolone and zoledronic acid. Due to progression of disease in December 2014, she commenced bortezomib and dexamethasone before proceeding to have an autologous stem cell transplant. She subsequently received monthly intravenous zoledronic acid infusions for 12 months then the frequency was reduced to every three months. In May 2019, she commenced third-line treatment with lenalidomide and dexamethasone. Zoledronic acid was ceased with the diagnosis of AFF.

Her other comorbidities included ischemic heart disease, chronic kidney disease, chronic pulmonary embolism, paroxysmal atrial fibrillation and hypertension. She lived at home with her husband and was independent with activities of daily living. She was not known to have significant vitamin D deficiency and had not sustained any other minimal trauma fractures.

Laboratory and medical imaging findings

Initial biochemistry revealed vitamin D level 55 nmol/L, creatinine 138 umol/L, corrected calcium 2.31 mmol/L, phosphate 0.73 mmol/L, and parathyroid hormone 114 pg/mL (15-68). Fasting C-telopeptide (CTX) level was 138 ng/L and procollagen type 1 N-terminal propeptide (P1NP) was 24 ug/L, reflective of long-term anti-resorptive therapy. Dual-energy x-ray absorptiometry (DEXA) scan revealed lumbar spine bone mineral density (BMD) of 1.226g/cm2 with T-score of 0.4 and left femoral neck BMD of 0.950g/cm2 with T-score 0.3.

Plain film radiography of the right hip 18-months post-IM nail insertion showed minimal interval bone remodelling without evidence of union. Computed tomography (CT) scan showed medial cortex union, and partial union at posterior cortex. 22-months post-operatively, repeat x-ray demonstrated persistent non-union of right AFF and new left femoral stress fracture with beaking of the lateral cortex of left femur.

Progress

Given persistent non-union of her right AFF, the orthopaedic team was hesitant to pursue surgical management of the left stress fracture. In consultation with her haematology team, she was commenced on teriparatide subcutaneous injections 20mcg daily for six months via compassionate access.

Brief outline of the literature

This case raises several interesting issues:

- Role of anabolic agents in fracture healing
- Role of anabolic agents in atypical femoral fracture
- Use of teriparatide in multiple myeloma or other paraprotein disorders

MM is a haematological malignancy characterised by clonal expansion of plasma cells.[1] Features include hypercalcemia, renal impairment, anaemia and diffuse osteopenia or focal lytic lesions.[1] Myeloma bone disease (MBD) is present in more than 80% patients with MM and results from plasma cell activation of osteoclast and suppression of osteoblast activity.[2] Intravenous bisphosphonates remain the standard of care for treatment and prevention of MBD and are administered every 3 to 4 weeks for 1-2 years.[2]

Long term bisphosphonate use is known to contribute to the development of AFF.[3] Most cases are treated surgically with intramedullary nailing however the procedure is associated with complications such as non-union and delayed union.[3] Currently there are no pharmacologic treatments approved for use in non-union. Several studies and case series have reported teriparatide, recombinant human parathyroid hormone, can enhance fracture healing time and union of AFF.[4]

There are however theoretical concerns about using teriparatide in MM. The use of teriparatide treatment for osteoporosis has previously been contraindicated in malignant bone disorders due to the increased incidence in osteosarcoma in rats in preclinical data.[5] Post-clinical studies have since found the incidence of osteosarcoma in patients using teriparatide is equivalent to incidence rates of osteosarcoma in the general population.[5]

There is also thought to be a potential role of parathyroid hormone–related protein (PTHrP) in MM pathogenesis and progression through osteoclast activation.[6] Whilst there is no evidence to demonstrate a direct causal link, there have been a small number of case reports of teriparatide use and MM development or recurrence. In one case report a patient presented with monoclonal gammopathy of uncertain significance (MGUS) and developed malignant melanoma post-teriparatide treatment.[7] In another case report MM was diagnosed soon after discontinuation of teriparatide treatment.[8] This association was disputed in a 12 month open label pilot study of 12 myeloma patients with previous bisphosphonate use who received subcutaneous teriparatide 20mcg daily. The results showed positive anabolic bone effects without an increase in myeloma disease activity or hypercalcemia.[9]

Take home messages

1) Teriparatide may be considered to improve fracture healing in AFF.

2) Despite theoretical concerns, early studies have shown that use of teriparatide for 12 months in patients with MM may have positive anabolic bone effects and does not appear to increase disease activity.

1. Quach H, Prince HM on behalf of Medical Scientific Advisory Group (MSAG). Clinical Practice Guideline Multiple Myeloma. Myeloma Australia; 2019.
2. Lee OL, Horvath N, Lee C, Joshua D, Ho J, Szer J, et al. Bisphosphonate guidelines for treatment and prevention of myeloma bone disease. Internal Medicine Journal.47(8):938-51.
3. Ebrahimpour A, Sadighi M, Hoveidaei AH, Chehrassan M, Minaei R, Vahedi H, et al. Surgical Treatment for Bisphosphonate-related Atypical Femoral Fracture: A Systematic Review. Archives of Bone & Joint Surgery.9(3):283-96.
4. Yoon BH, Kim KC. Does Teriparatide Improve Fracture Union?: A Systematic Review. Journal of Bone Metabolism.27(3):167-74.
5. Gilsenan A, Midkiff K, Harris D, Kellier-Steele N, McSorley D, Andrews EB. Teriparatide Did Not Increase Adult Osteosarcoma Incidence in a 15-Year US Postmarketing Surveillance Study. J Bone Miner Res. 2021;36(2):244-51.
6. Cafforio P, Savonarola A, Stucci S, De Matteo M, Tucci M, Brunetti AE, et al. PTHrP produced by myeloma plasma cells regulates their survival and pro-osteoclast activity for bone disease progression. J Bone Miner Res. 2014;29(1):55-66.
7. Koski AM, Sikio A, Forslund T. Teriparatide treatment complicated by malignant myeloma. BMJ Case Reports. 2010;13:13.
8. Forslund T, Koski AM, Koistinen A, Sikio A. Malignant myeloma in a patient after treatment for osteoporosis with teriparatide; a rare coincidence. Clinical Medicine Case Reports.1:119-22.
9. Diamond TH, Golombick T, Manoharan A, Ramakrishna R, Bryant C. Teriparatide (recombinant human parathyroid hormone 1-34) therapy in myeloma patients with severe osteoporosis and fractures despite effective anti-myeloma therapy and bisphosphonates: A pilot study. Am J Hematol. 2020.

Hypophosphatemic osteomalacia with suppressed bone turnover

Joanna Gong[1], Cherie Chiang[1], Christopher Yates[1]

1. Department of Diabetes and Endocrinology, Royal Melbourne Hospital, Parkville, Victoria, Australia

At the time of her initial presentation, Ms X was 26 years old with a history of narcolepsy and juvenile arthritis, characterised by pain, stiffness, erosive synovitis and enthesitis since age 13, with numerous immunosuppressants trialed in the past with limited success (etanercept, adalimumab, tocilizumab, methotrexate, leflunomide and abatacept). In the preceding two years, she had bilateral ulnar shortening osteotomies for painful ulnocarpal abutment, complicated by non-union requiring bone grafts. Ms X sought an endocrine opinion to assess her delayed bone healing, however shortly prior to initial review, she received an iron infusion that exacerbated mild pre-existing hypophosphatemia (nadir 0.35mmol/L) that in retrospect was first reported at age 19. For her juvenile arthritis, Ms X received intermittent courses of systemic steroids, however these were brief and insufficient to explain her poor bone health.

History revealed normal growth and development to achieve a height of 163cm and weight of 65kg, and Ms X was notably a competitive swimmer and medical graduate. She sustained no fractures as a child, however noted brittle dentition since her teens. There was no significant family history. In January 2020, investigations revealed a raised fractional excretion of phosphate of 25.65% (and low TmP/GFR 0.53), with an inappropriate FGF-23 of 78ng/L, associated with an unusually low bone turnover: alkaline phosphatase (39U/L), CTx 172ng/L and P1NP 21mcg/L (see Table 1). Screening for Fanconi's syndrome was negative. There was no evidence of hyperparathyroidism or vitamin D deficiency and DXA was unremarkable (April 2019 Z-scores: lumbar spine 0.1, total hip 0.0, femoral neck -0.2). Osteomalacia was confirmed on tetracycline double-labelled bone biopsy performed in October 2020. There was increased osteoid, no osteoclasts were identified, osteoblasts were scant and there was decreased blurred double labelling.

Targeted whole exome sequencing including known genetic causes of hypophosphatemic osteomalacia, hypophosphatasia and osteogenesis imperfecta were negative (see Table 2), and GaTate PET did not identify any mesenchymal tumours that could be causing tumour-induced osteomalacia. There was no evidence of Chiari malformation on MRI brain.

Ms X was managed with phosphate, colecalciferol and calcitriol supplementation, gradually titrated up to the current doses: phosphate phebra 1.5-2g daily in 2-3 divided doses, cholecalciferol 1000units daily and calcitriol 0.5mcg BD. Her most recent biochemistry on that regimen revealed a low normal phosphate of 0.83mmol/L, and calcium was 2.33mmol/L corrected. Unfortunately since her initial consultation, Ms X has sustained a right sixth rib fracture, bilateral cuboid stress fractures, a fracture of the left fourth and fifth metacarpals and her right ulnar shortening osteotomy site that was treated with a bone graft has not yet healed. Bone and joint pain did not improve following normalisation of her phosphate.

In summary, Ms X has hypophosphatemic osteomalacia in the context of inflammatory arthritis that appears to be genetic rather than acquired, given her young age of onset and lack of evidence of acquired causes such as tumour-induced osteomalacia on imaging. The atypical feature is the persistently suppressed bone turnover markers and the consequent delayed fracture healing.

Ms X's phenotype is most consistent with X-linked hypophosphatemia (XLH). XLH is the most common form of heritable rickets or osteomalacia, caused by loss of function mutations in the phosphate-regulating endopeptidase homolog, X-linked (PHEX) gene (Carpenter 2011). It is characterised by renal phosphate wasting and has a diverse presentation, varying from isolated hypophosphatemia to significant lower limb bowing and other musculoskeletal complaints.

While XLH frequently manifests in childhood, it may be identified in adulthood. Among other features, fractures, bone pain, abnormal dentition and enthesopathy may be present, all of which affected Ms X (Lambert 2019). Adults are also predisposed to secondary and tertiary hyperparathyroidism, in addition to metabolic disorders including obesity and cardiovascular disease (Lecoq 2020).

Traditional management includes supplementing phosphate and calcitriol. However, this often does not fully correct hypophosphatemia and bony manifestations. Burosumab (KRN23), a novel recombinant human antibody against FGF-23, seems to be a promising therapy. An open-label phase 2 trial of burosumab in children demonstrated improved renal tubular phosphate reabsorption, serum phosphate, linear growth, decreased pain and increased function (Carpenter 2018). Further, FGF-23 is affected by inflammation (Lang 2018) and its levels have been linked to the activity of inflammatory arthritis such as rheumatoid arthritis (Sato 2016), although further research into this relationship is required. This is pertinent to Ms X's case, and it may be useful to correlate inflammatory markers and disease activity with FGF-23 levels.

Despite fitting the clinical phenotype for XLH, it is peculiar that Ms X's gene testing was negative and her bone turnover markers have been persistently suppressed. This poses a diagnostic and management dilemma as genetic counselling for family members is limited and management is now guided by the clinical picture and consensus opinion. Ms X is on the waitlist for compassionate access to burosumab and receives regular surveillance and reviews in the meantime. The ultimate goal would be to achieve bone healing and prevent further fractures in the future.

Take home messages

1. Iron infusions may cause or exacerbate hypophosphatemia due to FGF-23 mediated urinary phosphate losses.
2. Tetracycline double-labelled bone biopsies are the gold standard for diagnosing osteomalacia.
3. X-linked hypophosphatemia is the most common heritable form of osteomalacia, and is characterised by FGF-23 mediated renal phosphate wasting. However, this is normally associated with elevated bone turnover markers, with the converse evident in Ms X.
4. A multidisciplinary approach is required to address the multisystem manifestations of this disease and burosumab is promising and the only targeted therapy available.

1. Carpenter TO, Imel EA, Holm IA, Jan de Beur SM and Insogna KL (2011) ‘A clinician's guide to X linked hypophosphatemia’, Journal of Bone and Mineral Research, 26(7):1381-1388.
2. Carpenter TO, Whyte MP, Imel EA, Boot AM, Högler W, Linglart A, Padidela R, Van’t Hoff W, Mao M, Chen CY and Skrinar A (2018) ‘Burosumab therapy in children with X-linked hypophosphatemia’, New England Journal of Medicine, 378(21):1987-1998.
3. Lambert AS, Zhukouskaya V, Rothenbuhler A and Linglart A (2019) ‘X-linked hypophosphatemia: management and treatment prospects’, Joint Bone Spine, 86(6):731-738.
4. Lang F, Leibrock C, Pandyra AA, Stournaras C, Wagner CA and Föller M (2018) ‘Phosphate homeostasis, inflammation and the regulation of FGF-23’, Kidney and Blood Pressure Research, 43(6):1742-1748.
5. Lecoq AL, Brandi ML, Linglart A and Kamenický P (2020) ‘Management of X-linked hypophosphatemia in adults’, Metabolism, 103:154049.
6. Sato H, Kazama JJ, Murasawa A, Otani H, Abe A, Ito S, Ishikawa H, Nakazono K, Kuroda T, Nakano M and Narita I (2016) ‘Serum fibroblast growth factor 23 (FGF23) in patients with rheumatoid arthritis’, Internal Medicine, 55(2):121-126.

Management of osteoporosis in end stage renal disease what to do when treatment fails

Elaine Jayadiwangsa[1]

1. Flinders Medical Centre, Bedford Park, SA, Australia

A 76 yo female was referred to metabolic bone clinic following a recent hospital admission for a L5 transverse spine and left ala of sacrum fracture after a fall from standing height. This was on the background of a history of osteoporosis diagnosed at age 60 for which she was managed on denosumab since 2019, with no history of missed or delayed dosing (last dose was administered in January 2022). Prior to this she was prescribed weekly alendronate. Her fracture history was significant for a previous right superior and inferior pubic rami fracture, sustained two months prior. Her other comorbidities include type 2 diabetes mellitus and hypertension. She has recently been diagnosed with end stage renal disease with an eGFR of 13 ml/min.

Her laboratory findings demonstrated stable renal function (urea 24.8 mmol/L, creatinine 289 umol/L, eGFR 13 ml/min/1.73m^2), normal calcium (corrected calcium 2.55 mmol/L) and vitamin D (80 nmol/L) and slightly elevated phosphate (1.71 mmol/L). Other secondary screens included a slightly elevated parathyroid hormone (7.4 pmol/L) reflecting secondary hyperparathyroidism, normal thyroid function tests (TSH 4.37 mIU/L), negative coeliac and myeloma screens. Her crosslaps were 380 ng/L and ALP 84 U/L.

Her most recent CT of her lumbar spine demonstrated acute bilateral L5 transverse process and left sacral ala fractures as well as a subacute right sacral ala fracture. There were chronic T11, T12, L1, L2 and L4 vertebral body fractures present.

Results of her previous DEXA scans are as follows:

	Region	BMD (g/cm^2)	T score
2021	Total right femur	0.706	-2.4
	Total left femur	0.768	-1.9
	AP spine L2-L4	1.066	-1.1
2017	Total left femur	0.696	-2.5
	AP spine L2-L4	0.899	-2.5

Despite improvements in her bone mineral density in both the spine and hip, Deidre has continued to sustain minimal trauma fractures thus raising the question of whether this represents failure of denosumab therapy and thus the potential role of anabolic agents such as teriparatide or romosozumab mindful of her history of end stage kidney disease.

Osteoporosis is characterised by impaired bone quality and quantity, resulting in increased risk of fracture. It can be difficult to diagnose in the setting of CKD and treatment options are limited when there is a co- existing CKD related mineral and bone disorder (CKD-MBD). This condition is characterised by alterations in calcium, phosphate, parathyroid and vitamin D metabolism, in addition to abnormalities in bone turnover and mineralisation. The gold standard of diagnosis is by an iliac crest bone biopsy, which occurs infrequently given the invasiveness of this procedure. Given this, the exclusion of CKD-MBD is difficult.

The treatment of osteoporosis is no different in stages 1 to 3 CKD compared to those with normal renal function. Those with moderate to severe CKD, this presents more of challenge. There are limited evidence-based guidelines on the management of osteoporosis in end stage renal disease who have continued to fracture despite previous bisphosphonate or denosumab therapy. Denosumab use in this cohort can be complicated by severe, symptomatic hypocalcaemia.

Anabolic agents such as teriparatide (recombinant peptide of human PTH) and more recently romosozumab, a monoclonal anti sclerostin antibody, have been increasing used in those who are deemed very high fracture risk and have continued to fracture despite being on antiresorptive therapy. Their role in end stage renal failure has been limited to either case reports or small observational retrospective or prospective studies. Post hoc analysis of the Fracture Prevention Trial demonstrated that teriparatide improved bone mineral density and was safe in patients with an eGFR as low as 30 ml/min/1.73m^2. A post marketing study in Japan of 1847 patients with osteoporosis and high fracture risk included those with stage 4 (n= 30) and 5 CKD (n =3). Bone mineral density increases were noted in those with stage 4 CKD and no adverse effects were observed in both groups[4]. Teriparatide may be beneficial in those with adynamic bone disease however this is based on data obtained in published case reports5.

There has been retrospective data showing romosozumab use in those with mild to moderate renal impairment (eGFR 30-60 ml/min/1.73m^2) reduced the risk of new vertebral fractures[2]. There is limited data available on the use of romosozumab in more severe kidney disease (eGFR < 30 ml/min/1.73m^2) for fracture prevention[2]. Romosozumab in a cohort of patients on haemodialysis demonstrated improvements in bone mineral density with increases in bone formation markers with no symptomatic hypocalcaemia and lower cardiovascular events compared with the untreated group6.

Both osteoporosis and CKD are common conditions that are increasing in prevalence given the current ageing population. With increasing severity of CKD, treatment choices are complex and difficult which is compounded by a paucity of trial data.

- The management of osteoporosis in end stage renal disease is complex especially in the setting of chronic kidney disease related bone mineral disorder.
- The risk of fragility fractures and associated fracture related mortality is high
- The role of anabolic agents such as teriparatide and romosozumab in end stage renal disease is limited to small cohort studies which have demonstrated favourable effects however further studies are required

1. Evenepoel P, Cunningham J, Ferrari S, Haarhaus M, Javaid MK, Lafage-Proust MH, Prieto-Alhambra D, Torres PU, Cannata-Andia J. (2021). 'European Renal Osteodystrophy (EUROD) workgroup, an initiative of the CKD-MBD working group of the ERA-EDTA, and the committee of Scientific Advisors and National Societies of the IOF', European Consensus Statement on the diagnosis and management of osteoporosis in chronic kidney disease stages G4-G5D. Nephrol Dial Transplant, Jan 1;36(1):42-59
2. Miller P. (2022). 'Osteoporosis in patients with chronic kidney disease: management', UpToDate, Retrieved June 4th, 2022 from https://www.uptodate.com/contents/osteoporosis-in-patients-with-chronic-kidney-disease-management?search=romosozumab&sectionRank=1&usage_type=default&anchor=H3065283159&source=machineLearning&selectedTitle=3~13&display_rank=2#H3065283159
3. Miller PD, Adachi JD, Albergaria BH, Cheung AM, Chines AA, Gielen E, Langdahl BL, Miyauchi A, Oates M, Reid IR, Santiago NR, Vanderkelen M, Wang Z, Yu Z. (2022). 'Efficacy and Safety of Romosozumab Among Postmenopausal Women With Osteoporosis and Mild-to-Moderate Chronic Kidney Disease', Journal of bone and mineral research : the official journal of the American Society for Bone and Mineral Research, 10.1002/jbmr.4563.
4. Nishikawa A, Yoshiki F, Taketsuna M, Kajimoto K, Enomoto H. Safety and effectiveness of daily teriparatide for osteoporosis in patients with severe stages of chronic kidney disease: post hoc analysis of a postmarketing observational study. Clin. Interv. Aging. 2016;11:1653–1659.
5. Palcu P, Dion N, Ste-Marie LG, Goltzman D, Radziunas I, Miller PD, Jamal SA 2015, 'Teriparatide and bone turnover and formation in a hemodialysis patient with low-turnover bone disease: a case report', American Journal of Kidney Diseases, Jun;65(6):933-6. Epub 2015 Apr 2.
6. Sato M, Inaba M, Yamada S, Emoto M, Ohno Y, Tsujimoto Y 2021, 'Efficacy of romosozumab in patients with osteoporosis on maintenance hemodialysis in Japan; an observational study'. Journal of Bone and Mineral Metabolism, Nov;39(6):1082-1090.

The smile of an angel

Ruveena Kaur[1], Zaven Panossian[1], Tim Cundy[2]

1. Endocrinology, Counties Manukau District Health Board, Auckland

2. Endocrinology, Auckland District Health Board, Auckland

Clinical case details

A 15 year-old female of Tongan heritage was referred to the endocrinology department with bilateral, multifocal, radiolucent lesions on mandibular X-rays. She had presented to an orthodontist for dental alignment with no prior history of facial pain, swelling or dental caries.

Developmental milestones were completed and puberty commenced with no delays. She was previously affected by sinusitis and perennial rhinitis, but is currently asymptomatic on no regular medications. She is one of six siblings, all of whom have similar facial features. Her father, multiple paternal aunts and uncles, also have a similar jaw structure.

On examination she appeared overweight, with a BMI calculated at 40.8 kg/m^2. Her face had a full and rounded appearance, with no evidence of exophthalmos. She had misaligned dentition, with no tenderness on palpation of her teeth. She had a normal cardiovascular examination. There were no clinical features of neurofibromatosis type 1 (NF-1), apart from a single café au lait spot on her thigh. There were no features consistent with Noonan's syndrome.

Lab and medical imaging findings:

She was normocalcemic and normophosphataemic on routine biochemistry, with a PTH of 2.2 pmol/L. ALP was 129 U/L and PINP 222 ug/L, both within the normal limits. She had mild vitamin D deficiency with a 25-hydroxy Vitamin D of 33 nmol/L, and was commenced on replacement. Creatinine was preserved at 63 umol/L.

X-ray of her mandible revealed large, multilocular lesions at the angle of the mandible bilaterally. A further small unilocular lesion is seen in the left anterior mandible.

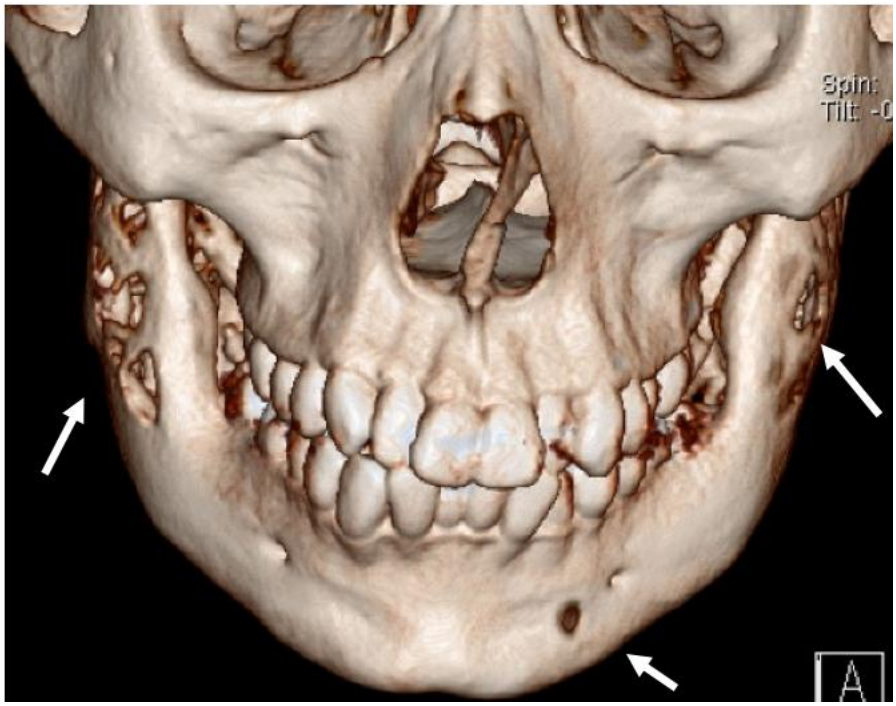

Figure 2: Computed tomography (CT) reconstruction showed bilateral multilocular lesions within the angle of the mandible and vertical rami, sparing the teeth.

DXA showed preserved bone density with a Z-score of +1.3 at the total lumbar spine and +2.4 at the hip. Biopsies of the mandibular lesions were consistent with multifocal, central giant cell granulomas.

Based on the clinical and family history, examination findings, imaging and biopsy results, the most likely diagnosis is cherubism of Grade I severity. The patient is awaiting a review by the genetic service. Given the absence of disfiguring facial appearance or dental pain, she has elected for a 'watch and wait' approach.

Brief outline of literature:

Cherubism is a variant of fibrous dysplasia, with the presentation ranging from painless, bilateral, jaw enlargement to the rarer, severe phenotype, associated with nasal obstruction and respiratory compromise(1, 2). The nomenclature 'cherubism' reflects the cherubs or angels of the Renaissance period, with the characteristic appearance of a rounded face and upturned eyes(3).

A family history is supportive, as seen in this case, with cherubism typically inherited in an autosomal dominant manner(1). In 2001, mutations in exon 9 of the *SH3BP2* gene were identified as the cause(4). Gain-of-function mutations in *SH3BP2* can result in inflammation and activation of osteoclasts, resulting in isolated bone resorption, cyst formation, and deposition of fibrous tissue in the jaws(5)

Radiological appearances include hyperlucent, well-defined, multilocular lesions. The mandible is almost always involved with varying involvement of the maxilla and zygoma. Severe cases can be associated with infiltration of the maxillary sinus and the orbital cavity, resulting in exophthalmos and limited eye movements(6).

Histological findings include clusters of giant cell granulomas within vascular fibrous connective tissue, which are non-specific and also seen in Brown's tumour, Central Giant Cell Granuloma (CGCG), Noonan syndrome and NF-1(5). Perivascular eosinophilic 'cuffing' is less common, but is pathognomonic of cherubism.

This rare, usually benign condition, begins with proliferative lesions in the jaw in childhood. The bony lesions typically regress following puberty, undergoing remodelling and filling in by woven bone(7). The majority of case reports have relied on expectant observation, with involution of the lesions seen on transition to adulthood. Medical management has been trialled with mixed success, including use of bisphosphonates, calcitonin, denosumab, imatinib, and tumour necrosis factor (TNF) inhibitors(1). In some cases surgery is performed, but has been associated with recurrence if undertaken too early(8).

Take home messages:

- Cherubism is a rare variant of fibrous dysplasia inherited in an autosomal dominant manner. The disease process usually involves the mandible, and occasionally the maxilla and/or zygoma.
- The infiltration of the jaws with fibro-osseous lesions begin in childhood but often spontaneously regresses following transition to adulthood.
- Histologically, clusters of giant cell granulomas are observed, although this is not pathognomonic for the condition, and the differential diagnosis must include Brown's tumour, CGCG, Noonan syndrome and NF-1.
- A watch-and-wait approach is commonly utilised in cherubism. For more severe cases, management with medical therapy such as bisphosphonates, calcitonin, denosumab, imatinib and more recently TNF inhibitors have been trialled with varying success. Surgery is reserved for the most severe of cases.

1. Chrcanovic BR, Guimaraes LM, Gomes CC, Gomez RS. Cherubism: a systematic literature review of clinical and molecular aspects. Int J Oral Maxillofac Surg. 2021;50(1):43-53.
2. Silva EC, de Souza PE, Barreto DC, Dias RP, Gomez RS. An extreme case of cherubism. Br J Oral Maxillofac Surg. 2002;40(1):45-8.
3. Ozkan Y, Varol A, Turker N, Aksakalli N, Basa S. Clinical and radiological evaluation of cherubism: a sporadic case report and review of the literature. Int J Pediatr Otorhinolaryngol. 2003;67(9):1005-12.
4. Ueki Y, Tiziani V, Santanna C, Fukai N, Maulik C, Garfinkle J, et al. Mutations in the gene encoding c-Abl-binding protein SH3BP2 cause cherubism. Nat Genet. 2001;28(2):125-6.
5. Reichenberger EJ, Levine MA, Olsen BR, Papadaki ME, Lietman SA. The role of SH3BP2 in the pathophysiology of cherubism. Orphanet J Rare Dis. 2012;7 Suppl 1:S5.
6. Sidorowicz W, Kubasiewicz-Ross P, Dominiak M. Familial cherubism: clinical and radiological features. Case report and review of the literature. Eur J Paediatr Dent. 2018;19(3):213-7.
7. Papadaki ME, Lietman SA, Levine MA, Olsen BR, Kaban LB, Reichenberger EJ. Cherubism: best clinical practice. Orphanet J Rare Dis. 2012;7 Suppl 1:S6.
8. Belloc JB, Divaris M, Cancemi GF, Vaillant JM. [Cherubism. Apropos of a major case]. Rev Stomatol Chir Maxillofac. 1993;94(3):152-8.

Treatment refractory post-operative hypocalcaemia

Thomas Nicholls[1], Cherie Chiang[1]

1. Endocrinology, The Peter MacCallum Cancer Centre, Melbourne, VIC, Australia

The Case

Mr CA is a 70 year old gentleman who was referred post obliteration of a tracheoesophageal fistula (TOF) with refractory hypocalcaemia secondary to surgical hypoparathyroidism. His background was most significant for transglottic laryngeal squamous cell carcinoma (T4N1) for which he underwent total laryngectomy and partial pharyngectomy in 2017. During this index operation, his right thyroid lobe was removed as were three parathyroid glands however he remained normocalcaemic in the community without calcium or Vitamin D supplementation. Mr CA continues to be in remission of his primary malignancy. Mr CA developed a TOF in February 2022 and following a failed repair was transferred to a tertiary service for re-do surgery. His pre-operative corrected calcium was 2.34 mmol/L [2.10-2.60] with a normal ionised calcium of 1.12 mmol/L [1.12 – 1.3]. During the re-do TOF repair his last parathyroid gland was unintentionally removed and Mr CA was referred to Endocrinology with a corrected calcium of 1.8, an ionized calcium of 0.77 and a PTH of <0.6 pmol/L [1.7-10]. His QTC segment was also prolonged at 521ms with runs of VT against a past history of a dilated cardiomyopathy. He remained hypocalcaemic requiring IV calcium gluconate despite escalating doses of calcitriol (5mcg QID) and calcium carbonate (5000mg QID) both given via PEG.

A 1, 25 (OH) Vitamin D level was found to be only 144pmol/L [50-190] despite 80 capsules daily of 0.25 mcg of calcitriol and therefore several strategies to improve bioavailability were trialled. Calcitriol was converted to a liquid calcitriol formulation to prevent any losses experienced when the medication was aspirated from the capsules. The PEG was extended to a PEJ due to nausea and this improved Mr CA's diarrhoea. Thyroxine and enteral nutrition were separated from calcium supplementation. Protein pump inhibition remained necessary in the context of gastrointestinal bleeding and calcium citrate was not readily available. An intravenous formulation of calcitriol was also trialled without significant improvement to hypocalcaemia.

Urinary losses were explored with a 24-hour urine collection, which did demonstrate an elevated calcium excretion 29.7 mmol/d [2.5 – 7.5]. With clinical polyuria of 4L per day, Mr CA likely had a tubular defect but no clear aetiology was determined and this self resolved. Hydrochlorothiazide 12.5mg BD was initiated to counter hypercalcuria and a repeat 24hr hour demonstrated its efficacy (calcium excretion 5.3 mmol/d). For approximately one month, Mr CA's corrected calcium remained stable with calcitriol 4mcg TDS, calcium carbonate 7000mg QID, calcium citrate 333mg / cholecalciferol 333 IU TDS and hydrochlorothiazide 25mg BD.

Mr CA's supplementation requirement fell at two major points. When Mr CA was switched from enteral nutrition to total parental nutrition (TPN), his calcitriol doses were down titrated to 3mcg TDS. Two months post initial admission, his calcitriol and calcium supplements were weaned to cessation as his corrected calcium improved (see Table 1). Mr CA was discharged for ongoing monitoring and supplement titration in the community.

Table 1- Calcium changes during admission

	Pre-Op	Post-Op	Stable	Discharge
Corrected Ca	2.34	1.8	2.37	2.39
Albumin	33	27	31	30
Ionised Ca	1.12	0.77	1.19	1.28
PTH	N/A	<0.6	<0.6	<0.6
Phosphate	0.99	0.91	1.54	1.77

Discussion

This case highlights a number of practical challenges associated with the inpatient management of surgical hypoparathyroidism. Firstly in the setting of enteral nutrition, the percutaneous endoscopic gastrostomy or jejunostomy tubes can interfere with delivery as calcitriol can adhere to the tubing.[1] Secondly, there can be multiple gastrointestinal barriers to calcium carbonate absorption including protein pump inhibition,[2] the latter of which can be managed with conversion to calcium citrate. A 1, 25 dihydroxycholecalciferol level can be used to prove absorption of calcitriol but should be interpreted in the context of the degree of supplementation, for example a normal level may be relatively low if large doses are being used. Finally, tubular defects resulting in hypercalcuria can prohibit effective calcium supplementation and hydrochlorothiazide can be an effective medication in this scenario.[3]

Take home messages

In the management of hypoparathyroidism:

- Delivery of calcitriol can be adversely affected by PEG/J administration as the medication can adsorb to the plastic tubing
- Calcium supplement absorption can be limited by diarrhoea, co-administration with enteral nutrition & thyroxine and gastric pH for calcium carbonate
- 1, 25 dihydroxycholecalciferol can be used to prove absorption of calcitriol however needs to be judged in relation to the level of supplementation given to the patient
- Hypercalcuria can limit calcium supplementation in hypoparathyroidism and can be combatted by the use of hydrochlorothiazide

1. Australia Don’t Rush to Crush Handbook (4th Edition). The Society of Hospital Pharmacists of Australia. MIMS Australia. 2022.
2. Graziani G, Badalamenti S et al. Calcium and phosphate plasma levels in dialysis patients after dietary Ca-P overload. Role of gastric acid secretion. Nephron. 2002; 91: 474-479.
3. Nijenhuis T, Hoenderop J et al. Thiazide-induced hypocalciuria is accompanied by a decreased expression of Ca2+ tranposrt proteins in kidney. Kidney International. 2003; 64: 555-564.

A cracking case

Emma Croker[1], Jasmine Wintour[1], Judy Luu[1]

1. John Hunter Hospital, New Lambton Heights, NSW, Australia

Clinical Case

A 22 year old woman, CG, presented with an atraumatic right distal femur fracture following two weeks of leg pain. X-ray confirmed transverse metaphyseal fracture **(Figure 1)**. CT and MRI suggested stress fracture **(Figure 2)**. She was otherwise healthy with no history of renal calculi or coeliac disease. Her past medical history includes previous intra-articular distal radius fracture after falling on outstretched hand, mild seasonal asthma and acne vulgaris requiring previous antibiotic use. She reports a normal developmental history with menarche occurring at age 12. She is nulliparous and takes levonorgestrol 150mcg/ethinyloestradiol 30mcg for menorrhagia. She is on no other regular medications or supplements. Her mother was diagnosed with ER positive breast cancer at age 48. There is no other family history of malignancy nor parathyroid disease, pituitary dysfunction or osteoporosis. CG works in an office-based job. She is a non-smoker and consumes alcohol rarely. Her diet is dairy inclusive, high in fibre and relatively low in meat. She does not participate in excessive physical activity.

Figure 1: X-rays of right distal femur demonstrating transverse metaphyseal fracture with periosteal new bone at the median margin.

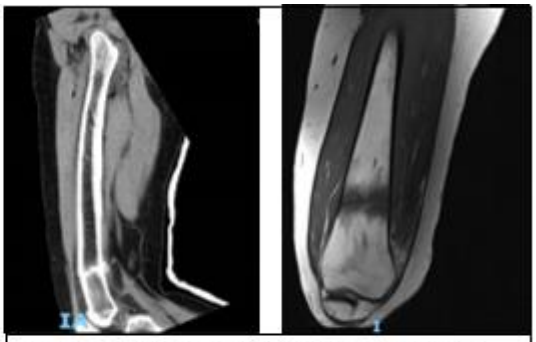

Figure 2: CT (left) and MRI (right) consistent with stress fracture.

On examination sclera were normal, there was no evidence of Cushingoid features, palpable lymphadenopathy or hyper-flexibility other than elbow hyper-flexion. She had normal dentition and palate.

Intra-operative bone biopsy from the fracture site was consistent with chronic inflammation without evidence of malignancy. Further imaging was attended including x-ray of the left femur given history of prodromal pain which identified stromal reaction to left distal femur in a similar location to that of the right **(Figure 3)**. Thoracic and lumbrosacral spine x-rays were unremarkable. Bone scan revealed previous second and ninth rib fractures. Bone mineral density (BMD) was very low for age (Z scores: L2-L4 -3.3, right femoral neck -1.6 and left femoral neck -1.6).

Figure 3: X-rays of left femur demonstrating stromal reaction.

Investigations for secondary causes of osteoporosis were unremarkable:

INVESTIGATION	RESULT	REFERENCE INTERVALS
CORRECTED CALCIUM	2.33 mmol/L	2.10-2.60
PHOSPHATE	1.16 mmol/L	0.75-1.50
MAGNESIUM	0.74 mmol/L	0.70-1.10
CREATININE	65 umol/L	45-90
24HR URINE CALCIUM	1.7 mmol/day	2.5-7.5
URINE CALCIUM/CREATININE RATIO	0.35	0.04-0.40
URINE TUBULAR RESORPTION OF PHOSPHATE	93%	85-95
VITAMIN D	142 nmo/L	
1,25-VITAMIN D	110 pmol/L	60-210
PTH	30 pg/mL	15-68
COELIAC SCREEN	Negative	
TSH	0.97 mIU/L	0.40-3.50
MYELOMA SCREEN	Negative	
P1NP	40 µg/L	<70
CTX	546 ng/L	100-600

CG subsequently attended prophylactic fixation of the left femur. Bone biopsy was attended with single labelled tetracycline labelling which demonstrated severe osteoporosis with reduced trabecular bone area and 'islands' of bone as well as reduced osteoid surfaces and thickness, reduced bone formation and osteoclast surfaces. Interestingly bone turnover markers were low despite recent fracture. CG represented with bilateral ankle pain. X-rays confirmed healing fracture in the right distal metaphysis of the tibia.

Genetic studies excluded osteogenesis imperfecta, Gaucher disease and homocystinuria. There are no plans to proceed to whole genome sequencing. Her mother and brother attended BMD which demonstrated osteopenia and low bone mineral density although not osteoporotic respectively. Management to date includes calcium supplementation and observation including annual BMD in keeping with CG's wishes to not commence Teriparatide at this time.

Literature **Review**

Osteoporosis is characterised by low bone mass and changes within the microarchitecture of bone resulting in increased risk of fragility fractures. Less commonly this occurs in pre-menopausal women. In this population there is often an underlying cause resulting in secondary osteoporosis. When no secondary cause is found in an otherwise healthy individual with normal gonadal function this is termed "idiopathic osteoporosis" (IOP).

Contributing factors may include low body weight, tobacco consumption and low calcium intake[1], however, there is a large genetic predisposition and family history of osteoporosis is more common in patients with IOP1 [1]. Despite studies involving whole exome sequencing the genetic aetiology is not identified in the majority of women (89%)[2]. This suggests the pathogenesis of idiopathic osteoporosis is heterogeneous which is further supported by the variety of clinical presentations and evidence of patients with high, normal and low bone turnover markers.

Uncoupling between resorption and formation results in net bone loss[1]. There is decreased initiation of remodelling cycles with more time in the resorption phase. In the formation phase, matrix is formed at a reduced rate with osteoid mineralisation occurring more slowly[3]. Osteoclast function is further implicated by the finding of elevated Tartrate-resistant acid phosphatase isoform 5b (TRAP5b), a specific osteoclast marker that correlates to either the number or the activity of differentiated osteoblasts and is independent to C-telopeptide (CTx) and N-telopeptides (NTx)[1]. Microcomputed tomography and microfinite element analysis has identified structural change within the microarchitecture contributing to reduced stiffness in both patients with IOP and those with idiopathic low bone mineral density[4,5].

IOP with high bone turnover have a biochemical pattern resembling idiopathic hypercalciuria, while microarchitectural deficits and reduced stiffness are most severe in those with the lowest bone formation ratio[4]. IOP with low bone turnover also had higher serum IGF-1 levels which suggests primary osteoblast dysfunction with resistance to IGF-1[4].

Treatment of IOP often includes an anabolic agent such as Teriparatide[6]. Interestingly, approximately 20% of patients demonstrate minimal response to Teriparatide. These patients generally have low bone turnover markers[7,8], which may implicate osteoblast dysfunction in the attenuation of the response to Teriparatide[9]. Response to Teriparatide is correlated to the increase of expression of the IGF-1 receptor (IGF-1R) on the surface of circulating osteoblast progenitor cells while lower IGF-1R expression is associated with higher body fat and lower BMD response[10]. Alternate treatment strategies such as combination therapy, romosozumab and the implications of future pregnancy will be reviewed in further detail.

Take home points:

- **IOP is a heterogenous disease including different levels of bone turnover activity and underlying pathogenesis**
- **Microarchitectural deficits contribute to reduced density and stiffness in both patients with fractures and those with idiopathic low bone mineral density**
- **In those with low bone turnover IOP, pathogenesis may be implicated by osteoblast dysfunction due to IGF-1 resistance**

1. Peris P, Ruiz-Esquide V, Monegal A, Alvarez L, Martínez de Osaba MJ, Martínez-Ferrer A, Reyes R, Guañabens N. Idiopathic osteoporosis in premenopausal women. Clinical characteristics and bone remodelling abnormalities. Clin Exp Rheumatol. 2008 Nov-Dec;26(6):986-91. PMID: 19210860.
2. Cohen A, Hostyk J, Baugh EH, Buchovecky CM, Aggarwal VS, Recker RR, Lappe JM, Dempster DW, Zhou H, Kamanda-Kosseh M, Bucovsky M, Stubby J, Goldstein DB, Shane E. Whole exome sequencing reveals potentially pathogenic variants in a small subset of premenopausal women with idiopathic osteoporosis. Bone. 2022 Jan;154:116253. doi: 10.1016/j.bone.2021.116253. Epub 2021 Nov 4. PMID: 34743040; PMCID: PMC8671293.
3. Donovan MA, Dempster D, Zhou H, McMahon DJ, Fleischer J, Shane E. Low bone formation in premenopausal women with idiopathic osteoporosis. J Clin Endocrinol Metab. 2005 Jun;90(6):3331-6. doi: 10.1210/jc.2004-2042. Epub 2005 Mar 22. PMID: 15784712.
4. Cohen A, Dempster DW, Recker RR, Stein EM, Lappe JM, Zhou H, Wirth AJ, van Lenthe GH, Kohler T, Zwahlen A, Müller R, Rosen CJ, Cremers S, Nickolas TL, McMahon DJ, Rogers H, Staron RB, LeMaster J, Shane E. Abnormal bone microarchitecture and evidence of osteoblast dysfunction in premenopausal women with idiopathic osteoporosis. J Clin Endocrinol Metab. 2011 Oct;96(10):3095-105. doi: 10.1210/jc.2011-1387. Epub 2011 Aug 10. PMID: 21832117; PMCID: PMC3200255.
5. Misof BM, Gamsjaeger S, Cohen A, Hofstetter B, Roschger P, Stein E, Nickolas TL, Rogers HF, Dempster D, Zhou H, Recker R, Lappe J, McMahon D, Paschalis EP, Fratzl P, Shane E, Klaushofer K. Bone material properties in premenopausal women with idiopathic osteoporosis. J Bone Miner Res. 2012 Dec;27(12):2551-61. doi: 10.1002/jbmr.1699. PMID: 22777919; PMCID: PMC3502637.
6. Soumya SL, Cherian KE, Kapoor N, Paul TV. Severe Idiopathic Osteoporosis in a Premenopausal Woman: A Case for Dual Therapy. J Midlife Health. 2020 Oct-Dec;11(4):260-263. doi: 10.4103/jmh.JMH_168_20. Epub 2021 Jan 21. PMID: 33767569; PMCID: PMC7978054.
7. Cohen A, Stein EM, Recker RR, Lappe JM, Dempster DW, Zhou H, Cremers S, McMahon DJ, Nickolas TL, Müller R, Zwahlen A, Young P, Stubby J, Shane E. Teriparatide for idiopathic osteoporosis in premenopausal women: a pilot study. J Clin Endocrinol Metab. 2013 May;98(5):1971-81. doi: 10.1210/jc.2013-1172. Epub 2013 Mar 29. PMID: 23543660; PMCID: PMC3644608.
8. Goetz TG, Nair N, Shiau S, Recker RR, Lappe JM, Dempster DW, Zhou H, Zhao B, Guo X, Shen W, Nickolas TL, Kamanda-Kosseh M, Bucovsky M, Stubby J, Shane E, Cohen A. In premenopausal women with idiopathic osteoporosis, lower bone formation rate is associated with higher body fat and higher IGF-1. Osteoporos Int. 2022 Mar;33(3):659-672. doi: 10.1007/s00198-021-06196-8. Epub 2021 Oct 19. PMID: 34665288.
9. Cohen A, Shiau S, Nair N, Recker RR, Lappe JM, Dempster DW, Nickolas TL, Zhou H, Agarwal S, Kamanda-Kosseh M, Bucovsky M, Williams JM, McMahon DJ, Stubby J, Shane E. Effect of Teriparatide on Bone Remodeling and Density in Premenopausal Idiopathic Osteoporosis: A Phase II Trial. J Clin Endocrinol Metab. 2020 Oct 1;105(10):e3540–56. doi: 10.1210/clinem/dgaa489. PMID: 32876328; PMCID: PMC8921657.
10. Cohen A, Kousteni S, Bisikirska B, Shah JG, Manavalan JS, Recker RR, Lappe J, Dempster DW, Zhou H, McMahon DJ, Bucovsky M, Kamanda-Kosseh M, Stubby J, Shane E. IGF-1 Receptor Expression on Circulating Osteoblast Progenitor Cells Predicts Tissue-Based Bone Formation Rate and Response to Teriparatide in Premenopausal Women With Idiopathic Osteoporosis. J Bone Miner Res. 2017 Jun;32(6):1267-1273. doi: 10.1002/jbmr.3109. Epub 2017 Mar 23. PMID: 28218468; PMCID: PMC5466483.

Rapidly progressive Charcot neuroarthropathy requiring below-knee amputation: an unfortunate outcome in a man with type 2 diabetes mellitus

Kay Hau Aaron Choy[1], Aviva Frydman[1], Michael McNamara[1], Mark Kotowicz[1, 2, 3]

1. Department of Endocrinology and Diabetes, Barwon Health, Geelong, Victoria, Australia

2. Deakin University, Geelong, Victoria, Australia

3. Melbourne Medical School-Western Campus, The University of Melbourne, Victoria, Australia

Introduction: Charcot neuroarthropathy (CN) is a complication of diabetic peripheral neuropathy. We present a case of diabetic foot infection (DFI) associated with CN.

Case: A 44-year-old male with type 2 diabetes, peripheral vascular disease, neuropathy and previous DFI, was admitted with right foot pain and redness. Barriers to effective diabetes care included depression and low health literacy, compounded by reduced in-person outpatient reviews amid the COVID-19 pandemic. Right foot assessment revealed cellulitis and a rocker-bottom deformity, with radiographic evidence of CN predominantly involving the navicular bone. He discharged against medical advice, leading to suboptimal foot care with CN management including offloading not being implemented. After six months, during which time he did not attend any podiatry clinic or the diabetic foot service and continued normal weight-bearing, he presented with increasing right foot pain and swelling, with a right ankle ulcer unresponsive to 5 months of oral antibiotics prescribed by his general practitioner. Rapid radiographic progression of CN, evidenced by complete destruction of the right tarsal bones, midfoot articulations and tarsometatarsal joints, was associated with MRI features of septic arthritis and tenosynovitis. The extent of his DFI was masked by the prolonged use of oral antibiotic therapy prior to admission, leading to delayed presentation and inadequately treated infection. His contralateral foot had no stigmata of DFI. He required a right below-knee amputation as his foot was deemed non-viable and underwent inpatient rehabilitation after surgery.

Conclusion: Our case highlights the devastating sequalae of suboptimally-treated CN. Despite multiple healthcare contacts and opportunities for interventions, appropriate management of CN was not initiated, suggesting a lack of awareness of its treatment and disease course among some healthcare professionals, although patient factors were also implicated. Increased vigilance and timely intervention of CN are vital to impede debilitating structural deformities and the risks of ulceration and amputation.

Serum sclerostin concentrations using the Diasorin assay correlate with renal function and physical activity

Shejil Kumar[1], Lucy Ding[1, 2], Paul Bonnitcha[2], Roderick Clifton-Bligh[1], Cameron Wood[2], Christian Girgis[1]

1. Endocrinology, Royal North Shore Hospital, Sydney, NSW, Australia

2. Clinical Chemistry, Royal North Shore Hospital, Sydney, NSW, Australia

Background: Sclerostin is an osteocyte-derived inhibitor of bone formation (1). Skeletal loading and the osteoanabolic agent romosozumab increase bone density via sclerostin downregulation/inhibition (1, 2). Sclerostin concentrations have been associated with skeletal loading (3, 4), and inversely associated with renal function (5). Data is scarce regarding association with renal function using the recently validated Diasorin assay, which is more specific for intact sclerostin than degradation fragments (6).

Methods: We conducted a cross-sectional study of serum sclerostin concentrations in different groups approximating different degrees of loading: active laboratory staff (n = 40), patients with recent femoral fracture (n = 39) and acute (<3 months, n = 10) and chronic (1-3 years, n = 5) spinal cord injury (SCI). We used an automated chemiluminescent sclerostin assay (LIAISON®, DiaSorin). Patients with predominantly stage 4-5 chronic kidney disease (CKD) (n = 25) were included to determine sclerostin associations with renal function.

Results: Serum sclerostin concentrations (pg/mL) among cohorts were: staff (median 176, IQR 122), femoral fracture (median 451, IQR 211), acute SCI (median 295, IQR 146) and chronic SCI (median 126, IQR 111). Mean sclerostin concentrations significantly differed between fully ambulant staff and less ambulant patients with femoral fracture and acute (but not chronic) SCI. The CKD cohort had highest sclerostin concentrations (median 676, IQR 811). Sclerostin had a strong negative association with eGFR ($r = -0.682$, $p < 0.001$), and strong positive association with creatinine ($r = 0.752$, $p < 0.001$). Using multivariate linear regression, sclerostin associations with eGFR and creatinine remained significant ($p < 0.001$).

Conclusions: Sclerostin concentrations are elevated in renal impairment using the Diasorin assay, suggesting elevated intact sclerostin rather than renally-excreted degradation products as the primary mechanism. This may represent impaired intact sclerostin excretion or a pathophysiological response to CKD. Use of this sclerostin assay should adjust for renal function.

1. Choi RB, Robling AG. The Wnt pathway: An important control mechanism in bone's response to mechanical loading. Bone. 2021 Dec;153:116087.
2. Cosman F, Crittenden DB, Adachi JD, et al. Romosozumab Treatment in Postmenopausal Women with Osteoporosis. N Engl J Med. 2016;375(16):1532-1543.
3. Omran A, Atanasova D, Landgren F, Magnusson P. Sclerostin: From Molecule to Clinical Biomarker. Int J Mol Sci. 2022;23(9):4751.
4. Costa AG, Cremers S, Bilezikian JP. Sclerostin measurement in human disease: Validity and current limitations. Bone. 2017;96:24-28.
5. Delanaye P, Paquot F, Bouquegneau A, et al. Sclerostin and chronic kidney disease: the assay impacts what we (thought to) know. Nephrol Dial Transplant. 2018;33(8):1404-1410.
6. Drake MT, Fenske JS, Blocki FA, et al. Validation of a novel, rapid, high precision sclerostin assay not confounded by sclerostin fragments. Bone. 2018;111:36-43.

A Maternal High Fat Diet Leads to Sex-Specific Programming of Mechanical Properties in Supraspinatus Tendons of Adult Rat Offspring

Scott M Bolam[1], Vidit V Satokar[1, 2], Subhajit Konar[1], Brendan Coleman[3], Paul Monk[1], Jillian Cornish[1], Jacob T Munro[1], Mark H Vickers[2], Ben B Albert[2], David S Musson[1]

1. University of Auckland, Grafton, AUCKLAND, New Zealand

2. Liggins Institute, University of Auckland, Auckland, New Zealand

3. Orthopaedics, Counties Manukau DHB, Auckland, New Zealand

Background: Over half of women of reproductive age are now overweight or obese. The impact of maternal high-fat diet (HFD) is emerging as an important factor in the development and health of musculoskeletal tissues in offspring, however, there is a lack of evidence examining its effects on tendon. Alterations in the early life environment during critical periods of tendon growth, therefore, have the potential to influence tendon health that crosses the lifespan. We hypothesised that a maternal HFD would alter biomechanical, morphological and gene expression profiles of adult offspring rotator cuff tendon.

Materials and Methods: Female Sprague-Dawley rats were randomly assigned to either: control diet (CD; 10% kcal from fat) or HFD (45% kcal from fat) 14 days prior to mating and throughout pregnancy and lactation. Eight female and male offspring from each maternal diet group were weaned onto a standard chow diet and then culled at postnatal day 100 for tissue collection. Supraspinatus tendons were used for mechanical testing and histological assessment (cellularity, fibre organisation, nuclei shape) and tail tendons were collected for gene expression analysis.

Results: A maternal HFD increased the elasticity (Young's Modulus) in the supraspinatus tendon of male offspring. Female offspring tendon biomechanical properties were not affected by maternal HFD. Gene expression of SCX and COL1A1 were reduced in male and female offspring of maternal HFD, respectively. Despite this, tendon histological organisation were similar between maternal diet groups in both sexes.

Conclusion: An obesogenic diet during pregnancy increased tendon elasticity in male, but not female, offspring. This is the first study to demonstrate that maternal diet can modulate the biomechanical properties of offspring tendon. A maternal HFD may be an important factor in regulating adult offspring tendon homeostasis that may predispose offspring to developing tendinopathies and adverse tendon outcomes in later life.

Methotrexate and diet's effect on trabecular long bone in a rat model of breast cancer

Bailey Deverell[1], Helen Tsangari[1], Hannah Wardill[1], Bonnie Williams[1], Joanne Bowen[1], Tania Crotti[1]

1. School of Biomedicine, The University of Adelaide, Adelaide, SA

INTRODUCTION

In advanced breast cancer, chemotherapies, such as methotrexate (MTX), are detrimental to the gut microbiota [1] and bone microarchitecture, increasing fracture risk [2]. Interplay between the gastrointestinal and skeletal systems, termed the "gut-bone axis", may reciprocally influence chemotherapy [3].

Given 90% of individuals treated for breast cancer with chemotherapy survive five-years post-diagnosis, understanding the effects of chemotherapies on bone is essential [4]. Diets that support gut health during chemotherapy may also be effective at mitigating bone loss. Thus, this study aimed to determine the effect of MTX +/- a hydrolysed protein (HP) diet on trabecular bone in long bones of a rat breast cancer model.

METHODS

Female dark agouti rats (n=32) were subcutaneously inoculated with mammary adenocarcinoma cells [5] then allocated to; vehicle control (VC; n=8), HP diet only (NT; n=8), MTX only (MTX; 2 mg/kg intramuscularly; n=8), and HP diet and MTX combination (NTMTX; n=8).

Rodents were given standard or HP diet (Nutricia Research) starting on day -14 then treated on days 0 and 1 with either MTX or vehicle and euthanised on day 4. Long bones were scanned via micro-CT and assessed for; trabecular thickness (Tb.Th.), trabecular number (Tb.N.), trabecular spacing (Tb.S.), bone volume (BV), and percent bone volume (BV/TV%).

RESULTS

A significant increase in Tb.Th. (p=0.0101), Tb.N. (p=0.0198), and BV/TV% (p=0.0054) was observed in NT rat tibia. No significant differences were observed in MTX and NTMTX rat tibia or femur.

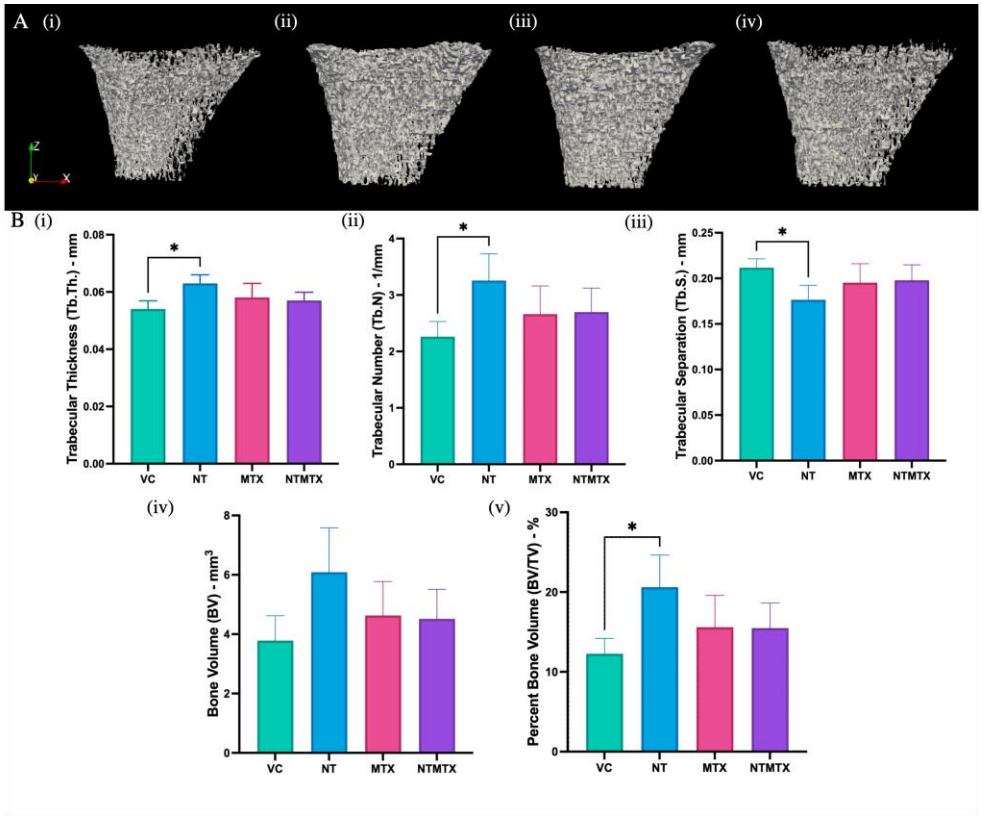

Figure 1: (A) High resolution 3D micro-CT models of right tibia; (i) VC (ii) NT (iii) MTX and (iv) NTMTX. (B) Histomorphometric analysis of right tibia trabecular microarchitecture by high resolution micro-CT. (i) Tb.Th. (ii) Tb.N. (iii) Tb.S. (iv) BV (v) BV/TV%.

CONCLUSION

Results indicate that HP diet increases bone volume, which may have a protective effect against MTX-induced bone loss.

1. Rodrigues FC, et al. (2012) J Med Food 15, 664-70.
2. Hain BA, et al. (2019). JCSM Rapid Commun.
3. Sjogren K, et al. (2012). J Bone Miner Res 27, 1357-67.
4. Youlden DR, et al. (2019). J Adolesc Young Adult Oncol.
5. Gibson R, et al. (2018) Chemotherapy 63, 284–292

Intramedullary nailing of tibial shaft fractures: a scoping review

Simon Thwaites[1], John Abrahams[2], Dominic Thewlis[1, 2], Mark Rickman[1, 2]

1. Centre for Orthopaedic and Trauma Research, University of Adelaide, Adelaide, SA, Australia

2. Department of Orthopaedics and Trauma, Royal Adelaide Hospital, Adelaide, SA, Australia

Intramedullary (IM) nailing is commonly used to treat tibial shaft fractures. Techniques to perform IM nailing vary, and studies comparing approaches show conflicting results [1,2]. The absence of a validated outcome measure specific to this cohort has led to a wide range of outcomes being used, making comparisons between studies difficult. This scoping review aimed to summarise the clinical and patient outcomes used to assess these fractures, and the nature of the publications. Literature reporting on tibial shaft fractures using any IM nailing approach were searched in online databases. Covidence™ was used for article screening and data extraction. We identified 433 articles with 165 papers included for final analysis. For in vivo studies, the most common patient and clinical outcomes were a binary assessment of knee pain (29%) (Fig.1), and union (51%), respectively. Most in vivo studies provided descriptions of locking (70%), fracture type/location (63%), open/closed fractures (76%), and reaming (60%), and did not include nail removal (73%). However, the majority did not describe the post-op weight-bearing regime (61%) or mechanisms of injury (55%). Nail insertion location was the most reported outcome for cadaveric studies (64%). The most reported follow-up times were 6 and 12 months (22%). Seventy-seven studies (47%) were published within the last decade, 58 (35%) originated from the USA, and 7 (4%) were level I evidence. We have shown that a wide range of outcomes are used to assess tibial shaft fractures treated with IM nailing. Notably, a number of the scores designed for other pathologies routinely used do not contain a kneeling component, shown to cause the most severe pain within this cohort [3]. Currently, no conclusive evidence exists to inform surgical decision making on an optimal IM nailing technique. This work highlights the need for a validated outcome measure designed specifically for this cohort.

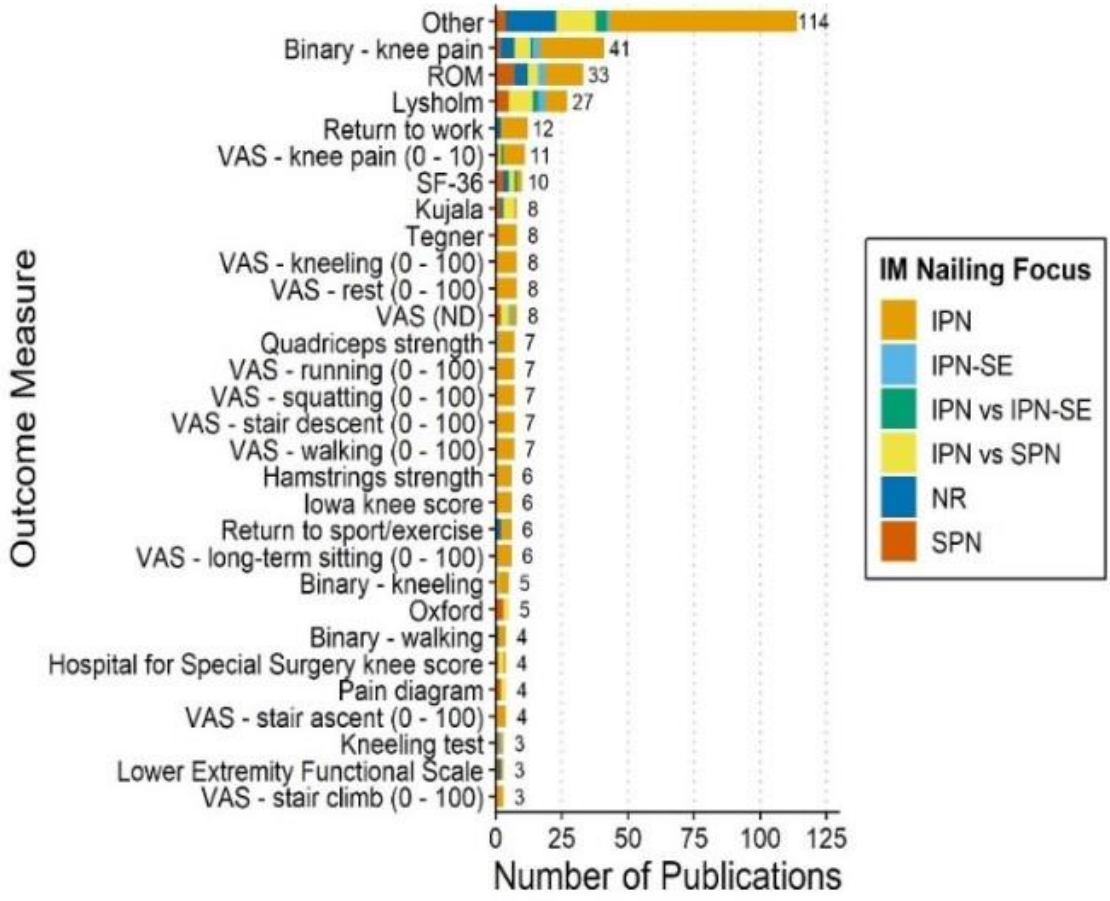

Fig.1: Patient outcomes used in in vivo studies. IPN - infrapatellar nailing; SE - semi-extended; NR - not reported; SPN - suprapatellar nailing; ROM - range of movement; VAS - visual analogue score; ND - no description

1. Sun et al. (2016) Int Orthop, 40(12):2611-7
2. Jones et al. (2014) J Orthop Trauma, 28(5):256-62.
3. Song (2012) J Orthop Trauma, 26(3):172-7

Regulation of blood-brain barrier by a subset of astrocytes that express osteocyte marker DMP-1

Delin Liu[2, 1], Hao Li[3], Peng Liao[3], Youshui Gao[3], Yigang Huang[3], Linjing Shi[4], Ziming Chen[1], Changqing Zhang[3], Ming-Hao Zheng[2, 1], Junjie Gao[3]

1. Centre for Orthopaedic Research, The University of Western Australia, Perth, Western Australia, Australia

2. Perron Institute for Neurological and Translational Science, Perth, Western Australia, Australia

3. Department of Orthopaedics, Shanghai Jiao Tong University Affiliated Shanghai Sixth People's Hospital, Shanghai, China

4. Department of Orthopaedics, The Second Affiliated Hospital of Zhejiang University School of Medicine, Hangzhou, China

Dentin matrix protein 1 (Dmp1), a marker of osteocyte that has been showed to be expressed in brain, but its biological function is still unknown[1, 2]. Using single cell RNA sequencing (scRNAseq) we revealed that Dmp1 was mainly expressed in astrocytes. Gene oncology analysis showed distinct difference in cell adhesion and projection between DMP-1 positive astrocytes (astrocytes^{DMP-1}) and Dmp1 negative astrocytes. In particular, astrocytes^{DMP-1} express much higher level of AQP4 compared to Dmp1 negative astrocytes. To investigate the role of astrocytes^{DMP-1}, we generated several mice lines including Dmp1^{Cre}-mGmT and Dmp1^{Cre}-COX8a^{Dendra2} fluorescent mice. *In vivo* confocal imaging indicated that astrocytes^{DMP-1} were mostly located around blood vessels and astrocytes^{DMP-1} transfer mitochondria through end-feet to endothelial cells. Interestingly, mitochondrial activity of astrocytes^{DMP-1} were decreased with increased aging. Co-culture of astrocytes and bEnd.3 endothelial cells demonstrated that astrocytes rescue endothelial oxidative stress via transferring mitochondria. Senescence of astrocytes compromised mitochondrial transfer efficiency *in vitro*, which is correlated with disrupted endoplasmic (ER)-mitochondria contact in astrocytes. Depletion of ER-mitochondria tethering protein Mfn2 in astrocytes^{DMP-1} resulted in dramatic blood-brain barrier (BBB) leakage *in vivo*. Mitochondrial transplantation assay showed that mitochondria acquired from astrocytes restored oxidative stress and wound healing ability of endothelial cells. In conclusion, we have identified a subset of astrocytes that express Dmp1. Astrocytes^{DMP-1} play a critical role in maintaining BBB via transferring mitochondria to vascular endothelial cells.

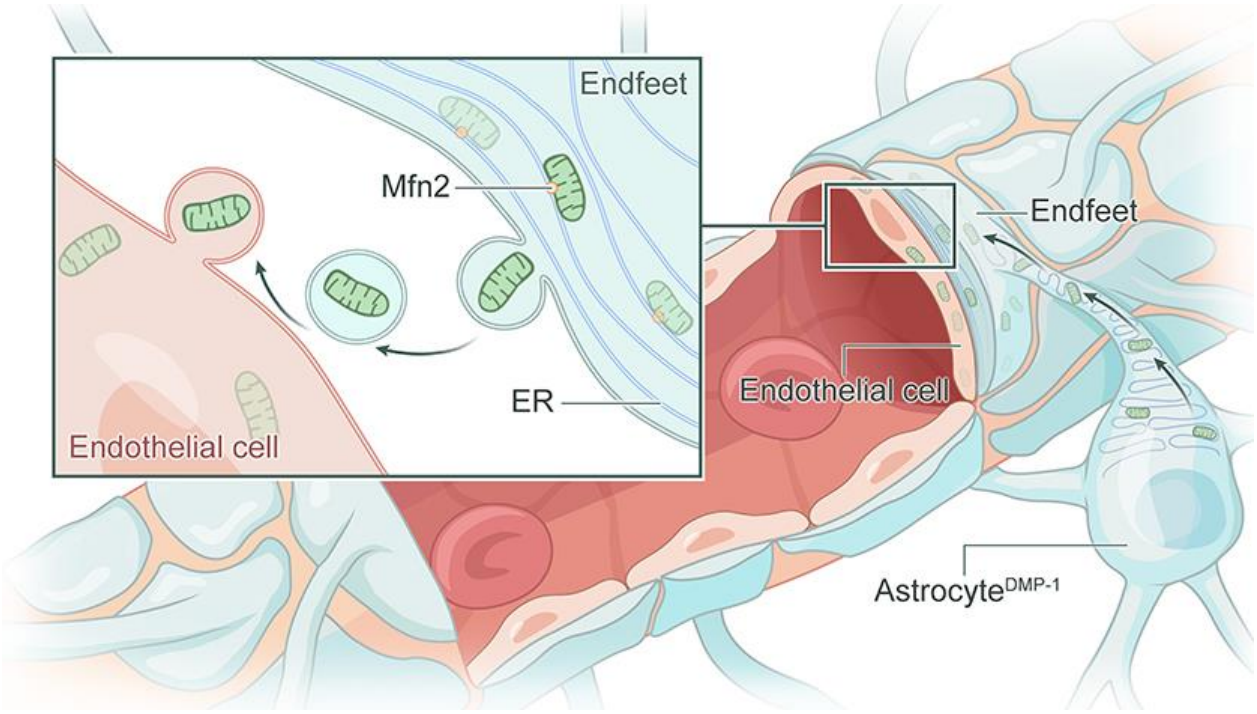

1. Terasawa M, Shimokawa R, Terashima T, Ohya K, Takagi Y, Shimokawa H. Expression of dentin matrix protein 1 (DMP1) in nonmineralized tissues. J Bone Miner Metab. 2004;22(5):430-438.
2. Lim J, Burclaff J, He G, Mills JC, Long F. Unintended targeting of Dmp1-Cre reveals a critical role for Bmpr1a signaling in the gastrointestinal mesenchyme of adult mice. Bone Res. 2017;5:16049.

245

Identification of epigenetic factors deregulated in skeletal stem cells during high fat/glucose mediated inhibition of bone formation.

Ensieh Hajimotallebi[1], Dimitrios Cakouros[1], Stan Gronthos[1], Nicholas Smith[1]

1. The university of Adelaide, Adelaide, SA, Australia

Individuals with type 2 diabetes are at higher risk of osteoporosis and major bone fractures independent of their body mass index (BMI). Bone marrow derived mesenchymal stem/ stromal cells (BMSC) derived from these patients exhibit reduced osteogenic potential and increased cell death. Currently, it is not known how high fat/glucose levels can suppress BMSC osteogenic differentiation potential. The present project examined the epigenetic mechanisms regulating BMSC dysfunction in response to high fat/glucose to identify targets for reversing high fat-mediated bone loss. We hypothesize that high fat/glucose levels lead to changes in BMSC epigenetic gene expression patterns that cause compromised bone formation. Ten-eleven translocation (Tet) family is a group of DNA demethylases, able to convert 5-methylcytosine (5-mC) to 5-hydroxymethylcytosine (5-hmC), an epigenetic marker in osteogenesis. Our studies have shown that *TET2* is essential in driving the differentiation of bone forming osteoblasts and high glucose level inhibits the expression of *TET1* and *TET2*. Furthermore, human BMSC grown in high glucose conditions were found to display increased level of cell death, senescence and oxidative stress, associated with decreasing cellular proliferation potential compared to BMSC cultured in regular growth media. To observe the effects of Tet molecules on bone formation in vivo, we generated a double *Tet1/Tet2* knockout mouse in the mesenchymal lineage using a Prx1:Cre driver mouse. The results found that Prx1:Cre *Tet1/Tet2* double knock out mice fed on high fat diet showed increased body fat and glucose tolerance and decreased bone density compared to Prx1:Cre control mice on the same diet. Understanding the role of epigenetic regulators in hyperglycaemic conditions will help to identify solutions to battle bone loss seen in diseases such as diabetes and osteoporosis. Given that epigenetic marks can be reversed by pharmacological inhibitors and altered via changes in diet and lifestyle, these targets are of unique therapeutic importance.

246

The osteoinductive potential of the nutrient inorganic components from the bone microenvironment for *in situ* bone tissue engineering

Yuqing Mu[1], Zhibin Du[1], Ross Crawford[1], Yin Xiao[1]

1. Queensland University of Technology, Kelvin Grove, QUEENSLAND, Australia

Inorganic ions actively participate in many biological processes, either as essential cofactors to enzymes and proteins or as regulatory molecules in ion channels or secondary signalling. Previous studies focused on the biological performances of individual ions on bone metabolism but overlooked the interactions among ions, and interactions between ions and other components in the localised microenvironment, i.e. cells and organic molecules. In other words, the influence of inorganic components from the bone microenvironment on bone metabolism, and their potential for future biomaterial design for bone tissue engineering remained unexplored.

We developed a low-temperature method for preparing monetite from the bovine femur and generated an ionic environment similar to the bone microenvironment. We found that these inorganic components from the bone microenvironment fostered osteogenesis by upregulating the expression of osteogenesis-related markers (RUNX2, ALP, BMP2, VEGF, OPN), and promoted mineralisation via intracellular mineralisation, without the need for an osteogenic environment. And we further confirmed the great regenerative capacity of inorganic components from the bone microenvironment *in vivo*. In a rat calvarial defect model, inorganic components from the bone microenvironment-incorporated collagen composite significantly promoted new bone formation in the defect area at 4 and 8 weeks post-operation, verifying the regenerative potential of the inorganic components from the bone microenvironment on in situ bone tissue regeneration in vivo.

Taken together, this is the first study investigating the influence of inorganic components from the bone microenvironment on bone metabolism. We demonstrated the great regenerative capacity of inorganic components from the bone microenvironment on bone tissue engineering. This would bring new insights to future biomaterial design for *in situ* bone tissue engineering, and provide directions for future studies on a deeper understanding of inorganic components in bone, and other biological processes.

Automated Grading System of Radiographic Knee Osteoarthritis Severity Using Deep Learning

Dinh-Tan Nguyen[2, 1], Duy K. Hoang[2, 1], Lan T. Ho-Pham[2], Tuan Nguyen[2, 1]

1. School of Biomedical Engineering, University of Technology Sydney, Sydney, NSW, Australia

2. Bone and Muscle Research Group, Ton Duc Thang University, Hochiminh City, Vietnam

Introduction: Knee osteoarthritis is a degenerative joint disease affecting the entire joints including cartilage, ligaments, bone and muscles. We aim to use artificial intelligence (AI, Deep Learning) in the screening of knee osteoarthritis (OA).

Objectives: We developed an automated model for staging knee osteoarthritis severity from radiographs, and we evaluated the prognostic performance of the automated model in the classification of OA.

Methods and Results: This study was a part of the Vietnam Osteoporosis Study (VOS) involved of 1503 women and 934 men aged 40 and older living in Ho Chi Minh city, Vietnam. Radiographs from the VOS staged by radiologists utilised the Kellgren-Lawrence (KL) score. Prior to the usage of those images as the input to a convolutional neural network model, they were standardized and augmented. The model was trained with 1945 plain Xray images, evaluated with 491 images. Applied object detection and other tools of deep learning (Grad-cam maps) were generated to reveal the features utilised (osteophyte formation) by the model to determine KL grades.

Our model was able to achieve 98% in the detection of the exact location of the knee joints and the label of different sides of the knees. The concordance between clinical diagnosis and AI-based classification of knee OA is significant, which the proportion of concordance was able to reach 79.8% (95% CI: 0.77, 0.82). Our model achieved with averagely 91.82% of specificity and 61,52% of sensitivity in all severity levels of knee OA. In terms of screening osteoarthritis, our model achieved 90% (95% CI: 0.87, 0.92) with 94% of sensitivity and 78% of specificity for classifying the knee OA and healthy people.

Conclusions: The AI-based model achieved high sensitivity and specificity in predicting osteoarthritis severity. The model can be used as a screening tool in high-volume setting to reduce clinical workload.

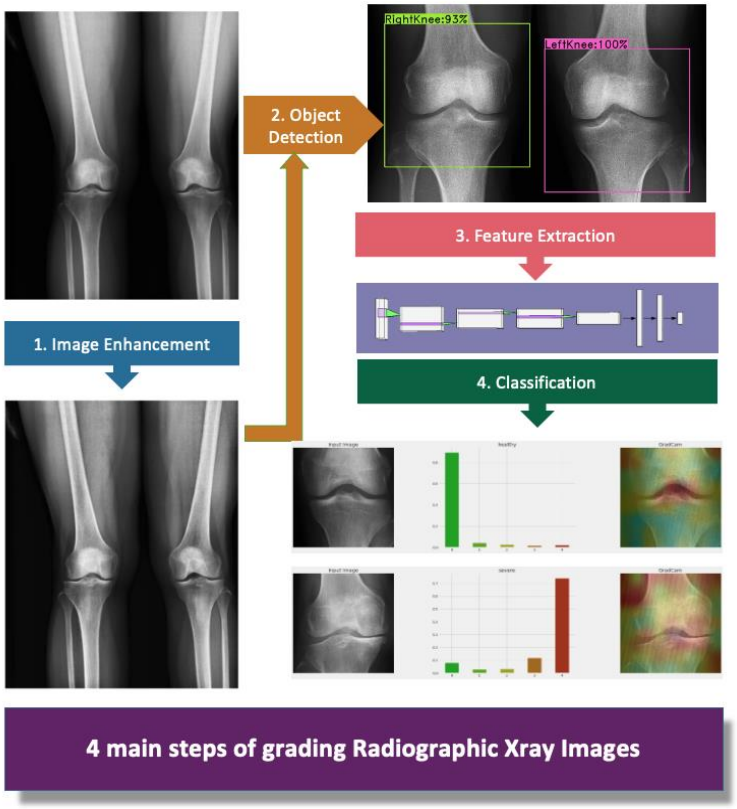

248

Pathogen-associated molecular patterns produced by infectious microbes worsen Neurogenic Heterotopic Ossifications after spinal cord injury

Selwin Gabriel Samuel[1], Hsu-Wen Tseng[1], Marjorie Salga[2], Whitney Fleming[1], Francois Genet[2], Kylie Alexander[1], Jean-Pierre Levesque[1]

1. Mater Research Institute - UQ, Woolloongabba, Brisbane, QLD, Australia

2. Department of Physical Medicine and Rehabilitation, Raymond Poincaré Hospital, Garches, France

Neurogenic heterotopic ossifications (NHOs) are pathological bone formations that develop in periarticular muscles after spinal-cord injury (SCI), traumatic brain injury (TBI), or stroke. As its pathophysiology is still obscure, there is a need to understand the factors that contribute to this pathology. We have established a mouse model for NHO by combining a complete spinal-cord transection together with an intramuscular injection of cardiotoxin into the hamstring muscles to cause muscle injury. Using this model, we have been able to identify numerous pathways that trigger NHO formation.

Retrospective studies have demonstrated that the prevalence of NHO is higher in patients with concomitant infections, particularly urinary tract infections and pneumonia. To demonstrate a direct link between infections and enhanced NHO formation, we employed purified pathogen-associated molecular patterns (PAMPs). C57BL/6 mice were subjected to a complete spinal-cord transection between T11-T13 vertebrae, followed by an intramuscular injection of cardiotoxin in the hamstring muscles. Mice additionally received intraperitoneal injections of purified PAMPs in different dosages, while control mice were injected with the vehicle. At 7- and 21-days post-surgery, NHO volumes were quantified using micro-computed tomography.

Bacterial PAMPs such as lipoteichoic acid (LTA) – TLR2 (Toll-like receptor-2) ligand, Pam2CSK4 - TLR2/6 ligand, GlcC14C18 – Mincle ligand, viral PAMPS such as Gardiquimod (TLR7/8 ligand), Poly(I:C) (TLR3, RIG1, MDA5, and PKR ligand), and a fungal PAMP Zymosan – Dectin1/2, TLR2/6 ligand significantly increased NHO volumes when compared to control mice. In support of these findings, receptors for the aforementioned PAMPs were expressed by sorted muscle macrophages and/or fibro-adipogenic progenitors.

These data illustrate that PAMPs exacerbate NHO development in mice. Our data are consistent with previous retrospective studies showing a higher prevalence of NHO in SCI patients with infections. This work highlights the necessity to increase microbe vigilance to reduce the incidence of NHO in SCI or TBI patients.

249

Clinical cardiovascular disease and long-term falls risk: The Perth Longitudinal Study of Ageing in Women

Abadi Kahsu Gebre[1, 2], Marc Sim[1, 3], Jack Dalla Via[1], Alexander Rodriguez[1, 4], Kun (Kathy) Zhu[3, 5], John Schousboe[6, 7], Jonathan Hodgson[1, 3], Catherine Bondonno[1, 3], Richard Prince[1, 3, 8], Joshua Lewis[1, 3, 9]

1. Nutrition & Health Innovation Research Institute, School of Medical and Health Sciences , Edith Cowan University, Joondalup, Western Australia, Australia

2. School of Pharmacy , Mekelle University, Mekelle , Tigray , Ethiopia

3. Medical School , The University of Western Australia, Perth, Western Australia, Australia

4. Bone and Muscle Health Research Group, Department of Medicine, School of Clinical Sciences at Monash Health, Faculty of Medicine, Nursing and Health Sciences, Monash University, Clayton, Victoria, Australia

5. Department of Endocrinology and Diabetes, Sir Charles Gairdner Hospital, Perth, Western Australia, Australia

6. Park Nicollet Osteoporosis Centre and HealthPartners Institute, HealthPartners, Minneapolis, Minnesota, USA

7. Division of Health Policy and Management, University of Minnesota, Minneapolis, Minnesota, USA

8. School of Public Health, Curtin University, Perth, Western Australia, Australia

9. Centre for Kidney Research, Children's Hospital at Westmead School of Public Health, Sydney Medical School, The University of Sydney, Sydney, New South Wales, Australia

Publish consent withheld

Poor alignment of a smaller femur with the upper body may contribute to increased fracture risk in women with POI

Navira Samad[1, 2], Hanh Nguyen[2], Roger Zebaze[2], Jasna Aleskova[1, 3], Julie Pasco[4, 5, 6, 7], Mark Kotowicz[8, 4, 5], Frances Milat[1, 9, 3], Peter Ebeling[1, 9], Amanda Vincent[1, 6]

1. Department of Endocrinology, Monash Health, Melbourne, Victoria, Australia

2. Department of Medicine Western Health, Monash University, Melbourne, Victoria, Australia

3. Hudson Institute of Clinical Research, Clayton, Melbourne, Victoria, Australia

4. IMPACT - Institute for Physical and Mental Health and Clinical Translation, Geelong, VIC, Australia, Deakin University, Geelong, Victoria, Australia

5. Department of Medicine, Western Health, The University of Melbourne, Melbourne, Victoria, Australia

6. Department of Epidemiology and Preventive Medicine, Monash University, Melbourne, Victoria, Australia

7. University Hospital Geelong, Barwon Health, Geelong, VIC, Australia

8. Department of Endocrinology & Diabetes, University Hospital Geelong, Barwon Health, Geelong, Victoria, Australia

9. Department of Medicine, School of Clinical Sciences, Monash University, Melbourne, Victoria, Australia

Background and objective: Resistance to hip fractures relies on adequate compressive strength, determined by femur alignment and geometry. Oestrogen is a crucial determinant of bone accrual, peak bone mass [1] and geometry [2]; however, premature ovarian insufficiency (POI) is characterised by hypoestrogenism. We hypothesised that hypoestrogenism as seen in women with POI is associated with an impaired femur alignment and/or smaller femoral size.

Methods: We conducted a cross-sectional, case-control study including 89 women with spontaneous normal karyotype (s-POI) or iatrogenic (i-POI) POI, aged 20-40 years (cases) compared with 89 age and BMI-matched population-based controls, from 2005-2021. Hip geometrical features using Lunar Advanced Hip Analysis (AHA) software were measured and the axis of the femoral shaft with the vertical (α)- an indicator of its alignment with the upper body was also calculated (Figure 1).

Results:

Median age (range) of POI diagnosis occurred at 35 (18-40) years; mean POI duration at time of DXA was 2.07 (range 0-13) years. Oestrogen therapy was recorded in 82% of POI women. Cross-sectional area at the femoral neck (CSA mm^2) was lower in POI women compared with controls (139.30 ± 29.08 vs 157.29 ± 22.26; p<0.001) (Table 1). The angle between the femur shaft axis and the upper body (α) was lower in POI women compared with controls (-2.34 ± 4.30 vs 1.24 ± 3.72; p<0.001). After adjustment for the differences in height and ethnicity among the controls and POI participants, cortical thicknesses and ratios, hip axis length, and buckling ratio were not significantly different between groups.

Conclusion and Inferences:

Women with POI exhibit a smaller femur that was poorly aligned with the upper body. Further research is needed to establish the role of this newly identified feature in fracture risk prediction in these patients and influence on therapeutic decisions.

		Control n = 89	All-POI n= 89	p-value	p-value adjusted	s-POI n = 39	i-POI n= 50	p-value	p-value adjusted [a]
HAL (mm)		104.74 ± 6.21	102.48 ±8.00	0.402	0.539	100.05 ± 8.90	104.34 ± 6.76	**0.003**	0.334
Geometrical parameters									
Neck	Cortical width (mm)	5.50 ± 2.20	5.11 ± 1.73	0.782	0.240	4.94 ± 1.60	5.23 ± 1.84	0.332	0.913
	Cortical ratio (%)	18.69 ± 7.60	17.88 ± 5.79	0.909	0.514	17.66 ± 5.52	18.04 ± 6.04	0.703	0.985
Shaft	Cortical width (mm)	5.15 ± 1.24	4.74 ± 1.18	0.025	0.250	4.73 ± 1.20	4.74 ± 1.48	0.019	0.240
	Cortical ratio (%)	17.38 ± 3.80	16.64 ± 3.85	0.274	0.479	16.17 ± 4.46	16.67 ± 4.05	0.317	0.555
Calcar	Cortical width (mm)	3.81 ± 0.96	3.56 ± 0.90	0.591	0.979	3.47 ± 0.80	3.64 ± 0.98	0.140	0.851
	Cortical ratio (%)	7.29 ± 1.73	7.183 ± 1.80	0.866	0.728	7.19 ± 1.32	7.18 ± 1.80	0.920	0.953
Strength indices									
CSA (mm^2)		157.29 ± 22.26	139.30 ± 29.08	**<0.001**	**0.011**	132.31 ± 28.88	144.74 ± 28.33	**<0.001**	**0.021**
CSMI (mm^4)		10605 ± 2784.45	8848.45 ± 2771.68	**<0.001**	**0.041**	8038.82 ± 2671.53	9479.96 ± 2723.01	**<0.001**	**0.047**
Section Modulus (mm^3)		665.21 ± 129.54	575.53 ± 150.88	**<0.001**	**0.037**	532.75 ± 144.66	6.8.89 ± 144.66	**<0.001**	**0.042**
SI		1.58 ± 0.44	1.390 ± 0.30	**0.001**	**<0.001**	1.41 ± 0.303	1.37 ± 0.30	**0.005**	**0.004**
Buckling ratio		3.35 ± 1.32	3.35 ± 1.26	0.496	0.632	3.39 ± 1.39	3.31 ± 1.16	0.958	0.900
Neck shaft angle (θ)		126.79 ± 4.13	127.34 ± 4.88	0.590	0.224	128.02 ± 5.74	126.80 ± 4.07	0.597	**0.217**
∝		1.24 ± 3.72	-2.34 ± 4.30	**<0.001**	**<0.001**	-5.11 ± 4.49	-1.32 ± 3.90	**<0.001**	**<0.001**
y		15.79 ± 1.52	15.23 ± 1.49	0.319	0.405	14.92 ± 1.55	15.47 ± 1.41	0.609	0.605
d1 (mm)		17.42 ±3.03	18.01 ± 3.41	0.222	0.093	17.49 ±3.31	18.42 ±3.46	0.192	0.195
d2 (mm)		46.32 ±4.72	46.38 ± 5.89	0.939	0.263	44.50 ±6.25	47.85 ± 5.20	**0.012**	0.535
d3 (mm)		31.83 ± 2.38	30.82 ± 2.33	**0.004**	0.317	30.33 ± 2.45	31.19 ± 2.17	**0.004**	0.449

Abbreviations: HAL- Hip axis length, CSA- Cross-sectional area at the femoral neck; CSMI- Cross-sectional moment of inertia; SI- strength index;; d1- distance from head centre to section of minimum CSMI along neck axis; d2- distance along the neck X is from the centre of the femoral head to the neck/ shaft axis intersection; d3- average diameter of the femoral neck; Y-distance from the center of mass to the superior neck margin; ∝- angle of shaft axis with respect to vertical.
[a] adjusted for height and ethnicity

Table-1: AHA derived hip geometrical and structural parameters in controls vs women with POI

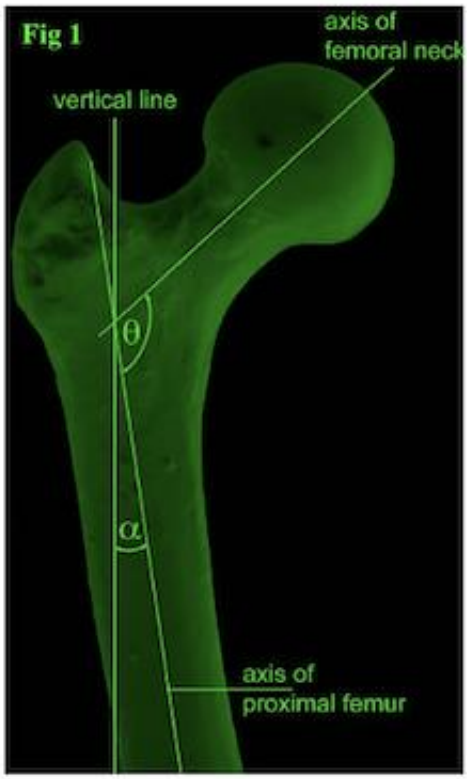

Figure 1: Diagram demonstrating angle of the hip to assess femoral alignment

1. Almeida, M., et al., Estrogens and Androgens in Skeletal Physiology and Pathophysiology. Physiol Rev, 2017. 97(1): p. 135-187.
2. Petit, M.A., et al., Femoral bone structural geometry adapts to mechanical loading and is influenced by sex steroids: the Penn State Young Women's Health Study. Bone, 2004. 35(3): p. 750-9.

Elevated bone-derived sclerostin in plasma is associated with high brain amyloid-β load in cognitively normal older adults

Jun Yuan[2, 1], Steve Pedrini[3], Pratishtha Chatterjee[3, 4], Bruno Meloni[1], Andrew Tai[2, 1], Junjie Gao[5], Frank Mastaglia[1], Charles Inderjeeth[6], Ralph Martins[3, 4], Minghao Zheng[2, 1]

1. Perron Institute for Neurological and Translational Science, Perth, Western Australia, Australia

2. Centre for Orthopaedic and Translational Research, School of Biomedical Sciences, University of Western Australia, M Block, WA, Australia

3. School of Medical and Health Sciences, Edith Cowan University, Joondalup, WA, Australia

4. Department of Biomedical Sciences, Macquarie University, North Ryde, NSW, Australia

5. Department of Orthopaedic Surgery, Shanghai Jiao Tong University Affiliated Sixth People's Hospital, Shanghai, China

6. Department of Rehabilitation & Aged Care, Sir Charles Gairdner Hospital, Nedlands, WA, Australia

Osteoporosis and Alzheimer's disease (AD) mainly affect older individuals, and the possibility of an underlying link contributing to their shared epidemiological features has rarely been studied. Interestingly, growing research has demonstrated that bone has endocrine-like functions by secreting various proteins that influence other body systems. In the current study, we investigated the association between levels of plasma sclerostin (SOST), a protein primarily produced by bone, and brain amyloid-beta (Aβ) load, a pathological hallmark of AD. A cohort of 100 older adults (66-89 years old) with normal global cognition (MMSE score >26) were enrolled for the study. Participants were divided into Aβ- (n = 65) and Aβ+ (n=35) groups based on their brain Aβ status assessed using positron emission tomography (PET) imaging. Plasma SOST concentrations were significantly elevated in Aβ+ participants ($p = 0.003$, $p^* = 0.008$), and were positively correlated with increasing brain Aβ load ($r_s = 0.321$, $p = 0.001$) before and after adjusting for covariates of age, gender and apolipoprotein E ε4 (APOE ε4) status. Furthermore, it was demonstrated that combining SOST with a base model built with AD risk factors including age, gender and APOE ε4 status had a higher diagnostic accuracy (AUC = 0.818, CI = 0.733 – 0.903) than using the base model alone (AUC = 0.787, CI = 0.693 – 0.882, $p = 0.228$). This study has identified a potential pathogenic association between bone and brain in older individuals, and highlights that plasma SOST levels may be associated with the pathology of AD.

Changes in body composition are associated with incident vertebral deformities over 10.7 years

Anuj Shah[1], Feitong Wu[1], Li Shean Toh[2], Flavia Cicuttini[3], Graeme Jones[1], Laura Laslett[1]

1. Menzies Institute for Medical Research, Univeristy of Tasmania, Hobart, TAS, Australia

2. School of Pharmacy, University of Nottingham, Nottingham, UK

3. Epidemiology and Preventive Medicine, Monash University, Melbourne, Victoria, Australia

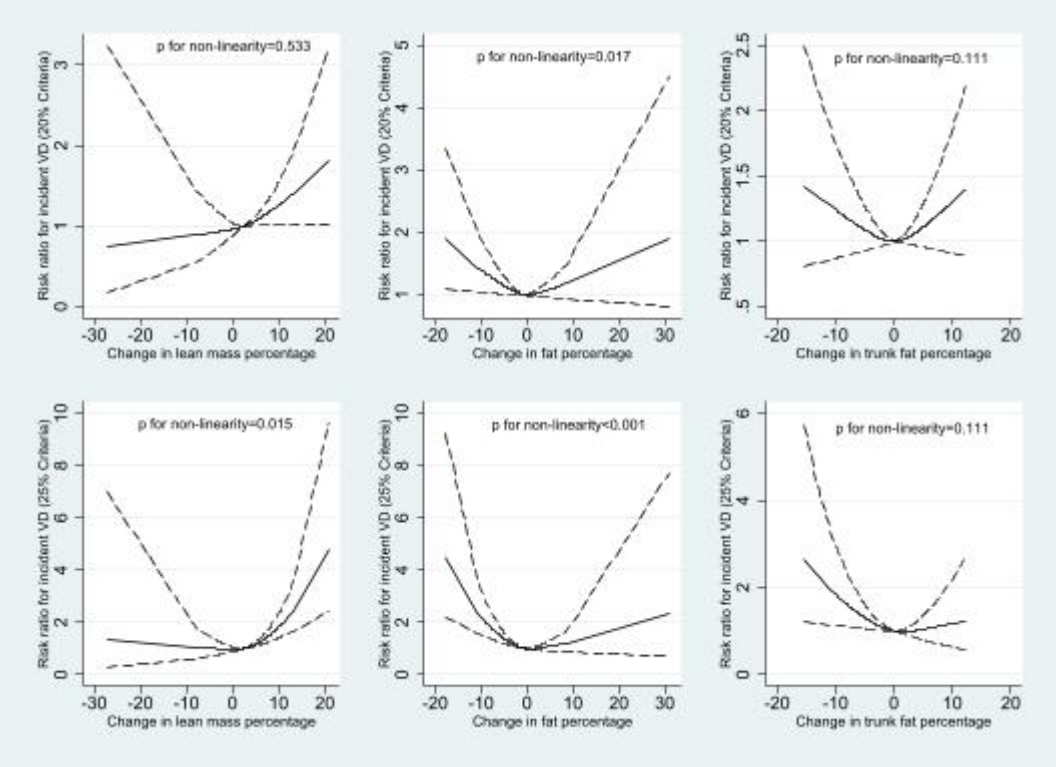

Purpose To examine the longitudinal associations between body composition and incident vertebral deformities (VDs) over 10.7 years in community dwelling adults aged 50-80 years.

Methods Participants (n=780, 50% female) underwent whole-body dual-energy X-ray absorptiometry (DXA) scans at baseline, 2.5, 5.1 and 10.7 years later which were used to obtain body composition measures and lateral vertebral scans. VD was defined using 2 criteria: ≥20% (mild), and ≥25% (moderate) reductions in vertebral height (anterior vs posterior height) from T4-L4. Incident VD was defined as new VD at any follow-up visit. Change in body composition measures was defined as the difference between the latest available data point and baseline.

Results New vertebral deformities were common over 10.7 years (53% mild VD, 37% moderate VD). Neither total fat mass or lean mass at baseline predicted incident deformities but increase in total fat mass reduced risk and increased lean mass percentage increased risk of mild and moderate VDs in both sexes. >10% increase in lean mas percentage increased risk of both mild and moderate VD in both sexes [(Males: IRR 1.96, 95%CI 1.26-3.04 for mild vs IRR 3.05, 95%CI 1.63-5.70 for moderate VD) ;(Females: IRR 1.59,95%CI 1.12-2.25 for mild vs IRR 2.91,95%CI 1.87-4.51 for moderate VD). Among women, change in fat percentage showed U shaped associations with incidence of both mild and moderate VD (p=0.017 and p<0.001, respectively). Change in lean percentage also showed non-linear association with moderate incident VDs (p=0.015).

Conclusions Baseline body mass did not predict incident vertebral deformities but change in mass did. While increasing lean mass percentage is associated with higher risk of incident VD, increasing total fat mass may be protective. Among women, associations between increased fat percentage and lean percentage, and incident VDs are non-linear in nature and may have a U-shape relationship.

Associations of Mechanical Loading from Physical Activity with Bone Mineral Density, Physical Function and Knee Impairment in Older Adults: the Tasmanian Older Adult Cohort (TASOAC) Study

Carrie-Anne Ng[1], Feng Pan[2], Dawn Aitken[2], Tania Winzenberg[2], Flavia Ciccuttini[3], Peter Ebeling[1], Graeme Jones[2], David Scott[1, 4, 2]

1. Department of Medicine, School of Clinical Sciences at Monash Health, Monash University, Clayton, Victoria, Australia

2. Menzies Institute for Medical Research, University of Tasmania, Hobart, Tasmania, Australia

3. Department of Epidemiology and Preventive Medicine, Monash University, Melbourne, Victoria, Australia

4. Institute for Physical Activity and Nutrition, School of Exercise and Nutrition Sciences, Deakin University, Burwood, Victoria, Australia

OBJECTIVE: Physical activity that induces high mechanical loading may benefit bone, but there are concerns of harm to joints in older adults. This longitudinal study aimed to investigate associations between loading intensities and application rates, estimated from self-reported physical activity, with bone mineral density (BMD), physical function, knee pain, knee cartilage defects and bone marrow lesions (BMLs) over 2.7 years.

METHODS: 943 community-dwelling older adults (mean age 63.0±7.5 years) from the Tasmanian Older Adult Cohort (TASOAC) study were assessed at baseline and 2.7 years later. Self-reported physical activity over the past year was assessed using the Global Physical Activity Questionnaire (GPAQ; estimates metabolic equivalents of task or METs), from which loading scores (product of peak force and application rate) were estimated using previously reported load ratings for different activities. Hip and lumbar spine BMD was measured by dual-energy x-ray absorptiometry scans, dynamometry assessed knee extension strength and the Western Ontario McMaster Osteoarthritis Index (WOMAC) assessed knee pain, stiffness and dysfunction (higher scores indicate poorer outcomes). Magnetic resonance imaging measured cartilage defects and BMLs at the medial and lateral tibia and femur. Linear mixed models investigated associations between physical activity scores and outcome measures accounting for repeated measures.

RESULTS: Loading scores, but not METS, were significantly positively associated with femoral neck BMD (standardised β=5.49mg/cm2 [95%CI=0.09, 10.9mg/cm2]) and knee extension strength (5.40kg [0.13, 0.95kg]) after adjustment for covariates including sex and body mass index. Neither loading scores nor METS were associated with spine BMD, WOMAC scores, knee cartilage defects or BMLs in unadjusted and adjusted models.

CONCLUSION: In community-dwelling older adults, self-reported physical activity of high and rapid impact maintains higher femoral neck BMD and knee extension strength over 2.7 years without apparent deleterious effects on knee joint structure or pain.

254

Understanding the contribution of immature myeloid cells to early melanoma establishment

Xiaoyu Hou[1], Arutha Kulasingh[1], Jazmina-Libertad Gonzalez-Cruz[1], James Wells[1]

1. UQDI/TRI, Woolloongabba, QLD, Australia

Immature myeloid cells are continually generated in the bone marrow of healthy individuals, where they differentiate into mature myeloid cells (such as neutrophils and monocytes) without causing detectable immunosuppression. However, in cancer, immature myeloid cells are known to be recruited to the tumour microenvironment and to differentiate into myeloid-derived suppressor cells with a potent ability to suppress various types of immune responses. The precise mechanisms that drive this differentiation remain unclear. In the laboratory, myeloid-derived suppressor cell differentiation is known to be induced through the interaction of peripheral blood mononuclear cells with melanoma cell lines, and in the clinic, myeloid-derived suppressor cell numbers accumulate in the blood of melanoma patients in all stages of disease, including in early-stage I patients. However, the absolute requirement for these cells in supporting the establishment of melanoma is not well understood. In my project, I will investigate whether immature myeloid cells play a fundamental role in tumour development by exploring the direct and indirect capacity of immature myeloid cells to impact tumour establishment and early growth. Initially, I will deplete immature myeloid cells before tumour challenge to determine the effects of depletion on tumour establishment. Next, I will co-inject immature myeloid cells and suboptimal numbers of tumour cells to determine whether immature myeloid cells offer a growth or survival advantage to emerging tumours. Finally, I will use a Nanostring GeoMx digital spatial profiling discovery approach to define where immature myeloid cells are physically located within emerging tumours, which cell they interact with, and which growth and angiogenic factors they produce. These observations could lead to novel approaches to exploit these insights to stop melanoma at an early stage.